The U.S. GOVERNMENT

IS ABSOLVED

FROM ANY LITIGATION WHICH MAY ENSUE FROM THE CONTRACTORS INFRINGING ON THE FOREIGN PATENT RIGHTS WHICH MAY BE INVOLVED.

REEL - C

484

A.T.I.

13979

UNCLASSIFIED

CORNELL AERONAUTICAL LABORATORY
OF CORNELL RESEARCH FOUNDATION, INC.
BUFFALO, N. Y.

REPORT NO. TB-405-F-3

DYNAMIC LONGITUDINAL STABILITY AND CONTROL FLIGHT TESTS OF A B-25J AIRPLANE. FORCED OSCILLATION AND STEP FUNCTION RESPONSE METHODS, UTILIZING AN A-12 AUTOMATIC PILOT.

Contract No. W33-038-ac-14248

Prepared BY Flight Research Department

G. F. Campbell

D. W. Whitcomb

W. O. Breuhaus

DATE 15 April 1947

NO. OF PAGES 165

Approved By W. F. Milliken, Jr., Assistant Manager.

I. C. Ross, Manager.

TABLE OF CONTENTS

TABLE OF CONTENTS CONT'D.

SUMMARY

With the advent of missiles, and rapid developments in conventional aircraft toward trans- and supersonic flight, an understanding and design knowledge of dynamic behavior is of increasing importance. Fundamental research in the development of new methods and techniques for the determination of dynamic characteristics in flight was initiated some three years ago through the joint efforts of the Air Materiel Command and what is now the Cornell Aeronautical Laboratory. The present report presents the detailed results of a particular phase of this general program.

A series of flight tests has been completed during which the dynamic response characteristics of an airplane to two different types of elevator motion were determined. These elevator motions were so chosen that they would be amenable to mathematical analysis and it was therefore possible to compare the experimental data with calculated response characteristics. Convenient forms of the equations of the motion of an airplane in its plane of symmetry have been developed and are included in this report.

It is shown that, based upon the well verified assumptions that the change of speed during control moments of normal rapidity is of negligible importance, the responses of the airplane may be obtained from expressions resembling that of the motion of a viscous damped, spring restrained mass.

The response characteristics of the airplane were measured during steady sinusoidal oscillations of the elevator and following abrupt (step) deflections of the elevator. Comparison of the experimentally determined response characteristics during sinusoidal oscillations with calculated responses indicated generally good agreement. However, the measured values of both the spring stiffness and the damping coefficient of the airplane were somewhat higher than the predicted values. An apparent lag between the motion of the airplane and the deflection of the elevator was found to exist during a number of the sinusoidal oscillations. A satisfactory explanation of this characteristic has not been advanced at the present time. Another characteristic for which no explanation has yet been found is an increasing apparent value of the stability derivative Z_w (which is directly proportional to the slope of the lift

curve of the airplane) as the frequency of the oscillation is increased. The transient responses following a step deflection of the elevator agree reasonably well with calculated responses. A time lag between the response of the airplane and the abrupt deflection of the elevator was noted.

A modified automatic pilot was used to obtain the desired elevator motion. The sinusoidal elevator deflection was superimposed on the normal stabilizing action of the automatic pilot so that the mean speed and flight path were maintained constant during the oscillation. During the step maneuver the elevator was moved to a new position and was held fixed in this position by the automatic pilot for the duration of the maneuver.

It is concluded that these tests confirm the feasibility of obtaining the dynamic longitudinal response characteristics of an airplane during flight by the selection of appropriate time histories of elevator movement.

INTRODUCTION

The results of a series of tests which have been conducted by the Flight Research Department of Cornell Aeronautical Laboratory to determine the dynamic longitudinal stability and control characteristics of an airplane by the forced oscillation technique are given in this report and these results are compared with calculated response characteristics. The responses of the airplane to step deflections of the elevator were also determined. The data reported herein are a part of those obtained during an extensive program of dynamic response measurements which is being carried out for the Aircraft Laboratory at Wright Field, under Contract No. W33-038-ac-14248, and covers all dynamic longitudinal tests made using a Sperry A-12 automatic pilot as a mechanism for oscillating the elevator of the airplane. A B-25J medium bombardment airplane was used for all tests.

It has been shown both experimentally and theoretically that the variation of speed which occurs during movements of the controls at normal rates is very small, and that this minor speed change has a negligible effect on the motion of the airplane. This permits considerable simplification of the theory of the motion of an airplane following movement of its elevator control, and convenient forms of the equations of motion of an airplane in its plane of symmetry are given in the appendices based on this assumption. These show that the variations of the normal acceleration and pitching velocity of an airplane may be expressed by second order differential equations analogous to the equation of motion of a spring restrained mass with viscous damping. This concept of effective spring stiffness and damping permits the construction by simple means of frequency response curves giving the amplitude and phase characteristics of the airplane in terms of the magnitude of the sinusoidal forcing function (which, in the case under consideration, is proportional to the elevator deflection) and its frequency. As is discussed in references (1) and (2), the analysis of the stability of closed loop dynamic systems (such as an airplane or missile equipped with an automatic pilot) is facilitated by the use of such frequency response data. Furthermore, the response to a step application of elevator deflection (forcing function) may be obtained quite simply from the second order system described and this response may be used in conjunction with the Duhamel integral for computing the response of the airplane corresponding to an arbitrary movement of the elevator.

The present flight investigation was undertaken in order to obtain a full scale flight check of the validity of the usual assumptions contained in theoretical treatments of the dynamic longitudinal stability of aircraft, and to develop a method for measuring the stability characteristics of airplanes and other flying devices for which

reliable stability parameters may not be available or cannot be obtained conveniently by theoretical analysis or wind tunnel testing. The frequency response curve of an aircraft (which is used as described in references (1) and (2) to investigate the stability characteristics of a combination of automatic pilot and airplane) may be obtained directly by this experimental technique. The forced oscillations method is thus of considerable utility in determining the response characteristics of an airplane.

The equations of motion of the airplane have been treated in terms of dimensional stability derivatives throughout this report. Although non-dimensionalized forms of the stability equations are in general use, it is thought that the dimensional form employed herein facilitates the interpretation of the equations. It is realized that, to ease comparison of the characteristics of airplanes of various sizes flying at different speeds and altitudes, the non-dimensional form is preferable. However, since the present tests were confined to tests of a single airplane at one altitude, it is believed that the dimensional form is advantageous in this case.

INDEX OF SYMBOLS, DEFINITIONS AND CONVENTIONS

b = Wing span - ft.

b = Equivalent control fixed airplane damping coefficient - 1/sec.

b' = Equivalent control free airplane damping coefficient - 1/sec.

c = Mean aerodynamic chord of wing - ft.

c_e = Elevator chord - ft.

c.g. = Center of gravity.

$C_h = \frac{HME}{\rho/2 S_e c_e U^2}$ - Elevator hinge moment coefficient.

$C_{h_\alpha} = \partial C_h / \partial \alpha_t$ - Elevator hinge moment coefficient due to angle of attack of the tail.

$C_{h_\delta} = \partial C_h / \partial \delta$ - Elevator hinge moment coefficient due to elevator deflection.

$C_L = L / \frac{\rho}{2} S U^2$ - Airplane lift coefficient.

$C_m = M / \frac{\rho}{2} S c U^2$ - Airplane pitching moment coefficient.

$C_{N_t} = N_t / \frac{\rho}{2} S_t U^2$ - Horizontal tail lead coefficient.

D = Differential operator = $\frac{d}{dt}$

F = Force or function - general.

f = Frequency - cycles/sec.

g = Acceleration due to gravity = 32.2 ft./sec.^{2}.

HME = Elevator hinge moment - lb. ft.

I_y = Airplane moment of inertia about the y axis - slug ft.^{2}.

K = Equivalent control fixed airplane spring constant - 1/sec.^{2}.

K' = Equivalent control free airplane spring constant - 1/sec.^{2}.

l_t = Tail length - ft. (considered positive).

M = Moment about the y axis - lb. ft.

$M_q = \partial M / \partial q \times \frac{1}{I_y}$, 1/sec.

$M_u = \partial M/\partial u \times 1/I_y$, 1/ft. - sec.

$M_w = \partial M/\partial w \times 1/I_y$, 1/ft. - sec.

$M_{\dot{w}} = \partial M/\partial \dot{w} \times 1/I_y$, 1/sec.^{2}.

m = Mass of airplane slugs.

$m_t = \partial C_{N_T}/\partial \alpha_t$ - Normal force slope of the horizontal tail.

mph = Miles per hour.

N_t = Normal horizontal tail load - lbs.

n = Acceleration along the Z axis at the c. g. (normal acceleration) - ft./sec.^{2}.

n_x = Acceleration along the x axis - ft./sec.^{2}.

$q = \dot{\theta}$ - Angular velocity about the y axis.

S = Wing area - ft.^{2}.

S_t = Horizontal tail area - ft.^{2}.

S_e = Elevator area, aft of hinge line - ft.^{2}.

T = Period of oscillation - seconds.

t = Time - seconds.

V = True airspeed - ft./sec.

u = Velocity increment along the y axis - ft./sec.

$\dot{u}$ = du/dt - Acceleration increment along the x axis due to changes in u. - ft./sec.^{2}.

w = Velocity increment along the Z axis - ft./sec.

$\dot{w}$ = dw/dt - Acceleration increment along the axis due to changes in w - ft./sec.^{2}.

X = Force along the x axis - lbs.

$X_q = \partial X/\partial q \times 1/m$ - ft./sec.

$X_u = \partial x/\partial u \times 1/m$ - 1/sec.

$X_w = \partial x/\partial w \times 1/m$ - 1/sec.

$X_\delta = \partial X / \partial \delta \times 1/m$ - ft./sec.^{2}.

$X_\theta = \partial X / \partial \theta \times 1/m$ - ft./sec.^{2}.

Z = Force along the z axis - lbs.

$Z_q = \partial Z / \partial q \times 1/m$ - ft./sec.

$Z_u = \partial Z / \partial u \times 1/m$ - 1/sec.

$Z_w = \partial Z / \partial w \times 1/m$ - 1/sec.

$Z_\delta = \partial Z / \partial \delta \times 1/m$ - ft./sec.^{2}.

$Z_\theta = \partial Z / \partial \theta \times 1/m$ - ft./sec.^{2}.

Greek Symbols

α = Wing angle of attack - degrees ~~or~~ radians.

α_t = Angle of attack of the horizontal tail - degrees ~~or~~ radians.

δ = Elevator deflection - degrees ~~or~~ radians.

ϵ = Angle of downwash - degrees or radians.

θ = Inclination of x axis with respect to the horizontal - degrees ~~or~~ radians.

$\lambda = -\left(\partial \alpha_t / \partial \delta\right)_{C_{N_t}}$ = Effective change of tail angle of attack due to elevator deflection.

ρ = Mass density of air - slugs/ft.^{3}.

ρ_0 = Sea level value of air density = 0.002378 slugs/ft.^{3}.

σ = Density ratio = ρ / ρ_0

ϕ = Phase angle - general - Phase relations indicated by subscripts. degrees

I can't tell what subscript system is.

ω = Angular frequency - radians/sec.

A bar placed over a variable indicates the maximum value of that variable during an oscillation. The amplitude may be either positive or negative, i.e. $\bar{n}$ is the maximum amplitude of the normal acceleration during an oscillation and may be either positive or negative.

Vertical bars placed around a variable indicate the positive value of that variable, i.e. $|n|$ is the positive value of the normal acceleration at a given instant. Thus $|\hat{n}|$ denotes the positive maximum value of the normal acceleration during an oscillation.

A dot placed over a variable indicates its derivative with respect to time. Two dots indicate the second derivative with respect to time, hence $\dot{n} = dn/dt$ and $\ddot{n} = d^2n/dt^2$, etc.

SIGN CONVENTIONS

Axes

x axis, or longitudinal axis, positive forward.

y axis, positive along right wing.

Z axis, positive downward.

Linear Displacements

A linear displacement along a positive reference axis is considered to be positive.

Angular Displacements

An angular displacement which is clockwise when viewed from the origin looking along a positive reference axis is considered to be positive.

Velocities and Accelerations

Velocities and accelerations, either linear or angular, are considered positive in the same sense as the corresponding displacements.

Control Surface Deflections

Positive elevator angle is associated with a downward movement of the elevator trailing edge.

Hinge Moment

Positive elevator aerodynamic hinge moment is that which tends to move the elevator in a trailing edge downward direction.

EQUIPMENT, INSTRUMENTATION AND METHOD OF TEST

All flight tests were conducted using a North American B-25J medium bombardment airplane. This airplane is a midwing, twin-engine monoplane powered by Wright R-2600-29 two-speed supercharged engines driving 3 bladed Hamilton Standard constant speed hydromatic 6359A-18 propellers. Fig. 1 is a photograph of this airplane, and a 3-view drawing of the airplane is included as Fig. 2. A tabulation of the primary physical characteristics of the airplane is given in Table I. All armament was removed from the airplane. The standard pitot tube installation was replaced by an NACA type free swiveling static tube and shielded total head tube mounted on a boom near the right wing tip.

A Sperry A-12 automatic pilot was installed in the airplane, and was suitably modified to permit using the automatic pilot as a mechanism for moving the elevator as desired. The sinusoidal oscillation of the elevator was obtained by feeding an oscillating voltage signal into the elevator position follow-up circuit so that a sinusoidal voltage was applied to the elevator servo. The sinusoidal voltage signal was produced by rotating an autosyn transmitter. The rotational velocity of the autosyn was varied to modify the elevator oscillation frequency, and the voltage output of the mechanical oscillator was varied to control the amplitude of the oscillation of the elevator.

The signal from the mechanical oscillator was superimposed on the normal rate and displacement signals from the vertical flight gyro of the automatic pilot. Thus the automatic pilot remained in operation during the oscillation, and the mean flight path of the airplane remained constant. The operation of the stabilizing elements of the automatic pilot resulted in a phase shift between the oscillator signal and the elevator motion, and a modification of the amplitude of elevator oscillation for a given oscillator voltage output. However, since the responses of the airplane are referred to the elevator motion throughout this report, the phase shifts and amplitude modifications due to the functioning of the automatic pilot are irrelevant. It was found necessary to control the mean flight path by leaving the automatic pilot in operation in order to prevent the speed of the airplane from slowly changing from the desired value during an oscillation.

The step deflection of the elevator was obtained by removing all signals from the vertical flight gyro to the elevator servo in steady flight at the desired speed and replacing the gyro signal with a constant voltage which maintained the elevator at the position necessary to maintain steady rectilinear flight at the desired speed. The airplane was thus trimmed in steady flight without automatic stabilization about the lateral axis. (Automatic control was maintained about the longitudinal and vertical axes). The step deflection of the elevator was then accomplished by suddenly applying a voltage to the elevator servo circuit. This voltage was maintained at a constant value for the deviation of the maneuver, and thus the elevator was maintained at a fixed deflection from its initial position.

The flight test data were recorded by a photo observer and a Consolidated Engineering Corporation recording oscillograph. Airspeed, altitude, and engine operating conditions were taken from the photo observer record. The following quantities were recorded on the oscillograph:

1. Normal acceleration.

2. Longitudinal acceleration.

3. Elevator angle.

4. Pitch angle.

5. Elevator hinge moment.

6. Horizontal tail load.

The normal and longitudinal accelerations were measured by Consolidated Engineering Corporation reluctance type electrical accelerometer pick-ups whose signals were amplified by electronic amplifiers before being fed into the galvanometers of the oscillograph.

The elevator position was obtained by recording the output of an autosyn transmitter which was driven by a linkage from the elevator horn. The pitch angle signal was taken from the pitch selsyn of a modified Minneapolis-Honeywell vertical flight gyro unit which was installed in the airplane as an attitude reference. The outputs of both the elevator position autosyn and the gyro pitch selsyn were amplified before being fed into their respective galvanometer circuits of the oscillograph.

Elevator hinge moment was obtained by recording the amplified signal of the unbalance of a Wheatstone bridge circuit of strain gages which was installed on the elevator horn.

A totalizing strain gage circuit was installed on the horizontal tail and the fuselage bulkheads supporting the horizontal tail. The circuit was so adjusted that its output was the same for a given loading of the tail no matter how the load was distributed. This permitted determination of the tail load from a single signal which was amplified and recorded on the oscillograph.

During the oscillation tests the airplane was carefully trimmed at the desired speed and altitude. The automatic pilot was then engaged, and the mechanical oscillator was adjusted to oscillate the elevator at the desired amplitude and frequency. After the oscillation of the airplane was established at the steady state condition the recording equipment was turned on and from 5 to 15 cycles were recorded. (The number of cycles recorded was usually greater at high frequencies than at low frequencies.) The frequency of oscillation was varied from 0.10 to 1.30 cycles per second in approximately 36 intervals. The double amplitude of the elevator oscillation was maintained at approximately 2° at all frequencies.

Oscillation tests were conducted at three speeds and six center of gravity positions at a pressure altitude of 10,000 feet. Oscillations were made at center of gravity positions of 22, 24, 26, 28, 30 and 32% MAC at a speed of 175 mph EAS. The tests were repeated at center of gravity positions of 22 and 26% at equivalent airspeeds of 135 and 200 mph.

The response of the airplane to a step deflection of the elevator was measured at 175 mph EAS and at center of gravity positions of approximately 24, 28, and 30% MAC.

The center of gravity was maintained at the desired position during all flights by transferring ballast within the airplane during flight. This was accomplished by pumping water from a tank located near the c. g. to another tank in the tail cone of the airplane, or vice versa.

DISCUSSION OF OSCILLATION THEORY

The theory of dynamic stability analysis by the oscillation method is based upon the fact that the airplane in flight represents a mechanical system made up of masses with inertia, and influenced by aerodynamic forces and moments.

It should be possible to obtain information concerning the dynamic characteristics of such a system by inducing forced oscillations at various frequencies and noting the characteristics of the ensuing motion. This is a method quite common in other fields of science, notably electrical engineering (reference (3)).

As applied specifically to the airplane, the oscillation method consists of applying sinusoidally varying aerodynamic moments by means of the control surfaces, which are oscillated by a suitably modified automatic pilot, at a controllable frequency and amplitude. The pertinent parameters of the motion are then simultaneously recorded as functions of time.

A brief analysis of the oscillation theory will be presented here and the significant aspects of this method discussed. For a detailed mathematical treatment together with a justification of certain assumptions, and complete definitions of various parameters, the reader is referred to Appendix A. All symbols and conventions are as previously defined.

The equations for the longitudinal motion of an airplane may be written as follows:

$$\dot{u} + g\theta = X_u u + X_w w \qquad (1)$$

$$\dot{w} - U_1 q = Z_u u + Z_w w \qquad (2)$$

$$\dot{q} = M_u u + M_w w + M_q q + M_{\dot{w}} \dot{w} + M_\delta \delta \qquad (3)$$

These equations represent the motion of a system having three degrees of freedom, namely u, w, and q. If it were possible to eliminate one degree of freedom either by a predetermined interrelation between the variables and forcing functions or by confining one's interest to a regime where the value of a particular variable is negligible in comparison to the others, a valuable simplification in the analysis would result.

It is well known that rapid changes in pitch and acceleration may take place with very small changes in airspeed. Examination of equations (1), (2), and (3) shows that if the effects of airspeed change were neglected, the problem of analysis would be greatly simplified.

To justify an assumption that variations in airspeed are negligible, calculations were made to determine the change in airspeed at various frequencies and its effect in comparison to those of the other variables. The effect was found to be small and essentially negligible as the frequencies approached that for the short period oscillation of the airplane. The variation in airspeed has decreased to approximately 0.10 times the change in vertical velocity w at this point and at a frequency of 0.50 radians/second has increased to approximately 0.50, the change in w. However the values of the derivatives dependent upon u are still small compared to those dependent upon w and q.

In addition to calculations, flight tests were made in which the change in airspeed and longitudinal acceleration were measured at different oscillation frequencies ranging from 0.50 to 8.0 radians/second. The greatest change in airspeed occurred at the lower frequency as would be expected. Measurements made with a calibrated airspeed indicator showed a maximum change at approximately 1.2 MPH at the lowest frequency, this change decreasing to essentially zero at 3 radians/second. Data obtained from longitudinal accelerometer records showed a maximum airspeed change of approximately 2.5 MPH at a frequency of 0.50 radians/second, this change decreasing to essentially zero at a frequency of 5.0 radians/second. Data from both sources are shown in Fig. 3.

It is justifiable therefore to assume that, if the lowest oscillation frequency is not appreciably less than 0.5 radians/second, the changes and rates of change of airspeed may be neglected in this analysis. Therefore

$$u = \dot{u} = 0$$

and equations (1), (2), and (3) become

$$s\theta = X_w w \tag{4}$$

$$\dot{w} - U_e q = Z_w w \tag{5}$$

$$\dot{q} - M_w w + M_q q + M_{\dot{w}} \dot{w} + M_\delta \delta \tag{6}$$

There are now three equations in two unknowns, namely w and q (or θ), since $M_\delta \delta$ is an arbitrary forcing function. However only equations (5) and (6) are independent, since equation (4) must be satisfied by the same conditions which satisfy equations (5) and (6).

By differentiation, suitable substitutions and rearranging, equations (5) and (6) can be written as

$$\ddot{w} - \left[M_q + Z_w + U M_{\dot{w}}\right]\dot{w} + \left[Z_w M_q - U M_w\right] w = U M_\delta \delta \tag{7}$$

$$\ddot{q} - \left[M_q + Z_w + U M_{\dot{w}}\right]\dot{q} + \left[Z_w M_q - U M_w\right] q = M_\delta \left[\dot{\delta} - Z_w \delta\right] \tag{8}$$

It is seen that the coefficients of $\dot{w}$ and $\dot{q}$ are the same, and that those of w and q are also identical.

Dimensionally

$$\left[M_q + Z_w + UM_{\dot{w}}\right] = \left(\frac{lb\text{-}ft\text{-}sec^2}{radian}\right)\left(\frac{1}{lb\text{-}ft\text{-}sec^2}\right) = \frac{1}{sec}, \text{ or } \left(\frac{lb\text{-}sec}{ft}\right)\left(\frac{ft}{lb\text{-}sec^2}\right) = \frac{1}{sec}$$

which represents a viscous damping proportional to angular velocity, divided by a moment of inertia, or a viscous damping proportional to a linear velocity, divided by a mass. This term may therefore be considered as an equivalent damping coefficient, in the analysis of the airplane motion.

Dimensionally

$$\left[Z_w M_q - UM_w\right] = \left(\frac{lb - ft}{radian}\right)\left(\frac{1}{lb \cdot ft\, sec^2}\right) = \frac{1}{sec^2} \quad or \quad \left(\frac{lb}{ft}\right)\left(\frac{ft}{lb\text{-}sec^2}\right) = \frac{1}{sec^2}$$

which represents a restoring moment proportional to a rotation, divided by a moment of inertia, or a restoring force proportional to a displacement divided by a mass. This term may therefore be considered as an equivalent spring constant in the analysis.

These two terms have been designated as follows

$$b = -\left[M_q + Z_w + UM_{\dot{w}}\right] \quad \text{Equivalent airplane damping coefficient} \tag{9}$$

$$k = \left[Z_w M_q - UM_w\right] \quad \text{Equivalent airplane spring constant} \tag{10}$$

Equations (7) and (8) now become

$$\ddot{w} + b\dot{w} + Kw = UM_\delta \dot{\delta} \quad \text{ft./sec.}^3 \tag{11}$$

$$\ddot{q} + bq + Kq = M_\delta\left[\dot{\delta} - Z_w \delta\right] \quad \frac{\text{radians}}{\text{sec.}^3} \tag{12}$$

Each of these equations now resembles that of the response of a simple single degree of freedom mechanical or electrical system under the influence of an arbitrary forcing function. The fact that the two important variables characterizing the airplane longitudinal motion have been separated into single independent differential equations greatly simplifies the analysis, and makes it possible to study the response of each variable separately.

An additional equation involving the normal acceleration may be obtained by noting that from equation (5)

$$n = \dot{w} - Uq = Z_{\dot{w}} \dot{w} \tag{13}$$

and making this substitution in equation (11) to obtain,

$$\ddot{n} + b\dot{n} + Kn = \bar{U} Z_w M_\delta \dot{\delta} \tag{14}$$

The airplane motion may now be determined in terms of w, q, or n, in response to any type of a forcing function that can be represented mathematically. The response to a unit step function as discussed later makes it possible to determine the response to any arbitrary forcing function since any control motion can be represented by a series of steps.

In this section the response to a sinusoidal forcing function only is considered. Time solutions for w, n and q in response to a sinusoidal elevator motion, where

$$\delta(t) = |\bar{\delta}| \sin \omega t \tag{15}$$

are derived in Appendix A. The results of these solutions are as follows:

$$\frac{w(t)}{|\bar{\delta}|} = \frac{UM_\delta}{\sqrt{(K-\omega^2)^2+(b\omega)^2}} \sin\left[\omega t + \tan^{-1}\frac{-b\omega}{K-\omega^2}\right] \tag{16}$$

$$\frac{n(t)}{|\bar{\delta}|} = \frac{UM_\delta Z_w}{\sqrt{(K-\omega^2)^2+(b\omega)^2}} \sin\left[\omega t + \tan^{-1}\frac{-b\omega}{K-\omega^2}\right] \tag{17}$$

$$\frac{q(t)}{|\bar{\delta}|} = \frac{M_\delta\sqrt{Z_w+\omega^2}}{\sqrt{(K-\omega^2)^2+(b\omega)^2}} \sin\left[\omega t + \tan^{-1}\frac{\omega(K-\omega^2)+Z_w b\omega}{-Z_w(K-\omega^2)+b\omega^2}\right] \tag{18}$$

The response of the airplane is best studied by noting the variation of the amplitude and phase relationships of each variable or the ratios of variables as a function of frequency. This gives information concerning resonances and attenuations of amplitude responses at various frequencies, and phase relations which may be interpreted as time lags between various factors in the motion. Flight test data showing the experimental variation of $\frac{n(t)}{|\bar{\delta}|}$ and $\frac{q(t)}{|\bar{\delta}|}$ both in amplitude and phase as functions of frequency are given in this report.

The values of b and k, the equivalent damping coefficient and spring constant, may be readily determined from the response data by means of the circle diagram as explained in the following section. The ability to visualize the motion of the airplane in the simple terminology of a b and k is of considerable value in the application of automatic flight controls to aircraft, in which case it is usually necessary to make a dynamic analysis of the aircraft and automatic control system combination. The advantage of being able to represent the airplane in any particular mode of longitudinal motion by a transfer function of second degree, greatly simplifies a very complicated problem of analysis. The term "transfer function" has been defined by Hall (reference (4)), and is a complex function relating the input and output of a system. Thus the acceleration transfer function of the airplane with respect to

the elevator angle, expressed in La Placian operator form (reference (5)) would be,

$$\frac{n(s)}{\delta(s)} = \frac{UM_\delta Z_w}{s^2 + bs + K} \tag{19}$$

or in terms of frequency where s has been replaced by $i\omega$

$$\frac{n(\omega)}{\delta(\omega)} = \frac{UM_\delta Z_w}{(K-\omega^2) + ib\omega} \tag{20}$$

In addition to the response relations discussed above, the variations of horizontal tail load and elevator hinge moment in response to a sinusoidal elevator motion can be both calculated and measured.

Since the variation of w, n, and q are known with respect to the elevator angle, it is possible to determine the variation of w, n, and q with respect to total elevator hinge moment. This information may be thought of as stick free dynamic stability data, if it is assumed that at the frequencies involved the inertia of the elevator control system produces negligible effects, (reference (6)).

The expression for variation of horizontal tail load coefficient with respect to elevator angle has been derived in Appendix A, and only the final result will be given here.

$$\frac{C_{n_t}}{|\bar{\delta}|} = \frac{m_t}{U}\sqrt{C^2+S^2}\,\sin\left(\omega t + \tan^{-1}\frac{C}{S}\right) \tag{21}$$

where

$$C = \frac{UM_\delta\left[\omega(K-\omega^2)\frac{\ell_t}{U}\frac{d\epsilon}{d\alpha} - b\omega\left(1-\frac{d\epsilon}{d\alpha}\right)\right] + M_\delta \ell_t\left[\omega(K-\omega^2) + Z_w b\omega\right]}{(K-\omega^2)^2 + (b\omega)^2} \tag{22}$$

and

$$S = \frac{UM_\delta\left[(K-\omega^2)\left(1-\frac{d\epsilon}{d\alpha}\right) + b\omega^2\frac{\ell_t}{U}\frac{d\epsilon}{d\alpha} + M_\delta \ell_t\left[-Z_w(K-\omega^2) + b\omega^2\right]\right]}{(K-\omega^2)^2 + (b\omega)^2} + U\lambda \tag{23}$$

The total elevator hinge moment coefficient variation with elevator angle is given by:

$$\frac{C_h}{|\bar{\delta}|} = \sqrt{C'^2 + S'^2}\,\sin\left(\omega t + \tan^{-1}\frac{C'}{S'}\right) \tag{24}$$

where

$$C' = \frac{C_{h_\alpha}}{\bar{U}\left[(K-\omega^2)^2+(b\omega)^2\right]}\left[-UM_\delta b\omega\left(1-\frac{d\epsilon}{d\alpha}\right)+\frac{d\epsilon}{d\alpha}(K-\omega^2)(\ell_t\omega M_\delta)\right. \quad (25)$$
$$\left. +\ell_t M_\delta\left[\omega(K-\omega^2)+Z_\omega b\omega\right]\right]$$

and

$$S' = C_{h_\delta}+\frac{C_{h_\alpha}}{\bar{U}\left[(K-\omega^2)^2+(b\omega)^2\right]}\left[UM_\delta\left(1-\frac{d\epsilon}{d\alpha}\right)(K-\omega^2)+\frac{d\epsilon}{d\alpha}\omega^2 b\,\ell_t M_\delta\right. \quad (26)$$
$$\left. +\ell_t M_\delta\left[-Z_\omega(K-\omega^2)+b\omega^2\right]\right]$$

Expressions are also determined for $/\bar{C}_n/$ and $/\bar{C}_h/$ as follows:

$$\frac{n}{/\bar{C}_h/} = \frac{\bar{U}M_\delta Z_\omega}{C_{h_\delta}\sqrt{(K'-\omega^2)^2+(b'\omega)^2}}\sin\left(\omega\tau+\tan^{-1}\frac{-b'\omega}{K'-\omega^2}\right). \quad (27)$$

and

$$\frac{\delta}{/\bar{C}_h/} = \frac{M_\delta}{C_{h_\delta}}\sqrt{\frac{Z_\omega{}^2+\omega^2}{(K'-\omega^2)^2+(b'\omega)^2}}\sin\left(\omega\tau+\tan^{-1}\frac{\omega(K'-\omega^2)+Z_\omega b'\omega}{-Z_\omega(K'-\omega^2)+b'\omega^2}\right) \quad (28)$$

where b' and k' are related to the expressions b and k (equations (9) and (10) respectively) by

$$b' = -\left[Z_\omega+M_{\dot\alpha}+UM_{\dot\omega}\right]+\left[M_\delta\frac{C_{h_\alpha}}{C_{h_\delta}}\frac{\ell_t}{\bar{U}}\left(1-\frac{d\epsilon}{d\alpha}\right)\right] = b+\left[M_\delta\frac{C_{h_\alpha}}{C_{h_\delta}}\frac{\ell_t}{\bar{U}}\left(1-\frac{d\epsilon}{d\alpha}\right)\right] \quad (29)$$

$$K' = \left[Z_\omega M_{\dot\alpha}-UM_\omega\right]+M_\delta\frac{C_{h_\alpha}}{C_{h_\delta}}\left(1-\frac{d\epsilon}{d\alpha}-\frac{\ell_t}{\bar{U}}Z_\omega\right) = K+\left[M_\delta\frac{C_{h_\alpha}}{C_{h_\delta}}\left(1-\frac{d\epsilon}{d\alpha}-\frac{\ell_t}{\bar{U}}Z_\omega\right)\right] \quad (30)$$

A knowledge of the variation of horizontal tail load with elevator angle under dynamic conditions is of value to the structural designer who must determine the magnitude of the maneuvering tail load. Experimental data of this type can serve as a check on the probable accuracy of the rather elaborate calculations usually necessary to determine by analytical means the tail load in response to rapid motions of the elevator. The tail load response to a step elevator input may be used to synthesize the response to any arbitrary elevator deflection.

The variation of elevator hinge moment with respect to elevator angle under dynamic conditions is of especial value to the designer of automatic flight controls or control boost systems, since this gives an indication of the power required to operate the control surfaces under rapidly varying conditions.

The response of the airplane as a function of the variation of hinge moment is of interest where automatic controls are employed which apply variable torques to the control system, such that the resulting control surface deflection is a function of this torque and the aerodynamic hinge moment. This is in contrast to automatic control systems which apply control surface deflections in response to error signals, and in which the applied torque is that required to give this deflection.

It has been assumed throughout this analysis that the forcing function is directly proportional to the elevator deflection and all responses have been determined on this basis. The true forcing function however is an aerodynamic moment and is correctly designated as $M_\zeta \delta$. This takes into account the possibility of a phase difference between δ and M_ζ, or that M_ζ may have complex components.

Since the test data show that the airplane does not behave as a simple system with constant coefficients under all conditions, there is the possibility that the various aerodynamic derivatives are functions of frequency and have an aerodynamic lag. Such a variation is not readily determinable, however, since many of the derivatives occur as products, for example $M_\zeta Z_w$, which makes it difficult to determine their values unless they are assumed to be real (that is, having no aerodynamic lag).

It would appear desirable to know the variation of the aerodynamic forcing moment as a function of time, and regard this as the true forcing function. This reasoning holds promise for a method of oscillation employing the application of a known moment. This method, which has been outlined in a previous report, (reference (7)) , makes use of an oscillating auxiliary lifting surface, installed in a suitable position on the airplane. The force which this surface applies to the airplane structure is measured and is a direct function of the applied aerodynamic moment.

DISCUSSION OF THE CIRCLE DIAGRAM

In the discussion of the oscillation theory, it was mentioned that the circle diagram was a useful method of presenting data and that only a simple computation was necessary to determine the values of b and k, the equivalent damping coefficient and spring constant, therefrom.

A complete theoretical development of the circle diagram together with an explanation of its numerous applications is presented in Appendix C. However, a simple explanation of this diagram will be given here.

The equation of a circle may be represented in polar form by,

$$R = D \cos \theta \tag{31}$$

where R is the radius vector for any value of θ. An examination of the airplane response equations indicates that they are of this form or may be converted thereto by a simple transformation.

Consider the expression for $\frac{\dot{n}}{|\bar{\delta}|}$, the first derivative with respect to time of the expression previously given for $\frac{n}{|\bar{\delta}|}$

$$\frac{\dot{n}}{|\bar{\delta}|} = \frac{U M_\delta Z_w}{\sqrt{\left(\frac{k}{\omega} - \omega\right)^2 + b^2}} \sin\left(\omega t + \tan^{-1} \frac{\frac{k}{\omega} - \omega}{b}\right) \tag{32}$$

The maximum amplitude of $\frac{\dot{n}}{|\bar{\delta}|}$ at any given frequency occurs when

$$\sin\left(\omega t + \tan^{-1} \frac{\frac{k}{\omega} - \omega}{b}\right) = 1 \tag{33}$$

and is given by

$$\frac{\dot{n}}{|\bar{\delta}|} = \frac{U M_\delta Z_w}{\sqrt{\left(\frac{k}{\omega} - \omega\right)^2 + b^2}} \tag{34}$$

It is evident that this expression can be written

$$\frac{\dot{n}}{|\bar{\delta}|} = \frac{U M_\delta Z_w}{b} \cos \phi_{\dot{n}_\delta} \tag{35}$$

where

$$\phi_{\dot{n}_\delta} = \tan^{-1} \frac{\frac{k}{\omega} - \omega}{b} \tag{36}$$

According to the definition given in equation (51) above, equation (35) represents a circle with diameter,

$$D = \frac{U M_\delta Z_w}{b} \tag{37}$$

This theoretical circle is shown in Fig. 4.

It is thus possible to plot the variation of $\frac{\dot{n}}{|\bar{\delta}|}$ as a circle, where the length of the radius vector and its angle with respect to the reference or diameter represent the maximum amplitude of $\dot{n}/|\bar{\delta}|$ and its phase respectively as functions of frequency. Flight test values of $\dot{n}/|\bar{\delta}|$ plotted as circles are shown in Figs. 6 through 16 of this report. Circle plots of $\frac{\dot{n}}{|\bar{C}_n|}$ are also included in these figures.

When $\phi_{\dot{n}_\delta}$ equals zero, the value of $\frac{\dot{n}}{|\bar{\delta}|}$ is a maximum which is known to occur at the undamped natural frequency ($\omega = \sqrt{K}$) of the system. If the phase angle is zero, its tangent is also zero and

$$\tan \phi_{\dot{n}_\delta} = \frac{\frac{K}{\omega_o} - \omega_o}{b} = 0 \tag{38}$$

where ω_o is the undamped natural frequency of the system, and is that frequency corresponding to the diameter of the circle. The value of k is immediately determined since

$$K = \omega_o^2 \tag{39}$$

The value of b may be obtained by knowing the value of tan $\phi_{\dot{n}_\delta}$ at any other frequency. For ease of computation it is convenient to choose the frequency so that $\phi_{\dot{n}_\delta}$ (measured from the diameter of the circle) = 45° or tan $\phi_{\dot{n}_\delta} = 1$. Thus

$$\tan \phi_{\dot{n}_\delta} = \frac{\frac{K}{\omega'} - \omega'}{b} = 1 \tag{40}$$

where ω' is the frequency where $\phi_{\dot{n}_\delta} = 45°$

and

$$b = \frac{K}{\omega'} - \omega' \tag{41}$$

By an analysis similar to that above, it can be shown that the variation of the maximum amplitude of $\dot{q}/|\bar{\delta}|$ with frequency may be plotted as a circle if it first be multiplied by the factor,

$$\cos\left(\tan^{-1}\frac{\omega}{-Z_w}\right) = \frac{-Z_w}{\sqrt{\omega^2 + Z_w^2}} \tag{42}$$

and if $\tan^{-1}\frac{\omega}{-Z_w}$ be subtracted from the phase angle of $\dot{q}$ with respect to δ. The resulting circle is given by

$$\frac{\dot{q}}{|\bar{\delta}|}\left(\frac{-Z_w}{\sqrt{\omega^2 + Z_w^2}}\right) = \frac{M_\delta Z_w}{b} \cos\left(\phi_{\dot{q}_\delta} - \tan^{-1}\frac{\omega}{-Z_w}\right) \tag{43}$$

Values of b and k can be obtained from these circles in the same manner as outlined above. Flight test values of

$$\frac{\dot{\theta}}{|\bar{\delta}|}\left(\frac{-Z_w}{\sqrt{\omega^2+Z_w^2}}\right) \quad \text{and} \quad \frac{\dot{\theta}}{|\bar{C_h}|}\left(\frac{-Z_w}{\sqrt{\omega^2+Z_w^2}}\right)$$

are plotted as circles in Figs. 6 through 16.

The values of b' and k', or the stick free equivalent damping coefficient and spring constant may be determined from the $\dot{n}/|\bar{C_h}|$ and $\frac{\dot{\theta}}{|\bar{C_h}|}\left(\frac{-Z_w}{\sqrt{\omega^2+Z_w^2}}\right)$ circles in the same manner as has been explained above.

The value of Z_w may be obtained by dividing $\frac{\bar{n}}{|\bar{\delta}|}$ by $\frac{\bar{\theta}}{|\bar{\delta}|}$ since it can be shown that

$$Z_w = -\frac{|\bar{n}|}{|\bar{\theta}|}\,\omega\sqrt{\frac{1}{U^2-\left(\frac{|\bar{n}|}{|\bar{\theta}|}\right)^2}} \qquad (44)$$

The diameter of either the $\frac{\dot{n}}{|\bar{\delta}|}$ or $\frac{\dot{\theta}}{|\bar{\delta}|}\cos\left(\tan\frac{\omega}{-Z_w}\right)$ circles will now give the value of M_δ since Z_w and b are known.

The theoretical circle shown in Fig. 4 lies in the first and fourth quadrants with the value of ϕ varying from +90° to -90° as the frequency goes from zero to infinity. In practice however, it will be found that while the $\frac{\dot{n}}{|\bar{\delta}|}$ and $\frac{\dot{\theta}}{|\bar{C_h}|}\cos\left(\tan^{-1}\frac{\omega}{-Z_w}\right)$ circles follow this convention, the $\frac{\dot{n}}{|\bar{C_h}|}$ and $\dot{\theta}/|\bar{\delta}|\cos\left(\tan^{-1}\frac{\omega}{-Z_w}\right)$ circles lie in the second and third quadrants. This is due only to the established sign conventions and variation of phase angles and is explained in greater detail in Appendix C.

It will be observed that the maximum diameter of the circles presented in this report do not lie on the reference axis as predicted by the theory, but make an angle with this axis. The value of this angle is different for the various circles. The reason for this tilt is not readily apparent since it does not appear to be a function of such factors as C.G. position or airspeed. If it is a function of frequency, its variation would be hard to determine since the circle diameter is always associated with essentially the same frequency for a given airplane and speed. As it appears on the circles, the tilt resembles a lagging phase angle. This suggests the possible conclusion that it represents an aerodynamic lag between δ and M_δ or that the aerodynamic forcing moment is not in phase with the elevator angle. Such phenomena have been investigated in tests on oscillating airfoils (references (8), (9), and (10).), and show that at the highest frequencies used in the dynamic stability tests, the lag between the surface deflection and aerodynamic moment is negligible compared to the observed tilt of a number of the circles.

Another possible cause of tilt could be variations of the moment of inertia during any one flight, which are a result of the ballast shift required to keep the c.g. position constant. The variation of moment of inertia during a given flight is seldom more than 5%, however. Calculations were made assuming a 10% change in moment of inertia during flight. This variation produced a diameter tilt of only 2°. Hence, this is not regarded as a primary cause of this phenomenon.

Inertia and damping effects of the elevator system are possible causes, but at the low test frequencies these effects are considered negligible, (references (6) and (11)).

A condition imposed when constructing the circles was that these circles should pass through the origin. In some cases it is evident that the best circle through the test points does not pass through the origin, and that in most cases the diameter of such a circle will be larger than that of the existing circle. This can be interpreted to mean that for any frequency there is a component of the variable possessing some magnitude and phase which when added vectorially to the theoretical value, would give the test value of the variable. Another interpretation is the possibility that a circle does not represent the configuration of test points but that they are more closely represented by a spiral. The theoretical equations for the circles can be converted to those for a spiral by assuming that any of the aerodynamic derivatives were complex, which of course lends strenth to the supposition that some of those derivatives may be functions of frequency.

Sufficient data is not yet available to establish the validity of the several reasons discussed for tilting of the circles. This is a problem which demands solution however because of its many important implications.

It should be pointed out that once the circles have been constructed, the diameter is used as the reference in determining values of k, k^1 , b, and b^1, rather than the reference axis used in constructing the circle.

It is evident that the circle diagram is a simple means of presenting the experimental data, and that much useful information may be obtained from it with a minimum of computation. It also, serves as a logical means of obtaining the average or faired values of test data, since in practice, the best circle is usually faired through the test points and the origin. Deviations from circularity give an immediate indication of discrepancies and errors or non-conformity of the airplane motion to the simple modes predicted by the theory.

DISCUSSION OF OSCILLATION DATA

The basic sinusoidal oscillation response data are presented as functions of the angular frequency of oscillation. These data are the ratios of steady-state response amplitudes to amplitudes of elevator deflection and phase angles between the responses and elevator position, and are plotted in Figs. 5a through 5k. The data were taken during flight at equivalent air speeds of 135, 175, and 200 mph, at a pressure altitude of 10,000 feet, and with center of gravity positions of 22, 24, 26, 28, 30 and 32 per cent mean aerodynamic chord.

The quantities recorded were the forced incremental elevator position, and the responses of the incremental normal acceleration at the center of gravity of the airplane, the incremental pitch angle, the incremental elevator hinge moment, the incremental horizontal tail load, and the incremental longitudinal acceleration.

In general the responses plotted into smooth curves with a small degree of scatter of the individual points. In some instances the scatter was greater, principally dus to the greater difficulty of reducing the data when the responses were small, or due to disturbances in the air.

Following the methods outlined, previously, circle diagrams were constructed of the normal acceleration and pitch responses (Figs. 6a through 16d) both with reference to elevator position and with reference to elevator hinge moment coefficient. In order to convert the responses to the form required for plotting as circle diagrams, it was necessary to differentiate them with respect to time. Since the variations are sinusoidal, this process is performed by multiplying the amplitude by the circular frequency ω, and by adding ninety degrees to the phase angle, i.e. $\frac{n}{|\delta|} = \omega \frac{n}{|\delta|}$, and $\phi_{n_\delta} = \phi_{n_\delta} + 90°$.

Values of the stability parameters, b, k, b' and k' are obtained from the individual circle diagrams as described in the preceding section and in Appendix C. In order to place these values on a comparable basis, they must be corrected to some standard value of the moment of inertia, since the moment of inertia about the lateral axis varied appreciably during these tests with shifts of center of gravity location. The mean moment of inertia for each flight condition is listed in Table IV. These values of I_y were obtained by adding the calculated effects of changes of load distribution to an estimated inertia in the basic loading condition. Since it was necessary to estimate the basic moment of inertia, the accuracy of the corrections to k, k', b and b' depends somewhat upon the accuracy of this estimate. Practical methods for obtaining the moments of inertia of large airplanes experimentally are now being investigated.

The corrected values of k, k', b, and b' are plotted against c.g. position at a constant speed (see Fig. 17). The results obtained from the normal acceleration responses and from the pitching velocity responses are in substantial agreement. Table IV shows the values of k, b, k' and b' as obtained from the circles and also corrected to a standard I_y. Both k and

k' decrease with a rearward shift of the c.g. position, denoting a decrease in dynamic stability with decreasing longitudinal static stability (M_w). The equivalent stiffness constant k is always greater than k', which means that, for the B-25J, the fixed-control stability is greater than the free control stability at all c.g. positions. Both b and b' remain practically constant as the c.g. position is altered, with b slightly larger than b' (signifying higher damping with fixed control than with free control for the B-25J). These trends are as predicted from the theory, as may be seen in Fig. 18 on which the theoretical values of these stability parameters are included.

The natural short period is given by $2\pi/\sqrt{K-(\frac{b}{2})^2}$ and critical damping of the motion (the damping at which the short period response of an airplane ceases to be oscillatory) occurs if $b = 2\sqrt{K}$. For the B-25J, $b/b_{critical}$ is equal to 0.54 at the 22% c.g. position and is equal to 0.99 at 32% c.g. position, thus indicating that, for c.g. positions aft of 32%, the short period longitudinal motion of the airplane is no longer oscillatory in nature. (See Fig. 19).

The data have been further reduced to obtain the aerodynamic derivatives which go to make up the forcing functions and the equivalent stiffness and damping constants of the differential equations of airplane response. Using the methods outlined in Appendix D, the derivatives determined were Z_w, M_δ, C_{h_δ}, C_{h_α}, $d\epsilon/d\alpha$, M_q, and $M_{\dot{w}}$. Table V shows a comparison of the experimentally determined values with those predicted from wind tunnel tests, physical dimensions, and other available data.

Fig. 20 is a plot of the apparent value of the stability derivative Z_w at several center of gravity positions as a function of the frequency of oscillation. The values of Z_w shown were obtained from the ratio of the experimental amplitudes of normal acceleration and pitch angle. It will be noted that the values of Z_w show a somewhat random scatter with center of gravity position, but that all of the curves show an increasing value of Z_w with increasing frequency. The value of Z_w should be independent of center of gravity position, and the scatter noted may be indicative of experimental error. No satisfactory explanation for the increase of the value of Z_w with increasing frequency has been advanced, and this trend is contrary to the theoretical effect of oscillations on Z_w in the range of frequencies under consideration. The ratio of the magnitude of Z_w of a wing during oscillation to the magnitude of Z_w in the static condition calculated in accordance with oscillating airfoil theory is shown on Fig. 21 for several aspect ratios. It will be noted that, for the usual range of aspect ratios, the variation of the estimated magnitude of Z_w is very small, but shows a tendency to decrease slightly with increasing frequency. The calculated phase angle between Z_w and w is shown on Fig. 21 for several aspect ratios. While the lag shown is small at small frequencies, it begins to become appreciable at the higher frequencies. A more complete treatment of the effect of sinusoidal oscillations on the aerodynamic characteristics of a wing alone is contained in Appendix E.

It is possible that the variation of Z_w shown on Fig. 20 may be due to the method of solution, which is based on differential equations, the constancy of the coefficients of which depend upon the assumption that the aerodynamic characteristics of the airplane are independent of frequency.

If this condition is not met, the solutions contained in Appendix A must be considered to be approximations, the accuracy of which depend upon the amount that the aerodynamic coefficients are influenced by the frequency of oscillation. It may be possible that the apparent variation of Z_w shown on Fig. 20 is caused by the combination of variation of all of the aerodynamic derivatives with frequency and the method of evaluation of Z_w. Further consideration must be given to this problem.

As a further comparison with the predicted values, Figs. 22a, 22b, 23a and 23B show the experimental and calculated response curves at 30% c.g. and speeds of 135, 175, and 200 mph EAS. The responses plotted are $\bar{n}/\delta$, $\bar{n}_{z_1}$, ϕ_{θ_δ}, and ϕ_{n_δ}. The trends are as predicted, and there is, in general, fair agreement between the calculated and experimental responses.

A comparison has been made between the calculated and measured horizontal tail load characteristics. The amplitude of the tail load coefficient per degree of elevator deflection and the phase of the tail load with respect to the elevator deflection is given in Figs. 24a and 24b, where these data are given for three different center of gravity positions of the airplane. The calculated load characteristics were obtained by the method for predicting tail loads which has been developed in Appendix A. The aerodynamic characteristics used for these calculations were obtained from estimates and from the results of wind tunnel tests of a model of the B-25 airplane. It will be observed that, while the trends of the experimental data are in general similar to those of the calculated tail loads, the quantitative agreement is not good. Since it has been found that the stability derivatives obtained from the response data by the method described in Appendix D differ somewhat from the wind tunnel and estimated values, the differences between the estimated and observed values of the tail load characteristics may be due to these variations of aerodynamic characteristics. Some analysis of the tail loads using aerodynamic data obtained from the oscillation responses indicated better agreement between the calculated and observed tail loads. However, since such parameters as M_w and the variation of the normal force coefficient of the horizontal tail with angle of attack cannot be determined from the oscillation data, a complete analysis of the tail loads based on aerodynamic characteristics obtained from flight measurements has not been made. Since the method of calculating the tail load during a sinusoidal oscillation given in Appendix A corresponds to a special case of the general method for determining the horizontal tail load during maneuvers (an example of which is contained in reference (12)), the comparison of calculated and experimental results given in Figs. 24a and 24b indicates that further consideration should probably be given to the problem of determining the horizontal tail load during maneuvers. A more extensive flight program to determine the correlation between calculated and actual tail loads during dynamic maneuvers of an airplane would be desirable, and should furnish valuable information concerning the adequacy of existing methods for predicting horizontal tail loads for structural design.

A comparison of the phase and amplitude of the elevator hinge moment coefficient per degree of elevator deflection as calculated and as determined from the flight test data may be found on Figs. 25a and 25b, where these quantities are shown as a function of the frequency of oscillation at three

center of gravity positions. The values of C_{h_δ} and C_{h_α} used in the calculations were obtained from reference (13), and are given in Table II. As in the case of the tail load coefficient, it will be observed that the agreement between the calculated and experimental hinge moment characteristics, while not exact, is qualitatively good. The calculated 180° phase angle at the 32% MAC c.g. position indicates free control instability in steady flight. It will be observed that the experimental variation of phase angle as a function of frequency shows no tendency to return toward zero phase angle at zero frequency (which is necessary for free control stability in steady flight).

DISCUSSION OF STEP FUNCTION THEORY

As has been discussed in a previous section of this report, the responses of the airplane following deflection of the elevator are given by,

$$\ddot{n} + b\dot{n} + kn = UM_\delta Z_\omega \delta \tag{45}$$

and

$$\ddot{q} + b\dot{q} + kq = M_\delta(\dot{\delta} - Z_\omega \delta) \tag{46}$$

where δ represents the incremental deflection of the elevator from its position in steady rectilinear flight, and in the general case is an arbitrary function of time.

If the elevator is deflected suddenly to a new and constant position, and this incremental step deflection is denoted by the symbol δ_1, the responses of the airplane may be shown to be of the following form for various relationships of b and k. Similar equations for changes of airplane angle of attack and the angle of attack of the horizontal tail may be found in reference (12). More detailed derivatives of the response equations given below are contained in Appendix B.

$b^2 < 4k$ (Oscillatory Motion)

$$\frac{n}{\delta_1} = \frac{UM_\delta Z_\omega}{k}\left[1 - e^{-\frac{b}{2}t}\sqrt{\frac{4k}{4k-b^2}}\sin\left(\frac{\sqrt{4k-b^2}}{2}t + \tan^{-1}\frac{\sqrt{4k-b^2}}{b}\right)\right] \tag{47}$$

$$\frac{q}{\delta_1} = -\frac{M_\delta Z_\omega}{k}\left[1 - e^{\frac{b}{2}t}\sqrt{\frac{\left(b+\frac{2k}{Z_\omega}\right)^2}{4k-b^2}}\sin\left(\frac{\sqrt{4k-b^2}}{2}t + \tan^{-1}\frac{\sqrt{4k-b^2}}{b+\frac{2k}{Z_\omega}}\right)\right] \tag{48}$$

$b^2 = 4k$ (Critical Damping)

$$\frac{n}{\delta_1} = \frac{UM_\delta Z_\omega}{k}\left[1 - e^{-\frac{b}{2}t}\left(1 + \frac{b}{2}t\right)\right] \tag{49}$$

$$\frac{q}{\delta_1} = \frac{-M_\delta Z_\omega}{k}\left[1 - e^{-\frac{b}{2}t}\left(1 + \left(\frac{b}{2} + \frac{k}{Z_\omega}\right)t\right)\right] \tag{50}$$

$b > 4k$. (Over Damped Motion)

$$\frac{n}{\delta_1} = \frac{U M_\delta Z_\omega}{k}\left[1 - e^{-\frac{b}{2}t}\sqrt{\frac{4k}{b^2-4k}}\sinh\left(\frac{\sqrt{b^2-4k}}{2}t + \tanh^{-1}\frac{\sqrt{b^2-4k}}{b}\right)\right] \qquad (51)$$

$$\frac{q}{\delta_1} = \frac{-M_\delta Z_\omega}{k}\left[1 - e^{-\frac{b}{2}t}\sqrt{\frac{\left(b+\frac{2k}{Z_\omega}\right)^2}{b^2-4k}}\sinh\left(\frac{\sqrt{b^2-4k}}{2}t + \tanh^{-1}\frac{\sqrt{b^2-4k}}{b+\frac{2k}{Z_\omega}}\right)\right] \qquad (52)$$

Included among the assumptions necessary for the development of the above equations are that (1) the speed remains constant; (2) the deviation of the position of the airplane longitudinal stability axis from the horizontal remains small; (3) the development of airplane pitching moment due to the instantaneous elevator deflection is also instantaneous.

The errors due to the first two assumptions will be small for a reasonable period of time provided that the elevator deflection is small. However, the elevator deflection must be sufficiently great that the responses are large enough to make possible accurate measurements. This is a problem connected with the sensitivity of the recording instrumentation.

Since it is not possible for the pitching moment due to elevator deflection to develop instantaneously, the predicted response will lead the experimental response by a small amount. It has been estimated from reference (9) that, based on the horizontal tail chord of the B-25J of 6.3 feet and a true flight speed of 300 feet per second, a time of approximately .09 seconds (4 to 4.5 chord lengths) would be required to develop the change of tail lift. As a result, the magnitude of the transient response at a given time will not be in agreement with the predicted value. The agreement between the slopes of the predicted and the experimentally determined transient responses at a given percentage of the steady state response however is not effected substantially by this condition at other than very low values of the response, and reasonable agreement may be expected until speed and attitude variations become important.

Since the terms outside of the brackets of equations (47) through (52) represent the steady state responses, the quantities within the brackets represent the ratio of the transients at any instant to the final values of the responsee. Denoting the steady state value of incremental normal acceleration corresponding to a step deflection of the elevator by the subscript "s", the theoretical value of the slope of the ratio of the normal acceleration at any instant to n_s is given by the following expressions:

For $b^2 < 4k$:

$$\left(\frac{\dot{n}}{n_s}\right) = e^{-\frac{b}{2}t}\left[\frac{2k \sin \frac{\sqrt{4k-b^2}}{2}t}{\sqrt{4k-b^2}}\right] \qquad (53)$$

For $b^2 = 4k$:

$$\left(\frac{\dot{n}}{n_s}\right) = \left(\frac{b}{2}\right)^2 e^{-\frac{b}{2}t}\,t \qquad (54)$$

$$= k e^{-\frac{b}{2}t}\,t \qquad (54a.)$$

For $b^2 > 4k$:

$$\left(\frac{\dot{n}}{n_s}\right) = e^{-b/2t}\left[\frac{2k \sinh \frac{\sqrt{b^2-4k}}{2}t}{\sqrt{b^2-4k}}\right] \qquad (55)$$

Similar relationships may be obtained for the rate of change of pitching velocity.

The theoretical values of the time, t, at any desired value of the ratio n/n_s may be determined for a series of values of b and k from equations (47), (49), or (51). These values of the time are substituted in equations (53), (54), or (55) to obtain the corresponding slopes. A general curve of the slope of the transient at a given response ratio may then be plotted as a function of b and k. An example of such a curve is given as Fig. 27, where the value of n/n_s has been plotted as a function of b and k when $n/n_s = 0.50$. Similar curves may be constructed for other values of the response ratio but the selection of these ratios should be restricted to values at which the comparison between theory and experiment may be expected to be valid.

Although it is theoretically possible to determine the values of b and k for an airplane which is less than critically damped by determining the decay and period of the oscillations following the application of the step forcing function, this method is not practical unless the damping of the system is light since otherwise the decay of the oscillation is very rapid and the period of the motion is extremely difficult to observe. It will be found in general that the damping of an airplane is too great to permit the determination of b and k from the measured decay and period of the oscillatory response to a step function. From equations (47) through (52) it may be seen that the steady state response of either n or q involves M_q, Z_w, k, $M_{\dot{w}}$ and (in the case of n) V. Therefore, if the aerodynamic derivatives $M_{\dot{w}}$ and Z_w

are known or may be evaluated by other experimental techniques, the value of k may be determined from the steady state response. The value of b corresponding to this value of k and the observed value of the slope of the transient at $n/n_s = 0.50$ may then be read directly from Fig. 27.

Other methods based on the LaPlace transform or Carson's integral are available for determining the stability constants b and k from step responses. However, these methods also require that the aerodynamic derivatives M_δ and Z_w be known, and so do not appear to offer advantages over the method outlined above.

It thus appears that, unless auxiliary tests are made, the step response does not permit evaluation of b and k of an airplane due to the high damping ratio which usually exists. In any event, it is not possible to extract the wealth of information from the step response which may be obtained from the oscillation data. Furthermore, due to the abruptness of the maneuver, the assumption that the aerodynamic forces and moments are in phase with the velocites which produce them is questionable during the early portion of the maneuver.

Although it appears doubtful that the response to a step elevator deflection above may be analyzed in terms of stability coefficients, these data may be useful for determining the motion of the airplane corresponding to an arbitrary movement of the elevator. If the response to a step deflection of the elevator is known, the motion of the airplane may be caloulated by the Duhamel integral. The use of this integral is described in Appendix B, where the use of a graphical method which employs a template of the time history of the response is explained. This template may be constructed according to the experimentally determined data.

DISCUSSION OF STEP FUNCTION DATA

The incremental change of normal acceleration following a step deflection of the elevator has been determined during flight tests at c.g. positions of 23.9%, 24.1%, 28.0%, and 30.0% MAC. The tests were made at an equivalent airspeed of 175 MPH and at a pressure altitude of 10,000 feet. The observed response ratios, n/n_δ, and the steady state responses are shown on Figs. 26a through 26d. The calculated response ratios are also included on these figures. The time lag required to develop the pitching moment following an abrupt elevator deflection is clearly evident from these figures. However, after a brief initial period, the shapes of the experimental response ratio curves agree closely with those of the theoretical curves until speed and attitude changes commence to become important. The theoretical response ratios are based on values of b and k which were determined by the oscillation technique, and were taken from Fig. 17.

The values of k and b were determined from the step data of Figs. 26a through 26d from the steady state value of the response and the slope of the transient response ratio curve at $n/n_\delta = 0.50$ as described under the discussion of the step function given in the preceding section. The values of M_δ and Z_w used in this analysis were obtained from the oscillation tests, and these values are shown in Table V. Values of b and k obtained from the step data and the estimated value of I_y for each step are given in Table VI. The values of k and b corrected to a common I_y of 60,000 slug feet^2 are also included in Table VI.

Fig. 28 shows a comparison of k and b obtained from the step data (using values of M_δ and Z_w from the oscillation tests) and k and b obtained from the oscillation data. The agreement between the results obtained by the two methods is quite good. However it must be remembered that it is not possible to analyze the step data in terms of k and b unless values of M_δ and Z_w are obtained from oscillation tests or by other means.

The agreement obtained does illustrate that, with the exception of the initial portion of the motion, the assumption of velocity derivatives (stability derivatives which do not depend upon the past history of the motion of the airplane) is as valid for estimating the response to a step deflection of the elevator as for estimating the steady state response to a sinusoidal forcing function.

CONCLUSIONS:

From the results of the flight tests which have been conducted, the following conclusions have been reached.

1. The change of flight velocity of the airplane was found to be negligible during sinusoidal oscillations over the range of frequencies at which the tests were conducted. (0.10 to 1.30 cycles per second). This result confirms theory, and permits treatment of the airplane as a two degree of freedom system.

2. The experimentally determined data plot well to form a circle diagram over a considerable range of frequencies of oscillation. Since this is characteristic of a linear second order differential equation with constant coefficients, it furnishes further evidence that the airplane may be treated as a two degree of freedom system, and that the variation of the aerodynamic stability coefficients or derivatives with frequency is minor over the range of frequencies which is of usual interest.

3. An apparent lag between the deflection of the elevator and the response of the airplane was observed from the circle diagrams, which in general had their diameters rotated in the lagging direction. This lag was in addition to the phase angle which would be calculated between the airplane response and the elevator angle at a given frequency. A satisfactory explanation of this characteristic has not been obtained at the present time.

4. The measured values of the stability coefficients b, k, b' and k' are in general agreement with calculated values based on aerodynamic data obtained from estimates and wind tunnel tests. The experimental values of k and k' are consistently greater than the theoretical values at all center of gravity positions at which the tests of the B-25J were conducted. The experimental values of b and b' were slightly greater than the theoretical values over the same range of center of gravity positions.

5. The agreement between values of b, k, b' and k' as obtained from normal acceleration response data and pitching velocity response data was found to be very good.

6. Values of the airplane stability derivatives calculated from the measured airplane response characteristics in general agree reasonably well with values taken from wind tunnel tests of the B-25 airplane and with estimates.

7. The apparent value of the stability derivative Z_w as determined from the ratio of the amplitudes of the responses of n and θ was higher than the value estimated from wind tunnel tests of the B-25 airplane, and increased as the frequency of the oscillation was increased. The variation of Z_w with frequency is opposite to that which would be expected from the theory of an oscillating airfoil. While no satisfactory explanation for

this trend is available at the present time, it may be possible that other stability characteristics than Z_w vary with frequency in such a manner that, when the apparent value of Z_w is calculated from the amplitude ratio mentioned above, the observed trend with frequency results.

8. The phase and amplitude of the variation of horizontal tail load coefficient variation during sinusoidal oscillations at various frequencies was in qualitative agreement with calculations, but the quantitative agreement was not particularly good. This is of interest since the method for calculating the tail loads was basically similar to general methods for predicting tail loads during maneuvers. Further investigation of this phase would be valuable for furnishing a check of structural load analysis methods.

9. The comparison between calculated and experimentally determined values of elevator hinge moment during sinusoidal oscillations was similar to that of the tail load coefficient variation in that, while the qualitative agreement was good, the quantitative agreement was only fair.

10. A time lag between the response of the airplane and the deflection of the elevator was observed following step deflections of the elevator. It is believed that this was due primarily to the time required for the lift due to elevator deflection to develop on the horizontal tail. The variation of normal acceleration in a step function maneuver agreed with the calculated variation once the initial time lag was exceeded.

11. The experimentally determined step function response may be used in conjunction with the Duhamel integral to obtain the response to an arbitrary movement of the elevator.

12. No method has been found at the present time for obtaining the values of the stability coefficients b and k from the step responses without the use of aerodynamic data obtained from other sources.

13. Using the portion of the step response following the initial time lag, and using values of the aerodynamic derivatives taken from the oscillation tests, the values of b and k obtained from the step responses agree very well with the values of these coefficients obtained from the oscillation tests.

14. The forced oscillation method is of considerable utility for determining the response characteristics of an airplane for use in the design of automatic pilots, and furnishes a method for measuring the stability characteristics of airplanes or other devices for which reliable stability parameters may not be available or cannot be obtained conveniently by theoretical analysis or wind tunnel testing.

APPENDIX A.

STEADY MOTION OF AN AIRPLANE DURING A SINUSOIDAL OSCILLATION OF THE ELEVATOR.

Introduction

A simplified treatment of the response in a vertical plane ("longitudinal motion") of an airplane due to movement of the elevators has been presented by E. V. Laitone in reference (13). This theory assumes that changes of the velocity along the flight path may be neglected during the period of the response of the airplane to the given control motion, thus reducing the motion to one of two degrees of freedom. (Pitching velocity and translational velocity along an axis fixed in the airplane and perpendicular to the flight path in steady flight.) The validity of this assumption has been verified by calculations made by classical methods in which speed variations have been considered, and have been found to be small, and by actual measured speed changes during sinusoidal oscillations in flight.

The same assumption is contained in references (12) and (15), which also treat the problem of the longitudinal motion of an airplane following movement of the elevators. Based on the simplification of constant speed, it has been shown that the response of the airplane in each of the two remaining degrees of freedom may be presented in a form analogous to the solution for the motion of a spring restrained mass having viscous damping. It is the purpose of this appendix to present the theory of response to a sinusoidal elevator motion in more detailed form than the presentation of reference (14), and to amplify this theory to include the response of the airplane to a sinusoidal variation of elevator hinge moment, and the variation of horizontal tail load and elevator hinge moment during sinusoidal oscillations.

Axes

Standard NACA stability axes are used throughout. These axes are fixed in the airplane with the origin at the airplane center of gravity, and are so oriented that the positive x axis is directed forward and parallel to the flight path in undisturbed flight. The positive y axis is perpendicular to the x axis and parallel to the plane of the wing (positive to starboard), and the positive z axis is perpendicular to the xy plane and is directed downward. The orientation of these axes with respect to airplane body axes varies with the initial angle of attack of the airplane in undisturbed flight, but these two systems of axes remain in a fixed relationship with respect to each other during a given oscillation or maneuver.

Symbols

A definition of the quantities which influence the longitudinal motion of the airplane is given below. A number of these quantities have a negligible effect on the motion of the airplane, but are included to give a complete picture of the variables which enter into the problem in the general case. With the exception of the pitching moment due to the time lag of downwash at the horizontal tail during maneuvers involving changes of angle of attack, all of the aerodynamic forces and moments are based on the conventional velocity derivatives which have been used for airplane stability analysis in the past. (See reference (16)).

U - Initial velocity along the x axis in undisturbed flight. Positive forward. ft./sec.

W - Initial velocity along the z axis in undisturbed flight. (Made zero by choice of axis orientation.)

u - Incremental velocity along the x axis of the airplane. Positive forward. ft./sec.

w - Incremental velocity along the z axis of the airplane. Positive downward. ft/sec.

θ - Pitch angle between the airplane x axis and the horizontal. Positive for nose-up displacements. Radians.

$q = \dot{\theta}$ - Pitching velocity about the y axis of the airplane. Positive for nose-up rates. Radians/sec.

M - Mass of airplane. Slugs.

I_y - Moment of inertia of airplane about the y axis. Slug $ft.^2$

n - Incremental total acceleration along the airplane z axis. Positive downward. $ft./sec.^2$

N_t - Incremental horizontal tail load from initial conditions. Considered positive upward. Pounds.

S_t - Area of horizontal tail. $ft.^2$

ℓ_t - Tail length. Distance from airplane center of gravity to the center of pressure of the tail. Considered positive. ft.

$C_{N_t} = \frac{N_t}{\frac{\rho}{2} U^2 S_t}$ - Incremental horizontal tail load coefficient.

HME - Incremental hinge moment of the elevator. Positive when it tends to deflect the trailing edge of the elevator downward. ft. lbs.

$C_e S_e$ - Product of the mean geometric chord aft of the hinge line and the area aft of the hinge line of the elevator. $ft.^3$

C_h - $\frac{HME}{\frac{\rho}{2} U^2 c_e S_e}$ Incremental elevator hinge moment coefficient. Positive when it tends to deflect the trailing edge downward.

$C_{h_\delta} = \frac{\partial C_h}{\partial \delta}$ - Rate of change of elevator hinge moment coefficient with elevator angle.

$C_{h_\alpha} = \frac{\partial C_h}{\partial \alpha_t}$ - Rate of change of elevator hinge moment coefficient with tail angle of attack.

a_t - Rate of change of tail normal force coefficient with respect to tail angle of attack. 1/radian.

$\lambda = -\left.\frac{\partial \alpha_t}{\partial \delta}\right)_{C_{N_t}}$ Effective change of angle of attack of the horizontal tail per unit elevator deflection.

X - Force along the airplane x axis. Positive forward. Pounds.

Z - Force along the airplane z axis. Positive downward. Pounds.

M - Pitching moment about airplane y axis. Positive for nose-up. ft. lbs.

δ - Indremental elevator deflection from initial position in undisturbed flight. Positive trailing edge downward. Radians.

α_t - Incremental change of tail angle of attack. Positive if it tends to produce a positive change in tail load coefficient.

$X_u = \frac{\partial X}{\partial u} \times \frac{1}{m}$ 1/sec.

$X_w = \frac{\partial X}{\partial w} \times \frac{1}{m}$ 1/sec.

$X_q = \frac{\partial X}{\partial q} \times \frac{1}{m}$ ft./sec.

$X_\delta = \frac{\partial X}{\partial \delta} \times \frac{1}{m}$ $ft./sec.^2$

$Z_u = \frac{\partial Z}{\partial u} \times \frac{1}{m}$ 1/sec.

$Z_w = \frac{\partial Z}{\partial w} \times \frac{1}{m}$ 1/sec.

$Z_q = \frac{\partial Z}{\partial q} \times \frac{1}{m}$ ft./sec.

$Z_\delta = \frac{\partial Z}{\partial \delta} \times \frac{1}{m}$ $ft./sec.^2$

$M_u = \frac{\partial M}{\partial u} \times \frac{1}{I_y}$ 1/ft. sec.

$M_w = \frac{\partial M}{\partial w} \times \frac{1}{I_y}$ 1/ft. sec.

$M_{\dot{w}} = \frac{\partial M}{\partial \dot{w}} \times \frac{1}{I_y}$ 1/ft.

$M_q = \frac{\partial M}{\partial q} \times \frac{1}{I_y}$ 1/sec.

$M_\delta = \frac{\partial M}{\partial \delta} \times \frac{1}{I_y}$ 1/sec.^{2}

A bar placed over a variable indicates the maximum value of that variable during an oscillation. The amplitude may be either positive or negative. i.e. $\bar{n}$ is the maximum amplitude of normal acceleration during an oscillation, and may be either positive or negative.

Vertical bars placed around a variable indicate the positive value of that variable. i.e., $|n|$ is the positive value of normal acceleration at a given instant. $|\bar{n}|$ is the positive maximum amplitude of normal acceleration during an oscillation.

Equations of Motion in the Plane of Symmetry

The equations of the motion of an airplane in the plane of symmetry are written below based upon the following assumptions:

(1) The reference axes are fixed in the airplane as has been described above in the section defining axes.
(2) The airplane is initially in horizontal flight.
(3) All disturbances are sufficiently small that angles may be considered equal to their tangents.
(4) All aerodynamic moments and forces (with the exception of the moment due to lag of downwash at the horizontal tail) are considered to vary directly with linear or angular velocities, and are therefore not dependent upon the past history of the airplane motion or on the linear or angular accelerations which exist at that moment.
(5) It is assumed that small lateral disturbances which may exist do not affect the aerodynamic forces or pitching moments in the plane of symmetry.
(6) Second order inertia terms resulting from the product of two infinitesimal velocities are neglected.

As described in reference (16), the equations of longitudinal motion may then be written:

$$(\dot{u} + g\theta) = X_u u + X_w w + X_q q + X_\delta \delta \qquad \text{(Eq. 1)}$$

$$(\dot{w} - Uq) = Z_u u + Z_w w + Z_q q + Z_\delta \delta \qquad \text{(Eq. 2)}$$

$$\dot{q} = M_u u + M_{\dot{w}} \dot{w} + M_q q + M_\delta \delta \qquad \text{(Eq. 3)}$$

The following simplifications may be made to equations 1, 2, and 3:

(1) As has been discussed previously, the variation of velocity along the x axis may be considered to be zero. Therefore equation 1 may be omitted, and u may be considered to be zero in equations 2 and 3.

(2) Z_q and Z_δ are small for conventional airplanes, and usually may be omitted without introduction of appreciable error.

Based upon these simplifications, equations 1, 2 and 3 may be rewritten as follows:

$$(\dot{w} - Uq) = Z_w w \qquad \text{(Eq. 4)}$$

$$\dot{q} = M_w w + M_{\dot{w}} \dot{w} + M_q q + M_\delta \delta \qquad \text{(Eq. 5)}$$

Solution of Equations of Motion:

Equations 4 and 5 are written in operational form (where $D = \frac{d}{dt}$)

$$(Dw - Uq) = Z_w w \qquad \text{(Eq. 6)}$$

$$Dq = (M_w + DM_{\dot{w}}) w + M_q q + M_\delta \delta \qquad \text{(Eq. 7)}$$

Equations 6 and 7 may be solved simultaneously by the usual methods to obtain w and q as functions of time. However, a more physically significant solution may be made if these equations are written in terms of the variables w and q, and these variables are then separated so that two second order differential equations are in a single variable. This separation of variables is now illustrated.

Equations 6 and 7 may be rearranged in the following manner:

$$(D - Z_w) w - Uq = 0 \qquad \text{(Eq. 6')}$$

$$-(DM_{\dot{w}} + M_w) w + (D - M_q) q = M_\delta \delta \qquad \text{(Eq. 7')}$$

To eliminate the pitching velocity, q, the usual algebraic operations are performed on equations 6' and 7'.

$$\frac{D - Z_w}{U} w - q = 0 \qquad \text{(Eq. 8)}$$

$$-\frac{D M_{\dot{w}} + M_w}{D - M_q} w + q = \frac{M_\delta \delta}{D - M_q} \qquad \text{(Eq. 9)}$$

Adding equations 8 and 9

$$\left(\frac{D - Z_w}{U} - \frac{D M_{\dot{w}} + M_w}{D - M_q}\right) w = \frac{M_\delta \delta}{D - M_q} \qquad \text{(Eq. 10)}$$

or

$$\left[(D - Z_w)(D - M_q) - U(D M_{\dot{w}} + M_w)\right] w = U M_\delta \delta \qquad \text{(Eq. 11)}$$

$$\left[D^2 - D Z_w - D M_q + Z_w M_q - D U M_{\dot{w}} - U M_w\right] w = U M_\delta \delta \qquad \text{(Eq. 12)}$$

Collecting terms,

$$\left[D^2 - D(Z_w + M_q + U M_{\dot{w}}) + (Z_w M_q - U M_w)\right] w = U M_\delta \delta \qquad \text{(Eq. 13)}$$

Now let $b = -(Z_w + M_q + U M_{\dot{w}})$ (Eq. 14)

$$k = (Z_w M_q - U M_w) \qquad \text{(Eq. 15)}$$

Then $\ddot{w} + b\dot{w} + kw = U M_\delta \delta$ (Eq. 16)

Since it is difficult to determine the translational velocity w along the z axis experimentally, but since the total acceleration n along the z axis may be determined quite simply, it is convenient to write equation 16 in terms of n rather than w.

By definition, $n = (\dot{w} - U q)$

and, from equation 4,

$$(\dot{w} - U q) = Z_w w$$

Therefore, $n = Z_w w$ (Eq. 17)

This result is to be expected, since w is proportional to the additional angle of attack required to develop the additional lift on the airplane which balances the inertia force due to the additional acceleration n.

Equation 16 may then be rewritten

$$\ddot{n} + b\dot{n} + k n = U M_\delta Z_w \delta \qquad \text{(Eq. 16')}$$

An equation for the pitching velocity may now be developed by similar algebraic operation on equations 6' and 7'.

$$w - \left(\frac{U}{D - Z_w}\right) q = 0 \qquad \text{(Eq. 18)}$$

$$-w + \left(\frac{D - M_q}{DM_{\dot{w}} + M_w}\right) q = \frac{M_\delta \delta}{DM_{\dot{w}} + M_w} \qquad \text{(Eq. 19)}$$

$$\left[-\left(\frac{U}{D - Z_w}\right) + \left(\frac{D - M_q}{DM_{\dot{w}} + M_w}\right)\right] q = \frac{M_\delta \delta}{DM_{\dot{w}} + M_w} \qquad \text{(Eq. 20)}$$

$$\left[(D - M_q)(D - Z_w) - U(DM_{\dot{w}} + M_w)\right] q = M_\delta \delta (D - Z_w) \qquad \text{(Eq. 21)}$$

$$\left[D^2 - DZ_w - DM_q + Z_w M_q - DUM_{\dot{w}} + UM_w\right] q = M_\delta \delta (D - Z_w) \qquad \text{(Eq. 22)}$$

$$\left[D^2 - D(Z_w + M_q + UM_{\dot{w}}) + (Z_w M_q - UM_w)\right] q = M_\delta \delta (D - Z_w) \qquad \text{(Eq. 23)}$$

$$\text{or} \quad \ddot{q} + b\dot{q} + kq = M_\delta (\dot{\delta} - Z_w \delta) \qquad \text{(Eq. 24)}$$

where b and k are defined by equations 14 and 15.

It has now been shown that, subject to the basic assumptions made in writing equations 1 through 5, the longitudinal motion of the airplane may be represented by two independent linear second order differential equations with constant coefficients which are summarized here as

$$\ddot{n} + b\dot{n} + kn = U M_\delta Z_w \delta \qquad \text{(Eq. 16')}$$

$$\ddot{q} + b\dot{q} + kq = M_\delta (\dot{\delta} - Z_w \delta) \qquad \text{(Eq. 24)}$$

where $b = -(Z_w + M_q + UM_{\dot{w}})$ (Eq. 14)

$k = (Z_w M_q - U M_w)$ (Eq. 15)

and $\delta = f(t)$

These equations are identical to those of the forced motion of a spring restrained mass with viscous damping (a conclusion which was also stated in reference (12)). The coefficient k is analogous to the spring deflection rate, and b is analogous to the viscous damping coefficient. Analogy may also be drawn to an electrical circuit containing inductance, resistance, and capacitance.

The form of equations 16' and 24 suggests that the coefficients of the equations may be determined by applying special types of forcing functions and observing the response of the airplane, a technique which has been employed in other forms of dynamic measurement and analysis for many years. The response of the airplane to a sinusoidal application of the forcing function (sinusoidal oscillation of the elevator) is next considered. The response of the airplane to a sudden (step) application of the forcing function is considered in appendix B. A method of analysis of the response data obtained during steady sinusoidal oscillations at various frequencies to obtain b and k, the coefficients of the equations of motion, is contained in appendix C, and a method of analysis to obtain the aerodynamic derivatives from these coefficients and other auxiliary data is contained in appendix D.

Steady State Motion of the Airplane Resulting From A Sinusoidal Oscillation of the Elevator.

Consider the special case in which the elevator is oscillated sinusoidally at a constant frequency and maximum amplitude. The elevator angle at any particular instant may then be written

$$\delta = |\bar{\delta}| \sin \omega t$$

where $|\bar{\delta}|$ is the positive maximum deflection of the elevator and ω is its circular frequency in radians per second.

To find the variation of the total incremental acceleration along the z axis at the airplane center of gravity,

$$\ddot{n}^{\circ} + b\dot{n}^{\circ} + kn = UM_{\delta} z_{w} \delta \qquad \text{(Eq. 16')}$$

$$\ddot{n}^{\circ} + b\dot{n}^{\circ} + kn = UM_{\delta} z_{w} |\bar{\delta}| \sin \omega t \qquad \text{(Eq. 25)}$$

The complete solution of equation 25 involves two additive parts--the complementary solution (obtained by placing the right hand side of the equation equal to zero) and the particular integral which is obtained by consideration of the right hand side of the equation. The complementary solution represents the transient of the motion, whereas the particular integral represents the steady state motion. Since, in this problem, we are interested in only the steady state response, the complementary solution need not be found.

The particular integral may be found most easily by operational methods.

$$\ddot{n} + b\dot{n} + Kn = U M_s Z_w |\bar{\delta}| \sin \omega t \qquad \text{(Eq. 25)}$$

Since $e^{i\omega t} = \cos \omega t + i \sin \omega t$

Then

$$(D^2 + bD + K)n = U M_s Z_w |\bar{\delta}| \, \jmath e^{i\omega t} \qquad \text{(Eq. 26)}$$

where $\jmath e^{i\omega t}$ represents the coefficient of the imaginary part of $e^{i\omega t}$

$$n = U M_s Z_w |\bar{\delta}| \frac{\jmath e^{i\omega t}}{D^2 + bD + K} \qquad \text{(Eq. 27)}$$

Now perform the operations indicated on $\jmath e^{i\omega t}$

Since $D e^{i\omega t} = (i\omega) e^{i\omega t}$

Then D may be replaced by $i\omega$

Therefore, equation 27 may be rewritten in the form

$$n = U M_s Z_w |\bar{\delta}| \frac{\jmath e^{i\omega t}}{(i\omega)^2 + b(i\omega) + K} \qquad \text{(Eq. 27')}$$

$$n = U M_s Z_w |\bar{\delta}| \frac{\jmath (\cos \omega t + i \sin \omega t)}{(K - \omega^2) + i(b\omega)} \qquad \text{(Eq. 28)}$$

Equation 28 is now rationalized.

$$n = U M_s Z_w |\bar{\delta}| \frac{\jmath (\cos \omega t + i \sin \omega t)}{(K - \omega^2) + i(b\omega)} \times \frac{(K - \omega^2) - i(b\omega)}{(K - \omega^2) - i(b\omega)} \qquad \text{(Eq. 29)}$$

$$n = U M_s Z_w |\bar{\delta}| \frac{(K - \omega^2) \sin \omega t - (b\omega) \cos \omega t}{(K - \omega^2)^2 + (b\omega)^2} \qquad \text{(Eq. 30)}$$

$$\frac{n}{|\bar{\delta}|} = \frac{U M_s Z_w}{(K - \omega^2)^2 + (b\omega)^2} \left[-(b\omega) \cos \omega t + (K - \omega^2) \sin \omega t \right] \qquad \text{(Eq. 31)}$$

Equation 31 may be simplified by use of the trigonometric identity,

$$A \cos \omega t + B \sin \omega t = \sqrt{A^2 + B^2} \sin \left(\omega t + \tan^{-1} \frac{A}{B}\right)$$

$$\frac{n}{|\bar{\delta}|} = \frac{U M_\delta Z_w}{\sqrt{(K-\omega^2)^2 + (b\omega)^2}} \sin \left[\omega t + \tan^{-1} \frac{-b\omega}{K-\omega^2}\right] \qquad \text{(Eq. 32)}$$

Equation 32 represents the steady state response of the incremental acceleration at the airplane center of gravity per unit maximum elevator deflection ((ft./sec.^{2})/rad.) as a function of the airplane stability characteristics and the circular frequency (in radians/second) of the elevator oscillation.

Equation 24 may now be solved in a similar manner to obtain the steady response of pitching velocity to the sinusoidal elevator deflection.

$$\ddot{q} + b\dot{q} + Kq = M_\delta (\dot{\delta} - Z_w \delta) \qquad \text{(Eq. 24)}$$

$$\delta = |\bar{\delta}| \sin \omega t$$

$$\dot{\delta} = \omega |\bar{\delta}| \cos \omega t$$

$$\ddot{q} + b\dot{q} + Kq = M_\delta |\bar{\delta}| (\omega \cos \omega t - Z_w \sin \omega t) \qquad \text{(Eq. 33)}$$

The steady state solution of equation 33 may be found by dividing the right hand side of the equation into two parts, solving for each part, and then adding these two separate solutions to obtain the total steady state solution. The procedure followed is exactly the same as that given above for the acceleration n, with the exception that the real part of $e^{i\omega t}$ $(\mathcal{R} e^{i\omega t})$ is considered when obtaining the solution of the term involving $\cos \omega t$.

By this method the steady state solution of equation 33 is found to be

$$\frac{q}{|\bar{\delta}|} = M_\delta \sqrt{\frac{Z_w^2 + \omega^2}{(K-\omega^2)^2 + (b\omega)^2}} \sin \left[\omega t + \tan^{-1} \frac{\omega(K-\omega^2) + Z_w b\omega}{-Z_w (K-\omega^2) + b\omega^2}\right] \qquad \text{(Eq. 34)}$$

Comparison of equations 32 and 34 shows that a simple relationship may be derived for obtaining Z_w from the ratio of the amplitudes of $\frac{n}{|\bar{\delta}|}$ and $\frac{q}{|\bar{\delta}|}$

From equation 32

$$\frac{|\bar{n}|}{|\bar{\delta}|} = \left| \frac{U M_\delta \bar{z} \omega}{\sqrt{(k-\omega^2)^2 + (b\omega)^2}} \right|$$

From equation 34

$$\frac{|\bar{q}|}{|\bar{\delta}|} = \left| M_\delta \sqrt{\frac{\bar{z}\omega^2 + \omega^2}{(k-\omega^2)^2 + (b\omega)^2}} \right|$$

Then,

$$\frac{|\bar{n}|}{|\bar{q}|} = \frac{\frac{|\bar{n}|}{|\bar{\delta}|}}{\frac{|\bar{q}|}{|\bar{\delta}|}} = \left| \frac{U}{\sqrt{1 + \left(\frac{\omega}{\bar{z}\omega}\right)^2}} \right| \qquad \text{(Eq. 35)}$$

Since the true speed and frequency of oscillation are known, the value of the derivative Z_w may be obtained from the ratio of the amplitude of the n and q responses during a steady sinusoidal oscillation.

Steady State Motion of the Airplane Resulting From A Sinusoidal Application of Elevator Hinge Moment.

If an airplane is disturbed from steady, rectilinear flight, the increment of elevator hinge moment coefficient (assuming that the trim tab position remains unchanged) will in general be a function of the change of elevator angle and tail angle of attack from their respective initial values; the aerodynamic hinge moment coefficient parameters of the elevator, C_{h_δ} and C_{h_α} ; the linear dimensions of the elevator; the equivalent airspeed; the aerodynamic hinge moment due to angular velocity of the elevator (aerodynamic damping); the total angular acceleration of the elevator and its moment of inertia; and the static mass unbalance of the elevator and the incremental normal acceleration at the horizontal tail.

An analysis of the order of magnitude of the above effects, however, shows that several of these variables may be omitted without introducing appreciable error. Thus, for small oscillations of the elevator and frequencies of oscillation in the range being considered, (ω less than 10 radians per second), the effects of the aerodynamic damping and moment of inertia of the elevator are negligible. The combination of incremental normal acceleration at the tail and elevator

mass unbalance may also usually be considered to have a negligible effect on the elevator hinge moment.

The incremental change of elevator hinge moment coefficient during a small disturbance of the airplane may then be expressed as

$$C_h = C_{h_\delta}\,\delta + C_{h_\alpha}\,\alpha_t \qquad \text{(Eq. 36)}$$

The change of tail angle of attack, α_t, is equal to the steady state change of tail angle of attack due to the velocity w, corrected for the effects of downwash lag and pitching velocity. Thus

$$\alpha_t = \left[\frac{w}{U}\left(1-\frac{d\epsilon}{d\alpha}\right) + \frac{d\epsilon}{d\alpha}\frac{\dot{w}}{U}\frac{l_t}{U} + q\frac{l_t}{U}\right] \qquad \text{(Eq. 37)}$$

Substituting equation 37 into equation 36 and solving for δ,

$$\delta = \frac{C_h - C_{h_\alpha}\left[\frac{w}{U}\left(1-\frac{d\epsilon}{d\alpha}\right) + \frac{d\epsilon}{d\alpha}\frac{\dot{w}}{U}\frac{l_t}{U} + q\frac{l_t}{U}\right]}{C_{h_\delta}} \qquad \text{(Eq. 38)}$$

From equation 6,

$$q = \frac{\dot{w} - Z_w w}{U}$$

Then

$$\delta = \frac{C_h}{C_{h_\delta}} - \frac{C_{h_\alpha}}{C_{h_\delta}}\left[\frac{1}{U}\left(1-\frac{d\epsilon}{d\alpha} - \frac{l_t}{U}Z_w\right)\right]w - \frac{C_{h_\alpha}}{C_{h_\delta}}\left[\frac{l_t}{U^2}\left(1+\frac{d\epsilon}{d\alpha}\right)\right]\dot{w} \qquad \text{(Eq. 39)}$$

Writing equation 16' (general equation for n) in terms of the basic aerodynamic derivatives,

$$\ddot{n} - (Z_w + M_q + UM_{\dot{w}})\dot{n} + (Z_w M_q - UM_w)n = UM_\delta Z_w\,\delta \qquad \text{(Eq. 16")}$$

Now, substituting equation 39 for δ in equation 16" and recognizing that $n = Z_w w$)

$$\ddot{n} - \left[Z_w + M_q + U\left(M_{\dot{w}} - M_\delta\frac{C_{h_\alpha}}{C_{h_\delta}}\frac{l_t}{U^2}\left(1+\frac{d\epsilon}{d\alpha}\right)\right)\right]\dot{n} + \left[Z_w M_q - U\left(M_w - M_\delta\frac{C_{h_\alpha}}{C_{h_\delta}}\frac{1}{U}\left(1-\frac{d\epsilon}{d\alpha} - \frac{l_t}{U}Z_w\right)\right)\right] = \frac{UM_\delta Z_w}{C_{h_\delta}}C_h \qquad \text{(Eq. 40)}$$

Equation 40 may be rewritten as

$$\ddot{n} + b'\dot{n} + k' n = \frac{U M_\delta Z_w}{C_{h_\delta}} C_h \qquad \text{(Eq. 40')}$$

where $$b' = -\left[Z_w + M_q + U\left(M_{\dot{w}} - M_\delta \frac{C_{h_\alpha}}{C_{h_\delta}} \frac{\ell_t}{U^2}\left(1 + \frac{d\epsilon}{d\alpha}\right)\right)\right] \qquad \text{(Eq. 41)}$$

or $$b' = b + \Delta b \qquad \text{(Eq. 41')}$$

where $$\Delta b = M_\delta \frac{C_{h_\alpha}}{C_{h_\delta}} \frac{\ell_t}{U}\left(1 + \frac{d\epsilon}{d\alpha}\right) \qquad \text{(Eq. 42)}$$

and $$k' = \left[Z_w M_q - U\left(M_w - M_\delta \frac{C_{h_\alpha}}{C_{h_\delta}} \frac{1}{U}\left(1 - \frac{d\epsilon}{d\alpha} - \frac{\ell_t}{U} Z_w\right)\right)\right] \qquad \text{(Eq. 43)}$$

or $$k' = k + \Delta k$$

where $$\Delta k = M_\delta \frac{C_{h_\alpha}}{C_{h_\delta}}\left(1 - \frac{d\epsilon}{d\alpha} - \frac{\ell_t}{U} Z_w\right) \qquad \text{(Eq. 43')}$$

$$\qquad \text{(Eq. 44)}$$

The variation of pitching velocity with elevator hinge moment may be arrived at by a similar method.

$$\delta = \frac{C_h - C_{h_\alpha}\left[\frac{w}{U}\left(1 - \frac{d\epsilon}{d\alpha}\right) + \frac{d\epsilon}{d\alpha}\frac{\dot{w}}{U}\frac{\ell_t}{U} + q\frac{\ell_t}{U}\right]}{C_{h_\delta}} \qquad \text{(Eq. 38)}$$

Equations 6' and 7' may now be rewritten as

$$(D - Z_w) w - U q = 0 \qquad \text{(Eq. 6')}$$

$$-(DM_{\dot{w}} + M_w) w + (D - M_q) q = \frac{M_\delta}{C_{h_\delta}}\left\{C_h - C_{h_\alpha}\left[\frac{w}{U}\left(1 - \frac{d\epsilon}{d\alpha}\right) + \frac{d\epsilon}{d\alpha}\frac{Dw}{U}\frac{\ell_t}{U} + \frac{q\ell_t}{U}\right]\right\} \qquad \text{(Eq. 45)}$$

Equation 45 may be rearranged to eliminate terms involving w and q on the right hand side, and w may be eliminated between the resulting equation and equation 6' in a manner similar to that used previously in deriving equation 24. The resulting equation for q is of the form

$$\ddot{q} + b'\dot{q} + k q = \frac{M_\delta}{C_{h_\delta}}\left(C_h^{\circ} - Z_w C_h\right) \qquad \text{(Eq. 46)}$$

where b' and k' are defined by equations 41 and 43.

The response of the airplane to a given elevator hinge moment has now been shown to be

$$\ddot{n} + b'\dot{n} + k' n = \frac{U M_\delta Z_w}{C_{h_\delta}} \dot{C}_h \qquad \text{(Eq. 40')}$$

$$\ddot{q} + b'\dot{q} + k' q = \frac{M_\delta}{C_{h_\delta}} \left(\dot{C}_h - Z_w C_h \right) \qquad \text{(Eq. 46)}$$

$$b' = b + \Delta b = -\left[Z_w + M_q + U M_{\dot{w}} \right] + \left[M_\delta \frac{C_{h_\alpha}}{C_{h_\delta}} \frac{l_t}{U} \left(1 + \frac{\partial \epsilon}{\partial \alpha} \right) \right] \qquad \text{(Eq. 41)}$$

$$k' = k + \Delta k = \left[Z_w M_q - U M_{\dot{w}} \right] + \left[M_\delta \frac{C_{h_\alpha}}{C_{h_\delta}} \left(1 - \frac{\partial \epsilon}{\partial \alpha} - \frac{l_t Z_{w_1}}{U} \right) \right] \qquad \text{(Eq. 43)}$$

where $C_h = f(t)$

Equations 40' and 46 are exactly analogous to equations 16' and 24. Therefore the response of the airplane to a sinusoidal elevator hinge moment may be obtained by analogy to equations 32 and 34. The desired equations of response to a sinusoidal elevator hinge moment are then

$$\frac{n}{|\bar{C}_h|} = \frac{U M_\delta Z_w}{C_{h_\delta} \sqrt{(k' - \omega^2)^2 + (b'\omega)^2}} \sin \left[\omega t + \tan^{-1} \left(\frac{-b'\omega}{k' - \omega^2} \right) \right] \qquad \text{(Eq. 47)}$$

$$\frac{q}{|\bar{C}_h|} = \frac{M_\delta}{C_{h_\delta}} \sqrt{\frac{Z_w^2 + \omega^2}{(k' - \omega^2)^2 + (b'\omega)^2}} \sin \left[\omega t + \tan^{-1} \left(\frac{\omega (k' - \omega^2) + Z_w b'\omega}{-Z_w (k' - \omega^2) + b'\omega^2} \right) \right] \qquad \text{(Eq. 48)}$$

where $C_h = |\bar{C}_h| \sin \omega t$

The response to a sinusoidal elevator hinge moment coefficient has thus been found to be similar to the response to a sinusoidal elevator angle. The stability coefficients, k and b and k' and b', differ from each other by increments defined by equations 41 through 44.

Variation of Horizontal Tail Load During the Steady Oscillation

The variation of the horizontal tail load during a sinusoidal oscillation may now be calculated (based on the assumptions inherent in the equations of motion given by equations 6' and 7') from the response equations derived in the previous sections.

The incremental tail load coefficient at any instant is

$$C_{N_t} = m_t \, \Delta\alpha_t \qquad \text{(Eq. 49)}$$

where $$\Delta\alpha_t = \Delta\alpha - \Delta\epsilon + \Delta\epsilon_{lag} + \frac{q\,l_t}{U} + \lambda\delta \qquad \text{(Eq. 50)}$$

$$\Delta\alpha_t = \frac{w}{U}\left(1 - \frac{d\epsilon}{d\alpha}\right) + \frac{d\epsilon}{d\alpha}\,\frac{\dot{w}}{U}\,\frac{l_t}{U} + \frac{q\,l_t}{U} + \lambda\delta \qquad \text{(Eq. 50')}$$

Then

$$C_{N_t} = \frac{m_t}{U}\left[\left(1 - \frac{d\epsilon}{d\alpha}\right)w + \frac{l_t}{U}\,\frac{d\epsilon}{d\alpha}\,\dot{w} + q\,l_t + U\lambda\delta\right] \qquad \text{(Eq. 51)}$$

Since $n = Z_w w$, then equation 51 may be written

$$\frac{C_{N_t}}{\delta} = \frac{m_t}{U}\left[\frac{1 - d\epsilon/d\alpha}{Z_w}\,\frac{n}{\delta} + \frac{l_t}{U}\,\frac{d\epsilon/d\alpha}{Z_w}\,\frac{\dot{n}}{\delta} + l_t\,\frac{q}{\delta} + U\lambda\right] \qquad \text{(Eq. 51')}$$

Now assuming $\delta = |\bar{\delta}| \sin \omega t$

From equation 32

$$\frac{n}{|\bar{\delta}|} = \frac{U M_\delta Z_w}{\sqrt{(K-\omega^2)^2 + (b\omega)^2}} \sin\left(\omega t + \tan^{-1}\frac{-b\omega}{K-\omega^2}\right) \qquad \text{(Eq. 32)}$$

or

$$\frac{n}{|\bar{\delta}|} = \frac{U M_\delta Z_w}{(K-\omega^2)^2 + (b\omega)^2}\left[(K-\omega^2)\sin\omega t - (b\omega)\cos\omega t\right] \qquad \text{(Eq. 32')}$$

Based on equation 32'

$$\frac{\dot{n}}{|\bar{\delta}|} = \frac{U M_\delta Z_w\,\omega}{(K-\omega^2)^2 + (b\omega)^2}\left[(b\omega)\sin\omega t + (K-\omega^2)\cos\omega t\right] \qquad \text{(Eq. 52)}$$

From equation 34

$$\frac{q}{|\delta|} = M_\delta \sqrt{\frac{Z_w^2 + \omega^2}{(K-\omega^2)^2 + (b\omega)^2}} \sin\left[\omega t + \tan^{-1} \frac{\omega(K-\omega^2) + Z_w b\omega}{-Z_w(K-\omega^2) + b\omega^2}\right] \qquad \text{(Eq. 34)}$$

or

$$\frac{q}{|\delta|} = \frac{M_\delta}{(K-\omega^2)^2 + (b\omega)^2}\left[(-Z_w(K-\omega^2) + b\omega^2)\sin\omega t + (\omega(K-\omega^2) + Z_w b\omega)\cos\omega t\right] \qquad \text{(Eq. 34')}$$

The equation for $\frac{C_{N_t}}{|\delta|}$ (equation 51') may now be rewritten based on the values of n, $\dot{n}$, and q given by equations 32', 52, and 34'. This results in the following equation for the tail normal force coefficient.

$$\frac{C_{N_t}}{|\delta|} = \frac{m_t}{U}\left\{\frac{U M_\delta \left(1 - \frac{d\epsilon}{d\alpha}\right)}{(K-\omega^2)^2 + (b\omega)^2}\left[(K-\omega^2)\sin\omega t - b\omega\cos\omega t\right]\right.$$

$$+ \frac{U M_\delta \frac{d\epsilon}{d\alpha}\frac{l_t}{U}\omega}{(K-\omega^2)^2 + (b\omega)^2}\left[(b\omega)\sin\omega t + (K-\omega^2)\cos\omega t\right]$$

$$+ \frac{M_\delta l_t}{(K-\omega^2)^2 + (b\omega)^2}\left[-(Z_w(K-\omega^2) + b\omega^2)\sin\omega t + (\omega(K-\omega^2) + Z_w b\omega)\cos\omega t\right]$$

$$\left. + \lambda U \sin\omega t\right\} \qquad \text{(Eq. 53)}$$

An examination of equation 53 shows that it is of the form

$$\frac{C_{N_t}}{|\delta|} = \frac{m_t}{U}\left\{C\cos\omega t + S\sin\omega t\right\} . \qquad \text{(Eq. 54)}$$

where C is the sum of the coefficients of the cosine terms within the braces of equation 53, and S is the sum of the coefficients of the sine terms within the braces of this equation.

It is then finally possible to write the equation for the variation of tail load during a sinusoidal oscillation of the elevator as

$$\frac{C_{N_t}}{|\bar{\delta}|} = \frac{m_t}{U}\sqrt{C^2 + S^2}\ \sin\left(\omega t + \tan^{-1}\frac{C}{S}\right) \qquad \text{(Eq. 55)}$$

$$C = \left[-\frac{U M_\delta b\omega\left(1-\frac{d\epsilon}{d\alpha}\right)}{(K-\omega^2)^2+(b\omega)^2} + \frac{U M_\delta (K-\omega^2)\omega\frac{l_t}{U}\frac{d\epsilon}{d\alpha}}{(K-\omega^2)^2+(b\omega)^2} + \frac{M_\delta l_t\left(\omega(K-\omega^2)+Z_w b\omega\right)}{(K-\omega^2)^2+(b\omega)^2}\right] \qquad \text{(Eq. 56)}$$

$$S = \left[\frac{U M_\delta (K-\omega^2)\left(1-\frac{d\epsilon}{d\alpha}\right)}{(K-\omega^2)^2+(b\omega)^2} + \frac{U M_\delta b\omega^2\frac{l_t}{U}\frac{d\epsilon}{d\alpha}}{(K-\omega^2)^2+(b\omega)^2} + \frac{M_\delta l_t\left(-Z_w(K-\omega^2)+b\omega^2\right)}{(K-\omega^2)^2+(b\omega)^2} + \lambda U\right] \qquad \text{(Eq. 57)}$$

and $\delta = |\bar{\delta}| \sin \omega t$

Variation of the Elevator Hinge Moment During the Steady Oscillation

As was pointed out in the derivation of the motion of the airplane corresponding to a sinusoidal variation of elevator hinge moment, a rigorous treatment of this elevator hinge moment would include the effects of the moment of inertia and mass unbalance of the elevator, and the aerodynamic damping of the elevator due to its angular velocity. It was pointed out, however, that these effects were of negligible magnitude at the frequencies of oscillation which are being considered here (ω less than 10 radians per second). Therefore, it is possible to represent the incremental change of elevator hinge moment coefficient during a small disturbance of the airplane by the expression

$$C_h = C_{h_\delta}\delta + C_{h_\alpha}\alpha_t \qquad \text{(Eq. 36)}$$

where

$$\alpha_t = \left[\frac{w}{U}\left(1-\frac{d\epsilon}{d\alpha}\right) + \frac{d\epsilon}{d\alpha}\frac{\dot{w}}{U}\frac{l_t}{U} + q\frac{l_t}{U}\right] \qquad \text{(Eq. 37)}$$

or, since $w = \frac{n}{Z_w}$

$$\alpha_t = \left[\frac{n}{UZ_w}\left(1-\frac{d\epsilon}{d\alpha}\right) + \frac{d\epsilon}{d\alpha}\frac{\dot{n}}{UZ_w}\frac{l_t}{U} + q\frac{l_t}{U}\right] \qquad \text{(Eq. 37')}$$

For a sinusoidal elevator motion,

$$\delta = |\delta| \sin \omega t$$

and from equations 32', 34' and 52

$$\frac{\eta}{|\delta|} = \frac{U M_\delta Z_w}{(K-\omega^2)^2+(b\omega)^2}\left[(K-\omega^2)\sin\omega t - (b\omega)\cos\omega t\right] \qquad \text{(Eq. 32')}$$

$$\frac{\dot{\eta}}{|\delta|} = \frac{U M_\delta Z_w \omega}{(K-\omega^2)^2+(b\omega)^2}\left[b\omega \sin\omega t + (K-\omega^2)\cos\omega t\right] \qquad \text{(Eq. 52)}$$

$$\frac{q}{|\delta|} = \frac{M_\delta}{(K-\omega^2)^2+(b\omega)^2}\left[(-Z_w(K-\omega^2)+b\omega^2)\sin\omega t + (\omega(K-\omega^2) + Z_w b\omega)\cos\omega t\right] \qquad \text{(Eq. 34')}$$

For the sinusoidal elevator motion equation 36 may now be written in the following form

$$\frac{C_h}{|\delta|} = C_{h_\delta}\sin\omega t + C_{h_\alpha}\frac{1}{U}\left\{\frac{U M_\delta (1-\frac{\partial\epsilon}{\partial\alpha})}{(K-\omega^2)^2+(b\omega)^2}\left[(K-\omega^2)\sin\omega t - b\omega\cos\omega t\right]\right.$$

$$+\frac{\partial\epsilon}{\partial\alpha}\frac{l_t}{U}\frac{U M_\delta \omega}{(K-\omega^2)^2+(b\omega)^2}\left[(b\omega)\sin\omega t + (K-\omega^2)\cos\omega t\right]$$

$$\left.+\frac{l_t M_\delta}{(K-\omega^2)^2+(b\omega)^2}\left[(-Z_w(K-\omega^2)+b\omega^2)\sin\omega t + (\omega(K-\omega^2)+Z_w b\omega)\cos\omega t\right]\right\} \qquad \text{(Eq. 58)}$$

Examination of equation 58 shows that it may be reduced to

$$\frac{C_h}{|\delta|} = C'\cos\omega t + S'\sin\omega t$$

where C' is the coefficient of the cosine terms of equation 58, and S' is the coefficient of the sine terms.

$$C' = \frac{C_{h_\alpha}}{U\left[(K-\omega^2)^2+(b\omega)^2\right]}\left\{-U M_\delta\left(1-\frac{\partial\epsilon}{\partial\alpha}\right)b\omega + \frac{\partial\epsilon}{\partial\alpha}l_t M_\delta\omega(K-\omega^2)\right. \qquad \text{(Eq. 59)}$$

$$\left.+ l_t M_\delta\left[\omega(K-\omega^2)+Z_w(b\omega)\right]\right\}$$

$$S' = C h_\xi + \frac{C h_\alpha}{U[(K-\omega^2)^2 + (b\omega)^2]} \left\{ U M_\delta \left(1 - \frac{d\epsilon}{d\alpha}\right)(K-\omega^2) + \frac{d\epsilon}{d\alpha} \ell_t M_\delta b\omega^2 \right.$$

$$\left. + \ell_t M_\delta \left[-Z_w (K-\omega^2) + b\omega^2 \right] \right\} \qquad \text{(Eq. 60)}$$

and

$$\frac{C_h}{|\bar{\delta}|} = \sqrt{C'^2 + S'^2} \sin\left(\omega t + \tan^{-1} \frac{C'}{S'}\right) \qquad \text{(Eq. 61)}$$

APPENDIX B.

MOTION OF AN AIRPLANE FOLLOWING A STEP DEFLECTION OF THE ELEVATOR, AND THE MOTION RESULTING FROM AN ARBITRARY ELEVATOR MOVEMENT.

Introduction

An analysis of the equations of motion of an airplane in a vertical plane following movement of the elevator was made in Appendix A, and this analysis was extended to include the steady response of the airplane to a sinusoidal oscillation of the elevator. In this appendix the general equations of the motion of the airplane are solved for the case of an instantaneous (or "step") deflection of the elevator. It is then shown that the response obtained from this solution may be used in conjunction with the Duhamel integral to obtain the motion of the airplane following any arbitrary time history of the movement of the elevator. A generally similar treatment has been made in reference (12).

Response of Normal Acceleration at the Center of Gravity of the Airplane Following a Step Deflection of the Elevator

As has been pointed out in Appendix A, the change of speed which occurs during ordinary movements of the elevator has a negligible effect on the motion of the airplane, and it is therefore permissible to reduce the problem to one of two degrees of freedom. Based on this assumption and assumptions common to the analysis of the dynamic stability of airplanes (see Appendix A), the motion of the airplane has been shown to be

$$\ddot{n} + b\dot{n} + kn = UM_{\sigma} Z_w \delta \qquad \text{(Eq. 1)}$$

$$\ddot{q} + b\dot{q} + kq = M_{\sigma}(\dot{\sigma} - Z_w \delta) \qquad \text{(Eq. 2)}$$

where $b = -(Z_w + Mq + UM_w^{\bullet})$ (Eq. 3)

$k = (Z_w M_q - UM_w)$ (Eq. 4)

and $\sigma = f(t)$

The definition of symbols used in equations (1) through (4) may be found in Appendix A.

It will be assumed that $\sigma = 0$ for all values of $t < 0$, and that $\sigma = \sigma_1$ for all values of $t > 0$. The solution of equations (1) and (2) for n and q will now be found. Since the transient of the resultant motion is of importance in this case, it is necessary that both the complementary and particular solutions of the equations be found.

Equation (1) may be rewritten:

$$(D^2 + bD + k)\, n = UM_\delta Z_w \delta_1 \qquad (1')$$

The complementary solution of this equation is of the form

$$C_1 e^{\gamma_1 t} + C_2 e^{\gamma_2 t}$$

where γ_1 and γ_2 are roots of the equation obtained by placing the right hand side of equation (1) equal to zero and substituting γ for the operator D.

$$\gamma^2 + b\gamma + k = 0$$

$$\gamma_1 = \frac{-b + \sqrt{b^2 - 4k}}{2}$$

$$\gamma_2 = \frac{-b - \sqrt{b^2 - 4k}}{2}$$

The particular integral of equation (1') is found to be

$$\frac{UM_\delta Z_w}{k} \delta_1$$

The complete solution may then be written:

$$\frac{n}{\delta_1} = C_1 e^{\frac{-b + \sqrt{b^2 - 4k}}{2} t} + C_2 e^{\frac{-b - \sqrt{b^2 - 4k}}{2} t} + \frac{UM_\delta Z_w}{k} \qquad \text{(Eq. 5)}$$

In order to evaluate the constants C_1 and C_2, equation (5) is differentiated, and the known values of n and $\dot{n}$ at t = 0 are substituted into equation (5) and its derivative.

$$\frac{\dot{n}}{\delta_1} = \frac{-b + \sqrt{b^2 - 4k}}{2} C_1 e^{\frac{-b + \sqrt{b^2 - 4k}}{2} t} + \frac{-b - \sqrt{b^2 - 4k}}{2} C_2 e^{\frac{-b - \sqrt{b^2 - 4k}}{2} t} \qquad \text{(Eq. 6)}$$

when $t = 0$, $\frac{n}{\delta_1} = 0$ and $\frac{\dot{n}}{\delta_1} = 0$

($\frac{\dot{n}}{\delta_1} = 0$ at $t = 0$ since there is no incremental force acting along the z axis at t = 0. This is true only if $Z_\delta \delta_1$ is of negligible magnitude.)

By placing these known boundary conditions in equations (5) and (6) the constants C_1 and C_2 are found to be

$$C_1 = -UM_\delta \frac{Z_w}{K} \left(\frac{b + \sqrt{b^2 - 4K}}{2\sqrt{b^2 - 4K}} \right) \qquad \text{(Eq. 7)}$$

$$C_2 = -UM_\delta \frac{Z_w}{K} \left(\frac{-b + \sqrt{b^2 - 4K}}{2\sqrt{b^2 - 4K}} \right) \qquad \text{(Eq. 8)}$$

Substituting the results of equations (7) and (8) into equation (5), the solution for the time history of the incremental normal acceleration at the center of gravity of an airplane following a step deflection of the elevator is

$$\frac{n}{\delta_1} = \frac{U M_\delta Z_w}{K}\left\{1 - e^{-\frac{b}{2}t}\left[\frac{(b+\sqrt{b^2-4K})e^{\frac{\sqrt{b^2-4K}}{2}t} - (b-\sqrt{b^2-4K})e^{-\frac{\sqrt{b^2-4K}}{2}t}}{2\sqrt{b^2-4K}}\right]\right\} \quad \text{(Eq. 9)}$$

The term outside of the braces of equation (9) is the steady stete response, and the terms within the braces contain the transient effects.

If the short period motion of the airplane is less than critically damped (as is frequently the case), then $b^2 < 4k$. Equation (9) may then be written more conveniently by making use of the transformations

$$e^{+i\frac{\sqrt{4K-b^2}}{2}t} = \cos\frac{\sqrt{4K-b^2}}{2}t + i\sin\frac{\sqrt{4K-b^2}}{2}t$$

and

$$e^{-i\frac{\sqrt{4K-b^2}}{2}t} = \cos\frac{\sqrt{4K-b^2}}{2}t - i\sin\frac{\sqrt{4K-b^2}}{2}t$$

Equation (9) may then be rewritten in the form

$$\frac{n}{\delta_1} = \frac{U M_\delta Z_w}{K}\left[1 - e^{-\frac{b}{2}t}\left(\cos\frac{\sqrt{4K-b^2}}{2}t + \frac{b}{\sqrt{4K-b^2}}\sin\frac{\sqrt{4K-b^2}}{2}t\right)\right] \quad \text{(Eq. 10)}$$

By making use of the relationship

$$A\cos\theta + B\sin\theta = \sqrt{A^2+B^2}\sin\left(\theta + \tan^{-1}\frac{A}{B}\right)$$

equation (10) may be further simplified by combining the cosine and sine terms into a single sine term when $b^2 < 4k$.

$$\frac{n}{\delta_1} = \frac{U M_\delta Z_w}{K}\left[1 - e^{-\frac{b}{2}t}\sqrt{\frac{4K}{4K-b^2}}\sin\left(\frac{\sqrt{4K-b^2}}{2}t + \tan^{-1}\frac{\sqrt{4K-b^2}}{b}\right)\right] \quad \text{(Eq. 11)}$$

If the airplane is more than critically damped ($b^2 > 4k$) equation (9) may be written most conveniently in terms of hyperbolic functions by means of the transformations

$$e^{\frac{\sqrt{b^2-4K}}{2}t} = \cosh\frac{\sqrt{b^2-4K}}{2}t + \sinh\frac{\sqrt{b^2-4K}}{2}t$$

and

$$e^{-\frac{\sqrt{b^2-4K}}{2}t} = \cosh\frac{\sqrt{b^2-4K}}{2}t - \sinh\frac{\sqrt{b^2-4K}}{2}t$$

$$\frac{n}{\delta_1} = \frac{UM_\delta Z_w}{K}\left\{1 - e^{-\frac{b}{2}t}\left[\cosh\frac{\sqrt{b^2-4K}}{2}t + \frac{b}{\sqrt{b^2-4K}}\sinh\frac{\sqrt{b^2-4K}}{2}t\right]\right\} \quad \text{(Eq. 12)}$$

By making use of the relationship

$$A\cosh\theta + B\sinh\theta = \sqrt{B^2 - A^2}\sinh\left(\theta + \tanh^{-1}\frac{A}{B}\right)$$

equation (12) may be further simplified by combining the cosh and sinh terms into a single sinh terms when $b^2 > 4K$.

$$\frac{n}{\delta_1} = \frac{UM_\delta Z_w}{K}\left\{1 - e^{-\frac{b}{2}t}\sqrt{\frac{4K}{b^2-4K}}\left[\sinh\left(\frac{\sqrt{b^2-4K}}{2}t + \tanh^{-1}\frac{\sqrt{b^2-4K}}{b}\right)\right]\right\} \quad \text{(Eq. 13)}$$

When $b^2 = 4K$, the motion corresponds to that of critical damping, and equation (5) is of the form

$$\frac{n}{\delta_1} = (c_1 + c_2 t)e^{-\frac{b}{2}t} + \frac{UM_\delta Z_w}{K} \quad \text{(Eq. 5')}$$

Based on the initial conditions that, when

$t = 0$, $\frac{n}{\delta_1} = 0$ and $\frac{\dot{n}}{\delta_1} = 0$

equation (5') reduces to

$$\frac{n}{\delta_1} = \frac{UM_\delta Z_w}{K}\left[1 - e^{-\frac{b}{2}t}\left(1 + \frac{b}{2}t\right)\right] \quad \text{(Eq. 14)}$$

Response of Pitching Velocity of the Airplane Following A Step Deflection of the Elevator

For $t > 0$, $\delta \approx \delta_1$ and $\dot{\delta} = 0$.

Therefore equation (2) may be written,

$$(D^2 + bD + K)q = -M_\delta Z_w \delta_1 \quad \text{(Eq. 2')}$$

By the same method used in obtaining equation (5), the complete solution of equation (2') is found to be

$$\frac{q}{\delta_1} = c_1 e^{\frac{-b+\sqrt{b^2-4K}}{2}t} + c_2 e^{\frac{-b-\sqrt{b^2-4K}}{2}t} - \frac{M_\delta Z_w}{K} \quad \text{(Eq. 15)}$$

The derivative of equation (15) is

$$\frac{\dot{q}}{\delta_1} = \left(\frac{-b+\sqrt{b^2-4K}}{2}\right) C_1 e^{\frac{-b+\sqrt{b^2-4K}}{2}t} + \left(\frac{-b-\sqrt{b^2-4K}}{2}\right) C_2 e^{\frac{-b-\sqrt{b^2-4K}}{2}t} \qquad \text{(Eq. 16)}$$

when $t = 0$, $\frac{q}{\delta_1} = 0$ and $\frac{\dot{q}}{\delta_1} = M_\delta$

The above boundary conditions, when substituted into equations (15) and (16), yield the following values of the constants

C_1 and C_2 :

$$C_1 = \frac{M_\delta Z_w}{K}\left[\frac{2\frac{K}{Z_w} + b + \sqrt{b^2-4K}}{2\sqrt{b^2-4K}}\right] \qquad \text{(Eq. 17)}$$

$$C_2 = \frac{M_\delta Z_w}{K}\left[\frac{-2\frac{K}{Z_w} - b + \sqrt{b^2-4K}}{2\sqrt{b^2-4K}}\right] \qquad \text{(Eq. 18)}$$

When the values of C_1 and C_2 from equations (17) and (18) are substituted into equation (16), the final form of the resultant expression is

$$\frac{q}{\delta_1} = -\frac{M_\delta Z_w}{K}\left\{1 - e^{-\frac{b}{2}t}\left[\frac{\left(b+\sqrt{b^2-4K}+2\frac{K}{Z_w}\right)e^{\frac{\sqrt{b^2-4K}}{2}t} - \left(b-\sqrt{b^2-4K}+2\frac{K}{Z_w}\right)e^{-\frac{\sqrt{b^2-4K}}{2}t}}{2\sqrt{b^2-4K}}\right]\right\} \qquad \text{(Eq. 19)}$$

Now, replacing the exponential terms within the brackets of equation (19) by their trigonometric equivalents, equations(19) may be written in the following convenient forms.

When $b^2 < 4k$

$$\frac{q}{\delta_1} = -\frac{M_\delta Z_w}{K}\left[1 - e^{-\frac{b}{2}t}\left(\cos\frac{\sqrt{4K-b^2}}{2}t + \frac{\left(b+\frac{2K}{Z_w}\right)}{\sqrt{4K-b^2}}\sin\frac{\sqrt{4K-b^2}}{2}t\right)\right] \qquad \text{(Eq. 20)}$$

OR

$$\frac{q}{\delta_1} = -\frac{M_\delta Z_w}{K}\left[1 - e^{-\frac{b}{2}t}\sqrt{1+\frac{\left(b+\frac{2K}{Z_w}\right)^2}{4K-b^2}}\sin\left(\frac{\sqrt{4K-b^2}}{2}t + \tan^{-1}\frac{\sqrt{4K-b^2}}{b+\frac{2K}{Z_w}}\right)\right] \qquad \text{(Eq. 21)}$$

When $b^2 > 4k$

$$\frac{q}{\delta_1} = -\frac{M_\delta Z_w}{K}\left\{1 - e^{-\frac{b}{2}t}\left[\cosh\frac{\sqrt{b^2-4K}}{2}t + \frac{\left(b+\frac{2K}{Z_w}\right)}{\sqrt{b^2-4K}}\sinh\frac{\sqrt{b^2-4K}}{2}t\right]\right\} \qquad \text{(Eq. 22)}$$

or

$$\frac{q}{\delta_1} = -\frac{M_\delta Z_w}{K}\left\{1 - e^{-\frac{b}{2}t}\sqrt{\frac{\left(b+\frac{2K}{Z_w}\right)^2}{b^2-4K}-1}\ \sinh\left(\frac{\sqrt{b^2-4K}}{2}t + \tanh^{-1}\frac{\sqrt{b^2-4K}}{b+\frac{2K}{Z_w}}\right)\right\} \quad \text{(Eq. 23)}$$

When $b^2 = 4K$, the motion corresponds to that of critical damping, and equations(15) is of the form

$$\frac{q}{\delta_1} = (C_1 + C_2 t)\, e^{-\frac{b}{2}t} - \frac{M_\delta Z_w}{K} \quad \text{(Eq. 15')}$$

and with the initial condition that, when $t = 0$, $\frac{q}{\delta_1} = 0$, $\frac{\dot{q}}{\delta_1} = M_\delta$

equation (15') reduces to

$$\frac{q}{\delta_1} = -\frac{M_\delta Z_w}{K}\left[1 - e^{-\frac{b}{2}t}\left(1 + \left(\frac{b}{2} + \frac{K}{Z_w}\right)t\right)\right] \quad \text{(Eq. 24)}$$

Equations 11, 13, 14 and 21, 23 and 24 give the most convenient forms for the variation of the n and q responses to a step deflection of the elevator for all possible relationships of b and k. Similar equations for the change of angle of attack of the airplane (which is similar to the change of n) following a step deflection of the elevator are given in reference (12).

Response of Normal Acceleration at the Center of Gravity and Pitching Velocity of an Airplane Following a Step Application of Elevator Hinge Moment.

Based on the assumptions that the effects of the moment of inertia and the mass unbalance of the elevator might be neglected, and that the hinge moment due to the angular velocity of the elevator is also negligible, the equations of motion following the application of hinge moment were obtained in Appendix A.

$$\ddot{n} + b'\dot{n} + K'n = \frac{U M_\delta Z_w}{C h_\delta} C_h \quad \text{(Eq. 25)}$$

$$\ddot{q} + b'\dot{q} + K'q = \frac{M_\delta}{C h_\delta}\left(\dot{C}_h - Z_w C_h\right) \quad \text{(Eq. 26)}$$

where $C_h = f(t)$

and K' and b' are defined by equations (41) and (43) of Appendix A.

The assumptions stated above are obviously violated during a step deflection of the elevator. However, the effects of inertia and damping will be appreciable only for a small time interval near zero, and the above equations are probably sufficiently accurate for the step application of small hinge moments. Furthermore, the theoretical response to a step application of hinge moment is useful for determining the response to an arbitrary time history of hinge moment by the Duhamel integral. (The use of the Duhamel integral is described in a later section of this Appendix.)

Equations (25) and (26) above are analogous to equations (1) and (2). It is therefore possible to write the equation of the, response of the airplane to a step hinge moment by direct analogy to equations 11, 13, 14, 21, 23 and 24.

When $b'^2 < 4k'$

$$\frac{n}{Ch_1} = \frac{UM_\delta Z_w}{Ch_\delta K'}\left[1 - e^{-\frac{b'}{2}t}\sqrt{\frac{4K'}{4K'-b'^2}}\,\sin\left(\frac{\sqrt{4K'-b'^2}}{2}t + \tan^{-1}\frac{\sqrt{4K'-b'^2}}{b'}\right)\right] \quad \text{(Eq. 27)}$$

$$\frac{q}{Ch_1} = -\frac{M_\delta Z_w}{Ch_\delta K'}\left[1 - e^{-\frac{b'}{2}t}\sqrt{\frac{1+\left(\frac{b'+2\frac{b'}{Z_w}}{2}\right)^2}{4K'-b'^2}}\,\sin\left(\frac{\sqrt{4K'-b'^2}}{2}t + \tan^{-1}\frac{\sqrt{4K'-b'^2}}{b'+\frac{2K'}{Z_w}}\right)\right] \quad \text{(Eq. 28)}$$

When $b'^2 > 4k'$

$$\frac{n}{Ch_1} = \frac{UM_\delta Z_w}{Ch_\delta K'}\left[1 - e^{-\frac{b'}{2}t}\sqrt{\frac{4K'}{b'^2-4K'}}\,\sinh\left(\frac{\sqrt{b'^2-4K'}}{2}t + \tanh^{-1}\frac{\sqrt{b'^2-4K'}}{b'}\right)\right] \quad \text{(Eq. 29)}$$

$$\frac{q}{Ch_1} = -\frac{M_\delta Z_w}{Ch_\delta K'}\left[1 - e^{-\frac{b'}{2}t}\sqrt{\frac{\left(b'+\frac{2K'}{Z_w}\right)^2}{b'^2-4K'} - 1}\,\sinh\left(\frac{\sqrt{b'^2-4K'}}{2}t + \tanh^{-1}\frac{\sqrt{b'^2-4K'}}{b'+\frac{2K'}{Z_w}}\right)\right] \quad \text{(Eq. 30)}$$

When $b'^2 = 4k'$

$$\frac{n}{Ch_1} = \frac{UM_\delta Z_w}{Ch_\delta K'}\left[1 - e^{-\frac{b'}{2}t}\left(1 + \frac{b'}{2}t\right)\right] \quad \text{(Eq. 31)}$$

$$\frac{q}{Ch_1} = -\frac{M_\delta Z_w}{Ch_\delta K'}\left[1 - e^{-\frac{b'}{2}t}\left(1 + \left(\frac{b'}{2} + \frac{K}{Z_w}\right)t\right)\right] \quad \text{(Eq. 32)}$$

Airplane Motion Following an Arbitrary Time History of Elevator Movement or an Arbitrary Application of Elevator Hinge Moment.

Having obtained the solution to the response of the airplane following a step deflection of the control, it is now possible to obtain the response associated with an arbitrary movement of the control by the use of the Duhamel integral. This method of obtaining the response in the general case of control motion has been pointed out in references (12),(14), and (17).

By the Duhamel integral (the derivation of which may be found in reference(18)), the desired responses to an arbitrary elevator motion are

$$q(t) = \int_0^t \frac{q}{\delta_1}(t-\tau)\, d\delta(\tau) = \int_0^t \frac{d\delta}{d\tau}(\tau)\, \frac{q}{\delta_1}(t-\tau)\, d\tau \qquad \text{(Eq. 33)}$$

$$n(t) = \int_0^t \frac{n}{\delta_1}(t-\tau)\, d\delta(\tau) = \int_0^t \frac{d\delta}{d\tau}(\tau)\, \frac{n}{\delta_1}(t-\tau)\, d\tau \qquad \text{(Eq. 34)}$$

Where q(t) and n(t) are the desired time histories of pitching velocity and normal acceleration,

and

$\frac{d\delta}{d\tau}(\tau)$ is the variation of $\frac{d\delta}{d\tau}$ with time.

$d\delta(\tau)$ is the variation of $d\delta$ with time.

$\delta(\tau)$ is the variation of elevator angle with time.

It is assumed that $\delta(0) = 0$

An alternate form of the Duhamel integral makes use of the response to a unit impulse, $\frac{d}{dt}\left(\frac{q}{\delta_1}\right)$ and $\frac{d}{dt}\left(\frac{n}{\delta_1}\right)$, rather than the response to a unit step application of the control. In this case the response is given by

$$q(t) = \int_0^t \delta(\tau) \left[\frac{d}{dt}\left(\frac{q}{\delta_1}\right)\right](t-\tau)\, d\tau \qquad \text{(Eq. 35)}$$

$$n(t) = \int_0^t \delta(\tau) \left[\frac{d}{dt}\left(\frac{n}{\delta_1}\right)\right](t-\tau)\, d\tau \qquad \text{(Eq. 36)}$$

Equations for the response to an arbitrary application of elevator hinge moment are obtained simply by replacing $\frac{n}{\delta_1}$ and $\frac{q}{\delta_1}$ in equations (33) through (36) by $\frac{n}{C_{h_1}}$ and $\frac{q}{C_{h_1}}$.

A simple graphical method of obtaining the solution of the Duhamel integral is given in reference (1). In this method the given elevator time history is divided into equal increments of deflection, and the midpoint of each of the resulting time intervals is noted.

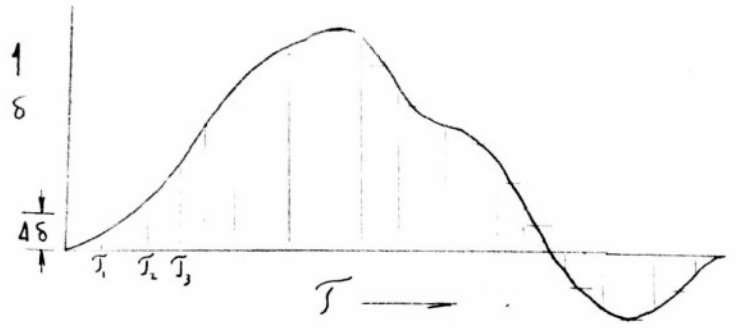

The response to a step deflection of the elevator of the chosen magnitude $\Delta\delta$ is computed by the methods described earlier in this appendix. A cardboard template of the computed response to the step deflection $\Delta\delta_1$ may then be constructed. The origin of the template is placed at the midpoint of the first increment of $\Delta\delta$ (at time τ_1), and the ordinate of the template is noted at a number of values of τ. The template is then shifted parallel to the τ axis until its origin is at τ_2. The ordinates of the template at each of the previously selected values of τ are then added to previous sum of the ordinates at each of these stations. This process is repeated throughout the duration of the control movement. The template is inverted when the increment of elevator movement is negative. Airplane response may be obtained rapidly and easily by this method.

The graphical solution of the Duhamel integral may also be made using a template constructed according to response data which have been obtained experimentally for a given airplane by measuring in flight the response to a step deflection of the elevator.

APPENDIX C

DERIVATION OF CIRCLE DIAGRAM PRESENTATION OF AIRPLANE RESPONSE DATA DURING A SINUSOIDAL OSCILLATION

Introduction

It is shown that the form of the equation for the change of normal acceleration at the center of gravity of an airplane during a sinusoidal oscillation at constant speed is such that a polar diagram of the amplitude of the time rate of change of normal acceleration per degree elevator deflection ($\dot{n}/|\delta|$) plotted as the radius and the phase difference between $\dot{n}$ and δ plotted as the polar angle will form a circle which has its center on the polar axis, and which passes through the origin. Although the pitching velocity data cannot be plotted directly as a circle, it is shown that these data may be transformed so that they will also plot as a circle. The circular form of the data is useful for several reasons. The known geometric shape of the plot facilitates accurate fairing of the experimental points, and, as will be shown, the calculation of b and k from the circle diagram is very simple. Additional information concerning aerodynamic parameters may be obtained from the diameter of the circle.

Various electrical circuits show frequency response characteristics which may be represented by the circle diagram when these circuits are excited by a sinusoidal forcing function. For this reason the circle diagram has been used in the electrical field for many years. A description of this diagram as used in various electrical applications is contained in reference (7). However the existence of a circular polar diagram of airplane response characteristics may be shown most directly by analytic geometry and without reference to an electrical analogy, and this approach is employed in the proof which follows.

Circle Diagram of Normal Acceleration Response to a Sinusoidal Oscillation of the Elevator

From Appendix A, (Equation 16'), the expression for variation of normal acceleration at the airplane center of gravity is

$$\ddot{n} + b\dot{n} + kn = \left(UM_\delta Z_w\right)\delta \qquad \text{(Eq. 1)}$$

where the above quantities are defined in the list of symbols included in Appendix A.

If $\delta = |\bar{\delta}| \sin \omega t$.

$$\frac{\ddot{n}}{|\bar{\delta}|} + \frac{b\dot{n}}{|\bar{\delta}|} + \frac{kn}{|\bar{\delta}|} = UM_\delta Z_w \sin \omega t \qquad \text{(Eq. 2)}$$

From the solution of (Eq. 2) (see Appendix A), the response of normal acceleration to a steady sinusoidal elevator motion is found to be

$$\frac{n}{|\bar{\delta}|} = \frac{UM_\delta Z_w}{\sqrt{(k-\omega^2)^2 + (b\omega)^2}} \sin\left(\omega t + \tan^{-1}\frac{-b\omega}{k-\omega^2}\right) \qquad \text{(Eq. 3)}$$

where ϕ_{n_δ} = (phase angle between n and δ) = $\tan^{-1}\frac{-b\omega}{k-\omega^2}$ (Eq. 4)

By differentiation of (Eq. 3),

$$\frac{\dot{n}}{|\delta|} = \frac{UM_\delta Z_w}{\sqrt{(k-\omega^2)^2 + (b\omega)^2}}\ \omega \cos\left(\omega t + \tan^{-1}\frac{-b\omega}{k-\omega^2}\right) \qquad \text{(Eq. 5)}$$

Since $\cos\alpha = \sin\left(\alpha + \frac{\pi}{2}\right)$

$$\frac{\dot{n}}{|\delta|} = \frac{UM_\delta Z_w}{\sqrt{(K-\omega^2)^2 + (b\omega)^2}}\ \omega \sin\left(\omega t + \frac{\pi}{2} - \tan^{-1}\frac{b\omega}{K-\omega^2}\right) \qquad \text{(Eq. 6)}$$

But $\frac{\pi}{2} - \tan^{-1} x = \tan^{-1}\frac{1}{x}$ therefore,

$$\frac{\dot{n}}{|\delta|} = \frac{UM_\delta Z_w}{\sqrt{(K-\omega^2)^2 + (b\omega)^2}}\ \omega \sin\left(\omega t + \tan^{-1}\frac{K-\omega^2}{b\omega}\right) \qquad \text{(Eq. 7)}$$

Factoring out the circular frequency, ω,

$$\frac{\dot{n}}{|\delta|} = \frac{UM_\delta Z_w}{\sqrt{\left(\frac{K}{\omega}-\omega\right)^2 + b^2}} \sin\left(\omega t + \tan^{-1}\frac{\frac{K}{\omega}-\omega}{b}\right) \qquad \text{(Eq. 8)}$$

and

$$\phi_{\dot{n}_\delta} = \tan^{-1}\frac{\frac{K}{\omega}-\omega}{b} \qquad \text{(Eq. 9)}$$

Comparing ϕ_{n_δ} and $\phi_{\dot{n}_\delta}$ from (Equations 4 and 9),

$$\phi_{\dot{n}_\delta} = \phi_{n_\delta} + \frac{\pi}{2} \qquad \text{(Eq. 10)}$$

or the phase of the "velocity" (first derivative) vector may be found by adding 90° to the experimentally determined "displacement" vector. (From the form of (Eq. 1), n is analogous to the displacement term, $\dot{n}$ is analogous to the velocity term, and $\ddot{n}$ is analogous to the acceleration term of the familiar mass-spring-damping equation).

From (Equations 7 and 8), the maximum value of $\frac{\dot{n}}{|\delta|}$ is obtained when $\sin(\omega t + \phi_{\dot{n}_\delta})$ is equal to 1, and its value is

$$\frac{\dot{n}}{|\delta|} = \frac{UM_\delta Z_w\,\omega}{\sqrt{(K-\omega^2)^2 + (b\omega)^2}} = \frac{UM_\delta Z_w}{\sqrt{\left(\frac{K}{\omega}-\omega\right)^2 + b^2}} \qquad \text{(Eq. 11)}$$

Similarly, the maximum value of $\frac{n}{|\delta|}$ is obtained from (Eq. 3).

$$\frac{\bar{n}}{|\delta|} = \frac{UM_\delta Z_w}{\sqrt{(K-\omega^2)^2 + (b\omega)^2}} \qquad \text{(Eq. 12)}$$

Comparison of (Equations 11 and 12) shows that

$$\frac{\dot{n}}{|\delta|} = \frac{\bar{n}}{|\delta|}\ \omega \qquad \text{(Eq. 13)}$$

where $\frac{\bar{n}}{|\delta|}$ is obtained directly from the experimental data.

Since (Eq. 9) $\tan\phi_{\dot{n}_\delta} = \frac{\frac{K}{\omega}-\omega}{b}$

Then $\cos\phi_{\dot{n}_\delta} = \frac{b}{\sqrt{\left(\frac{K}{\omega}-\omega\right)^2 + b^2}}$ (Eq. 14)

The maximum amplitude of $\frac{\dot{n}}{|\delta|}$ at a given circular frequency may then be written by combining (Eqs. 11 and 14).

$$\frac{\dot{n}}{|\delta|} = \frac{UM_\delta Z_w}{b} \cos \phi_{\dot{n}_\delta} \qquad \text{(Eq. 15)}$$

The polar equation of a circle which passes through the origin and whose center lies on the polar axis is given by the equation.

$$r = D \cos \Theta \qquad \text{(Eq. 16)}$$

where r is the length of the polar radius, D is the diameter of the circle, and Θ is the polar angle.

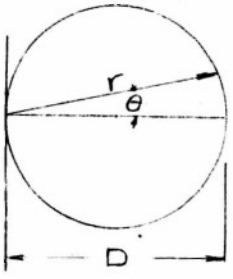

It is seen by comparing (Eq. 15) with (Eq. 16) that a polar plot of $\frac{\dot{n}}{|\delta|}$ and $\phi_{\dot{n}_\delta}$ will form a circle having the diameter $\frac{UM_\delta Z_w}{b}$.

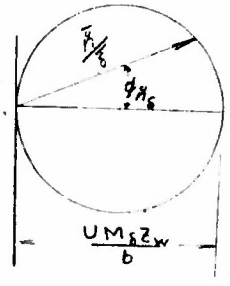

Inspection of (Eq. 15) shows that $\frac{\dot{n}}{|\delta|}$ is a maximum when $\cos \phi_{\dot{n}} = 1$. Thus $\frac{\dot{n}}{|\delta|}$ is a maximum when $\phi_{\dot{n}_\delta} = 0$.

Since, from (Eq. 9), $\tan \phi_{\dot{n}_\delta} = \frac{k - \omega}{b}$, then $\phi_{\dot{n}} = 0$ when $\frac{k}{\omega_o} - \omega_o = 0$, or

$$k = \omega_o^2 \qquad \text{(Eq. 17)}$$

Therefore, the stability constant k may be found from (Eq. 17), where ω_o is the circular frequency of the oscillation at which the $\frac{\dot{n}}{|\delta|}$ vector becomes the diameter of the circle. (Natural frequency of the system.)

To find b, let $\phi_{\dot{n}_\delta} = +\frac{\pi}{4}$

From (Eq. 9) and the above

$$\tan \phi_{\dot{n}_\delta} = \frac{k_{\omega_o} - \omega'}{b} = 1$$

$$b = k_{\omega_o} - \omega' \qquad \text{(Eq. 18)}$$

where k has been obtained from (Eq. 19), and ω' is the circular frequency at which $\phi_{\dot{n}_\delta} = +\frac{\pi}{4}$.

The use of the circle diagram thus not only is an aid in the fairing of the experimental data, but also permits rapid and simple evaluation of the desired stability constants, b and k.

Additional information may be obtained from the circle diagram by recognizing that the diameter of the circle is $\frac{UM_\delta Z_w}{b}$ and is also equal to $\frac{\dot{n}}{|\delta|}$ when $\omega = \omega_o$.

Z_w may be evaluated from the expression

$$\frac{|\bar{n}|}{|\bar{q}|} = \left| \frac{U}{\sqrt{1 + \left(\frac{\omega}{Z_w}\right)^2}} \right| \qquad \text{(See Appendix A)}$$

Z_w is known to be usually negative, and this sign may be fixed by inspection.

Since b has been determined from (Eq. 18), and U and $\frac{\dot{n}}{|\delta|}$ are known, the value of M_δ may be obtained.

When plotting the data, it may be found that the circle which best fits the points is not centered on the polar axis, but lies on a line which passes through the origin and forms an angle Λ with the polar axis. The possible causes of this rotation might include an aerodynamic lag between the deflection of the elevator and the development of the forcing moment, or a phase relationship between the true and indicated elevator angles. It is believed that the latter factor has been completely corrected for. However, no satisfactory explanation of this phenomenon has been arrived at at this time, and additional work must be done to find the cause of this characteristic.

When the center of the circle is on a line inclined to the polar axis, this line is used as the basic reference for determining k and b. The assumption is made that the observed phase shift does not vary with frequency, and that the data plots as a circle about the displaced reference axis.

Circle Diagram of Normal Acceleration Response to a Sinusoidal Application of Elevator Hinge Moment

In Appendix A it was shown that the response of normal acceleration to a steady sinusoidal application of elevator hinge moment coefficient was

$$\frac{n}{|C_h|} = \frac{UM_\delta Z_w}{C_{h_\delta} \sqrt{(k' - \omega^2)^2 + (b'\omega)^2}} \sin\left[\omega t + \tan^{-1}\left(\frac{-b'\omega}{k' - \omega^2}\right)\right] \qquad \text{(Eq. 19)}$$

Comparison of (Eq. 19) with (Eq. 3) shows that the two expressions are of identical form, except that the amplitude term of (Eq. 19) has been divided by C_{h_δ} and primed values of k and b have replaced the usual values of k and b of (Eq. 3). (See (Eqs. 41' and 43') of Appendix A for the definitions of k, b, k' and b'.)

It is therefore possible to show that a polar plot of $\frac{\dot{n}}{|C_h|}$ and $\phi_{\dot{n}_{C_h}}$ will form a circle similar to that formed by the $\frac{\dot{n}}{|\delta|}$ data, and that the diameter of this circle will be $\frac{UM_\delta Z_w}{C_{h_\delta} b'}$.

It should be noted here that, if the amplitude ratio $\frac{\bar{n}}{|\bar{C}_h|}$ is considered to be defined when

$$\sin\left[\omega t + \tan^{-1}\left(\frac{-b'\omega}{K'-\omega^2}\right)\right] = 1, \text{ then } \frac{\bar{n}}{|\bar{C}_h|} = \frac{UM_\delta Z_w}{C_{h_\delta}\sqrt{(K'-\omega^2)^2+(b'\omega)^2}}.$$

Since M_δ, Z_w, and C_{h_δ} are all usually negative, the amplitude $\frac{\bar{n}}{|\bar{C}_h|}$ will usually also be negative. Also it may be seen that the phase angle

$$\phi_{n_{C_h}} = \tan^{-1}\left(\frac{-b'\omega}{K'-\omega^2}\right)$$

varies from 0 to $-\pi$ as ω varies from 0 to ∞. Now, since $\phi_{\dot{n}_{C_h}} = \phi_{n_{C_h}} + \frac{\pi}{2}$, the value of $\phi_{\dot{n}_{C_h}}$ varies from $+\frac{\pi}{2}$ to $-\frac{\pi}{2}$ in the first and second quadrants. The circle diagram resulting from the simultaneous values of positive polar angles and negative polar radii lies to the left of the origin, and resembles the $\frac{\dot{n}}{|\dot{\delta}|}$ circle diagram rotated through the angle π. (Exactly the same diagram would be obtained if the phase were determined between the positive value of $\dot{n}$ and the peak hinge moment $|\bar{C}_h|$, for in this case the phase angles would be π greater than the phase angles determined above, and the polar radii measured along these lines would be positive).

The values of k' and b' are found from the hinge moment circle in exactly the same manner as the values of k and b are determined from the elevator deflection circle. The required relationships are given by (Eqs. 17 and 18).

Method for Obtaining Values of k and b of Points Which Do Not Lie on the Circle Diagram

A semi-empirical method for correcting the values of k and b of points at particular frequencies which fail to lie on the faired circle by a small distance may be arrived at in the following manner.

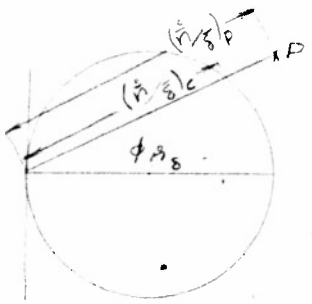

Let the subscript c denote the properties of points lying on the circle, and the subscript p denote the properties of the point P.

k_c and b_c (the k and b of all points on the circle) are obtained from (Eqs. 17 and 18).

Assume that the point P lies on a new circle, and compute k_p and b_p in terms of the characteristics of the known circle.

From (Eq. 15):

$$\frac{\dot{\bar{n}}}{|\bar{\delta}|} = \frac{UM_\delta \bar{Z}_w}{b} \cos \phi_{\dot{n}_\delta} \qquad \text{(Eq. 15)}$$

Assume that $UM_\delta \bar{Z}_w$ is the same at point P as it is on the circle.

Then, for a given value of $\phi_{\dot{n}_\delta}$,

$$\frac{\left(\frac{\dot{\bar{n}}}{|\bar{\delta}|}\right)_p}{\left(\frac{\dot{\bar{n}}}{|\bar{\delta}|}\right)_c} = \frac{b_c}{b_p} \qquad \text{(Eq. 20)}$$

$$\text{Let } \beta' = \frac{\left(\frac{\dot{\bar{n}}}{|\bar{\delta}|}\right)_c}{\left(\frac{\dot{\bar{n}}}{|\bar{\delta}|}\right)_p} \qquad \text{(Eq. 21)}$$

$$b_p = \beta' b_c \qquad \text{(Eq. 22)}$$

From (Eq. 9):

$$\tan \phi_{\dot{n}_\delta} = \frac{\frac{K}{\omega} - \omega}{b}$$

Now, for a given value of $\phi_{\dot{n}_\delta}$,

$$\frac{\frac{K_p}{\omega_p} - \omega_p}{b_p} = \frac{\frac{K_c}{\omega_c} - \omega_c}{b_c} \qquad \text{(Eq. 23)}$$

$$\frac{K_p}{\omega_p} - \omega_p = \frac{b_p}{b_c}\left(\frac{K_c}{\omega_c} - \omega_c\right) = \beta'\left(\frac{K_c}{\omega_c} - \omega_c\right) \qquad \text{(Eq. 24)}$$

where β' is defined by (Eq. 21).

(Eq. 24) may be written in the form

$$\frac{K_p}{\omega_p} - \omega_p = b_c\, \beta' \tan \phi_{\dot{n}_\delta} \qquad \text{(Eq. 25)}$$

Then

$$K_p = \omega_p \left(b_c\, \beta' \tan \phi_{\dot{n}_\delta} + \omega_p\right) \qquad \text{(Eq. 26)}$$

Therefore, the value of k and b of points which deviate from the circle diagram by a small amount may be approximated by the following relations:

$$b_p = \beta' b_c \qquad \text{(Eq. 22)}$$

$$K_p = \omega_p \left(b_c\, \beta' \tan \phi_{\dot{n}_\delta} + \omega_p\right) \qquad \text{(Eq. 26)}$$

where the subscript c refers to the circle and p refers to the point.

$$\beta' = \left(\frac{\dot{\bar{n}}}{|\bar{\delta}|}\right)_c \Big/ \left(\frac{\dot{\bar{n}}}{|\bar{\delta}|}\right)_p$$

(both taken at the same value of $\phi_{\dot{n}\dot{\delta}}$).

ω_p is the circular frequency at the point being considered.

b_c is obtained from (Eq. 18).

$\phi_{\dot{n}\dot{\delta}}$ is the phase angle between the reference line and the vector $\left(\frac{\dot{\bar{n}}}{|\bar{\delta}|}\right)_p$

Circle Diagram of Pitching Velocity Response to A Sinusoidal Oscillation of the Elevator.

It is necessary to perform certain transformations of the pitching velocity data in order that it will plot as a circle diagram. These transformations will be derived below. However, further geometric properties of the circle will first be discussed, and these properties will be used as a guide for selecting the required transformations of the pitching velocity data.

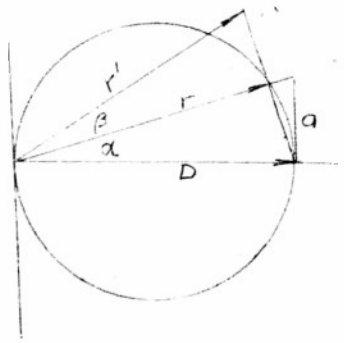

From the geometric characteristics of similar triangles

$$\frac{D}{\sqrt{D^2 + a^2}} = \frac{r}{D} \qquad \text{(Eq.27)}$$

$$r = \frac{D}{\sqrt{1 + \left(\frac{a}{D}\right)^2}} \qquad \text{(Eq. 28)}$$

but $\frac{a}{D} = \tan \alpha$

therefore $$r = \frac{D}{\sqrt{1+\tan^2\alpha}} \qquad \text{(Eq. 29)}$$

and $$r' \cos\beta = r \qquad \text{(Eq. 30)}$$

Now consider the form of the equation of rate of change of pitching velocity per unit elevator deflection during a sinusoidal oscillation.

From the equation for pitching velocity (see Appendix A),

$$\frac{q}{|\bar{\delta}|} = M_\delta \sqrt{\frac{Z_w^2+\omega^2}{(K-\omega^2)^2+(b\omega)^2}}\, \sin\left(\omega t + \tan^{-1}\frac{\omega(K-\omega^2)+Z_w b\omega}{-Z_w(K-\omega^2)+b\omega^2}\right) \qquad \text{(Eq. 31)}$$

The rate of change of pitching velocity is obtained from equation (31) by methods similar to those employed in obtaining equation (8), and is found to be

$$\frac{\dot{q}}{|\bar{\delta}|} = M_\delta \sqrt{\frac{Z_w^2+\omega^2}{(K-\omega^2)^2+(b\omega)^2}}\, \omega \sin\left(\omega t + \tan^{-1}\frac{-Z_w(K-\omega^2)+b\omega^2}{-\omega(K-\omega^2)-Z_w b\omega}\right) \qquad \text{(Eq. 32)}$$

Using the relation $\tan(\alpha+\beta) = \dfrac{\tan\alpha+\tan\beta}{1-\tan\alpha\tan\beta}$,

equation (32) may be rewritten

$$\frac{\dot{q}}{|\bar{\delta}|} = \frac{M_\delta}{b\sqrt{1+\left(\frac{K/\omega-\omega}{b}\right)^2}} \sqrt{Z_w^2+\omega^2}\, \sin\left(\omega t + \tan^{-1}\frac{K/\omega-\omega}{b} + \tan^{-1}\frac{\omega}{-Z_w}\right)$$

$$= -\frac{M_\delta Z_w}{b\sqrt{1+\left(\frac{K/\omega-\omega}{b}\right)^2}} \sqrt{1+\left(\frac{\omega}{-Z_w}\right)^2}\, \sin\left(\omega t + \tan^{-1}\frac{K/\omega-\omega}{b} + \tan^{-1}\frac{\omega}{-Z_w}\right) \qquad \text{(Eq. 33)}$$

Now, from equation (9),

$$\frac{K/\omega-\omega}{b} = \tan\phi_{\dot{n}_\delta}$$

and let $$\frac{\omega}{-Z_w} = \tan\phi'$$

where $$\phi' = \phi_{\dot{q}_\delta} - \phi_{\dot{n}_\delta}$$

The rate of change of pitching velocity then takes the form

$$\frac{\dot{q}}{|\bar{\delta}|} = -\frac{M_\delta Z_w}{b\sqrt{1+\tan^2\phi'}\,\dot{\phi}_{n_\delta}}\sqrt{1+\tan^2\phi'}\;\sin\left[\omega t + \tan^{-1}\frac{\frac{K}{\omega}-\omega}{b} + \tan^{-1}\frac{\omega}{-Z_w}\right] \qquad \text{(Eq. 34)}$$

From the known characteristic that the product of two vectors is obtained by multiplying their amplitudes and adding their phases, it will be seen that $\frac{\dot{q}}{|\bar{\delta}|}$ may be considered to be the vector product of the two vectors,

$$-\frac{M_\delta Z_w}{b\sqrt{1+\tan^2\phi'}\,\dot{\phi}_{n_\delta}} \qquad \text{and} \qquad \sqrt{1+\tan^2\phi'}$$

rotating at the uniform angular velocity ω.

The amplitude of the rate of change of the pitching velocity is

$$\frac{\dot{\bar{q}}}{|\bar{\delta}|} = -\frac{M_\delta Z_w}{b\sqrt{1+\tan^2\phi'}\,\dot{\phi}_{n_\delta}}\sqrt{1+\tan^2\phi'} \qquad \text{(Eq. 35)}$$

Comparison of equations (29) and (35) indicates that, if equation (35) is divided by the vector $\sqrt{1+\tan^2\phi'}$, the resulting vector will form a circle as the frequency of oscillation (and, therefore, $\dot{\phi}_{n_\delta}$) is varied.

$$\sqrt{1+\tan^2\phi'} = \frac{1}{\cos\phi'} = \frac{1}{\cos\left(\tan^{-1}\frac{\omega}{-Z_w}\right)} \qquad \text{(Eq. 36)}$$

$$\frac{\dot{\bar{q}}}{|\bar{\delta}|}\cos\phi' = -\frac{M_\delta Z_w}{b\sqrt{1+\tan^2\phi'}\,\dot{\phi}_{n_\delta}} \qquad \text{(Eq. 37)}$$

or

$$\frac{\dot{\bar{q}}}{|\bar{\delta}|}\cos\left(\tan^{-1}\frac{\omega}{-Z_w}\right) = -\frac{M_\delta Z_w}{b\sqrt{1+\tan^2\phi'}\,\dot{\phi}_{n_\delta}} \qquad \text{(Eq. 37')}$$

Equations (37) and (37') are analogous to equation (30).

Therefore it has been demonstrated that the pitching velocity characteristics are analogous to the quantities used in equations (27) through (30), where the correspondence is as follows.

$\frac{\dot{q}}{|\delta|} \sim r$ $\quad \phi_{\dot{q}_\delta} = \alpha$ $\quad -\frac{M_\delta Z_w}{b} \sim D$

$\frac{\dot{q}}{|\delta|}\cos(\tan^{-1}\frac{\omega}{-Z_w}) \sim r$ $\quad \tan^{-1}\frac{\omega}{-Z_w} = \beta$

The circle diagram of pitching velocity data may be constructed graphically by the following method.

1. Obtain $\frac{\dot{q}}{|\delta|}$ and $\phi_{\dot{q}_\delta}$ at a given frequency from the experimental data. (This may be done by multiplying the amplitude of the pitching velocity data by ω, and by adding 90° to the phase of the pitching velocity, or by multiplying by and adding 180° to the corresponding characteristics taken from pitch angle data). Plot this vector.

2. Subtract $\tan^{-1}\frac{\omega}{-Z_w}$ from the vector of step 1, and draw a line from the tip of the vector perpendicular to the line so determined. The intersection between these two lines will be a point on the circle.

Examination of the equation of $\frac{q}{|\delta|}$ indicates that it is similar to $\frac{n}{|C_h|}$ in that the amplitude will usually be negative when $\sin(\omega t + \phi_{q_\delta}) = 1$. This characteristic has been described above in the discussion of the $\frac{n}{|C_h|}$ circle, and it was shown that the $\frac{n}{|C_h|}$ circle lies to the left of the origin. From (Eq. 32)

$$\phi_{q_\delta} = \tan^{-1}\frac{-Z_w(\mu-\omega^2)+b\omega^2}{-\omega(\mu-\omega^2)-Z_w b\omega}$$

and this angle varies from $+\pi/2$ to 0 in a positive direction as ω varies from 0 to ∞. Also $\tan^{-1}\frac{\omega}{-Z_w}$ varies from 0 to $+\pi/2$ in a positive direction as ω varies from 0 to ∞. Therefore $(\phi_{q_\delta} - \tan^{-1}\frac{\omega}{-Z_w})$ varies from $+\pi/2$ to $-\pi/2$ through the first and second quadrants as ω varies from 0 to ∞. Now, since $\cos(\tan^{-1}\frac{\omega}{-Z_w})$ is usually positive and (as noted above) $\frac{q}{|\delta|}$ is usually negative, their product will be negative, and the resulting vectors of tie circle diagram will lie in the third and second quadrants. Therefore this diagram will be on the left hand side of the origin. The same conclusion would have been reached if the positive amplitude of $\frac{q}{|\delta|}$ and its associated phase had been considered, for in this case each phase angle would have been 180° greater and the polar radius would have been negative, thus forming the same family of vectors which was obtained above.

The construction of the circle from $\frac{\dot{q}}{|\delta|}$ and $\phi_{\frac{\dot{q}}{\delta}}$ is shown graphically below.

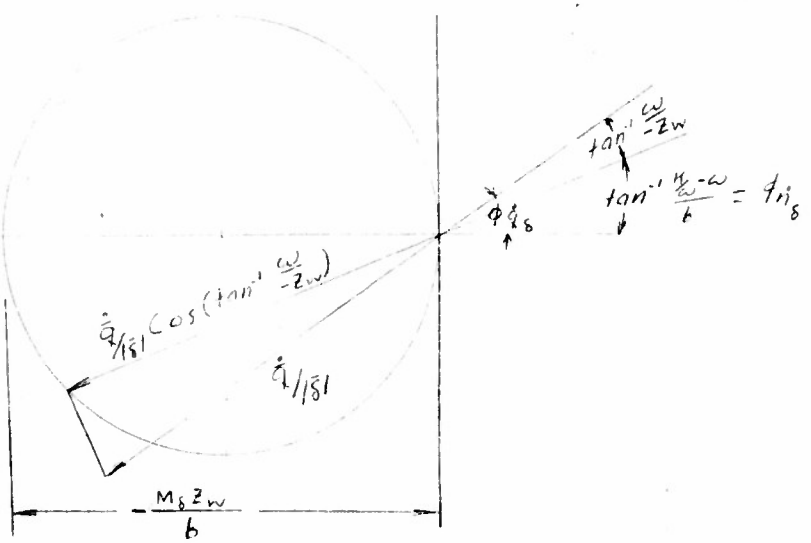

Circle Diagram of Pitching Velocity Response to A Sinusoidal Application of Elevator Hinge Moment

The variation of pitching velocity due to a sinusoidal application of elevator hinge moment was shown in Appendix A to be

$$\frac{q}{K_H} = \frac{M_\delta}{C_{h_\delta}} \sqrt{\frac{Z_w^2+\omega^2}{(K'-\omega^2)^2+(b'\omega)^2}}\ \sin\left(\omega t + \tan^{-1}\frac{\omega(K'-\omega^2)+Z_w b'\omega}{-Z_w(K'-\omega^2)+b'\omega^2}\right)$$

(Eq. 38)

Comparison of (Eq. 38) with (Eq. 31) indicates that $\frac{q}{|C_h|}$ is identical to $\frac{\dot{q}}{|\delta|}$ except that the amplitude of the oscillation is divided by C_{h_δ}, and k' and b' replace k and b.

$\frac{\dot{q}}{K_H}$ and $\phi_{\frac{\dot{q}}{C_h}}$ will then plot as a circle if the same operations are performed on these quantities which were performed on $\frac{\dot{q}}{|\delta|}$ and $\phi_{\frac{\dot{q}}{\delta}}$. The diameter of the resultant circle will be $-\frac{M_\delta Z_w}{C_{h_\delta}}$. Since both M_δ and C_{h_δ} will usually be negative, their ratio will be positive, and the circle diagram of $\frac{\dot{q}}{|K_H|}\cos(\tan^{-1}\frac{\omega}{-Z_w})$ and $(\phi_{\frac{\dot{q}}{C_h}} - \tan^{-1}\frac{\omega}{-Z_w})$ will lie to the right of the origin.

APPENDIX D.

METHOD OF ANALYSIS OF SINUSOIDAL OSCILLATION DATA TO OBTAIN STABILITY DERIVATIVES.

Since the equations developed in Appendices A and C have been found to satisfactorily predict the experimental responses, a means is desired for determining from the experimental data the various derivatives involved in the equations. The purpose of this appendix is to outline a method of analysis of the measured oscillation data to obtain the airplane stability derivatives.

The process is one of attempting to isolate the individual quantities as much as possible..

The steps are as follows:

1. Obtain Z_w vs. ω from the amplitude ratios of θ and n.

$$\frac{\bar{\theta}}{\bar{n}} = \frac{\sqrt{1+(\omega/Z_w)^2}}{U\omega}$$

2. Obtain M_δ from the diameter of the $\frac{\dot{n}}{|\delta|}$ circle. Diam. $= \frac{U M_\delta Z_w}{b}$

3. Obtain C_{h_δ} from the diameter of the $\frac{\dot{n}}{|C_h|}$ circle. Diam. $= \frac{U M_\delta Z_w}{b' C_{h_\delta}}$

$$C_{h_\delta} = \frac{\text{Diam. of } \frac{\dot{n}}{|\delta|} \text{ circle} \times b}{\text{Diam. of } \frac{\dot{n}}{|C_h|} \text{ circle} \times b'}$$

4. Obtain values of k and b (fixed control) from the $\frac{\dot{n}}{|\delta|}$ circles.

5. Obtain values of k' and b' (free control) from the $\frac{\dot{n}}{|C_h|}$ circles.

6. Obtain C_{h_α} from the relations between free control and fixed control parameters.

$$C_{h_\alpha} = \frac{(b'-b) + \frac{l_t}{U}(K'-K)}{M_\delta/C_{h_\delta} \cdot \frac{l_t}{U}\left(2 - \frac{l_t}{U} Z_w\right)}$$

7. Obtain $\frac{d\epsilon}{d\alpha}$ from the same relations.

$$\frac{d\epsilon}{d\alpha} = \frac{b'-b}{\frac{M_\delta}{C_{h_\delta}} \cdot \frac{l_t}{U} \cdot C_{h_\alpha}} - 1$$

8. M_w cannot be obtained from the oscillation data. Therefore it is necessary to calculate thie derivative from either wind

tunnel data or from static longitudinal stability flight test data. M_w may then be obtained from the relationship

$$M_w = \frac{\rho U}{2} \frac{S c}{I_Y} \frac{\partial C_L}{\partial \alpha} \frac{\partial C_m}{\partial C_L}$$

where $\frac{\partial C_L}{\partial \alpha}$ is per radian.

$$\text{or } M_w = -c \frac{m}{I_Y} Z_w \frac{\partial C_m}{\partial C_L}$$

It is assumed that $\frac{\partial C_m}{\partial C_L} \simeq \frac{\partial C_m}{\partial C_Z}$

The value of $\frac{\partial C_m}{\partial C_L}$ may be obtained from static stability flight test deta by locating the fixed control neutral point. The value of $\frac{\partial C_m}{\partial C_L}$ is then given approximately by

$$\frac{\partial C_m}{\partial C_L} = cg - np$$

where cg is the location of the center of gravity in fraction of the MAC.
np is the location of the neutral point in fraction of the MAC.

The value of $\frac{\partial C_m}{\partial C_L}$ may also be obtained by shifting ballast in flight (thus producing e known change of moment about a given point) and noting the lift coefficient at which the airplane trims with the elevator held fixed in its given position. This procedure may then be repeated for severel different ballast locations and a curve of C_m vs. C_L at a given elevetor angle will thus be defined.

9. Obtain M_q from the value of k.

$$M_q = \frac{k + UM_w}{Z_w}$$

10. Obtain $M_{\dot{w}}$ from the value of b.

$$M_{\dot{w}} = -\frac{(b + Z_w + M_q)}{U}$$

Using the above procedure, the following stability parameters have been determinsd: k, b, k', b', Z_w, M_ζ, C_{h_ζ}, C_{h_α} and $d\epsilon/d\alpha$

If the value of M_w may be found by other methods, M_q and $M_{\dot{w}}$ may also be determined.

APPENDIX E.

EFFECT OF OSCILLATION FREQUENCY ON THE LIFT OF THE AIRPLANE.

A theoretical investigation has been made to determine stability derivatives of a monoplane airfoil in steady sinusoidal motion by the theory of an oscillating airfoil as presented by Theodorsen. (Reference (11)). The problem is that of the wing alone in vertical translatory oscillation and rotating about an arbitrary fixed axis parallel to its span.

For the case of an airfoil alone in vertical translatory oscillation, the displacement of every point of the airfoil can be written as:

$$h = h_0 e^{i\omega t} = h_0 (\cos \omega t + i \sin \omega t) \tag{1}$$

and then

$$w = \dot{h} = h_0 i\omega e^{i\omega t} = h_0 (-\omega \sin \omega t + i\omega \cos \omega t)$$

$$\dot{w} = \ddot{h} = -h_0 \omega^2 e^{i\omega t} = h_0 (-\omega^2 \cos \omega t - i\omega^2 \sin \omega t)$$

The force acting on the airfoil in the two dimensional case as derived by Theodorsen is:

$$L = \rho b^2 \pi \dot{h}^{\circ} + 2\pi \rho U b C(K) Q \tag{2}$$

where L is positive upward and

b = 1/2 wing chord
U = velocity at infinity
k = reduced frequency = $\frac{\omega b}{U}$
$C(K) = F(K) + i G(K)$
$Q = \dot{h} = w$

Substituting in (2) and taking the imaginary part:

$$L = 2\pi \rho U b (h_0 \omega) \sqrt{F^2 + G^2} \cos (\omega t + \tan^{-1} \tfrac{G}{F}) + \pi \rho b^2 (-h_0 \omega^2) \sin \omega t \tag{3}$$

$$L_w = 2\pi \rho U b \sqrt{F^2 + G^2} \cos (\omega t + \tan^{-1} \tfrac{G}{F}) \tag{4}$$

$$L_{\dot{w}} = \pi \rho b^2 \sin \omega t \tag{5}$$

For the case of an airfoil alone in rotational oscillation, the angular displacement of every point of an airfoil can be written as:

$$\alpha = \alpha_0 e^{i\omega t} = \alpha_0 (\cos \omega t + i \sin \omega t) \tag{6}$$

and then

$$q = \dot{\alpha} = \alpha_0 i\omega e^{i\omega t} = \alpha_0 (-\omega \sin \omega t + i\omega \cos \omega t)$$

$$\dot{q} = \ddot{\alpha} = -\alpha_0 \omega^2 e^{i\omega t} = \alpha_0 (-\omega^2 \cos \omega t - i\omega^2 \sin \omega t)$$

The lift force can then be written:

$$L = \rho b^2 (U\pi \dot{\alpha} - \pi b a \ddot{\alpha}) + 2\pi \rho U b C(k) Q \qquad (7)$$

where, for this case: $Q = U\alpha + b(\tfrac{1}{2} - a)\dot{\alpha}$

where "a" is the center of rotation in (fraction of m.a.c. $-\frac{1}{2}$).

Letting a = 0 for an airfoil rotating about its midpoint, substituting in (7) and using the imaginary part:

$$L = \rho b^2 \pi U \alpha_0 \omega \sqrt{(1+F)^2 + G^2} \cos\left(\omega t + \tan^{-1} \frac{G}{1+F}\right)$$

$$+ 2\pi \rho U^2 b \alpha_0 \sqrt{F^2 + G^2} \cos(\omega t - \tan^{-1} F/G) \qquad (8)$$

$$L_\alpha = 2\pi \rho U^2 b \sqrt{F^2 + G^2} \cos(\omega t - \tan^{-1} F/G) \qquad (9)$$

$$L_q = \pi \rho b^2 U \sqrt{(1+F)^2 + G^2} \cos\left(\omega t + \tan^{-1} \frac{G}{1+F}\right) \qquad (10)$$

$$L_{\dot{q}} = 0 \qquad (11)$$

Jones (reference (9)) gives approximate equations for Theodorsen's F and G functions which corrects the theory for application to a wing of finite aspect ratio.

$$2\pi F = C_0 + C_1 \frac{k^2}{k^2 + r_1^2} + C_2 \frac{k^2}{k^2 + r_2^2} \qquad (12)$$

$$2\pi G = -C_1 \frac{r_1 k}{k^2 + r_1^2} - C_2 \frac{r_2 k}{k^2 + r_2^2} \qquad (13)$$

where C_0, C_1, C_2, r_1, and r_2 are constants depending upon the aspect ratio and k is the reduced frequency, $\frac{\omega b}{U}$.

The stability derivatives, Z_w, $Z_{\dot{w}}$, Z_q, and $Z_{\dot{q}}$, for a monoplane airfoil in pitching motion and oscillating about its midpoint can be determined from the preceding analysis.

$$Z_w = -\frac{1}{2\tau} \frac{dC_L}{d\alpha} \sqrt{F^2 + G^2} \cos\left(\omega t + \tan^{-1} \frac{G}{F}\right)$$

$$Z_{\dot{w}} = \frac{1}{2} \frac{\pi}{\tau} \frac{b}{U} \sin \omega t$$

$$Z_q = -\frac{b}{4\tau} \frac{dC_L}{d\alpha} \sqrt{(1+F)^2 + G^2} \cos\left(\omega t + \tan^{-1} \frac{G}{1+F}\right.$$

$$Z_{\dot{q}} = 0$$

where $T = m/\rho U S$, and F and G are corrected for finite aspect ratio by (12) and (13).

The ratio of the amplitude of Z_w for the oscillating airfoil to Z_w for the infinite airfoil in steady state has been plotted against frequency, ω, in Fig. 21a. For the aspect ratio and frequency range of the B-25, the variations in the magnitudes of the amplitudes of these derivatives are small enough to be considered negligible. Z_q varies less than 3% and $Z_{\dot{w}}$ less than 4%. The variation of the calculated phase of Z_w is plotted as a function of frequency in Fig. 21b. It will be noted that the phase variation becomes appreciable at the higher frequencies.

A more extensive study is being made to determine the variations with frequency of oscillations of all the stability derivatives for the entire airplane including the influence of the fuselage and tail surfaces in steady sinusoidal motion.

REFERENCES

(1) R. T. Jones and L. Sternfield, "A Method for Predicting the Stability in Roll of Automatically Controlled Aircraft Based on the Experimental Determination of the Characteristics of an Automatic Pilot" NACA RM L6K12, dated 17 January 1947.

(2) H. Greenberg, "Frequency Response Method for Determination of Dynamic Stability Characteristics of Airplanes with Automatic Controls" NACA TN 1229, dated March, 1947.

(3) Kennelley, "Electrical Vibration Instruments", MacMillan, dated 1923.

(4) A.C. Hall, "Analysis and Synthesis of Linear Servomechanisms", The Technology Press, Cambridge, Mass., dated 1946.

(5) Gardner and Barnes, "Transients in Linear Systems", John Wiley and Sons, New York, N.Y., dated 1942.

(6) Jones & Cohon, "An Analysis of the Stability of an Airplane with Free Controls," NACA TR709, dated 1941.

(7) Sager and Walter, "Application of Proposed Longitudinal Oscillation Method to the B-25J Airplane," Cornell Aeronautical Laboratory, Report TB405-F-2. dated 5 August 1946.

(8) Reid and Vincenti, "An Experimental Determination of the Lift of an Oscillating Airfoil", Journal of the Aeronautical Sciences, Vol. 8, No. 1, November, 1940.

(9) R. T. Jones, "The Unsteady Lift of a Wing at Finite Aspect Ratio," NACA TR 681, 1940.

(10) Silverstein & Joyner, "Experimental Verification of the Theory of Oscillating Airfoils," NACA TR673, 1939.

(11) T. Theodorsen, "General Theory of Aerodynamic Instability and the Mechanism of Flutter", NACA TR496, 1935.

(12) H.A. Pearson, "Derivation of Charts for Determining the Horizontal Tail Load Variation with any Elevator Motion" NACA Advance Restricted Report, dated January 1943.

(13) R.M. Crane, "Computation of Hinge Moment Characteristics of Horizontal Tails from Section Data", NACA CB 5B05, dated April, 1945.

(14) E.V. Laitone, "A New Approach to the Analysis of Airplane Motion," Cornell Aeronautical Laboratory, dated March 1946.

(15) H.W. Sibert, "Longitudinal Stability Equations for the Short Period Oscillation," AAF Memorandum Report No. ENG-51-4567-2, dated March, 1944.

(16) W.F. Durand, "Aerodynamic Theory" - Volume V.

(17) R.T. Jones, "Calculation of the Motion of Airplanes under the Influence of Irregular Disturbance," Journal of the Aeronautical Sciences, Vol. 3, No. 12, PP 419-425, October, 1936.

(18) Th. V. Karman and M.A. Biot, "Mathematical Methods in Engineering," McGraw and Hill Book Company, New York, 1940.

(19) Anonymous, "Aerodynamic Dimensional Data on the B-25J Airplane," North American Aviation, Inc., Report No. NA-5927, dated 24 January 1944.

TABLE I

Physical Dimensions of B-25J

Weight	26,000	lbs.
Wing Area	610	ft.^{2}
Root Chord	154.60	in.
Tip Chord	64.24	in.
Taper Ratio	.415	
Span	67.56	ft.
Aspect Ratio	7.48	
MAC	116.16	in.
Location of L. E. of MAC relative	12.68	in. aft.
to L. E. of wing at basic root chord	9.11	in. above
Airfoil Sections		
Root	NACA 23017	
Tip	NACA 4409R	
Horizontal Tail Area	132.4	ft.^{2}
Span	266	in.
Chord, Root	89.63	in.
Tip	61.11	in.
Mean Chord	75.37	in.
Aspect Ratio	3.71	
Taper Ratio	.68	
Elevator Area (Total)	40.4	ft.^{2}
Span (one)	108.25	in.
Chord	28.88	in.
Motion	25°	up
	10°	down
Vertical Tail Area (Total)	91.0	ft.^{2}
Tail Length	25.9	ft.
Moment of Inertia about Y axis	60,000	slug ft.^{2} (estimated)

Dimensions from reference (19).

TABLE II

Estimated and Wind Tunnel Values
of Aerodynamic Data

$$\partial C_L/\partial \alpha = 5.25$$

$$(\partial C_L/\partial \alpha)_t = 3.41$$

$$\partial C_m/\partial \alpha = -.525$$

$$\partial C_m/\partial \delta = -1.09$$

$$\partial \epsilon/\partial \alpha = 0.45$$

$$\partial C_h/\partial \delta = -.183$$

$$\partial C_h/\partial \alpha_t = -.149$$

All slopes are per radian.

TABLE III

Equations for Evaluating Stability Derivatives

$$Z_w = -\frac{dC_L}{d\alpha}\frac{\rho U S}{2m}$$

$$M_\delta = \frac{dC_m}{d\delta}\frac{\rho U^2 S c}{2 I_Y}$$

$$M_w = \frac{dC_m}{d\alpha}\frac{\rho U S c}{2 I_Y}$$

$$M_{\dot{w}} = -\left(\frac{dC_L}{d\alpha}\right)_t \frac{d\epsilon}{d\alpha}\frac{\rho S_t l_t^2}{2 I_Y}\frac{q_t}{q}$$

$$M_q = -\left(\frac{dC_L}{d\alpha}\right)_t \frac{\rho U S_t l_t^2}{2 I_Y}\frac{q_t}{q} - M_{q\,WING}$$

$$C_{h_\delta} = dC_h/d\delta$$

$$C_{h_\alpha} = dC_h/d\alpha_t$$

$$b = -Z_w - M_q - U M_{\dot{w}}$$

$$K = Z_w M_q - U M_w$$

$$b' = b + M_\delta \frac{C_{h_\alpha}}{C_{h_\delta}}\frac{l_t}{U}\left(1 + \frac{d\epsilon}{d\alpha}\right)$$

$$K' = K + M_\delta \frac{C_{h_\alpha}}{C_{h_\delta}}\left(1 - \frac{d\epsilon}{d\alpha} - \frac{l_t}{U} Z_w\right)$$

TABLE IV.

STABILITY CONSTANTS DETERMINED FROM

CIRCLE DIAGRAMS (Figs. 6-16)

(a) Determined Directly from Circle Diagrams.

EAS MPH	C.G. %MAC	Determined from $\dot{\rho}/\beta$ circles. k $1/sec^2$	b $1/sec$	k' $1/sec^2$	b' $1/sec$	Determined from $\dot{\phi}/\beta$ circles. k $1/sec^2$	b $1/sec$	k' $1/sec^2$	b' $1/sec$
175	22	8.40	3.28	-	-	8.94	3.64	-	-
"	24	8.70	3.78	7.07	2.54	7.62	3.58	4.72	2.11
"	26	6.96	3.30	-	-	7.08	3.56	-	-
"	26	6.50	3.40	2.69	2.51	6.60	3.74	3.24	2.31
"	28	6.92	3.87	3.06	1.47	6.55	3.69	2.60	2.71
"	30	5.20	3.31	2.17	3.28	5.61	2.73	.51	2.55
"	32	3.84	3.69	1.64	2.57	3.57	3.84	1.17	2.58
135	22	5.15	4.02	3.58	2.36	4.84	2.60	3.00	2.53
"	26	3.84	2.61	2.13	2.65	3.35	2.97	1.69	2.20
200	22	12.25	4.55	8.11	3.48	4.60	6.43	7.55	2.92
"	26	11.70	5.76	3.96	3.68	8.08	5.66	2.69	3.17

(b) Corrected to Standard I_y of 60,000 slug $ft.^2$

EAS MPH	C.G. %MAC	Est. I_y slug ft^2	Determined from $\dot{\rho}/\beta$ circles. k $1/sec^2$	b $1/sec$	k' $1/sec^2$	b' $1/sec$	Determined from $\dot{\phi}/\beta$ circles. k $1/sec^2$	b $1/sec$	k' $1/sec^2$	b' $1/sec$
175	22	47250	7.04	2.94	-	-	7.48	3.25	-	-
"	24	52050	6.85	3.21	5.57	2.26	6.00	3.08	3.72	1.92
"	26	62750	7.20	3.38	-	-	7.33	3.64	-	-
"	26	61625	6.80	4.50	2.81	2.57	6.90	3.85	3.39	2.36
"	28	69900	7.11	3.94	3.14	1.48	6.72	3.75	2.77	2.75
"	30	50250	6.06	3.66	2.53	3.62	7.10	3.12	.65	2.89
"	32	49100	4.75	4.28	2.06	2.89	4.41	4.45	1.45	1.90
135	22	50200	4.21	3.46	2.93	2.10	3.96	2.30	2.45	2.24
"	26	62100	3.98	2.67	2.20	2.71	3.46	3.03	1.75	2.24
200	22	64000	10.25	4.05	6.79	3.14	12.22	5.62	6.32	2.68
"	26	74225	12.50	6.05	4.22	3.83	8.60	5.93	2.86	3.28

TABLE V

Experimental and Predicted Derivatives
From Sinusoidal Oscillation Data

c. g. at 26% MAC — 10,000 ft. pressure altitude

	175 MPH. EAS		200 MPH. EAS	
	Predicted	Experimental (from faired curves vs. c.g.)	Predicted	Experimental (from Flight 82)
K	5.43	7.00	7.09	11.70
K'	2.30	3.75	3.00	3.96
b	2.98	3.45	3.40	5.76
b'	2.10	2.40	2.40	3.63
Diam. of η_δ Circle	.471	.394	.700	.506
Diam. of η_{C_h} Circle	-209	-97	-311	-156
dC_m/dC_L	- .100	--	- .109	--
M_δ	- 8.366	- 6.71	- 10.94	- 10.29
M_w	- .0135	- .0163 * $\left(Z_w \times \frac{m}{I_Y} \times \frac{dC_m}{dC_L}\right)$	-.0176	- .0226 * $\left(Z_w \times \frac{m}{I_Y} \times \frac{dC_m}{dC_L}\right)$
M_q	- 1.342	- 1.702	- 1.753	- 2.96
$M_{\dot{w}}$	- .00200	- .00166	- .00262	- .00433
Z_w	- 1.038	- 1.25	- 1.185	- 1.60
C_{h_δ}	- .0032	- .0059	- .0032	- .0051
C_{h_α}	- .0026	- .0064	- .0026	- .0088
$d\epsilon/d\alpha$	.45	.67	.45	.656

* Used in determining M_q and $M_{\dot{w}}$

TABLE VI

Results from Experimental Step Functions

175 MPH. EAS 10,000 ft. pressure altitude

C. G.	Estimated I_Y	(η/δ) Steady State	Slope When $\frac{n}{n_s}=.5$	K	b	K	b
						Corrected to St'd. I_Y	
% MAC	Slug Ft.^{2}	g/degree	1/sec.	1/sec.^{2}	1/sec.	1/sec.^{2}	1/sec.
23.9	60310	.187	1.304	7.25	3.28	7.29	3.29
24.1	48350	.194	1.266	8.71	4.25	7.01	3.66
28	54538	.241	1.140	6.21	3.28	5.65	3.10
30	66850	.237	.830	5.16	3.92	5.75	4.22

$M_\delta = -6.71 \times \frac{60,000}{I_Y}$

$Z_\omega = -1.25$

} from experimental sinusoidal oscillation data (Table V).

INDEX TO FIGURES

Figure	Title
19	Experimental Valuos of the Damping Ratio and Natural Short Period vs. c.g., 175 mph. EAS
20	Experimental Apparent Z_w vs ω at Various c.g.'s, 175 mph. EAS
21a, b	Theoretical Effect of the Frequenoy of Oscillation on the Amplitude and Phase of Z_w
22a, b	Experimental and Calculated Values of $\frac{\dot{\theta}}{\delta}$ and $\phi_{\dot{\theta}_\delta}$ vs. ω, 26% c.g. at Various Speeds
23a, b	Experimental and Calculated Values of $\frac{n}{\delta}$ and ϕ_{n_δ} vs. ω, 26% c.g. at Various Speeds
24a, b	Experimental and Calculated Values of $\frac{C_{N_\delta}}{\delta}$ and $\phi_{C_{N_\delta}}$ vs. ω, 175 mph. EAS at Various c.g. Positions
25a, b	Experimental and Calculated Values of $\frac{C_h}{\delta}$ and $\phi_{C_{h_\delta}}$ vs. ω, 175 mph. EAS at Various c.g. Positions
26a, b, c, d	Experimental and Calculated Time Histories of Normal Acceleration Response to Elevator Step Reflection, 175 mph. EAS, 23.9%, 24.1%, 28% and 30% c.g.
27	Calculated Slope of $\frac{n}{n_s}$ Response at $\frac{n}{n_s} = 0.5$
28	Experimental Values of k and b vs. c.g. from Normal Acceleration Responsos to Elevator Step Defleotions, 175 mph. EAS

Three-Quarter Front View - B-25J

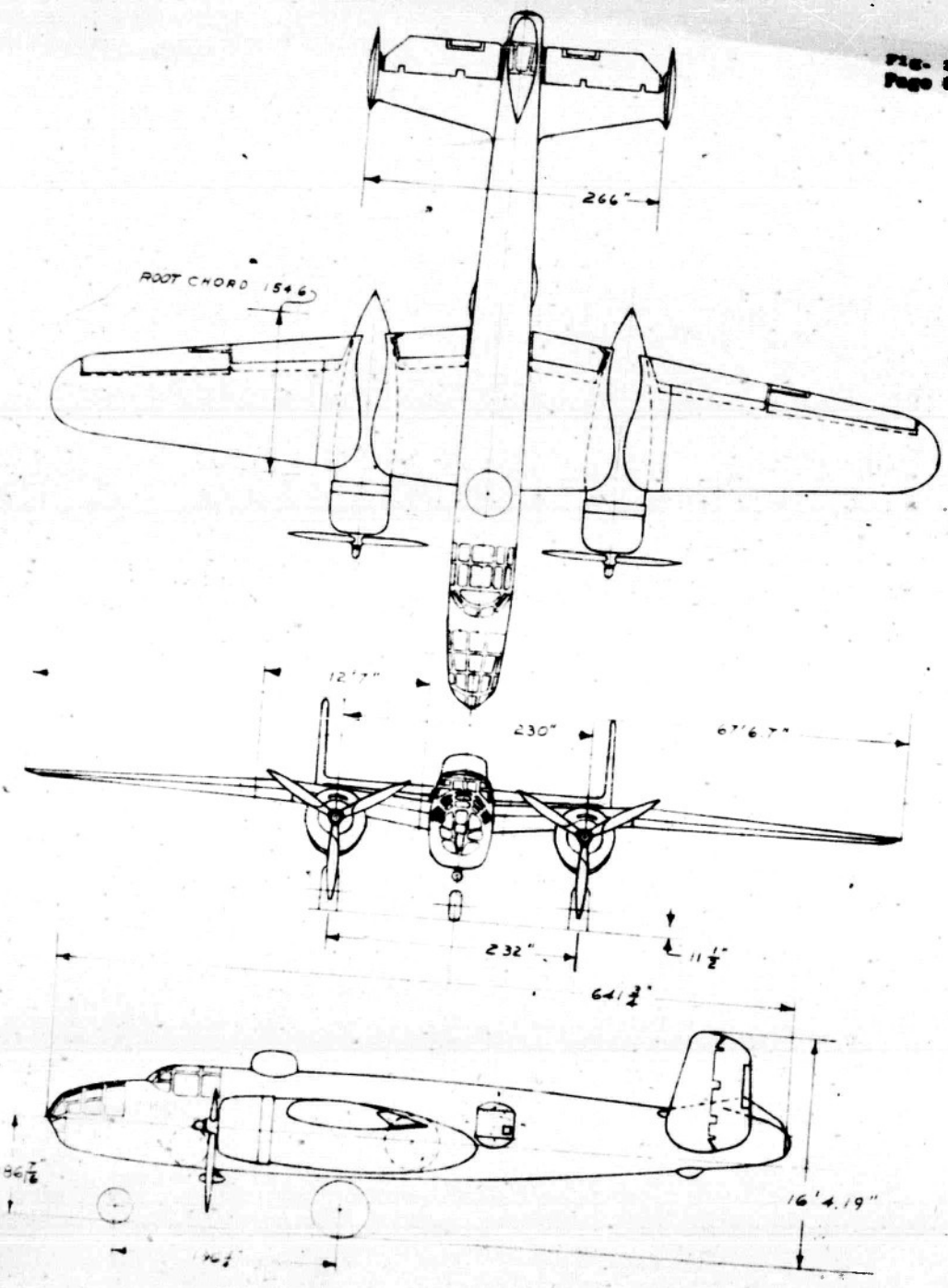

THREE VIEW DRAWING B-25 J

B-25 J 43-3892

VARIATION OF SPEED DURING SINUSOIDAL OSCILLATIONS

CALCULATED FROM LONGITUDINAL ACCELERATION RECORDS MEASURED IN FLIGHT

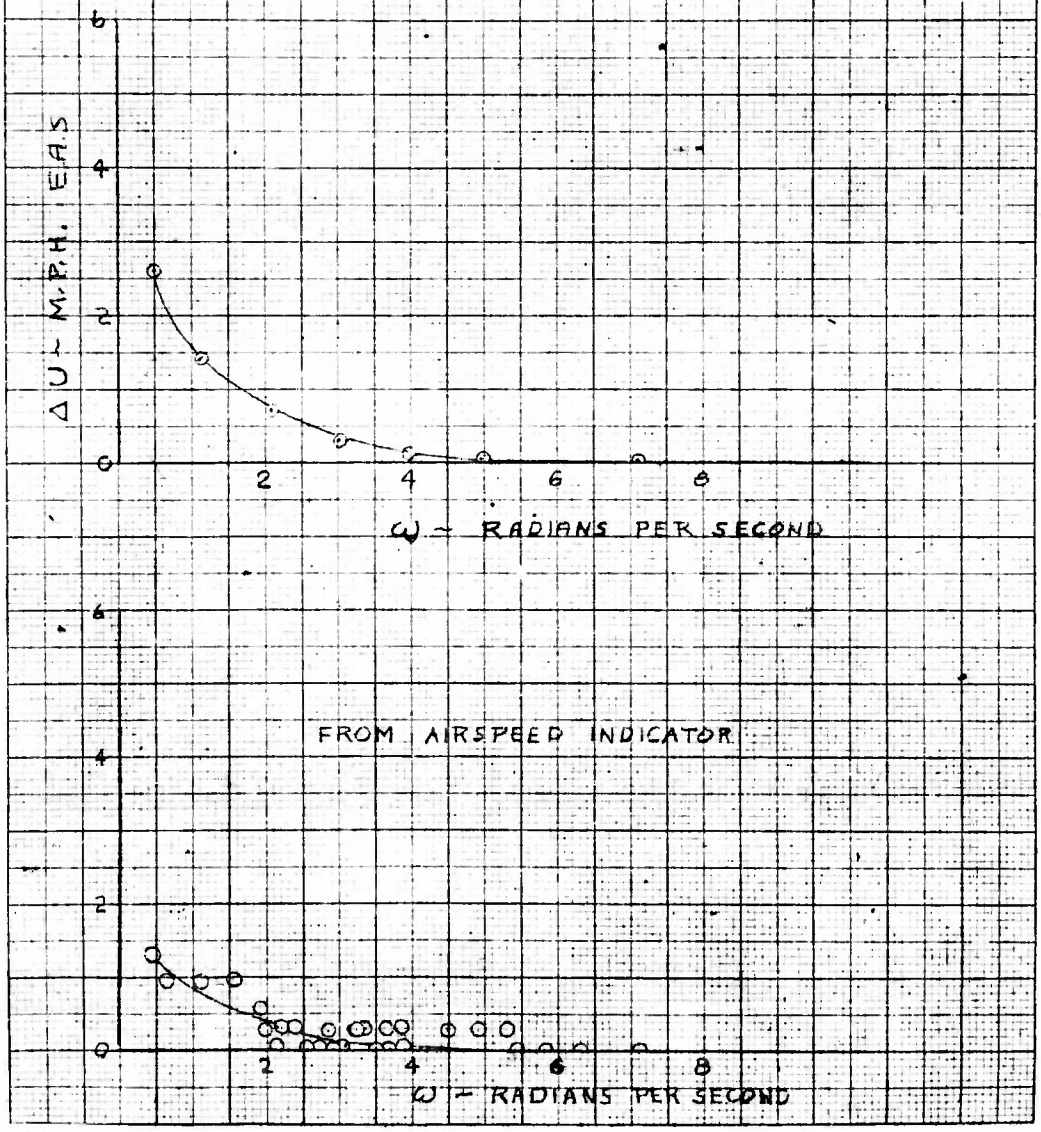

THEORETICAL VARIATION OF $\frac{\dot{\bar{n}}}{|\bar{\delta}|} = \frac{U M_\delta Z_w}{b} \cos \phi_{\dot{n}_\delta}$ WITH FREQUENCY

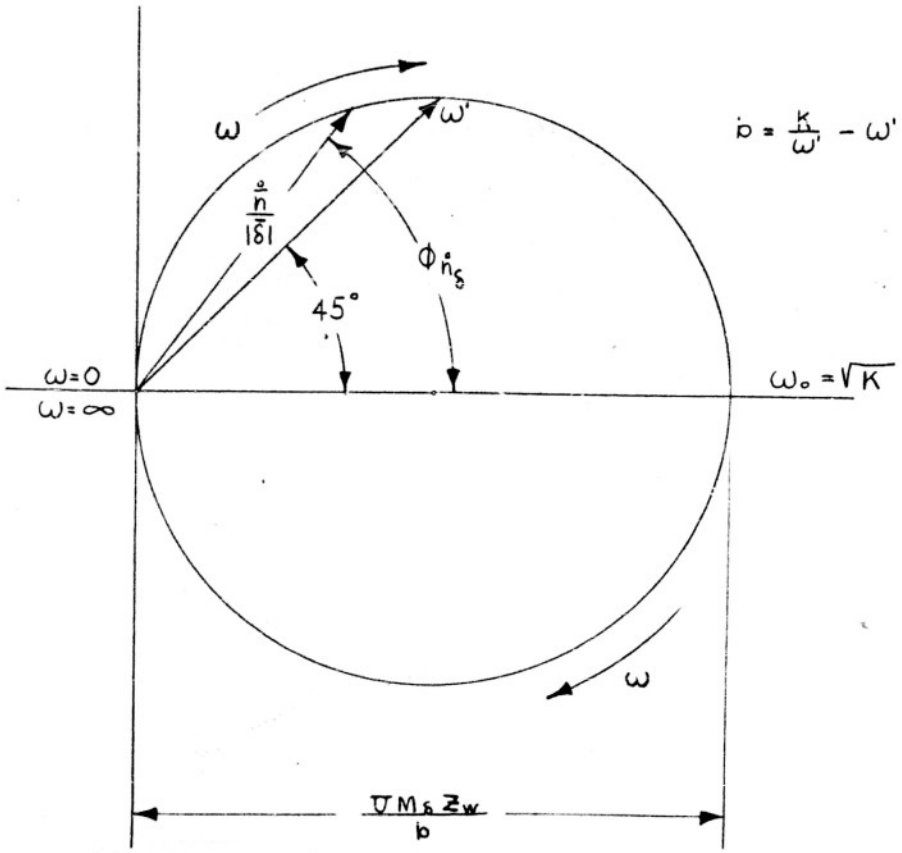

4-9-47 TCB

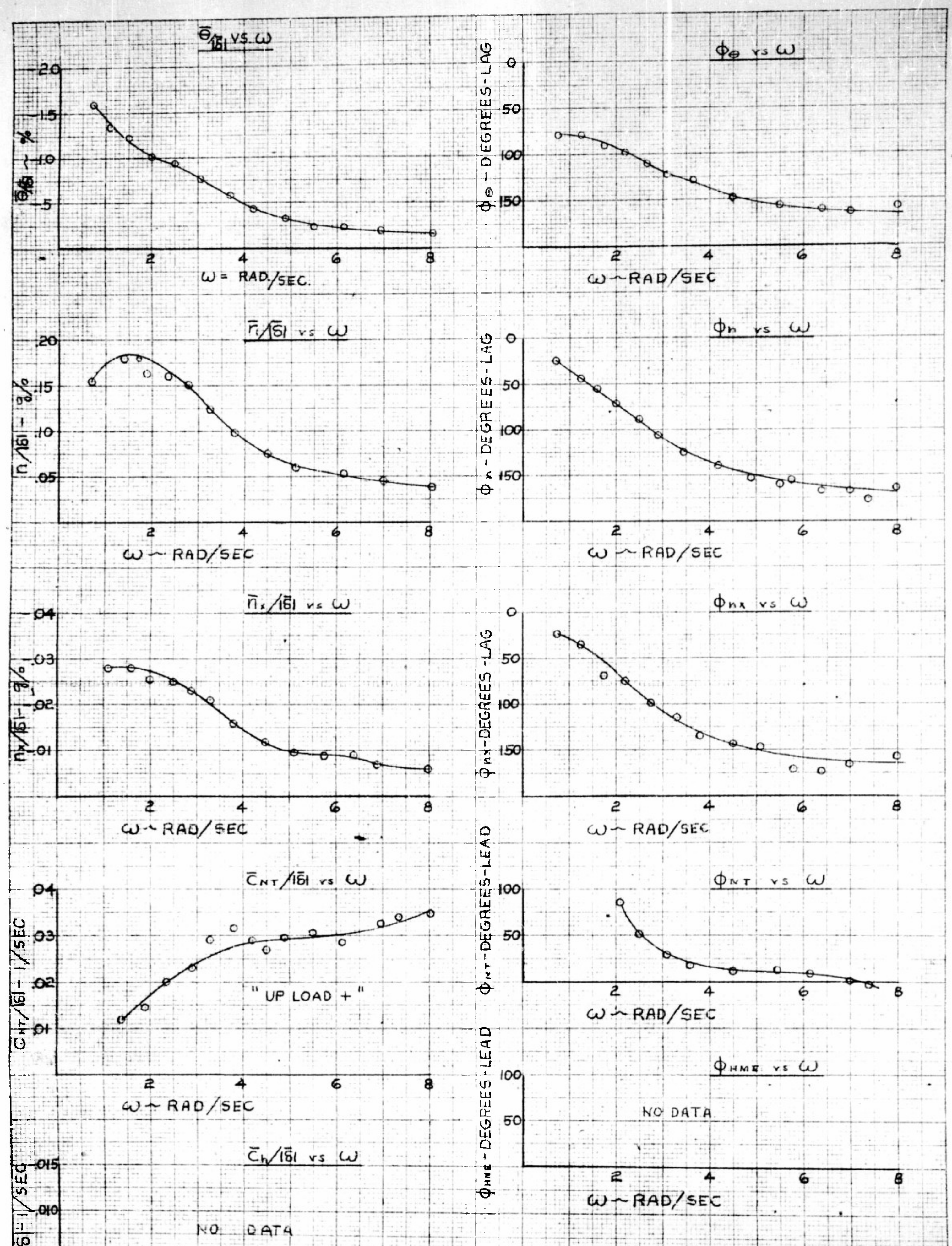

B25 J FLIGHT 77 11-6-46

CONDITIONS: CONSTANT POWER, TRIMMED AT 22 % MAC., 175 MPH. EAS. AT 10,000 FT., PRESSURE ALTITUDE OF 10,000 FT., CONSTANT SPEED OF 175 MPH. EAS.

Fig. 5a
Page 92

KEUFFEL & ESSER CO., N. Y. NO. 359-11LG
(8 × 10 to the inch, 80 lines accented)
MADE IN U.S.A.

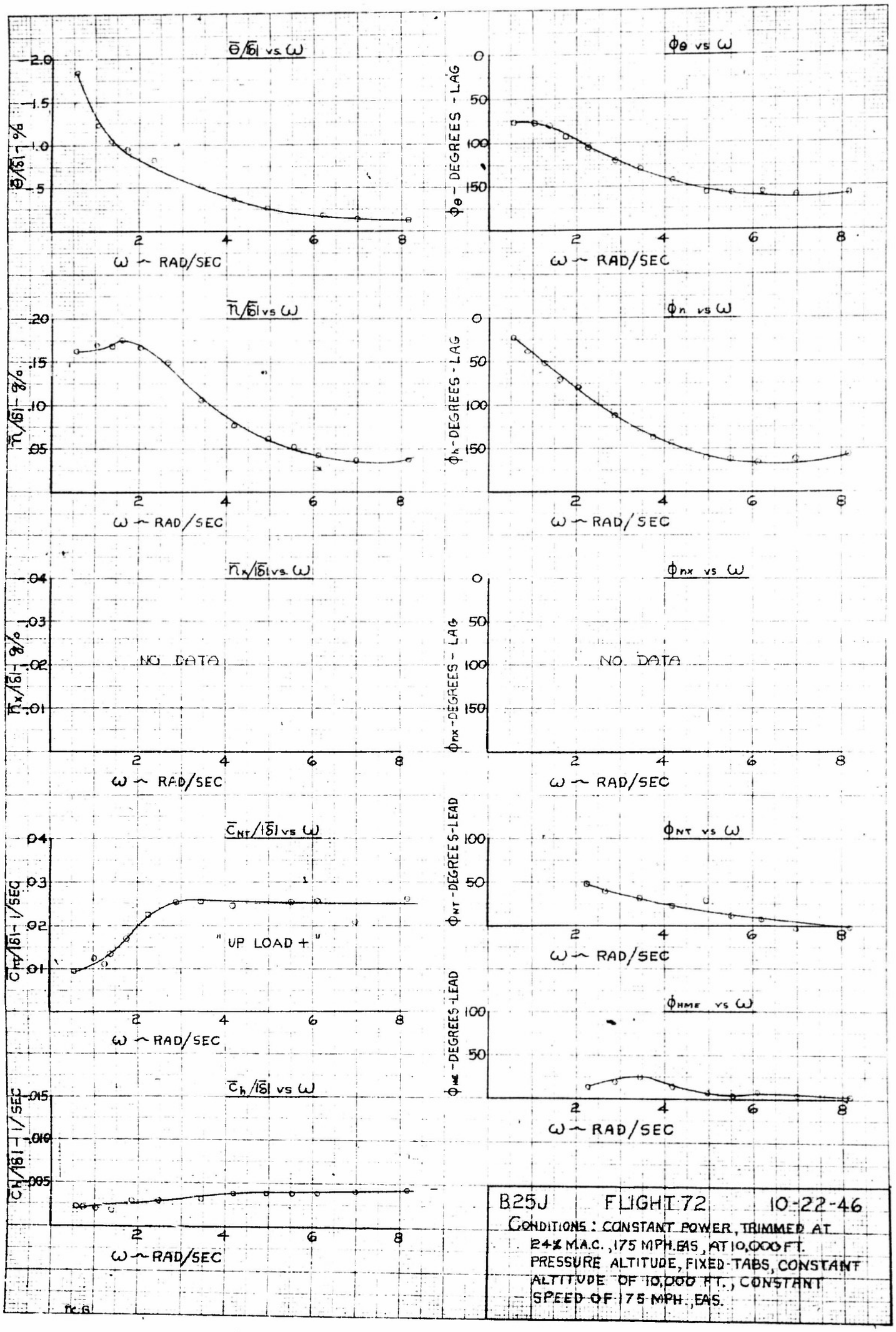

B25J FLIGHT 72 10-22-46

CONDITIONS: CONSTANT POWER, TRIMMED AT 24% M.A.C., 175 MPH. EAS, AT 10,000 FT. PRESSURE ALTITUDE, FIXED-TABS, CONSTANT ALTITUDE OF 10,000 FT., CONSTANT SPEED OF 175 MPH. EAS.

Fig. 5b
Page 93

KEUFFEL & ESSER CO., N. Y. NO. 389-11-LG
10 × 10 to the inch, 5th line accented.
MADE IN U. S. A.

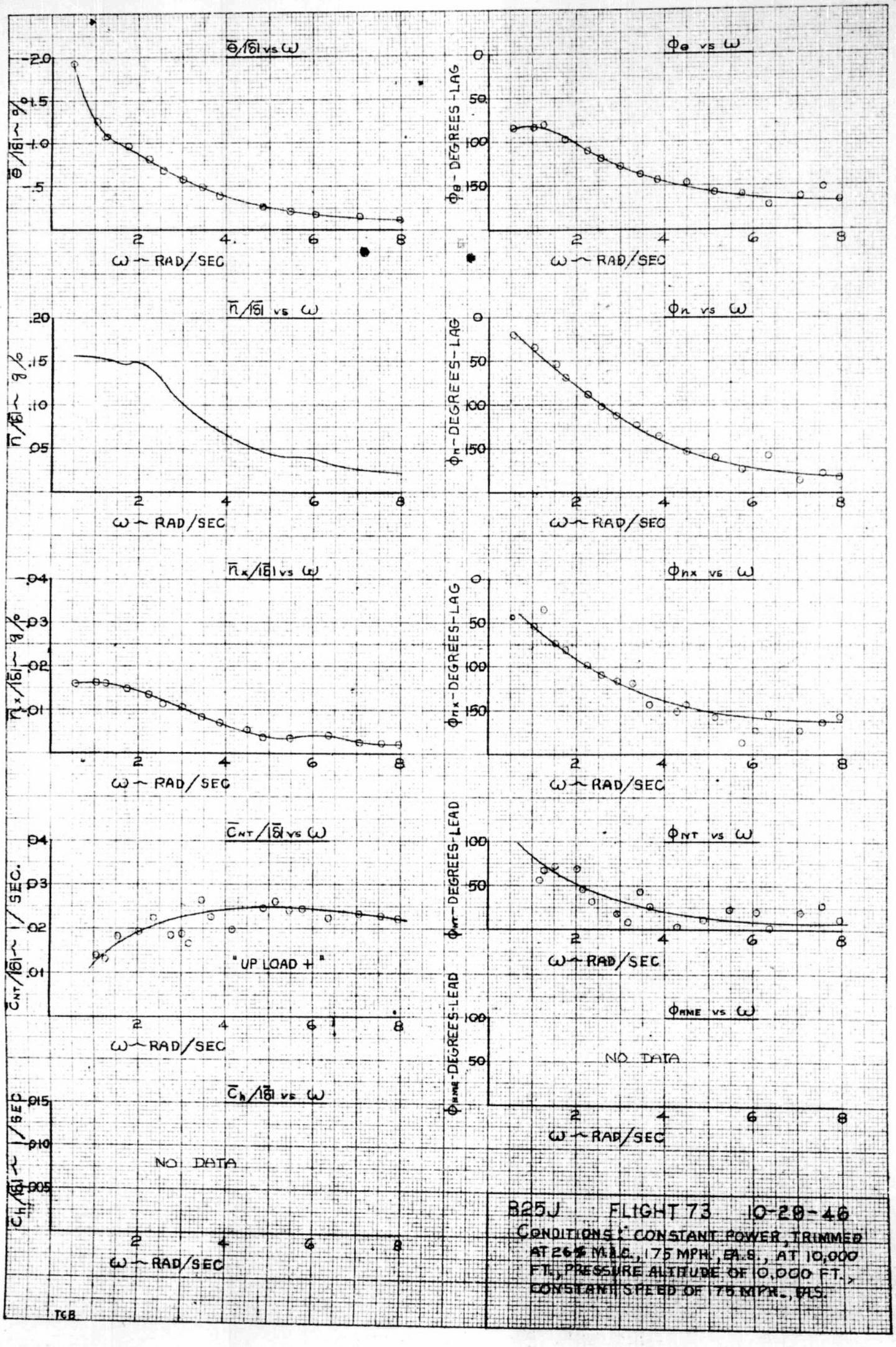

Fig. 50
Page 64

KEUFFEL & ESSER CO., N. Y. NO. 358-1110
10 X 10 to the ½ inch, 5th lines accented
MADE IN U.S.A.

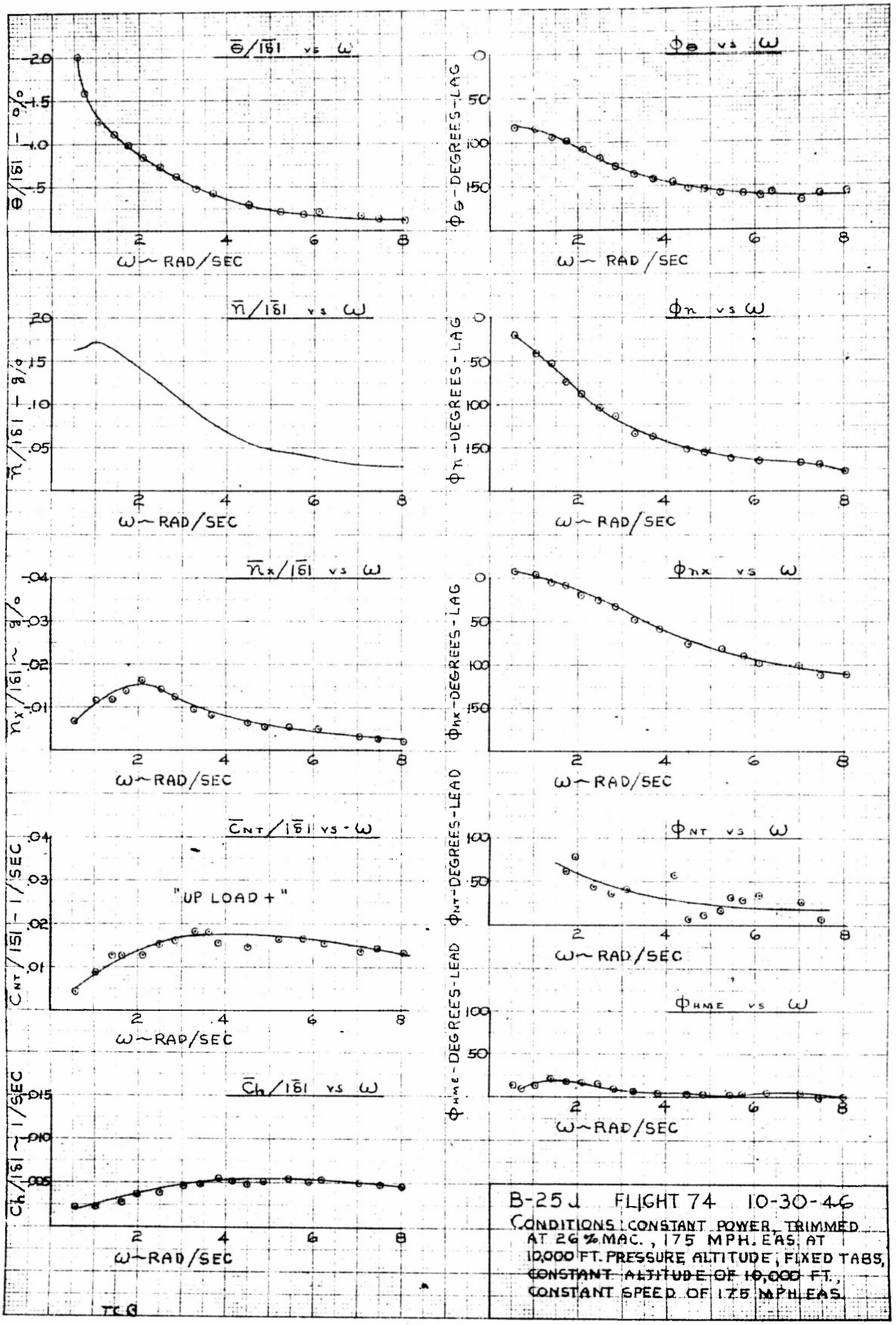

B-25 J FLIGHT 74 10-30-46

CONDITIONS: CONSTANT POWER, TRIMMED AT 26% MAC., 175 MPH. EAS AT 10,000 FT. PRESSURE ALTITUDE, FIXED TABS, ~~CONSTANT ALTITUDE OF 10,000 FT.~~, CONSTANT SPEED OF 175 MPH EAS.

Fig. 5d
Page 95

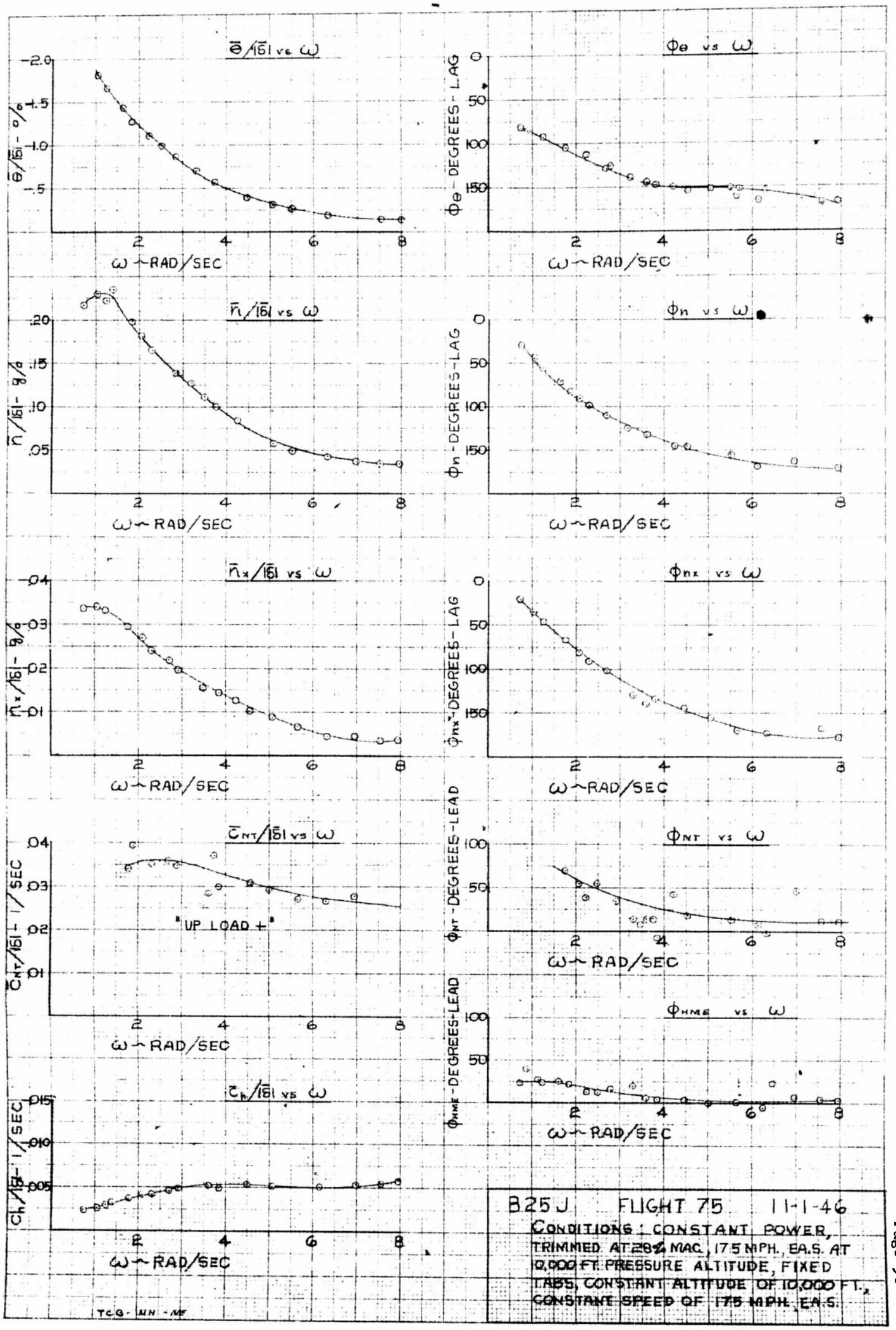

Fig. 59
Page 96

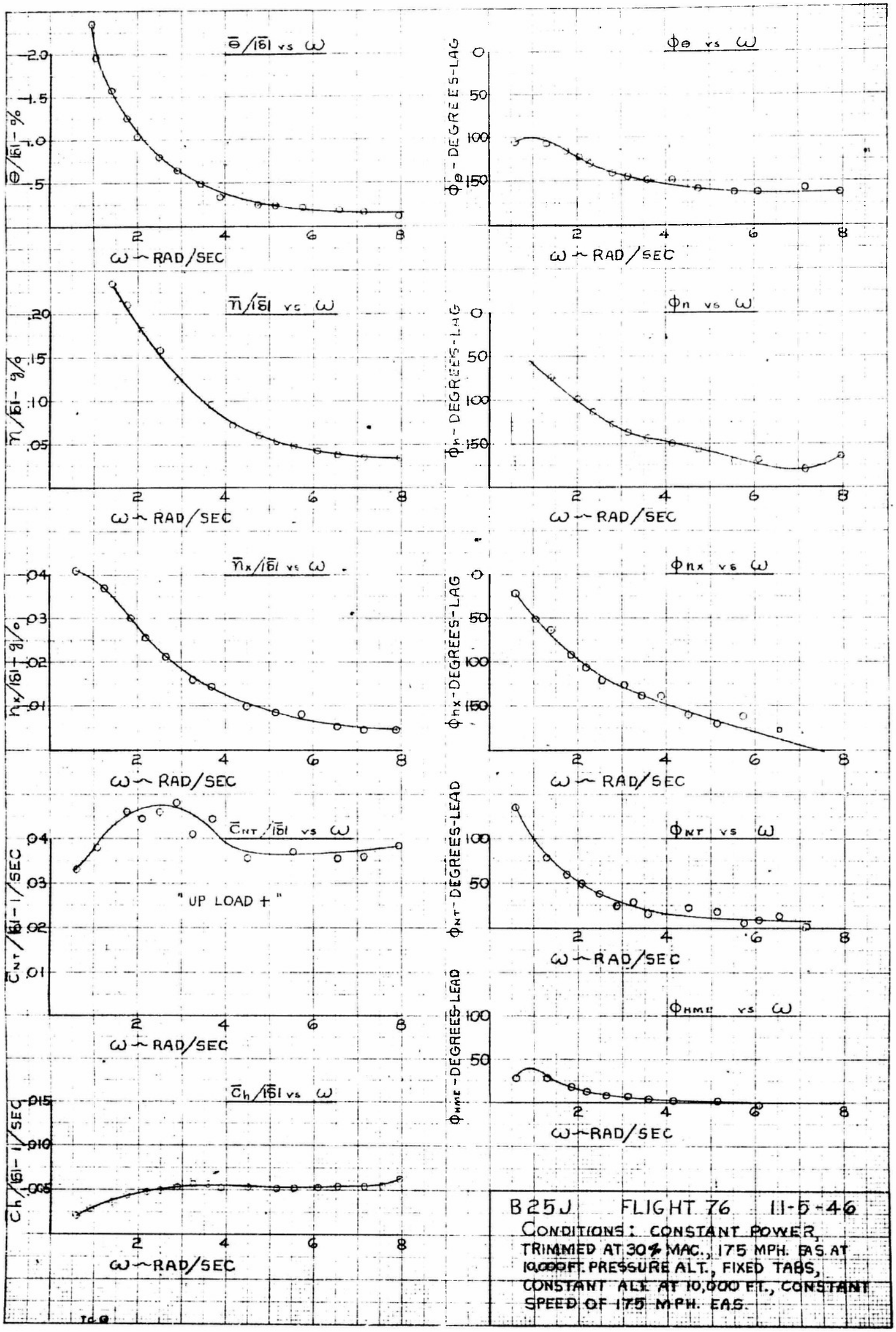

B25J FLIGHT 76 11-5-46

CONDITIONS: CONSTANT POWER, TRIMMED AT 30% MAC., 175 MPH. EAS AT 10,000 FT. PRESSURE ALT., FIXED TABS, CONSTANT ALT. AT 10,000 FT., CONSTANT SPEED OF 175 MPH. EAS.

Fig. 51
Page 97

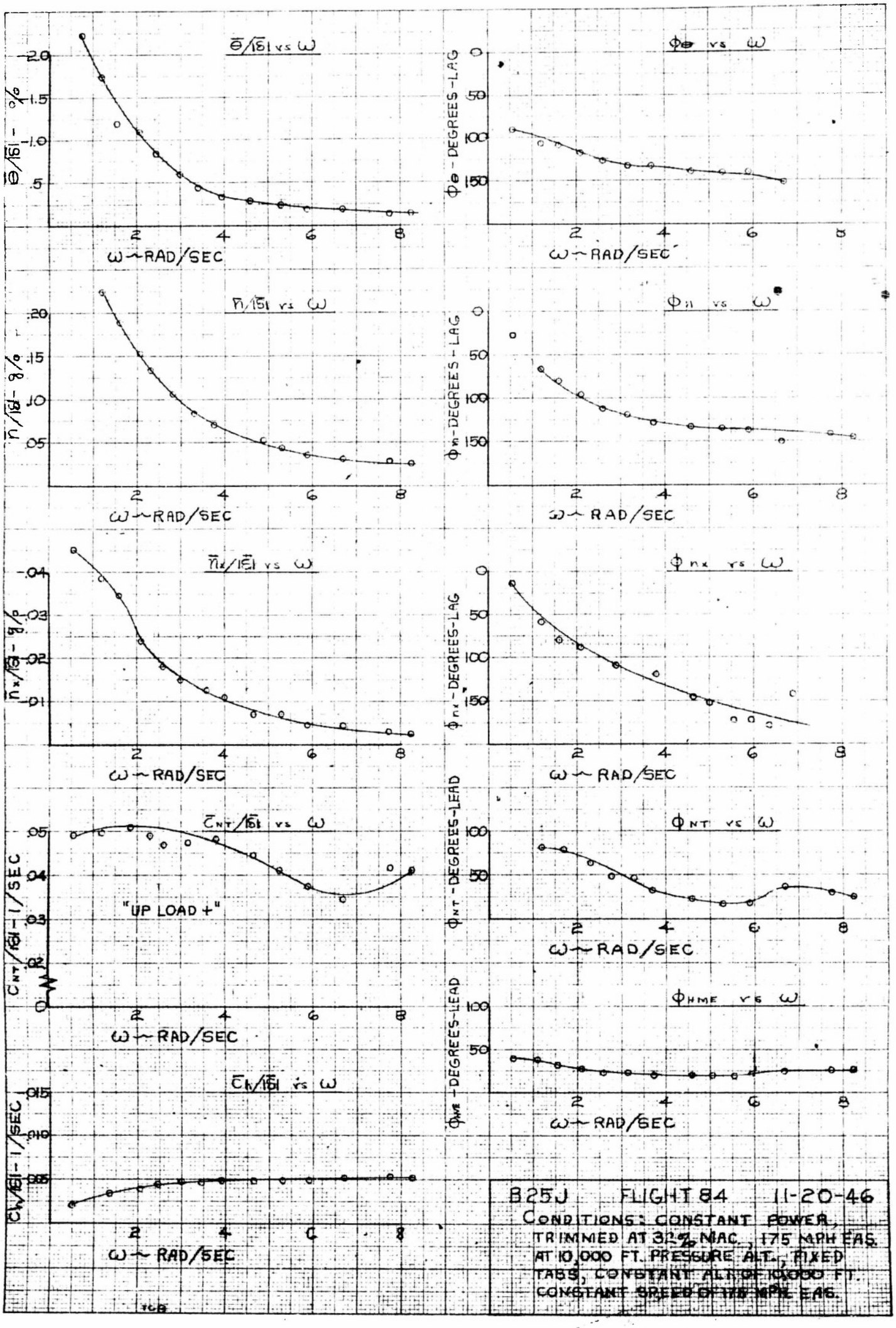

B25J FLIGHT 84 11-20-46

CONDITIONS: CONSTANT POWER, TRIMMED AT 3½ NAC., 175 MPH EAS. AT 10,000 FT. PRESSURE ALT., FIXED TABS, CONSTANT ALT. OF 10,000 FT. CONSTANT SPEED OF 175 MPH EAS.

Fig. 58
Page 98

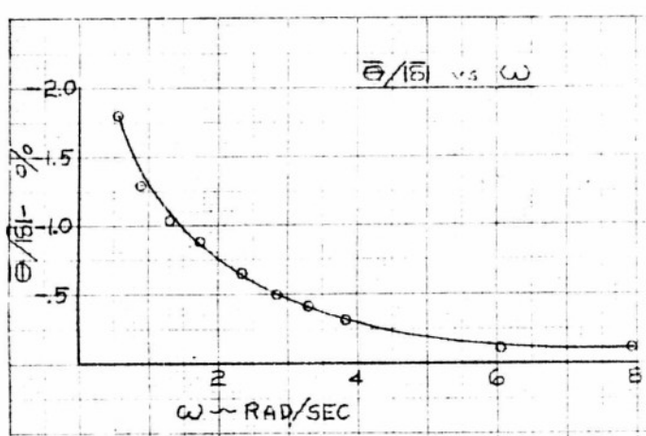

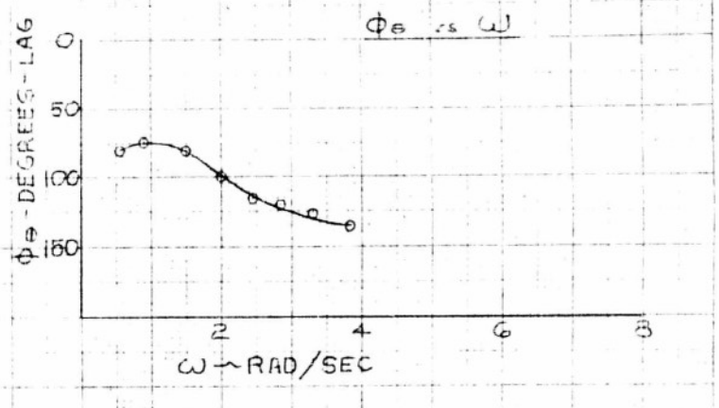

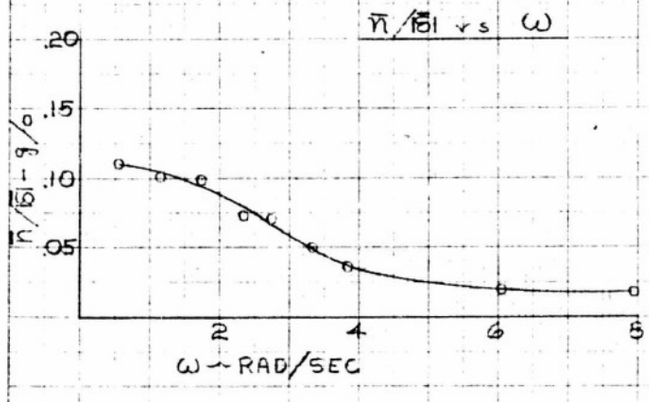

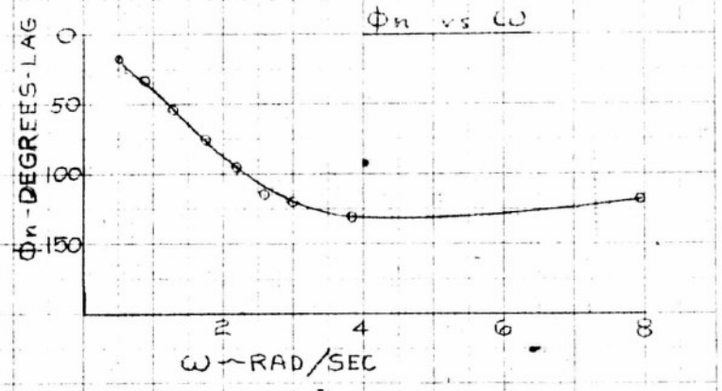

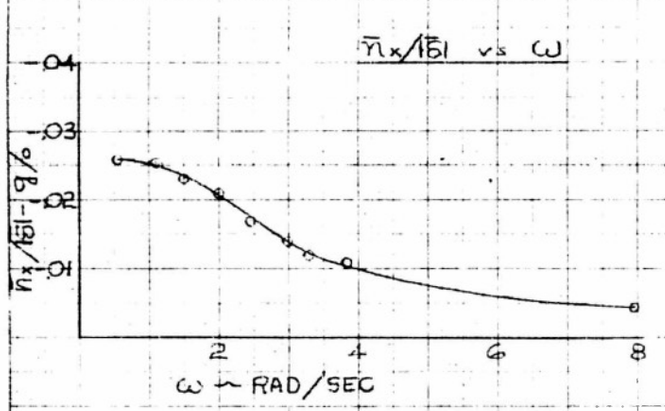

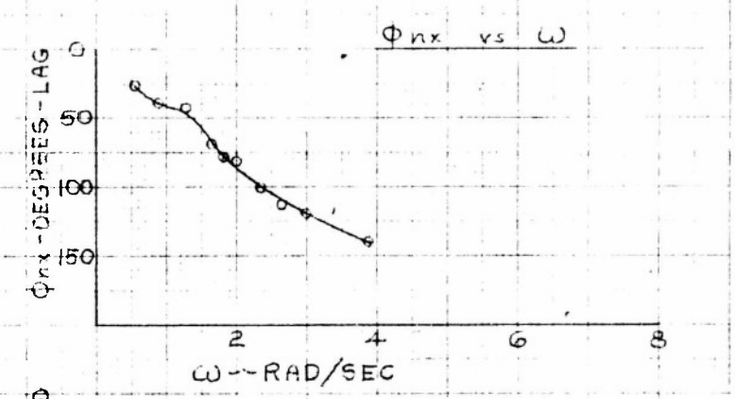

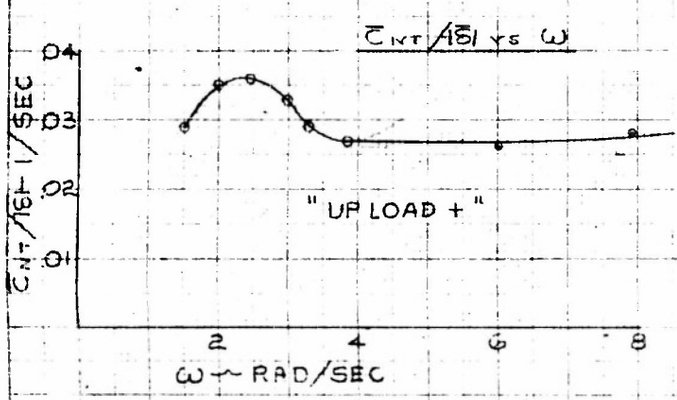

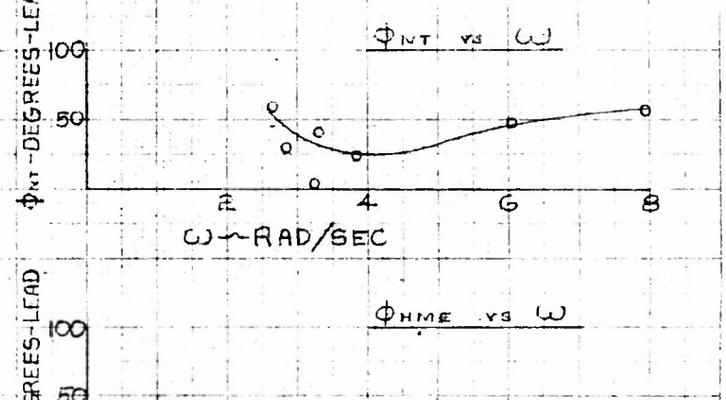

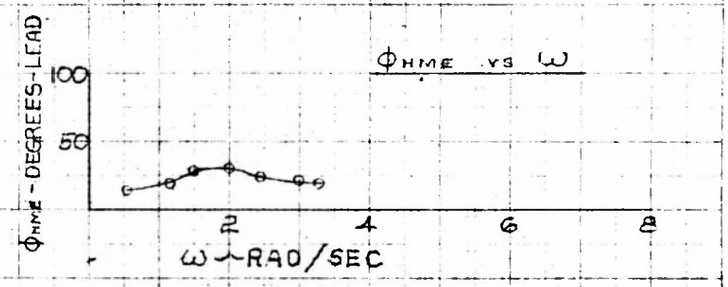

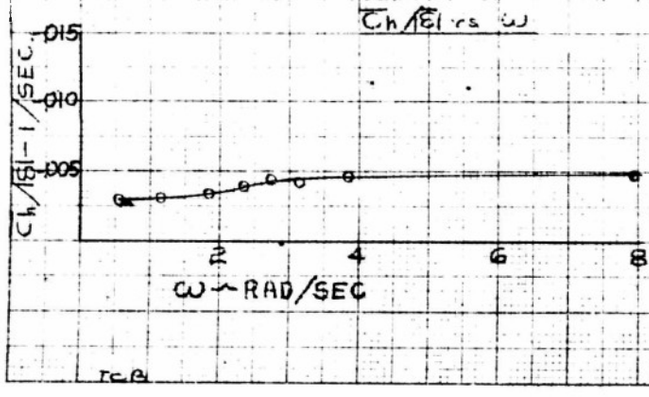

B25J FLIGHT 78 11-8-46
CONDITIONS: CONSTANT POWER, TRIMMED AT 22" MAG., 185 MPH. E.A.S. AT 10,000 FEET PRESSURE ALT., FIXED TABS, CONSTANT ALT. OF 10,000 FT., CONSTANT SPEED OF 135 MPH. E.A.S.

Fig. 5h
Page 69

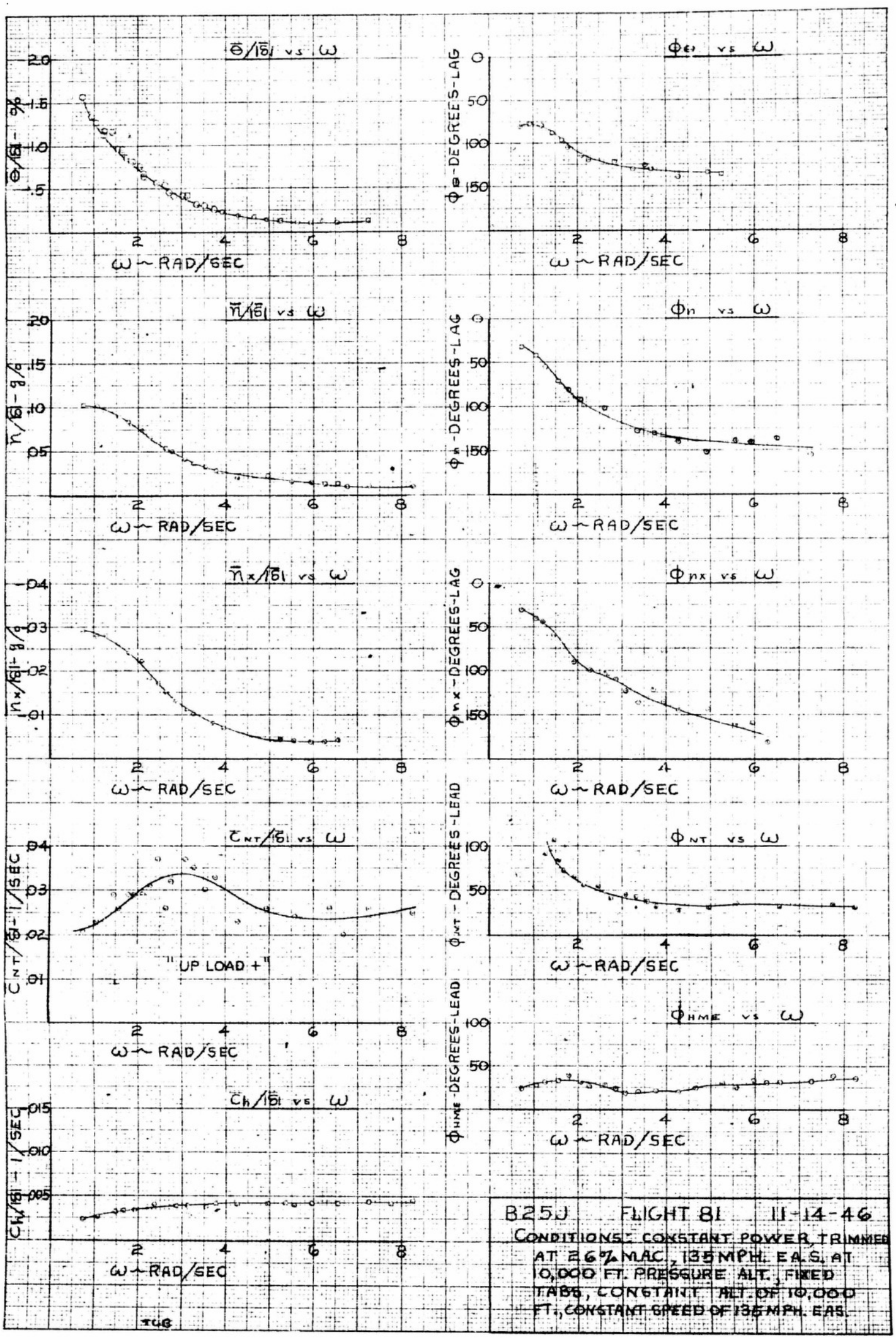

B25J FLIGHT 81 11-14-46

CONDITIONS: CONSTANT POWER, TRIMMED AT 26% MAC, 135 MPH. E.A.S. AT 10,000 FT. PRESSURE ALT., FIXED TABS, CONSTAINT ALT. OF 10,000 FT., CONSTANT SPEED OF 135 MPH. EAS.

TUG

Fig. 51
Page 100

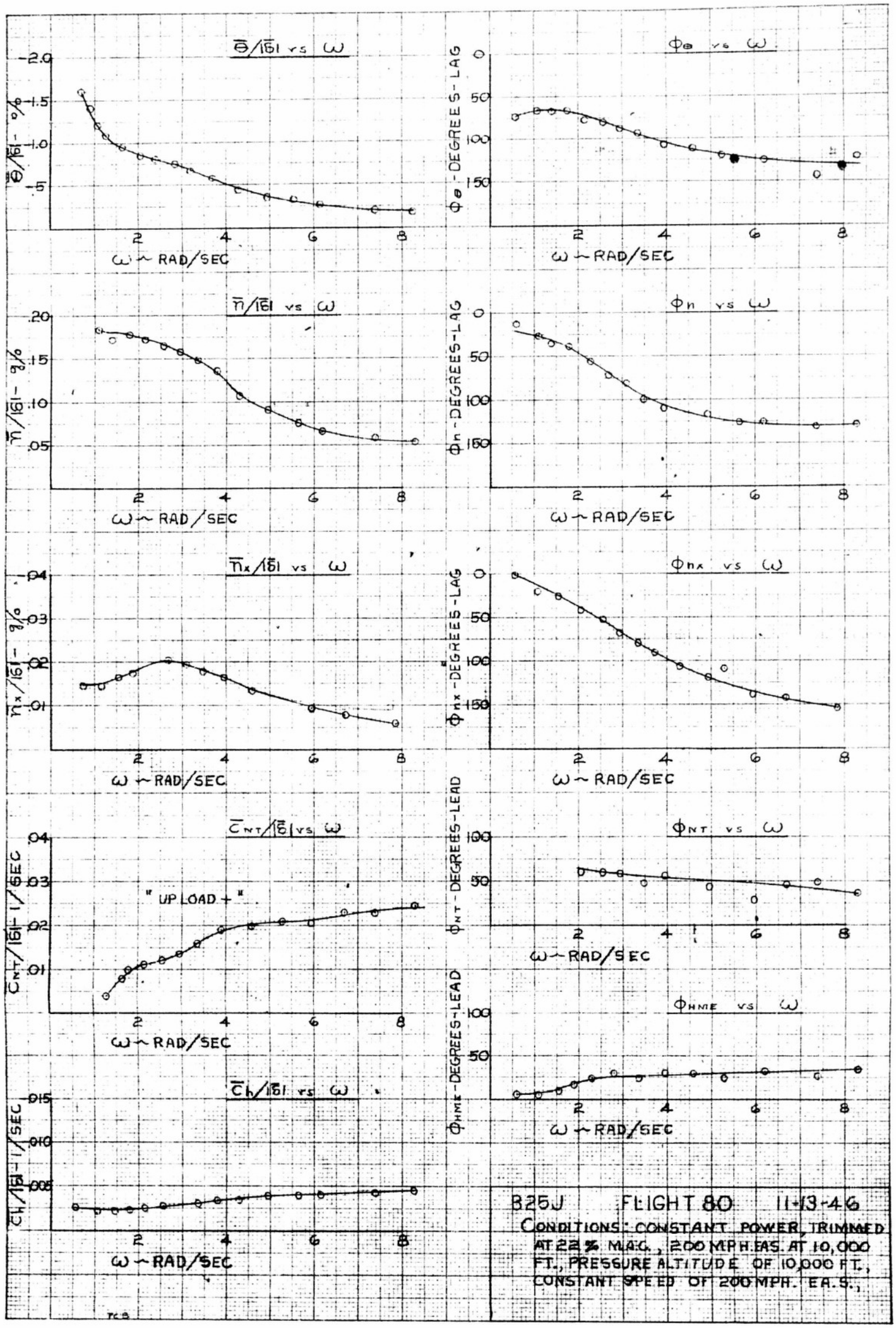

Fig. 5J
Page 101

KEUFFEL & ESSER CO. N. Y. NO. 359-1160

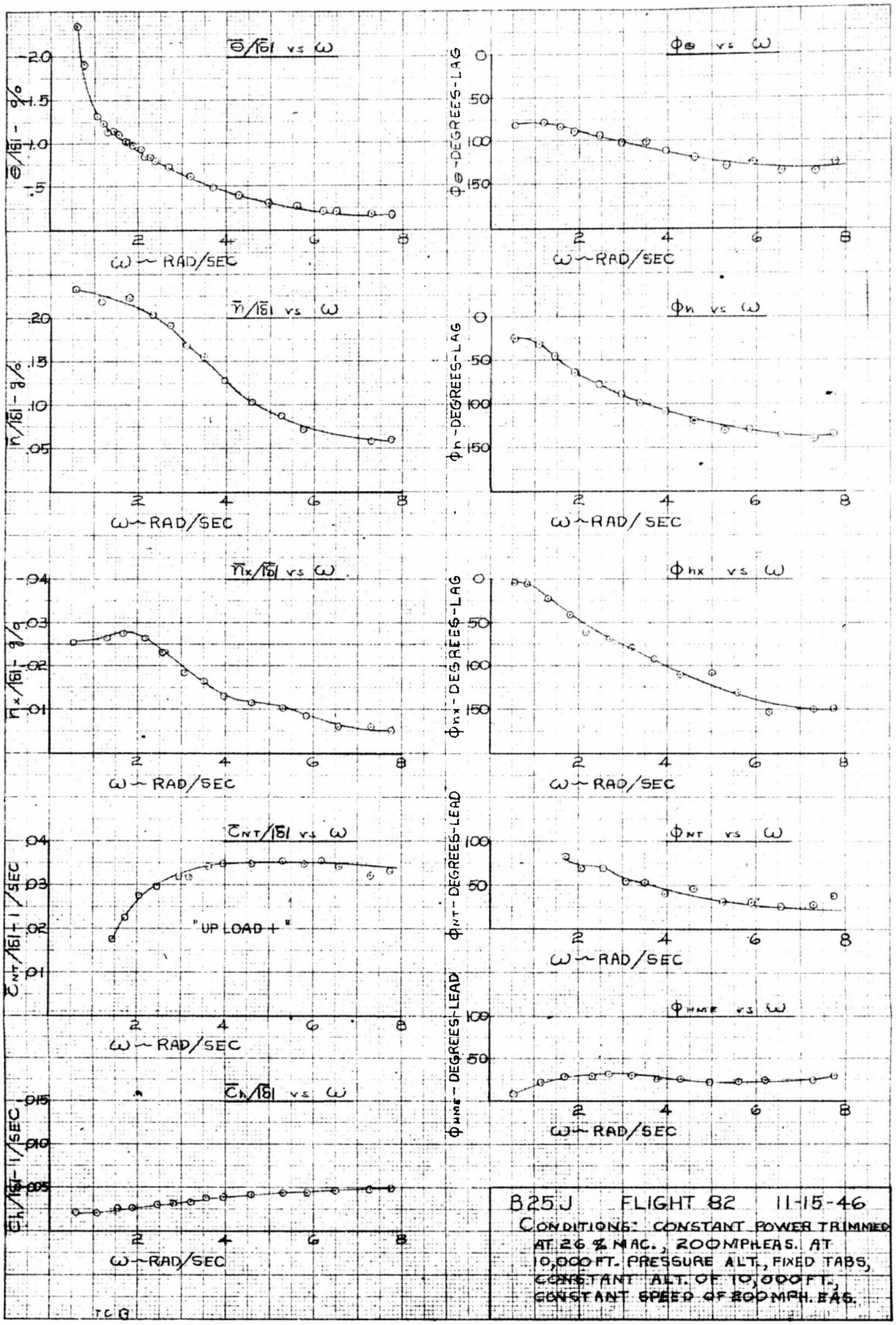

B25J FLIGHT 82 11-15-46

CONDITIONS: CONSTANT POWER TRIMMED AT 26 % MAC., 200 MPH EAS. AT 10,000 FT. PRESSURE ALT., FIXED TABS, CONSTANT ALT. OF 10,000 FT., CONSTANT SPEED OF 200 MPH. EAS.

Fig. 5k
Page 102

CIRCLE DIAGRAM

VARIATION OF $\frac{|n|}{|\delta|}$ AND $\phi^{\circ}_{n_s}$ WITH FREQUENCY

3 25J 43-3892 FLIGHT 77
C.G. - 22.0 %
E.A.S. - 175 M.P.H.

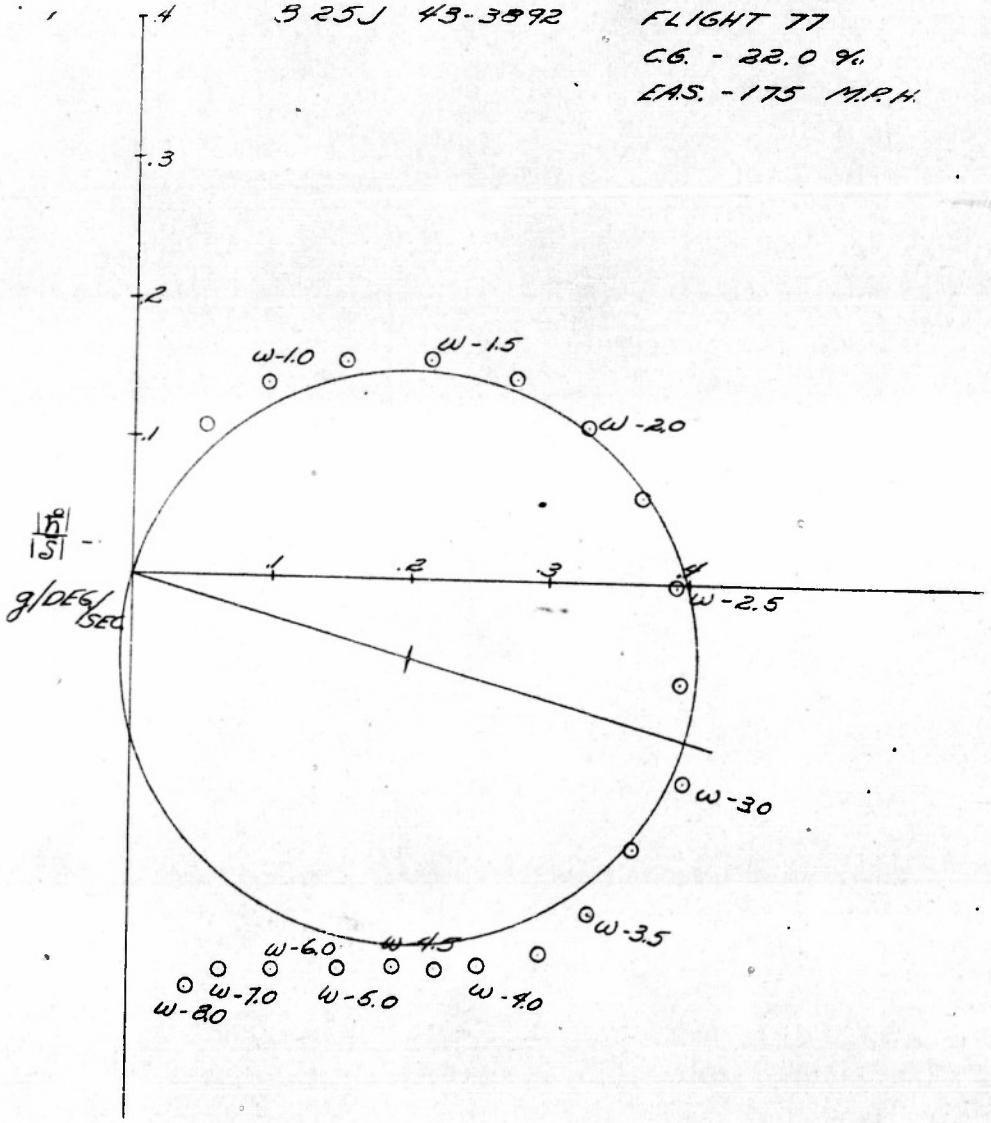

CIRCLE DIAGRAM

VARIATION OF $\frac{\dot{q}}{|\delta|} \cos(\tan^{-1}\frac{\omega}{-Z_w}) \angle(\phi_{\frac{q}{\delta}} - \tan^{-1}\frac{\omega}{-Z_w})$ WITH FREQUENCY

B25J 43-3892
FLIGHT 77

C.G -22 %
E.A.S - 175 M.P.H.

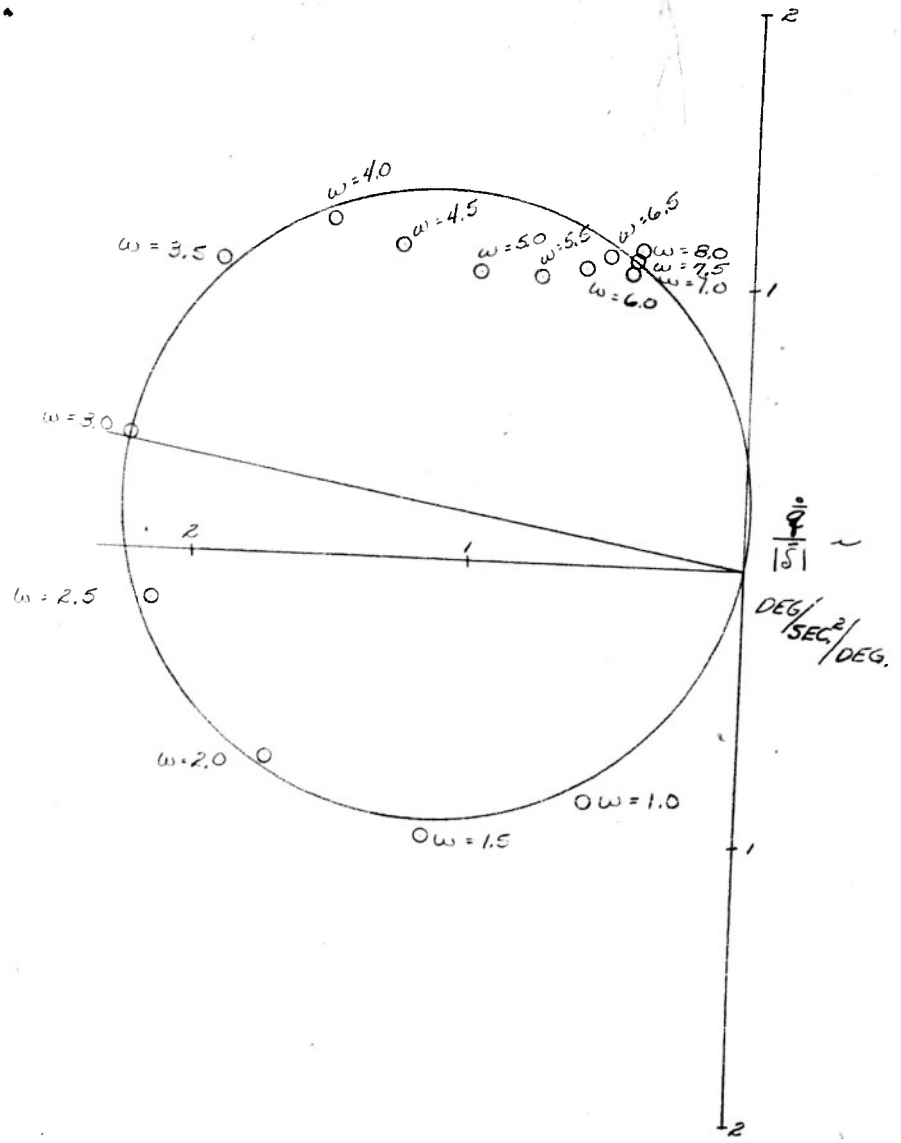

CIRCLE DIAGRAM

VARIATION OF $\frac{|\eta|}{|\delta|}$ AND $\phi_{\frac{\eta}{\delta}}^{\circ}$ WITH FREQUENCY

B25J 43-3892

FLIGHT 72
C.G. - 24.0 %
E.A.S. - 175 M.P.H.

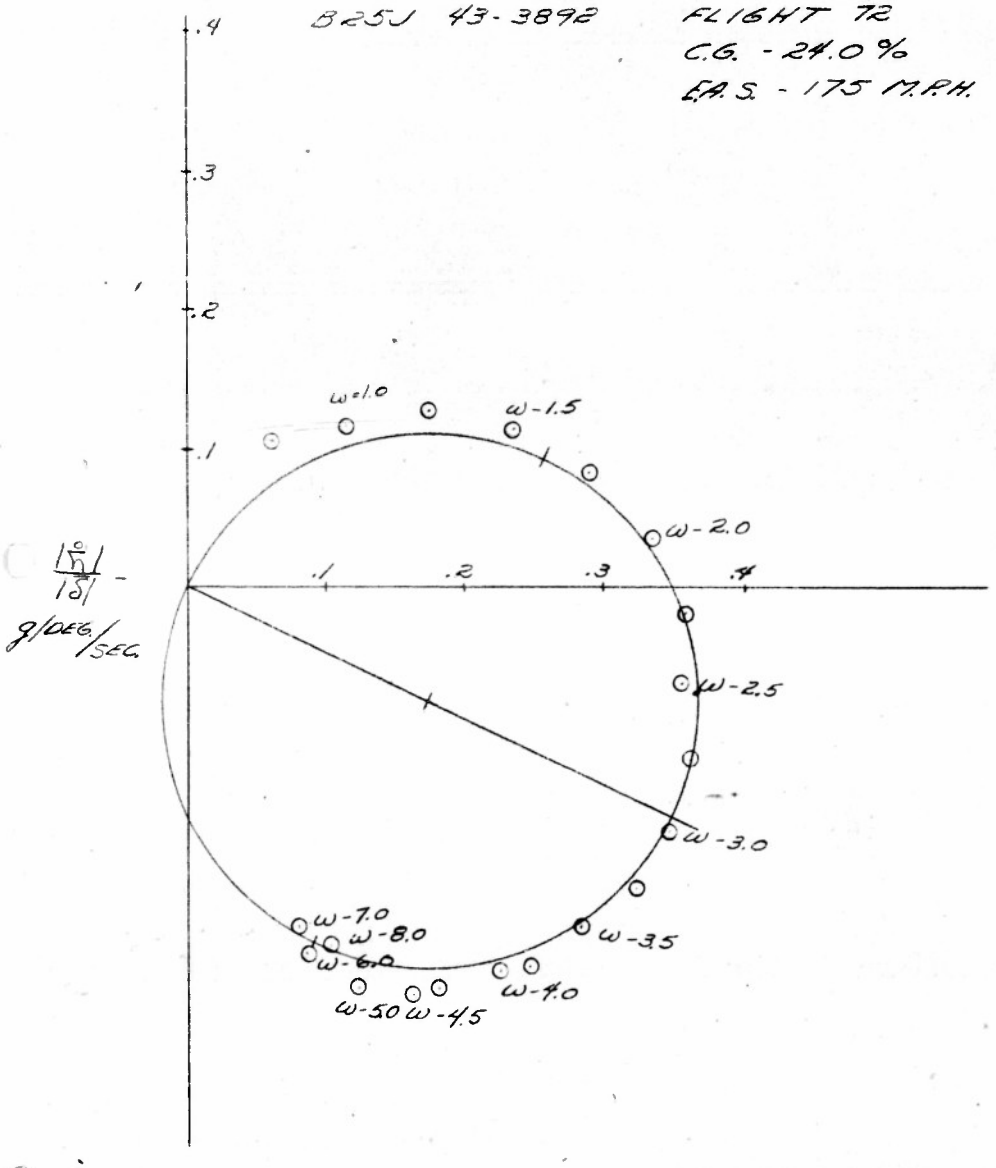

JER 1-7-47

CIRCLE DIAGRAM

VARIATION OF $\frac{\ddot{\theta}}{|\ddot{\theta}|}\cos\left(\tan^{-1}\frac{\omega}{-2\zeta\omega}\right)$ & $\left(\phi_{\frac{\ddot{\theta}}{\theta}} - \tan^{-1}\frac{\omega}{-2\zeta\omega}\right)$ WITH FREQUENCY.

B25J 43-3892
FLIGHT 72

C.G. = 24%
E.A.S. = 175 M.P.H.

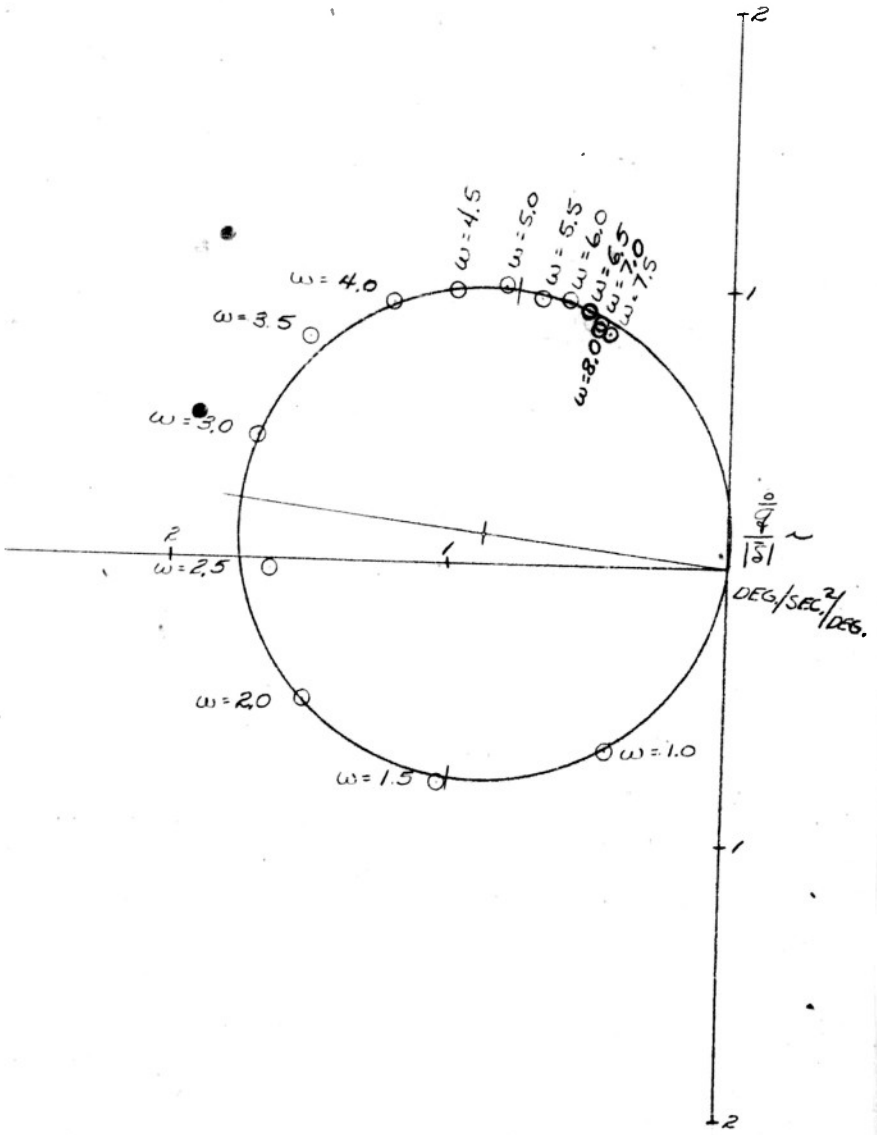

CIRCLE DIAGRAM

VARIATION OF $\frac{\dot{h}}{C_R}$ AND $\phi_{\frac{\dot{h}}{C_R}}$ WITH FREQUENCY

B25J 43-3892
FLIGHT 72

C.G. = 24 %
E.A.S. = 175 MPH

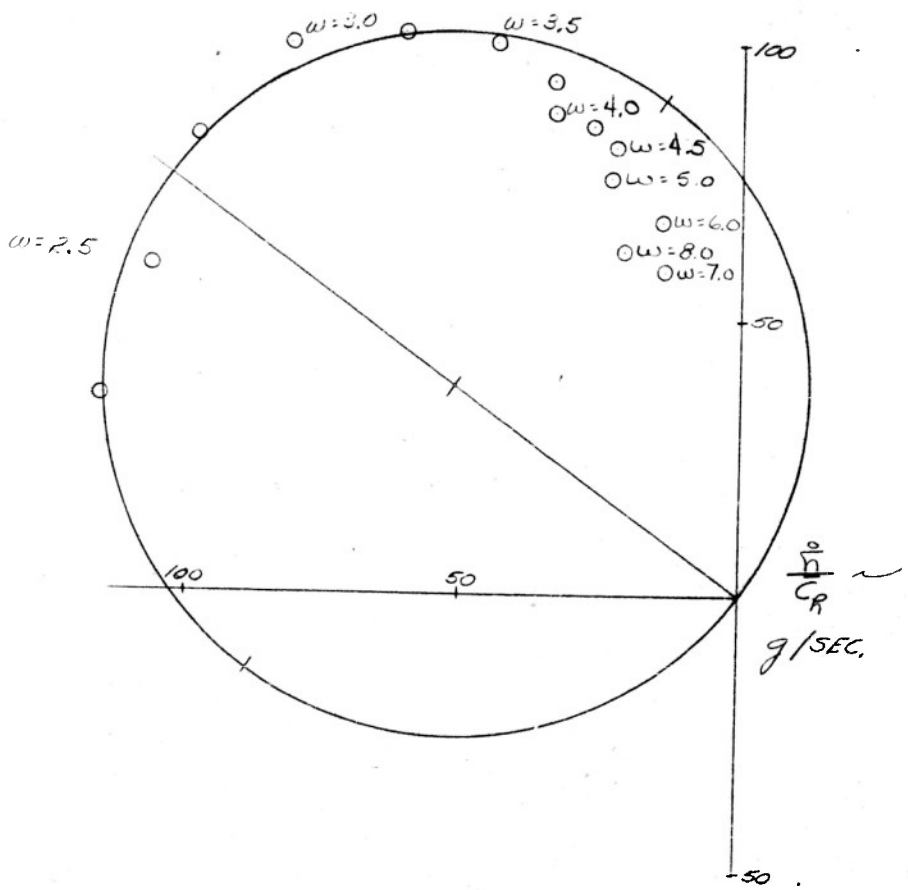

CIRCLE DIAGRAM

VARIATION OF $\frac{\partial}{\partial}/C_{N_\alpha} \cos\left(\tan^{-1}\frac{\omega}{-\frac{1}{2}\omega}\right) \frac{1}{\pi}\left(\gamma_{\frac{\partial}{\partial}} - \tan^{-1}\frac{\omega}{-\frac{1}{2}\omega}\right)$ WITH FREQUENCY

B25J
FLIGHT 72

C.G. = 24% MAC
E.A.S. = 175 MPH.

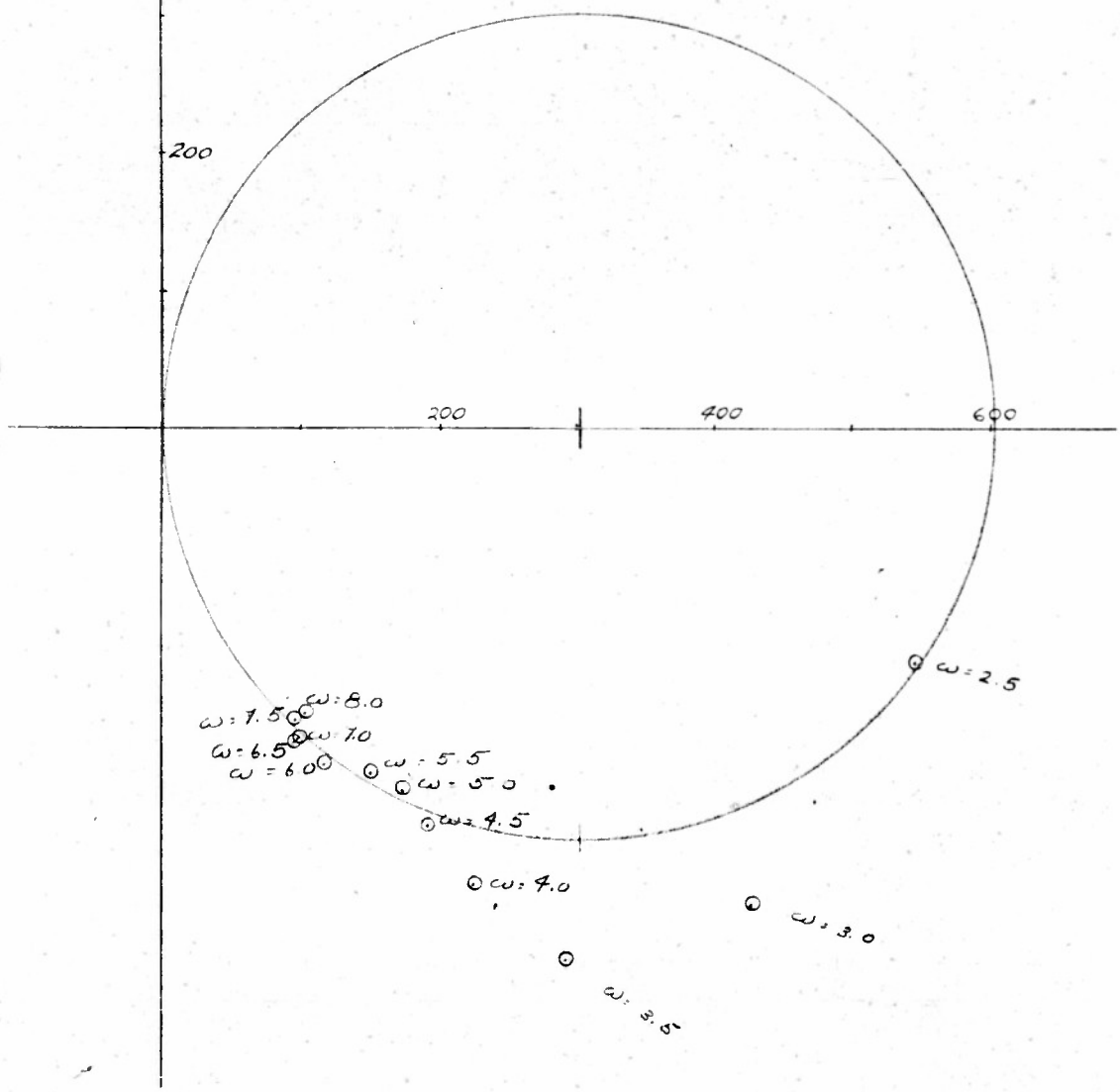

CIRCLE DIAGRAM

VARIATION OF $\frac{|\ddot{n}|}{|\ddot{\delta}|}$ AND $\phi_{\frac{\ddot{n}}{\ddot{\delta}}}$ WITH FREQUENCY

825 J 43-3892
FLIGHT 73

C.G. = 26 %
E.A.S. = 175 MPH

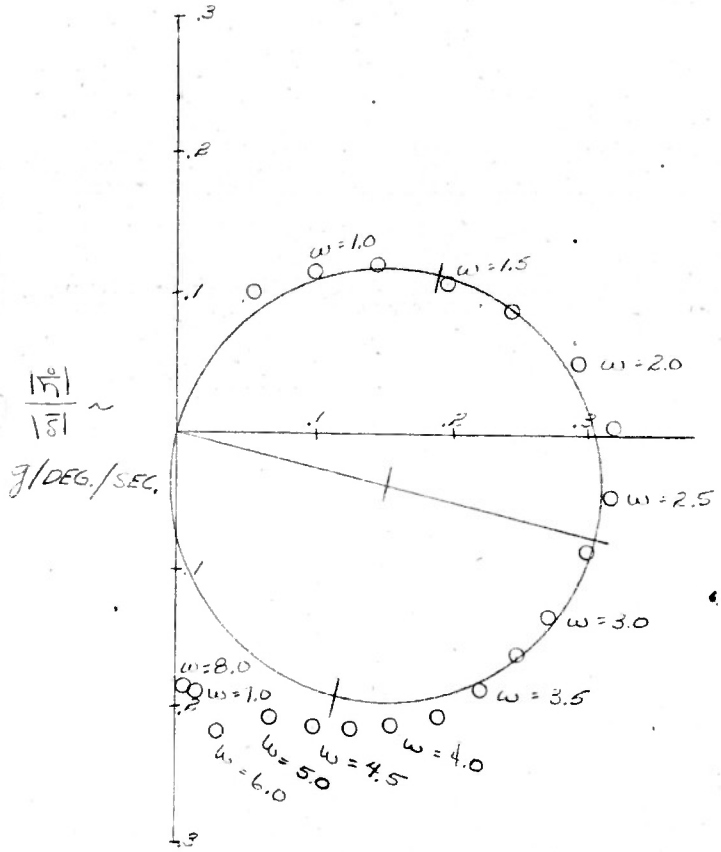

CIRCLE DIAGRAM.

VARIATION OF $\frac{\ddot{\phi}}{\delta}$ COS $(TAN^{-1}\frac{\omega}{2\zeta\omega})$ $\frac{\ddot{\phi}}{\delta}$ $(\phi_{\frac{\ddot{\phi}}{\delta}} - TAN^{-1}\frac{\omega}{2\zeta\omega})$ WITH FREQUENCY

B25J 43-3892
FLIGHT 73

C.G. = 26 %
E.A.S. = 175 M.P.H.

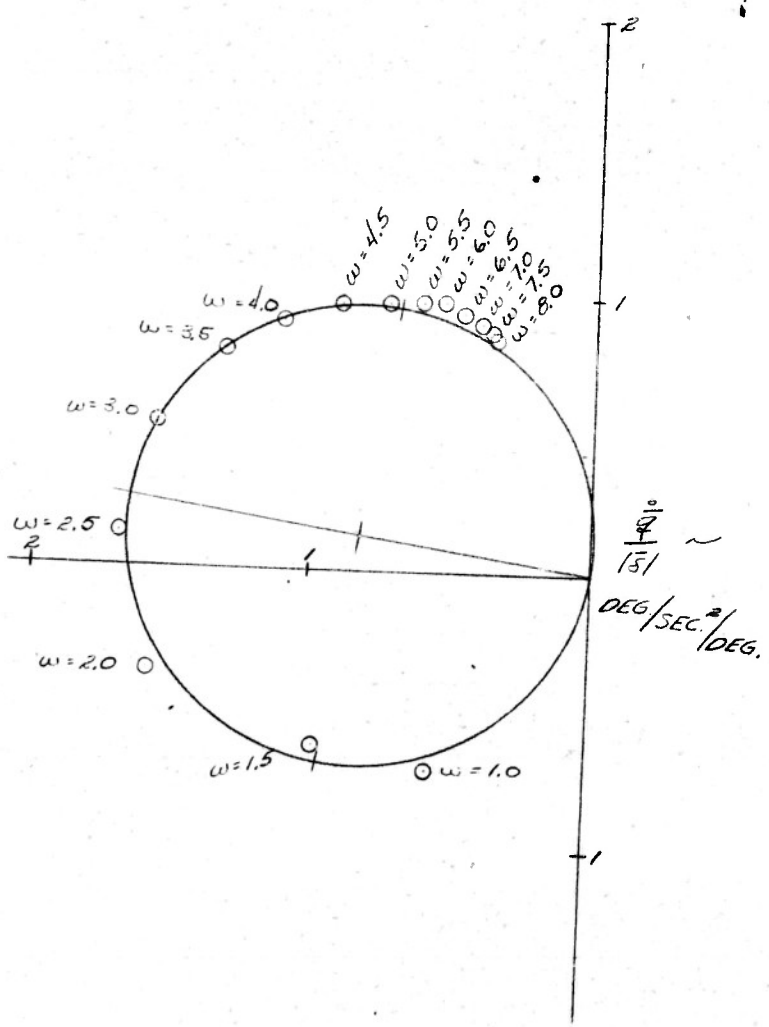

CIRCLE DIAGRAM

VARIATION OF $\frac{|\bar{n}|}{|\bar{\delta}|}$ AND ϕ_{n_s} WITH FREQUENCY

B25J 43-3892 C.G. = 26. %
FLIGHT 74 E.A.S. = 175 M.P.H.

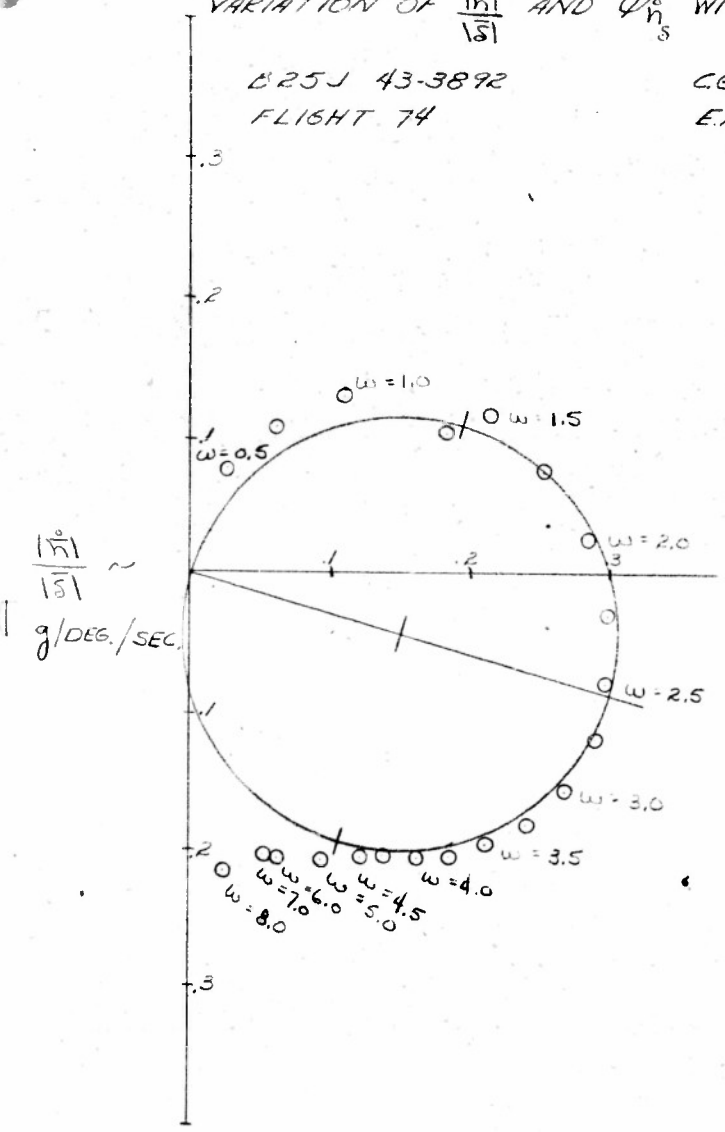

$\frac{|\bar{n}|}{|\bar{\delta}|}$ ~ g/DEG./SEC.

CIRCLE DIAGRAM

VARIATION OF $\frac{\ddot{\phi}}{|\delta|}\cos\left(\tan^{-1}\frac{\omega}{-\frac{1}{2}w}\right)$ & $\left(\phi_{\frac{\ddot{\phi}}{\delta}}^{\circ} - \tan^{-1}\frac{\omega}{-\frac{1}{2}w}\right)$ WITH FREQUENCY

B 25 J 43-3892
FLIGHT 74

C.G. = 26 %
E.A.S. = 175 MPH

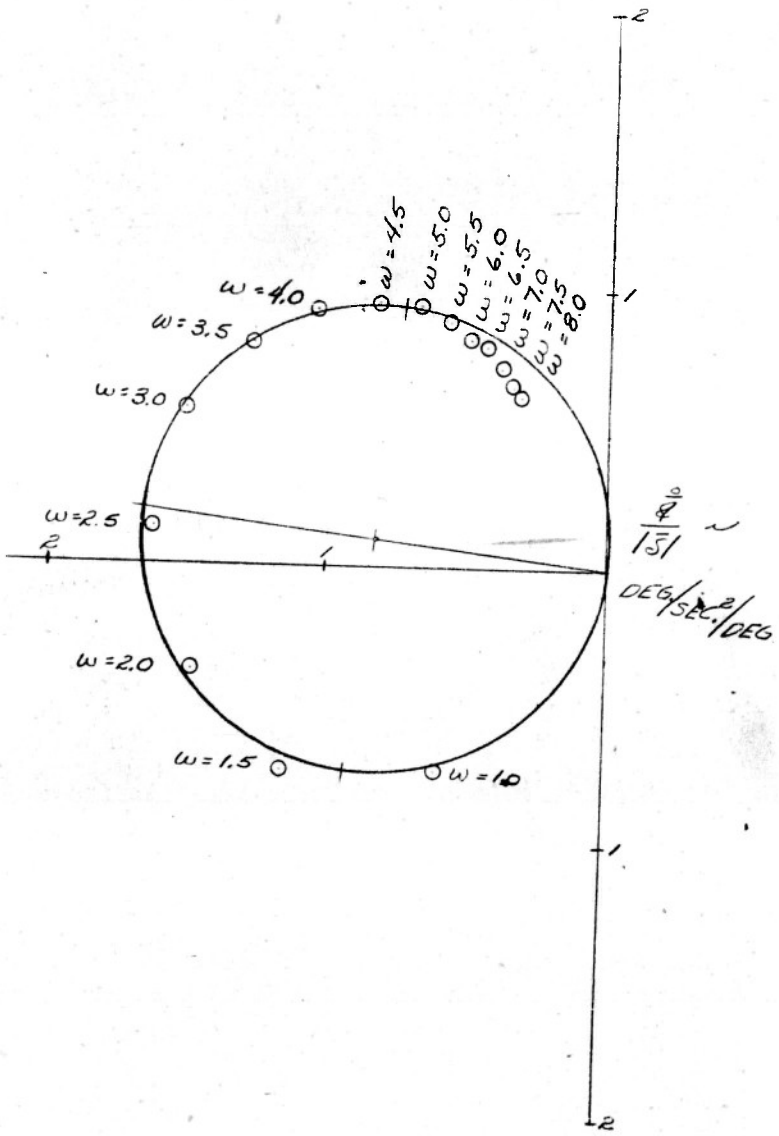

CIRCLE DIAGRAM

VARIATION OF $\frac{n^o}{C_R}$ AND $\phi_{\frac{n}{C_R}}$ WITH FREQUENCY

825J 43-3892
FLIGHT 74

C.G. = 26 %
E.A.S. = 175 M.P.H.

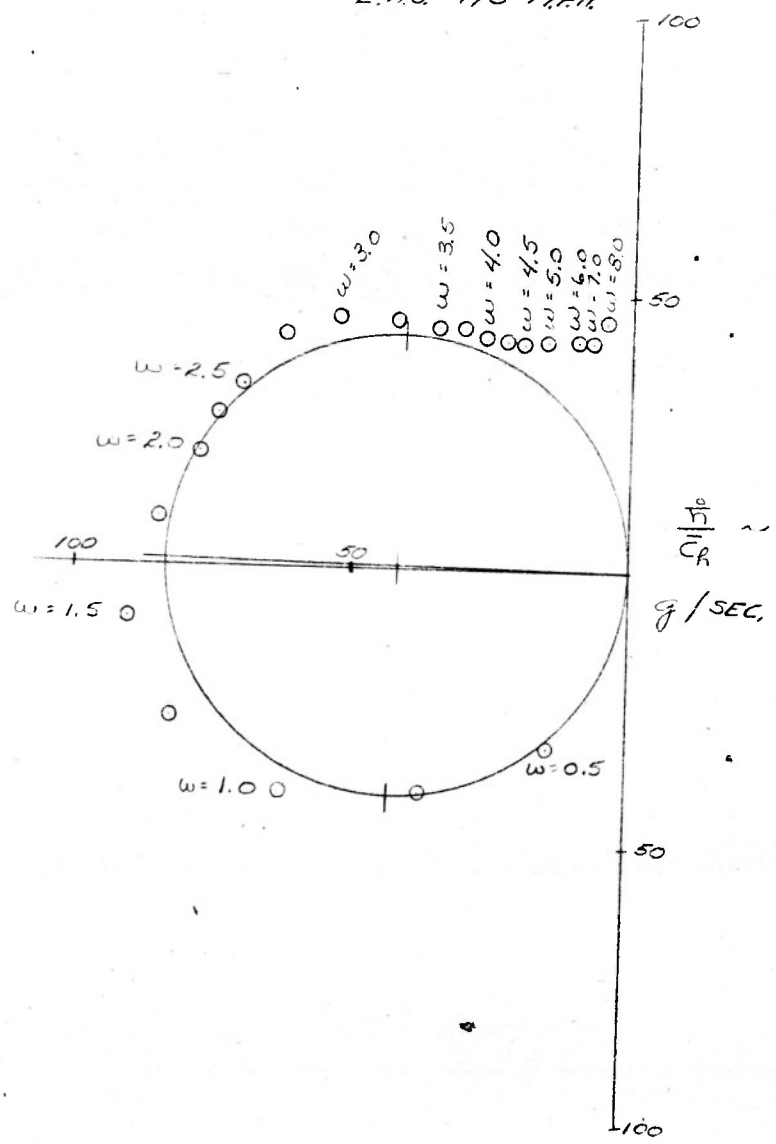

CIRCLE DIAGRAM

VARIATION OF $\frac{\hat{q}}{\alpha}C_{L_\alpha}\cos(\tan^{-1}\frac{\omega}{2\omega})\,\xi_T(\phi_{\frac{\hat{q}}{\alpha}_{C_{L_\alpha}}} - \tan^{-1}\frac{\omega}{-2\omega})$ WITH FREQUENCY

B25J
FLIGHT 74

C.G. = 26% M.A.C.
E.A.S. = 175 M.P.H.

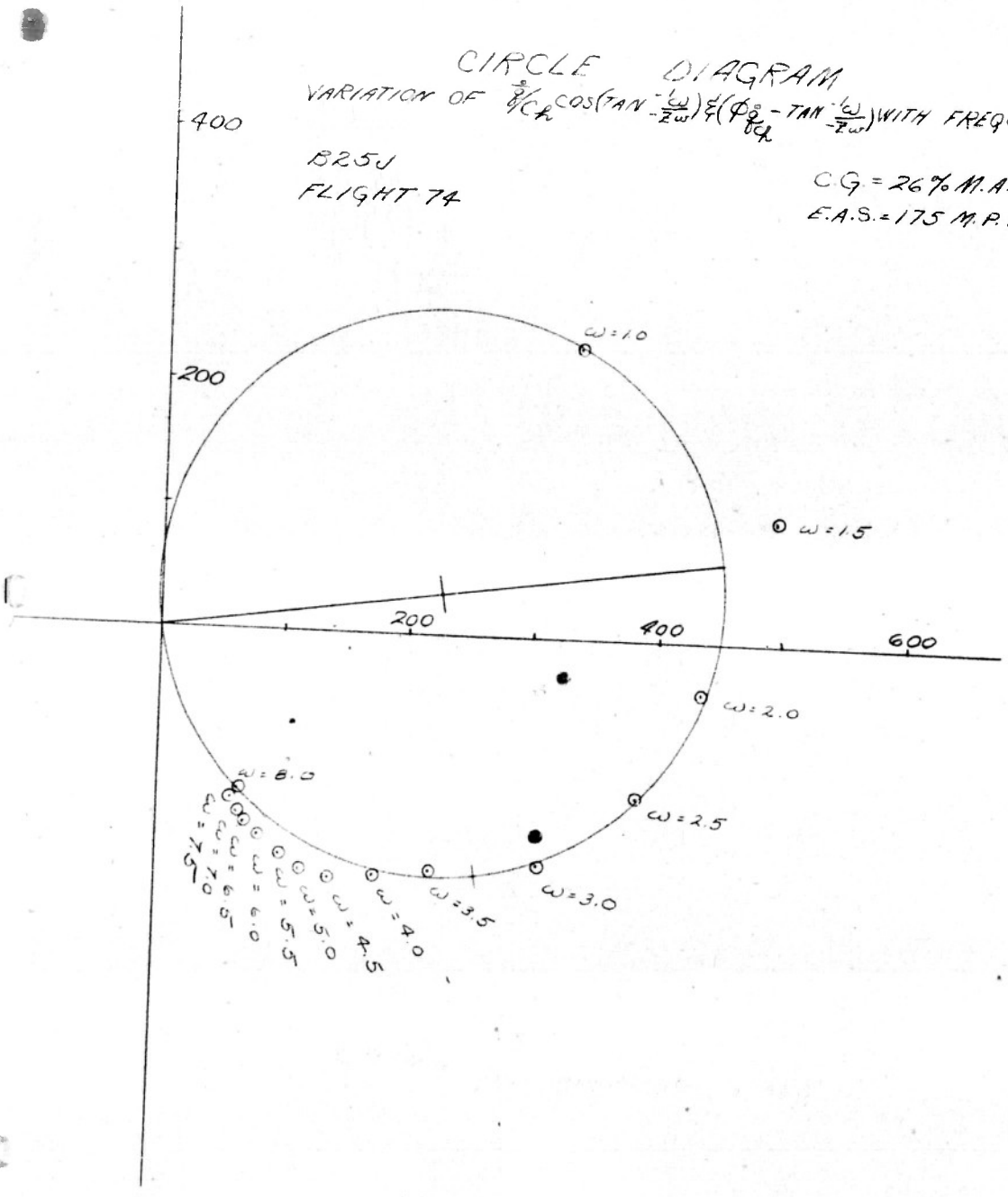

CIRCLE DIAGRAM

VARIATION OF $\frac{|n_z|}{|\delta|}$ AND ϕ_{n_z} WITH FREQUENCY

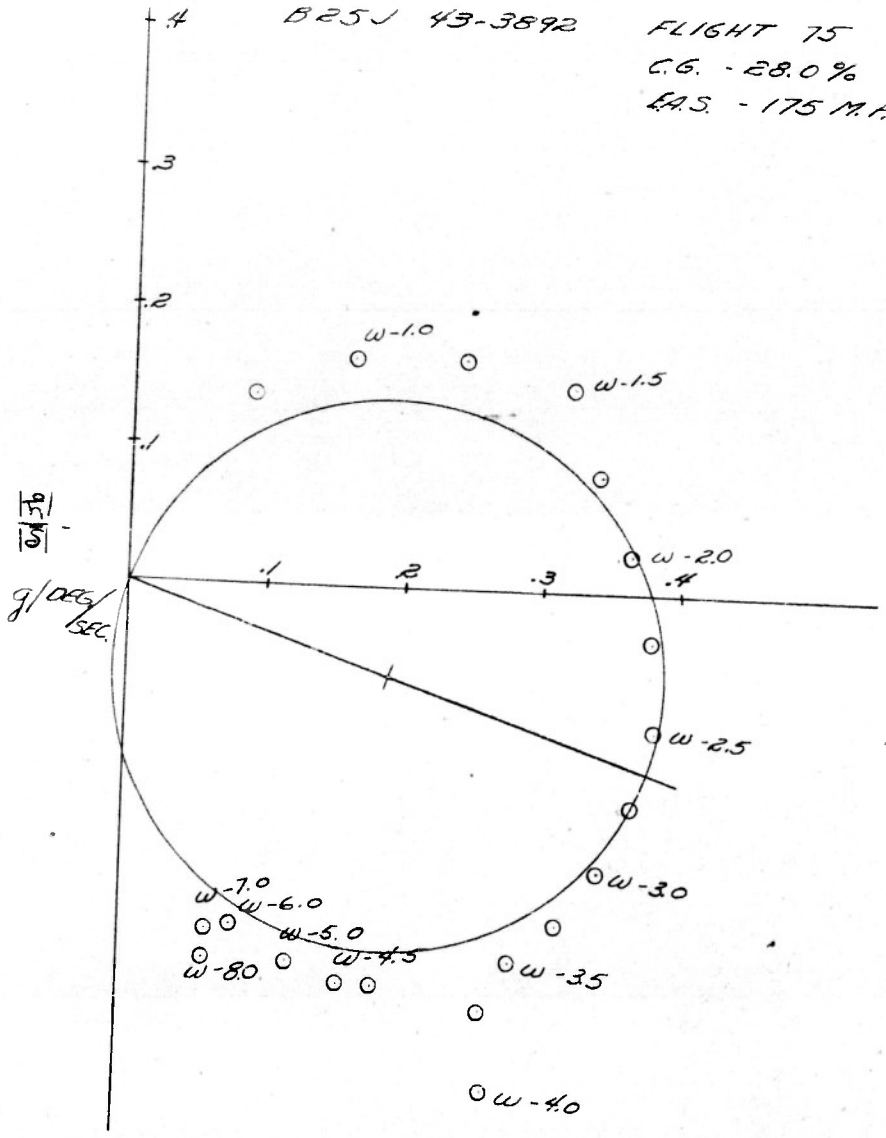

JEF 1-7-47

CIRCLE DIAGRAM

VARIATION OF $\frac{\dot{\theta}}{|\delta|}\cos\left(\tan^{-1}\frac{\omega}{-Z_w}\right)\angle\left(\phi_{\frac{\dot{\theta}}{\delta}} - \tan^{-1}\frac{\omega}{-Z_w}\right)$ WITH FREQUENCY

B 25 J 43-3892
FLIGHT 75

C.G. - 28 %
E.A.S. - 175 MPH

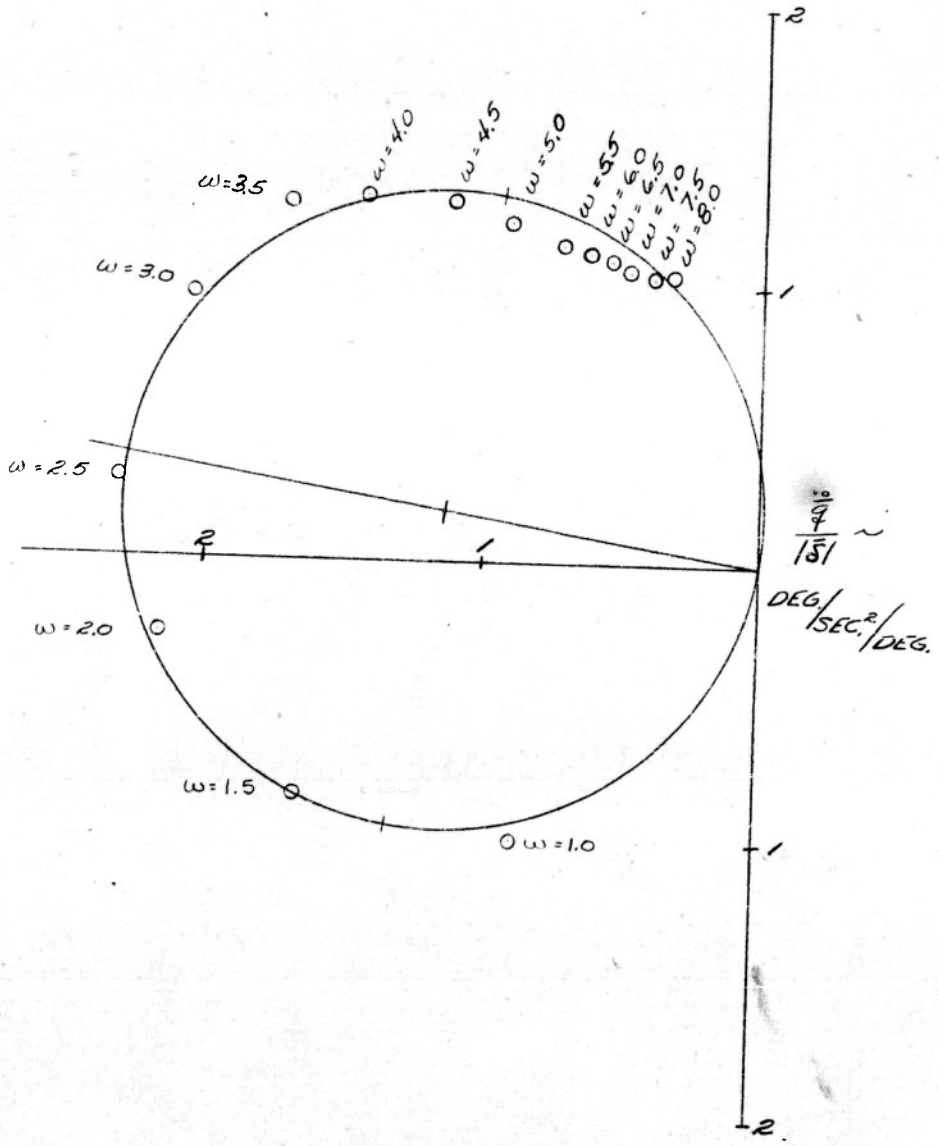

CIRCLE DIAGRAM

VARIATION OF $\frac{\Pi}{C_R}$ AND $\phi_{\frac{\Pi}{C_R}}$ WITH FREQUENCY

B25J 43-389.2
FLIGHT 75

C.G. = 28 %
E.A.S. = 175 M.P.H

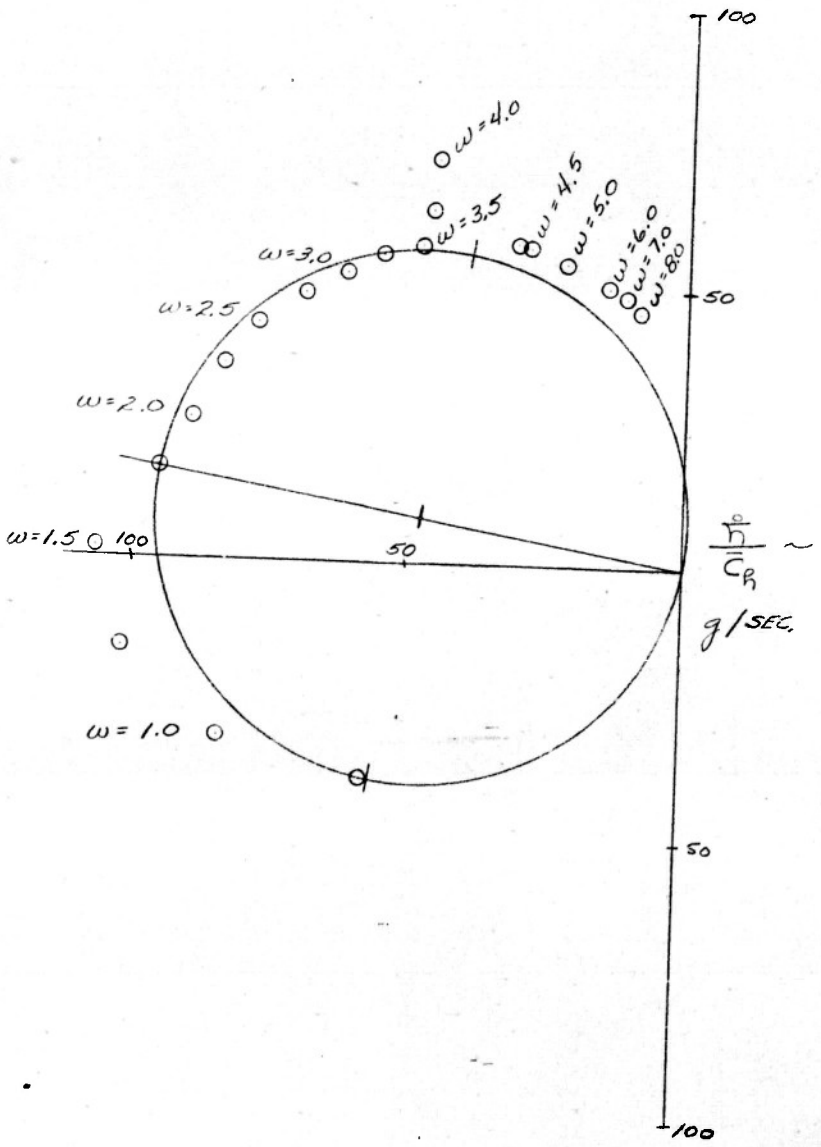

CIRCLE DIAGRAM

VARIATION OF $\frac{a}{\theta}/C_R \cos(\tan^{-1}\frac{\omega}{2\omega}) \epsilon^{\frac{1}{2}}(\phi_{\theta C_R} - \tan^{-1}\frac{\omega}{2\omega})$ WITH FREQUENCY

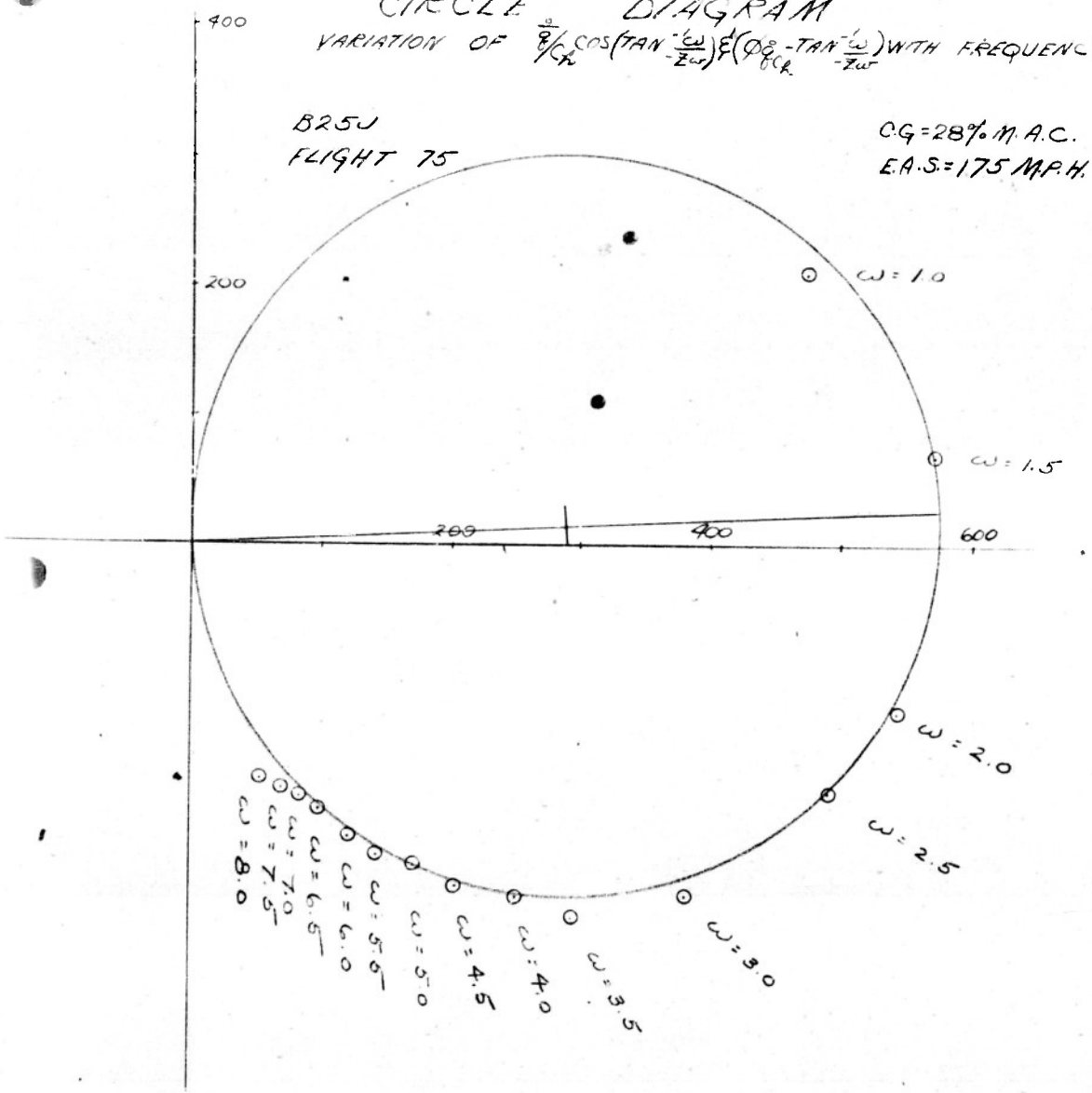

MH

CIRCLE DIAGRAM

VARIATION OF $\frac{|n|}{|\delta|}$ AND ϕ_n° WITH FREQUENCY

B25J 43-3892 FLIGHT 76
C.G - 30.0 %
I.A.S. - 175 M.P.H.

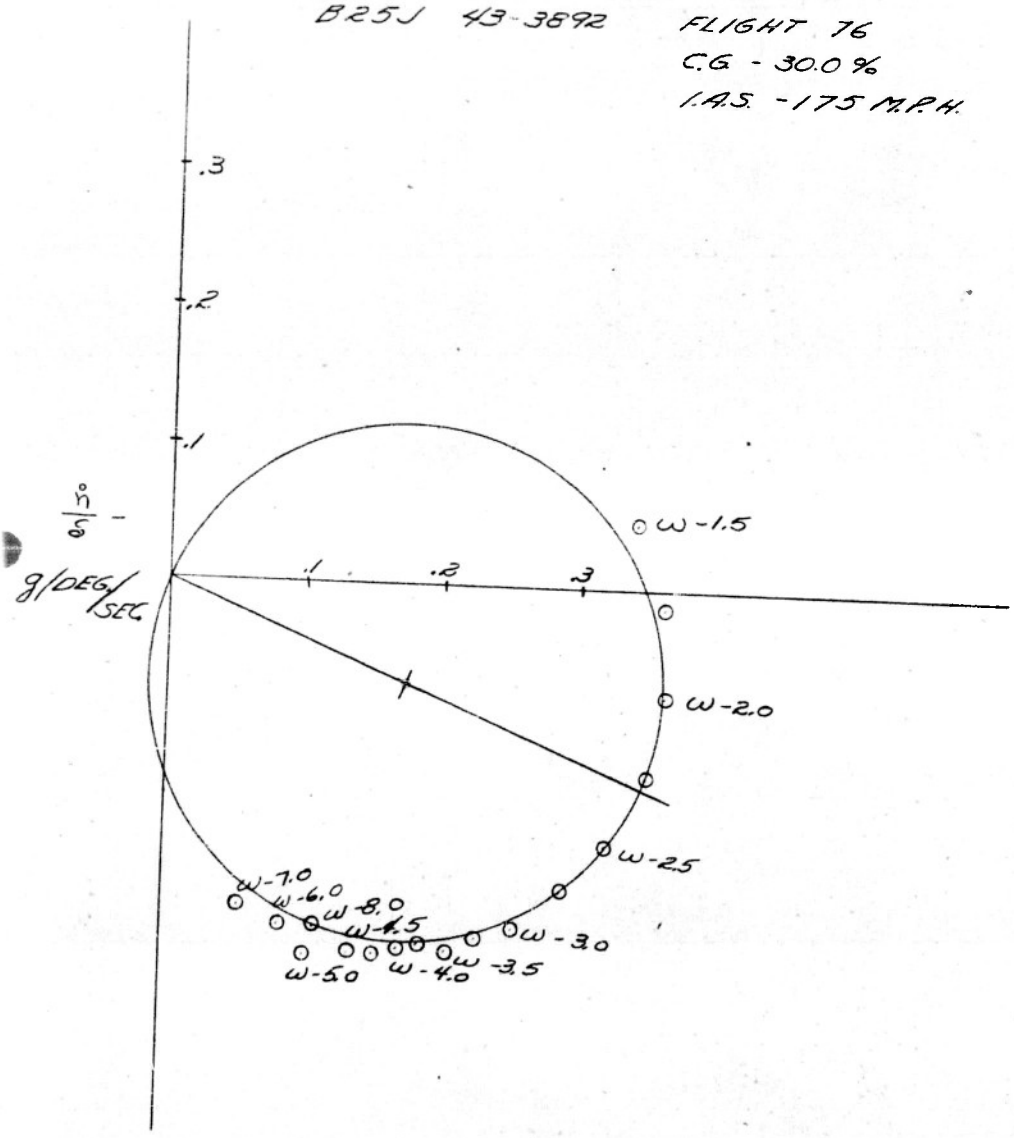

JEE 1-7-47

CIRCLE DIAGRAM

VARIATION OF $\frac{\dot{q}}{|\Delta|}\cos(\tan^{-1}\frac{\omega}{-2w})\,\mathcal{F}(\frac{\dot{q}}{\dot{q}_s}-\tan^{-1}\frac{\omega}{-2w})$ WITH FREQUENCY

B25J 43-3892
FLIGHT 76

C.G. = 30 %
E.A.S. = 175 MPH

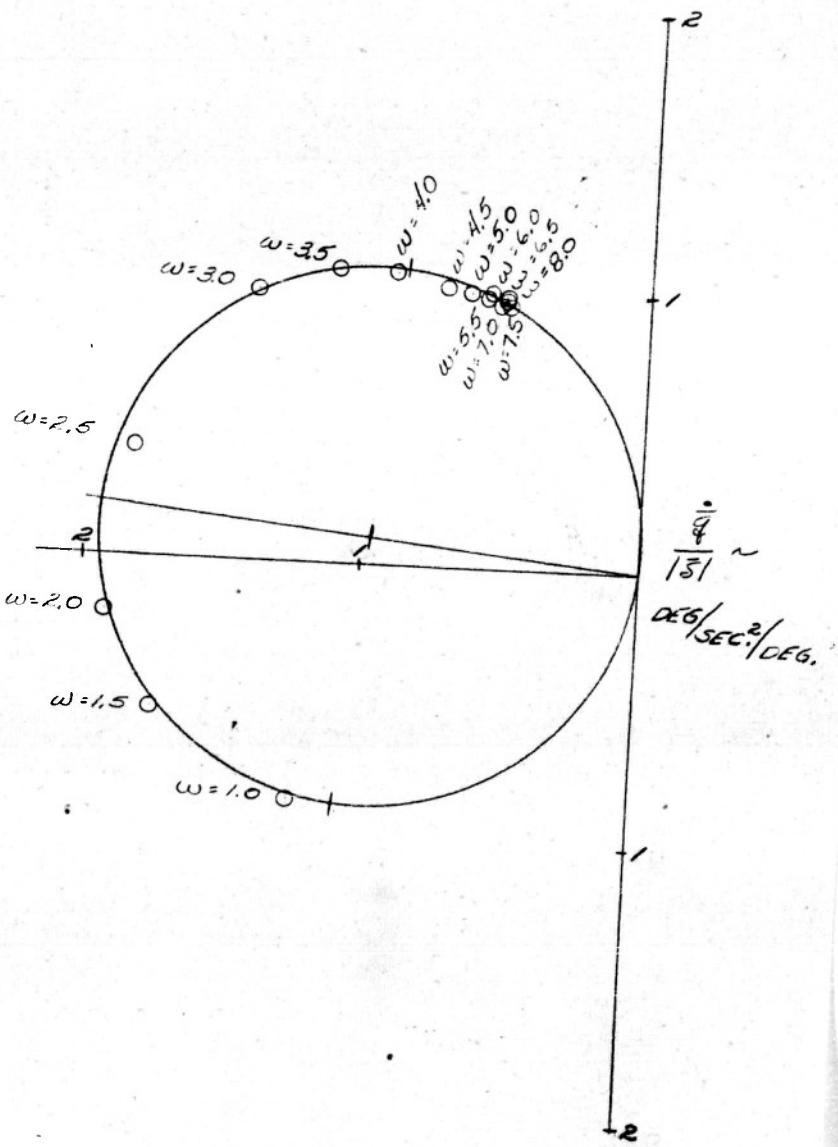

CIRCLE DIAGRAM

VARIATION OF $\frac{n}{C_R}$ AND $\phi_{\frac{n}{C_R}}$ WITH FREQUENCY

B25J 43-3892
FLIGHT 76

C.G. = 30 %
E.A.S. = 175 MPH.

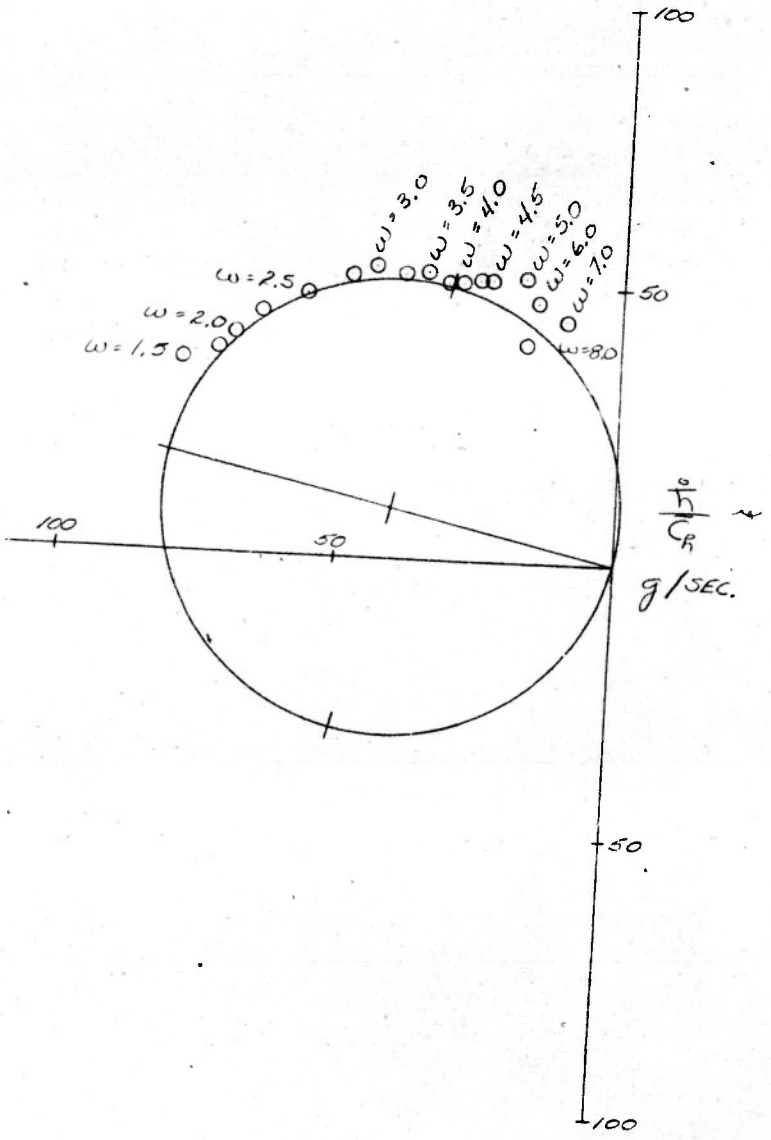

CIRCLE DIAGRAM

VARIATION OF $\frac{a}{\alpha_R}\cos(\tan^{-1}\frac{\omega}{-\frac{1}{T_{\omega_1}}}+\epsilon(\phi_{\frac{a}{\alpha_R}}-\tan^{-1}\frac{\omega}{-\frac{1}{T_{\omega_2}}})$ WITH FREQUENCY

B25J
FLIGHT 76

C.G. = 30% M.A.C.
E.A.S. = 175 M.P.H.

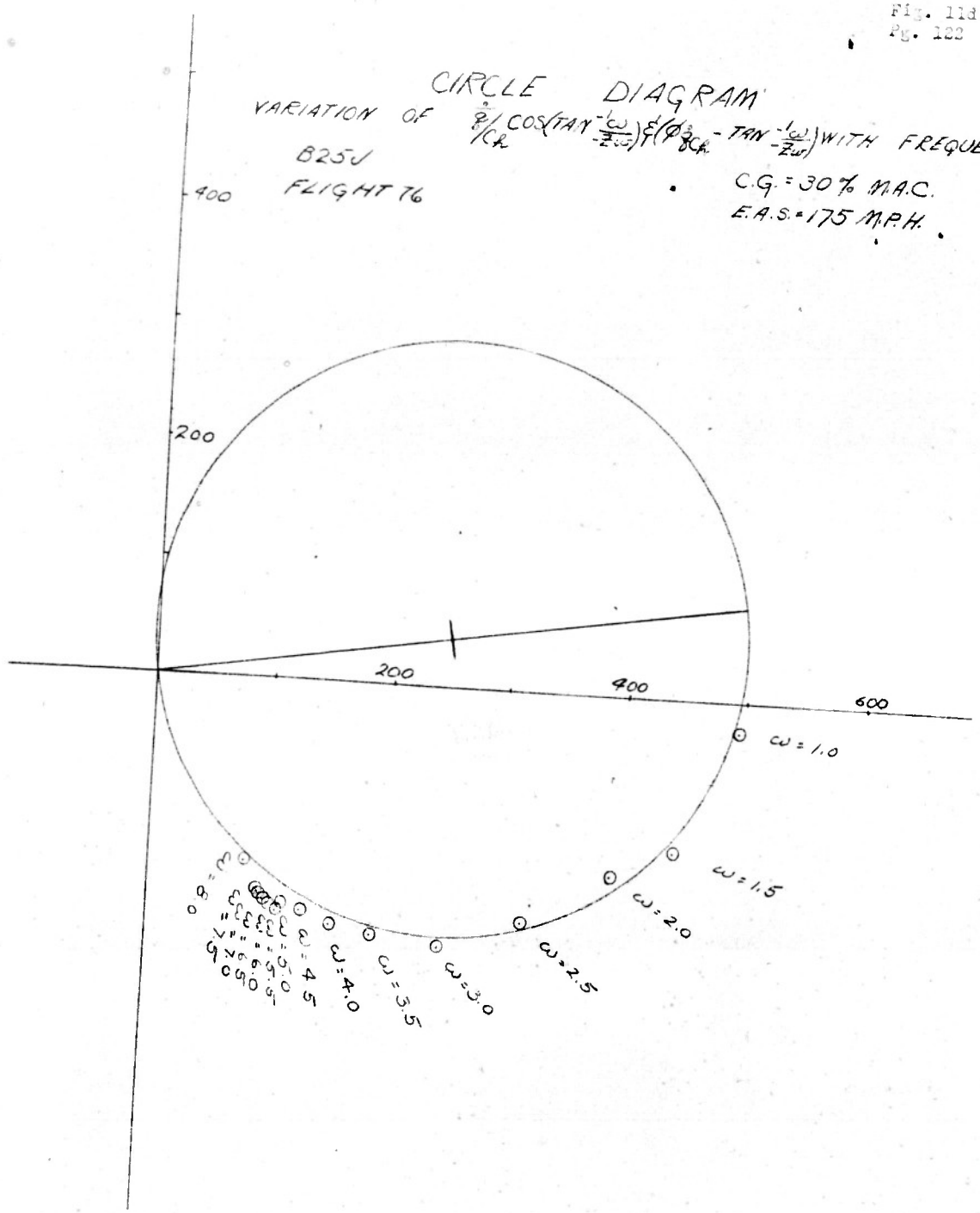

M/H

CIRCLE DIAGRAM
VARIATION OF $\frac{|n_\theta|}{|\delta|}$ AND $\phi_{n_\delta}^\circ$ WITH FREQUENCY

B25J 43-3892 FLIGHT 84
C.G. - 32.0%
E.A.S. - 175 M.P.H.

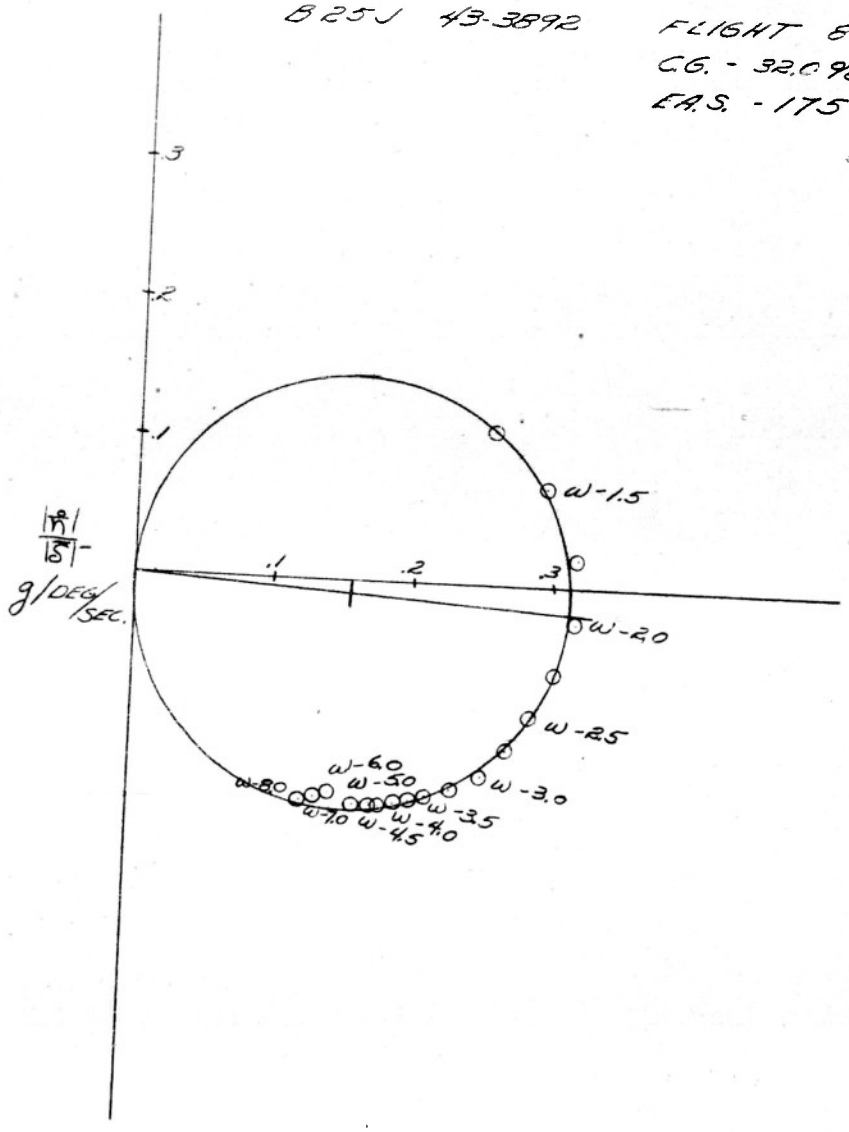

CIRCLE DIAGRAM

VARIATION OF $\frac{\dot{\theta}}{\theta}/\theta_1 \cos(\tan^{-1}\frac{-\omega}{2\omega_1}) \pm (\phi_{\dot{\theta}} - \tan^{-1}\frac{\omega}{-2\omega_1})$ WITH FREQUENCY

B25J
FLIGHT 84

C.G. = 32% M.A.C.
E.A.S. = 175 M.P.H.

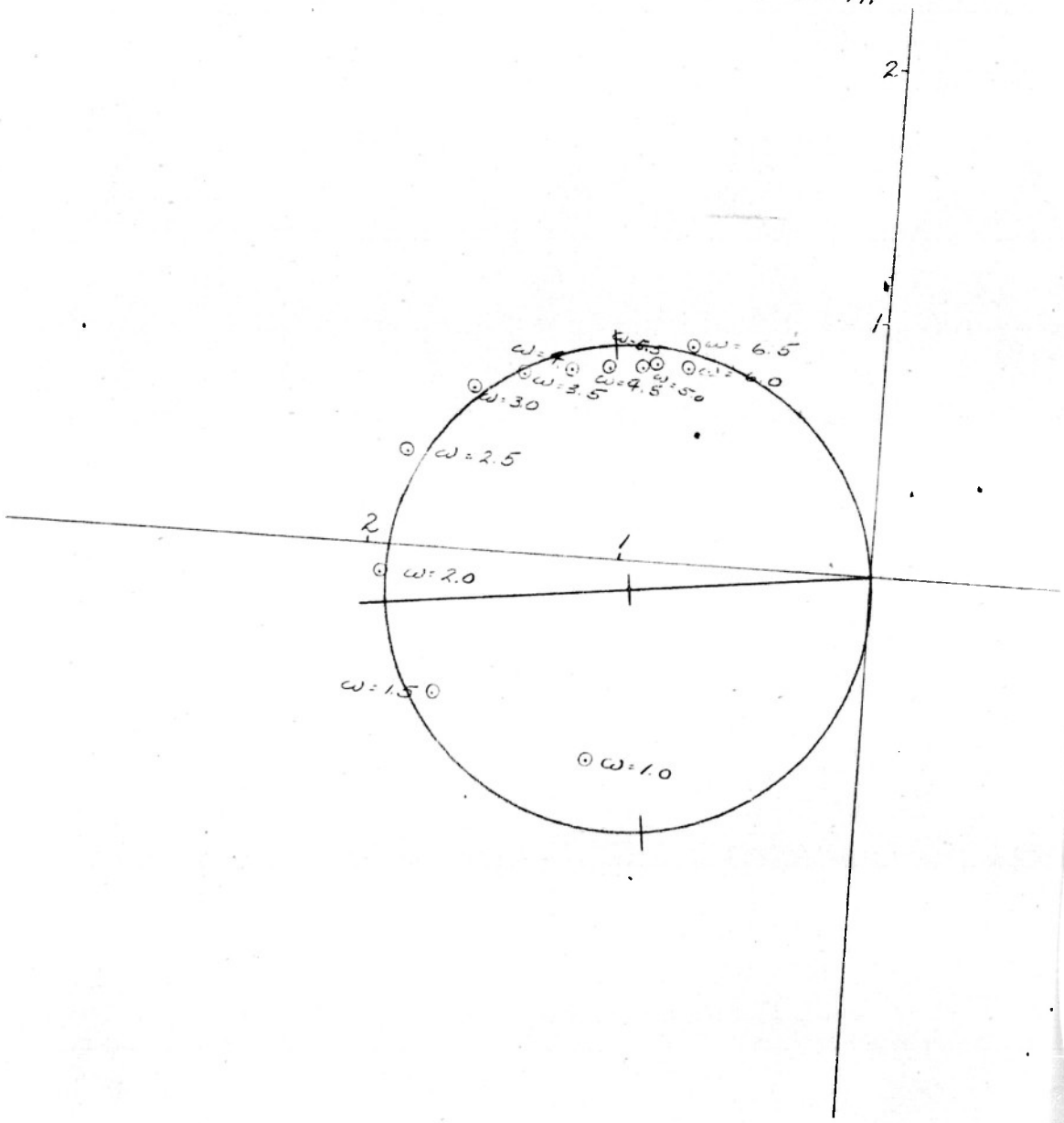

CIRCLE DIAGRAM

VARIATION OF $\frac{\dot{n}}{C_R}$ AND $\phi_{\frac{\dot{n}}{C_R}}$ WITH FREQUENCY

825J 43-3892
FLIGHT 84

C.G. = 32 %
E.A.S. = 175 M.P.H.

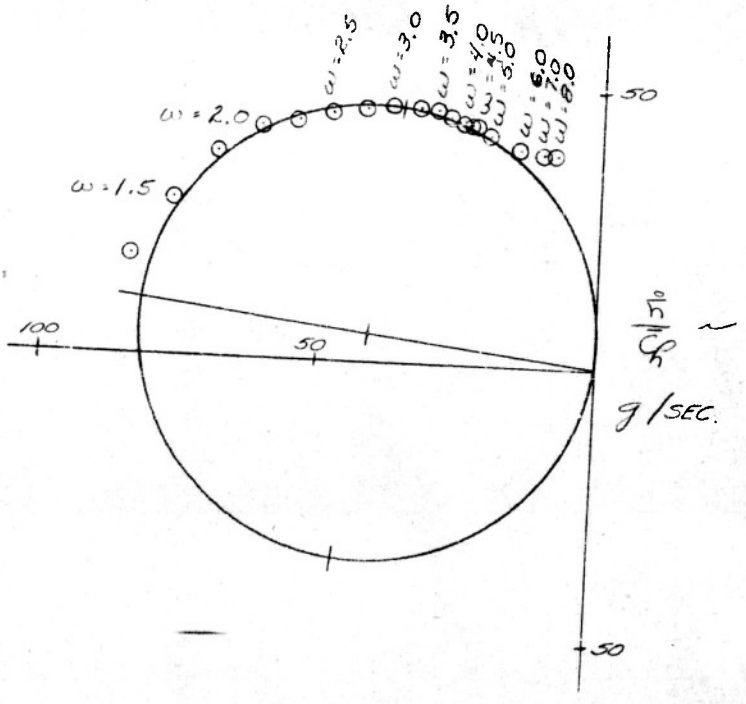

CIRCLE DIAGRAM

VARIATION OF $\frac{\pm}{7}/C_R \cos(\tan^{-1}\frac{\omega}{-2\omega r}) \not\in (\phi_{\frac{\delta}{C_R}} - \tan^{-1}\frac{\omega}{-2\omega r})$ WITH FREQUENCY

B25J
FLIGHT 84

C G = 32 % M.A.C.
E.A.S. = 175 M.P.H.

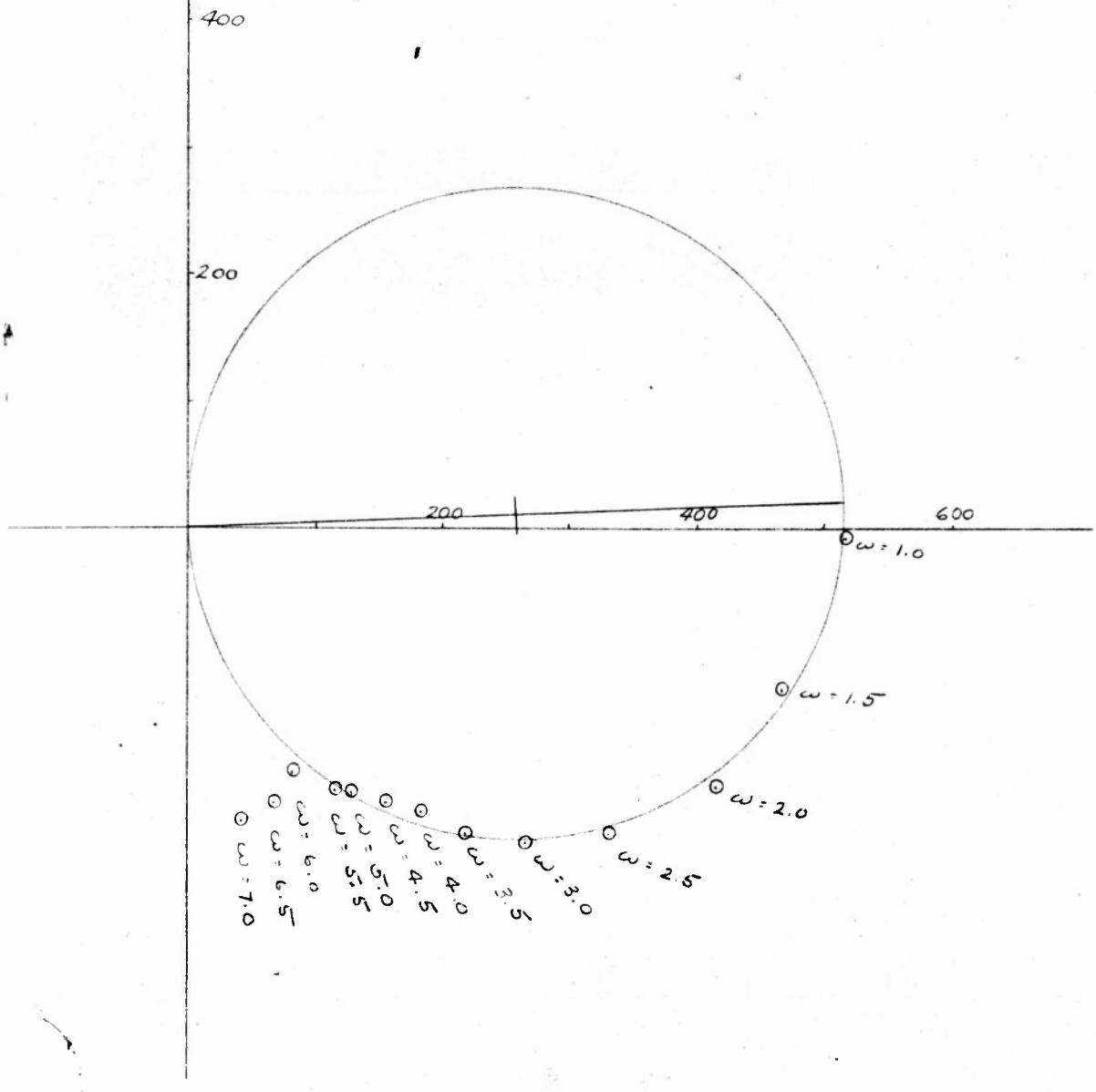

CIRCLE DIAGRAM
VARIATION OF $\frac{|n_z|}{|\delta|}$ AND ϕ_{n_z} WITH FREQUENCY

B25J 43-3892 FLIGHT 78
C.G. - 22.0%
E.A.S. - 135 M.P.H.

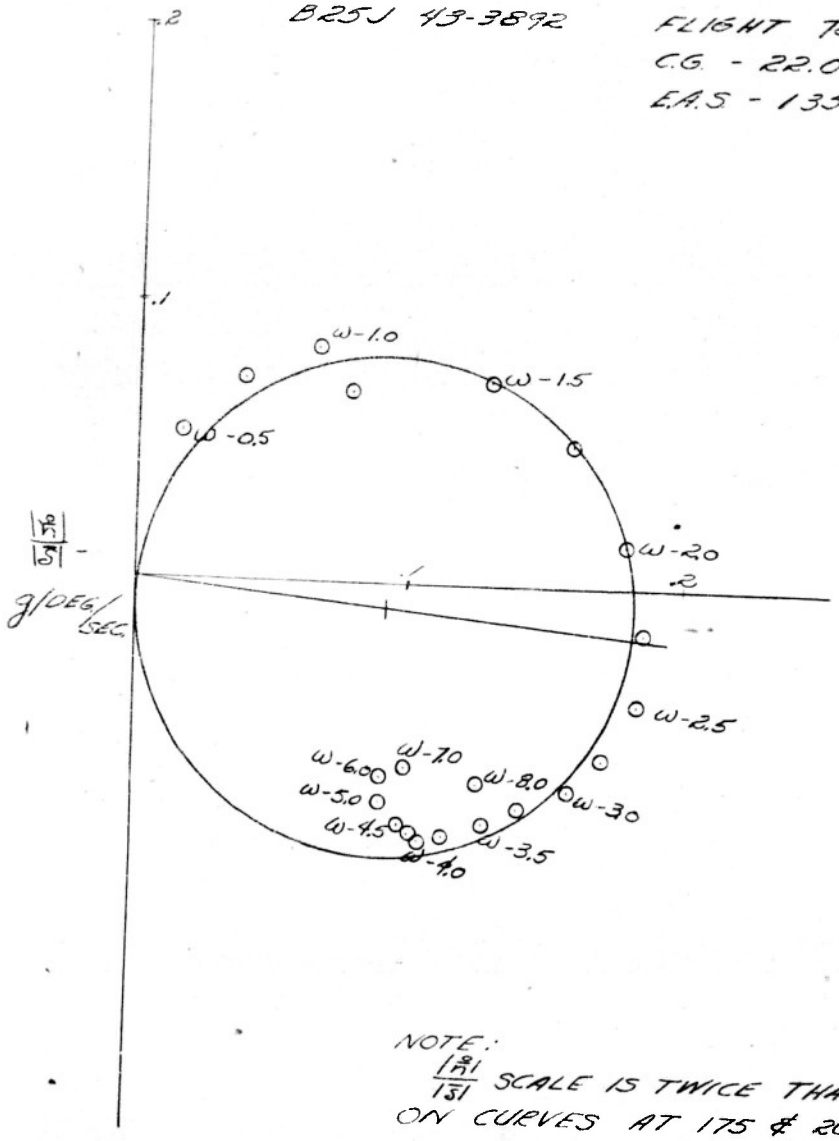

NOTE:
$\frac{|n_z|}{|\delta|}$ SCALE IS TWICE THAT USED ON CURVES AT 175 & 200 MPH

CIRCLE DIAGRAM

VARIATION OF $\frac{\bar{\dot{\theta}}}{|\delta|}\cos\left(\tan^{-1}\frac{\omega}{-Z_\omega}\right)$ & $\left(\phi_{\dot{\theta}\delta} - \tan^{-1}\frac{\omega}{-Z_\omega}\right)$ WITH FREQUENCY

B25J
FLIGHT 78

C.G. = 22% M.A.C.
E.A.S. = 135 M.P.H.

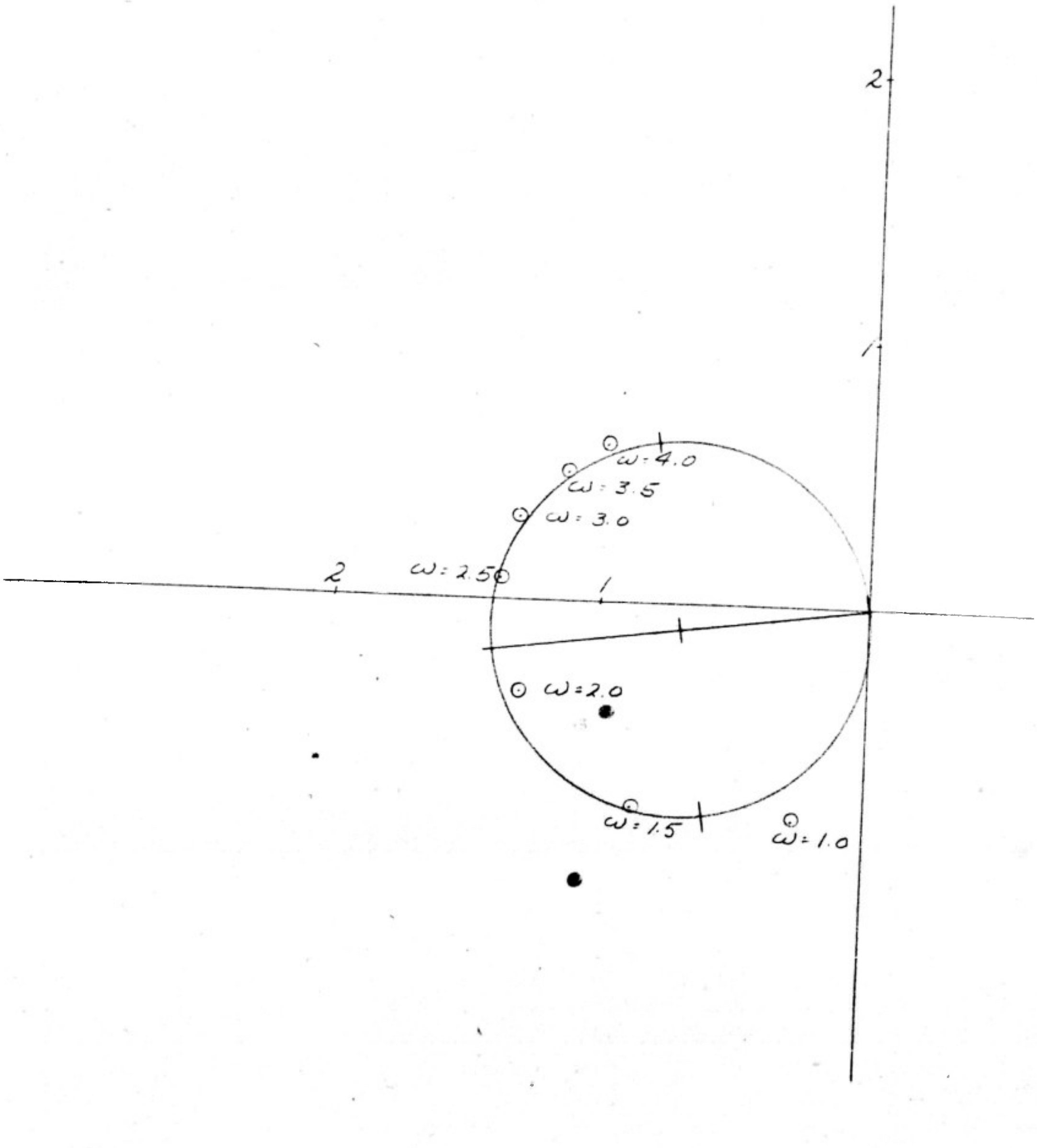

CIRCLE DIAGRAM

VARIATION OF $\frac{\dot{n}}{C_R}$ AND $\phi_{\frac{\dot{n}}{C_R}}$ WITH FREQUENCY

B 25J 43-3892
FLIGHT 78

C.G. = 22 %
E.A.S. = 135 M.P.H.

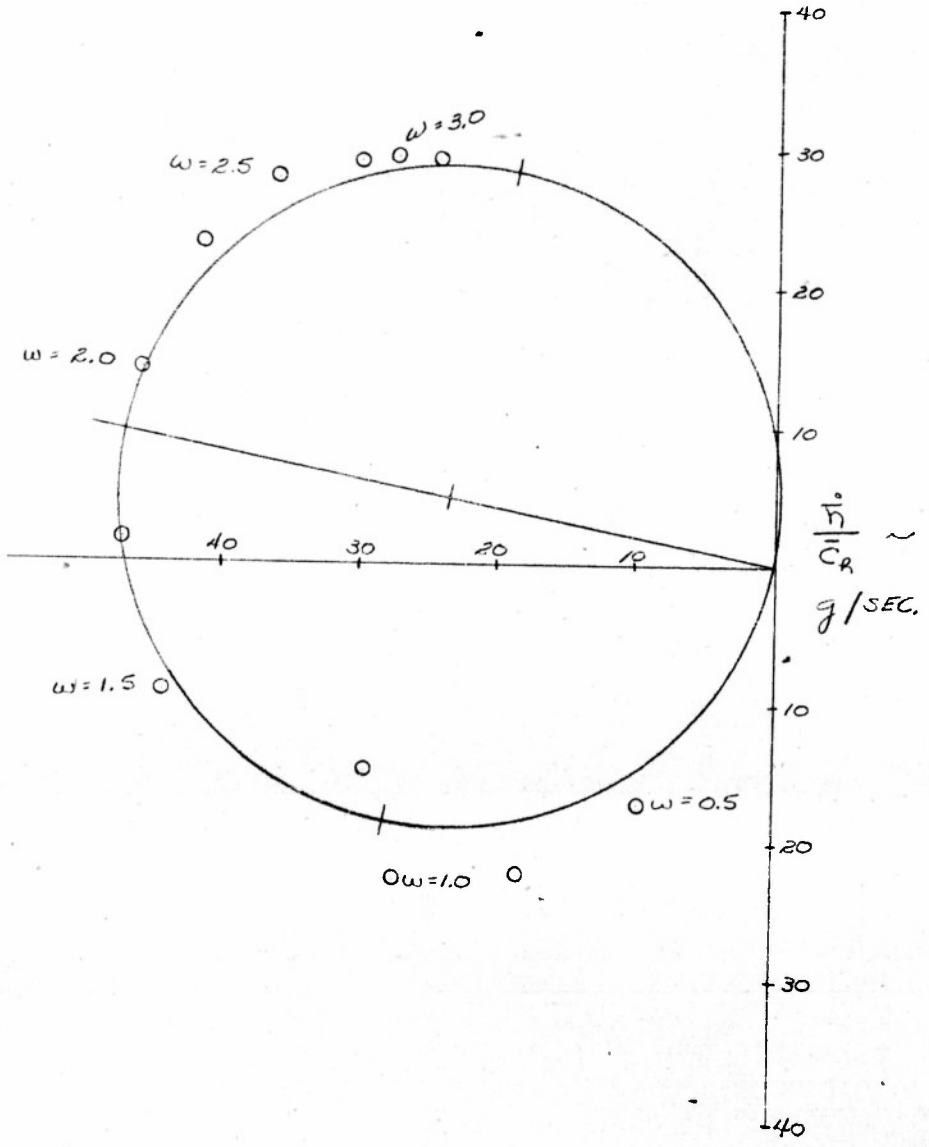

CIRCLE DIAGRAM

VARIATION OF $\frac{\dot{q}}{C_R}\cos\left(\tan^{-1}\frac{\omega}{-2\omega_{sp}}\right)\epsilon\left(\phi_{\frac{\dot{q}}{\delta_R}} - \tan^{-1}\frac{\omega}{-2\omega n}\right)$ WITH FREQUENCY

B25J
FLIGHT 78

C.G. = 22% MAC
E.A.S. = 135 M.P.H.

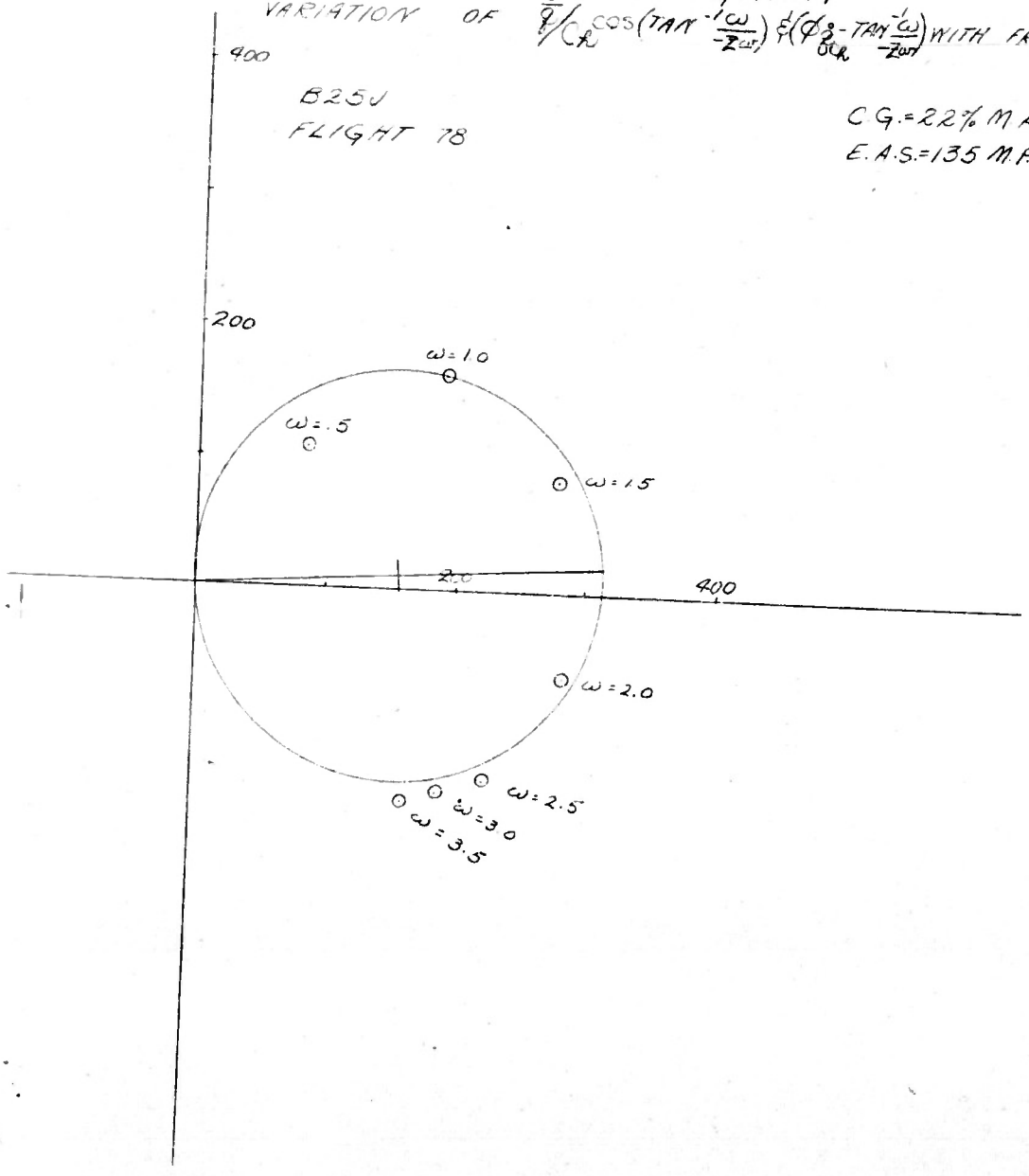

MH

CIRCLE DIAGRAM

VARIATION OF $\frac{|n|}{|\delta|}$ AND $\phi_{n_\delta}^{\circ}$ WITH FREQUENCY

B25J 43-3892

FLIGHT 81
C.G. - 26.0 %
EAS - 135 M.P.H.

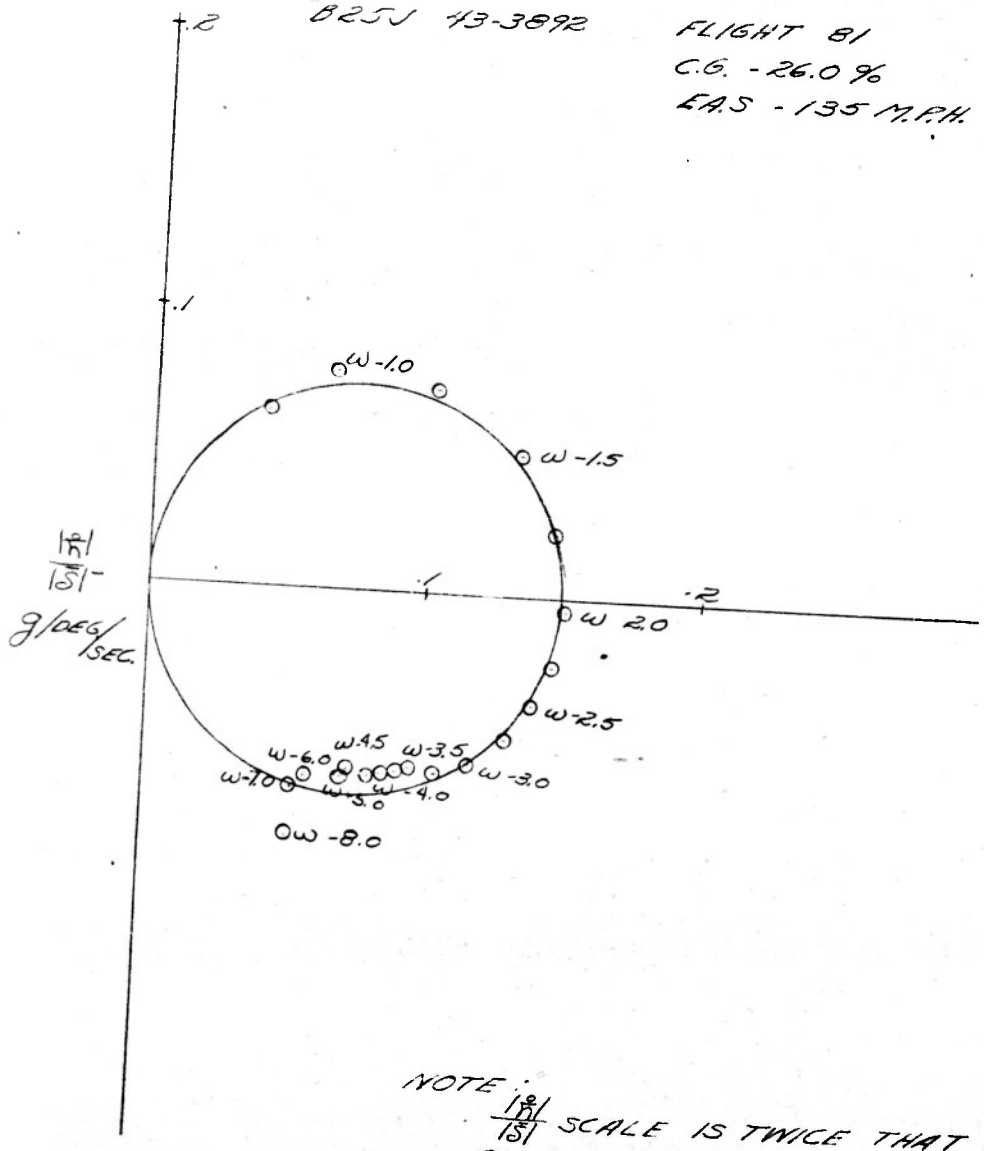

NOTE: $\frac{|n|}{|\delta|}$ SCALE IS TWICE THAT USED ON CURVES AT 175 & 200 MPH.

CIRCLE DIAGRAM

VARIATION OF $\frac{\theta}{|\delta|}\cos(\tan^{-1}\frac{\omega}{-2\omega}) \angle(\phi_{\dot{\theta}} - \tan^{-1}\frac{\omega}{-2\omega})$ WITH FREQUENCY

B-25J
FLIGHT 81

C.G. = 26% M.A.C.
E.A.S. = 135 M.P.H.

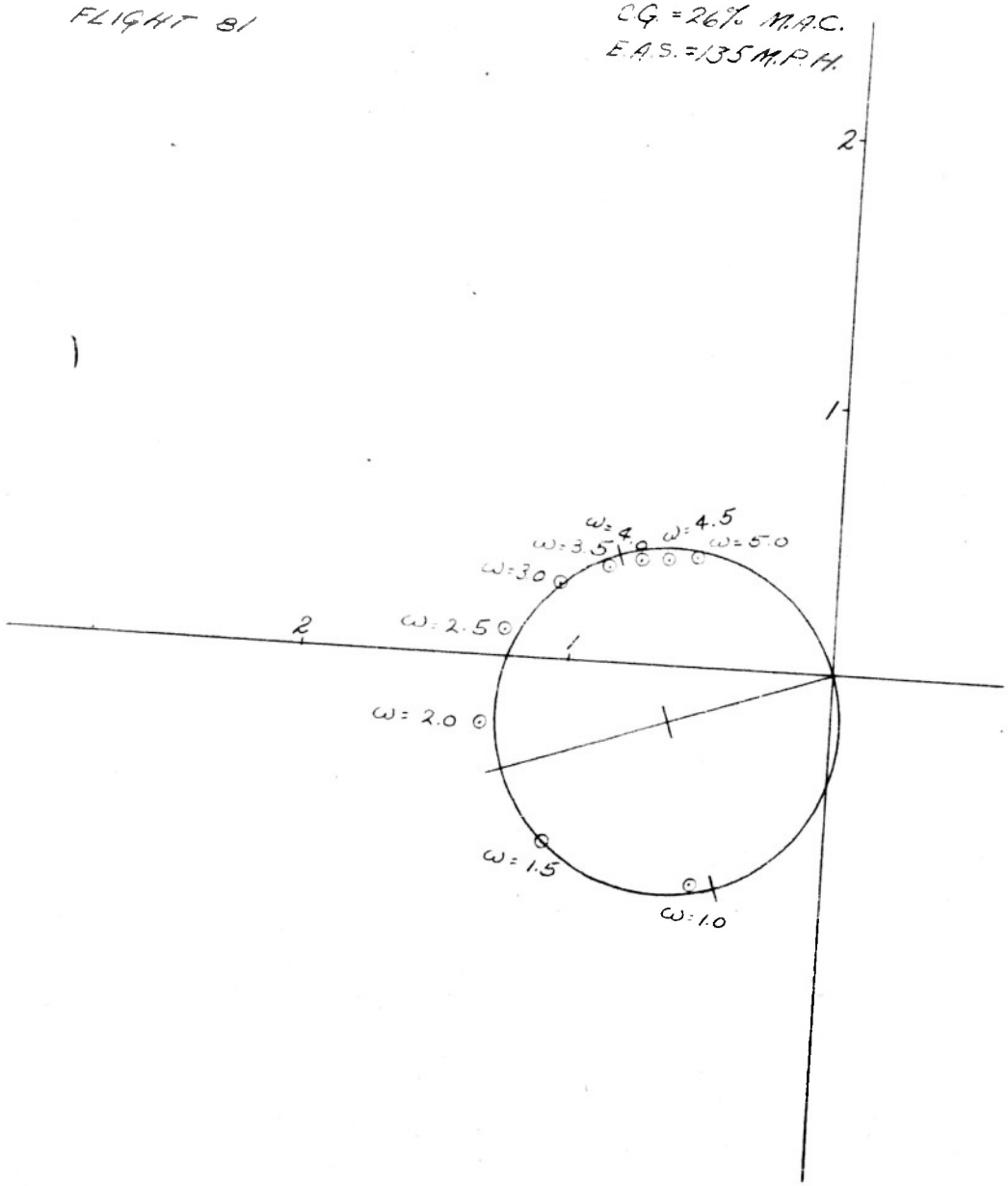

CIRCLE DIAGRAM

VARIATION OF $\frac{\dot{n}}{C_R}$ AND $\phi_{\frac{\dot{n}}{C_R}}$ WITH FREQUENCY

B25J 43-3892
FLIGHT 81

C.G. = 26 %
E.A.S. = 135 MPH

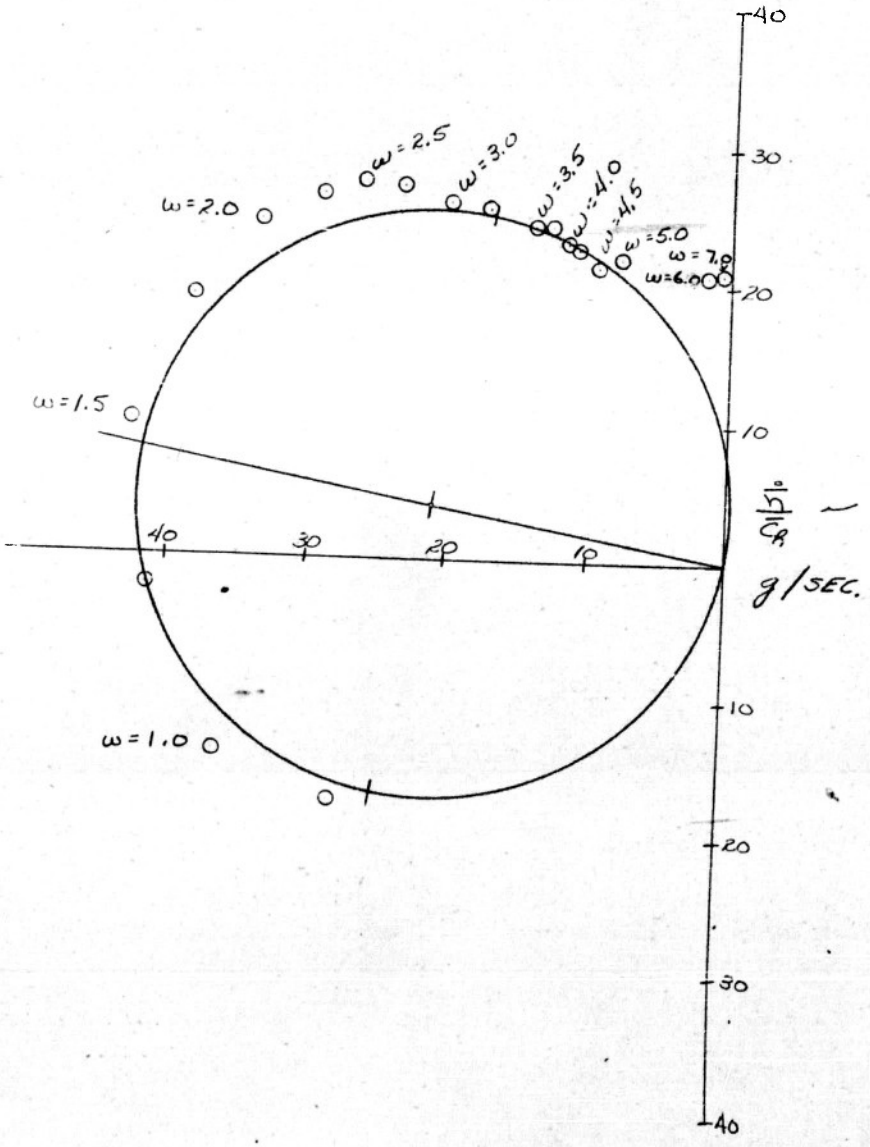

ICO 2 24-47

CIRCLE DIAGRAM

VARIATION OF $\frac{\ddot{\theta}}{\dot{\theta}_{ch}} \cos(\tan^{-1}\frac{\omega}{-\frac{1}{2}\omega}) \; \& \; (\phi \frac{\dot{\phi}}{\dot{\theta}_{ch}} - \tan^{-1}\frac{\omega}{-\frac{1}{2}\omega})$ WITH FREQUENCY

B25J
FLIGHT 81

C.G = 26% M.A.C.
E.A.S. = 135 M.P.H.

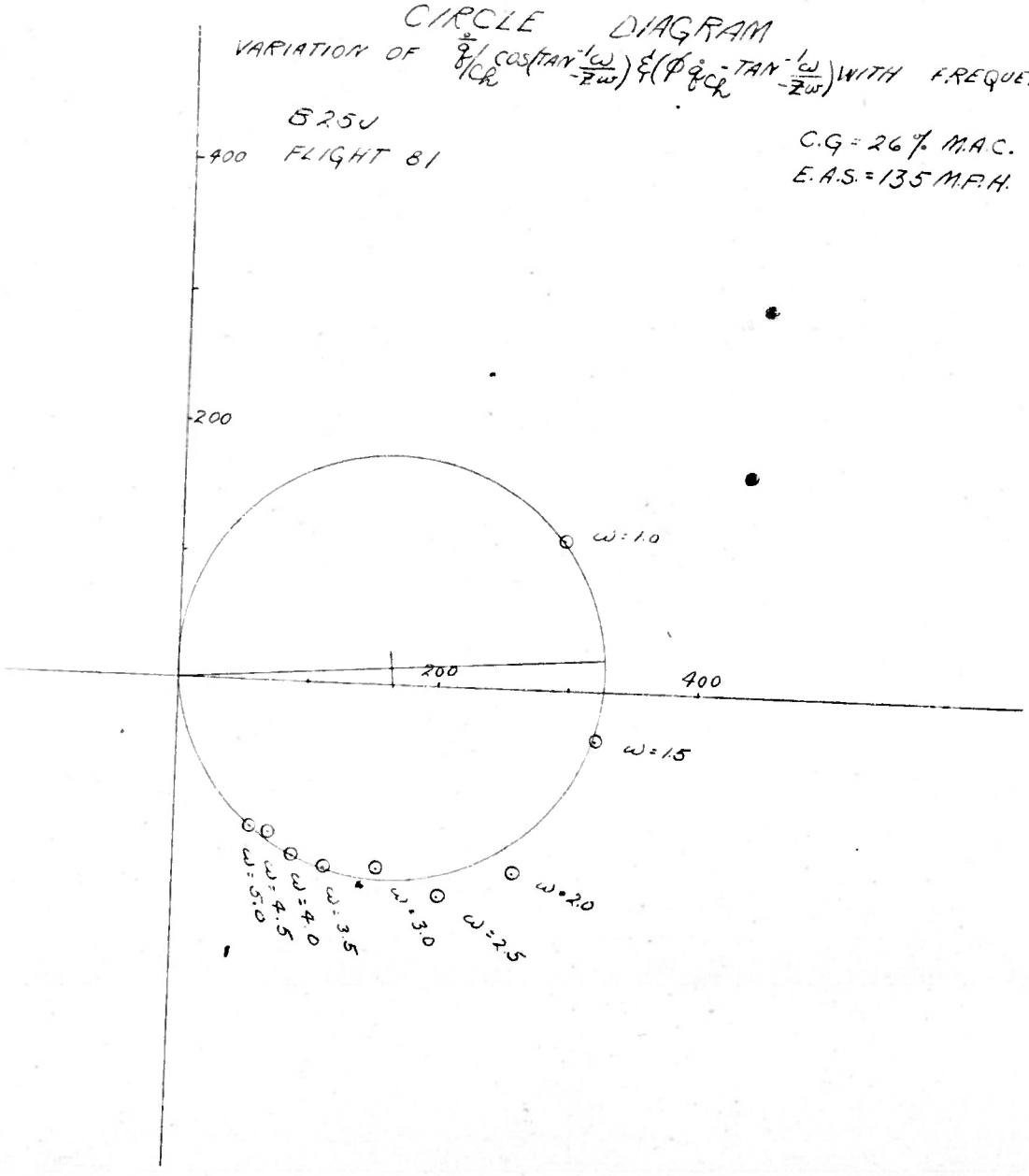

CIRCLE DIAGRAM

VARIATION OF $\frac{|n_\phi|}{|\delta|}$ AND $\phi_{n_\phi}^{\circ}$ WITH FREQUENCY

B25J 43-3892 FLIGHT 80

C.G. - 22.0%

E.A.S. - 200 M.P.H.

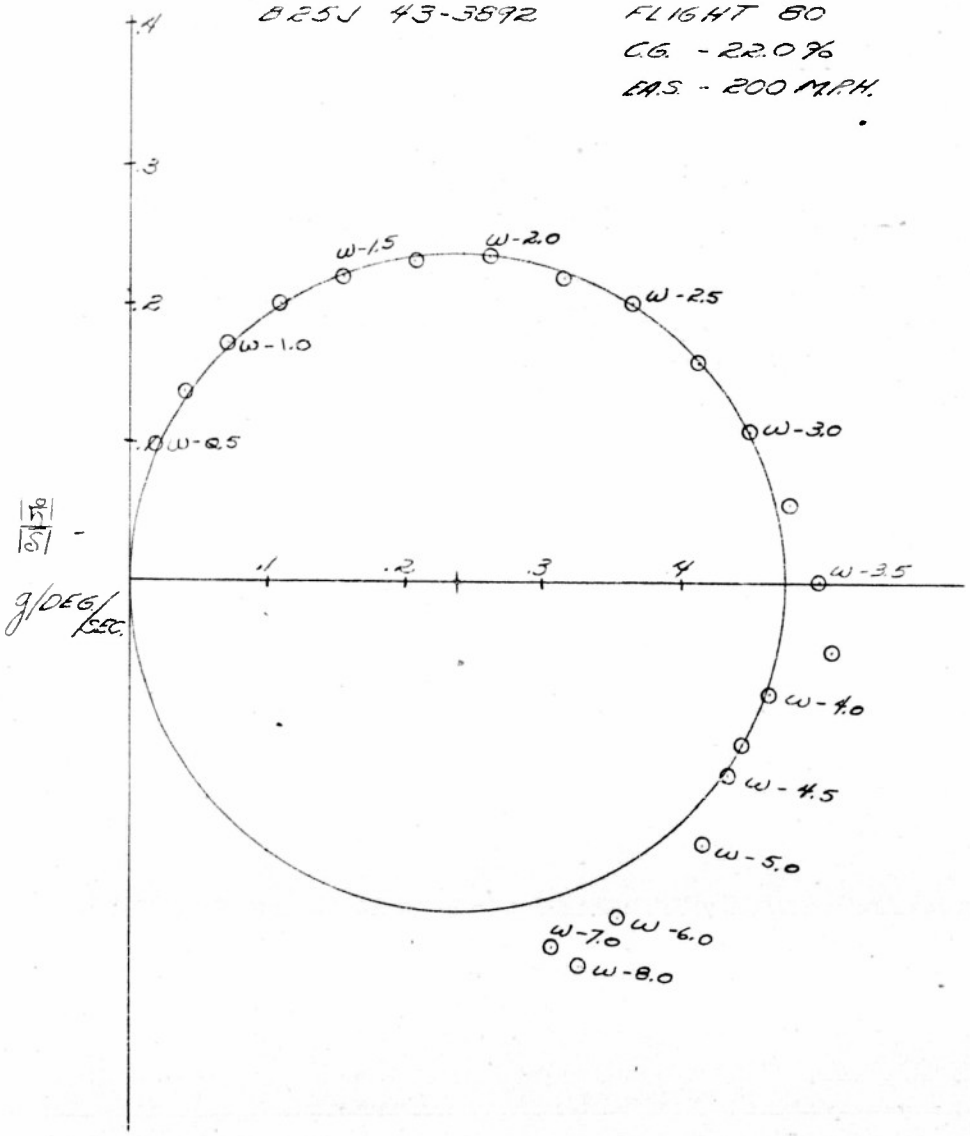

CIRCLE DIAGRAM

VARIATION OF $\frac{n_z}{\delta_1} \cos(\tan^{-1}\frac{\omega}{-z\omega}) + (\phi^\circ_{\frac{n_z}{\delta_s}} - \epsilon_{\tan^{-1}\frac{\omega}{-z\omega}})$ WITH FREQUENCY

FLIGHT 80
C.G. = 22 % M.A.C.
E.A.S. = 200 M.P.H.

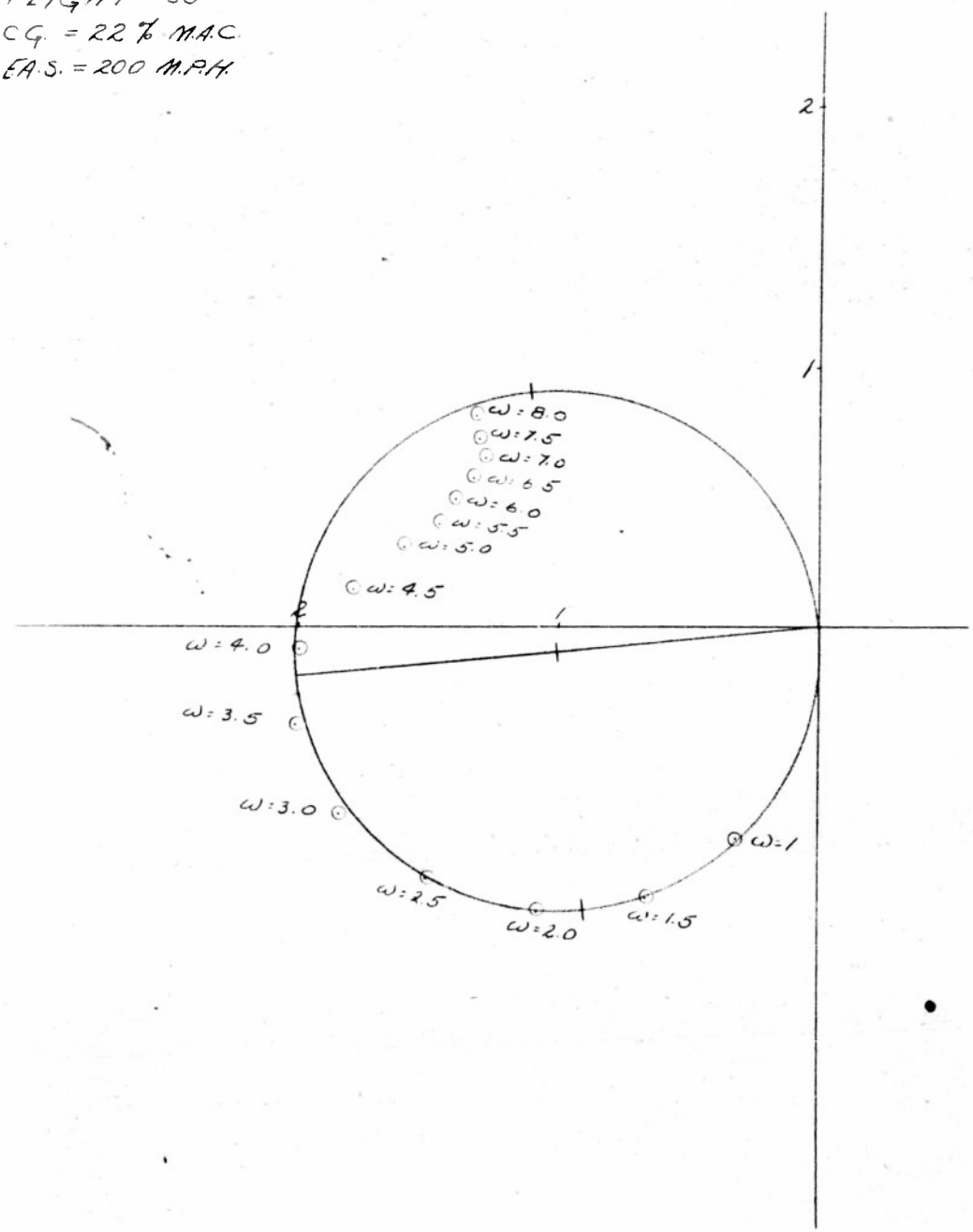

CIRCLE DIAGRAM

VARIATION OF $\frac{\dot{n}}{C_R}$ AND $\phi_{\frac{\dot{n}}{C_R}}$ WITH FREQUENCY

B 25J 43-3892 C.G. = 22 %

FLIGHT 80 E.A.S. = 200 MPH

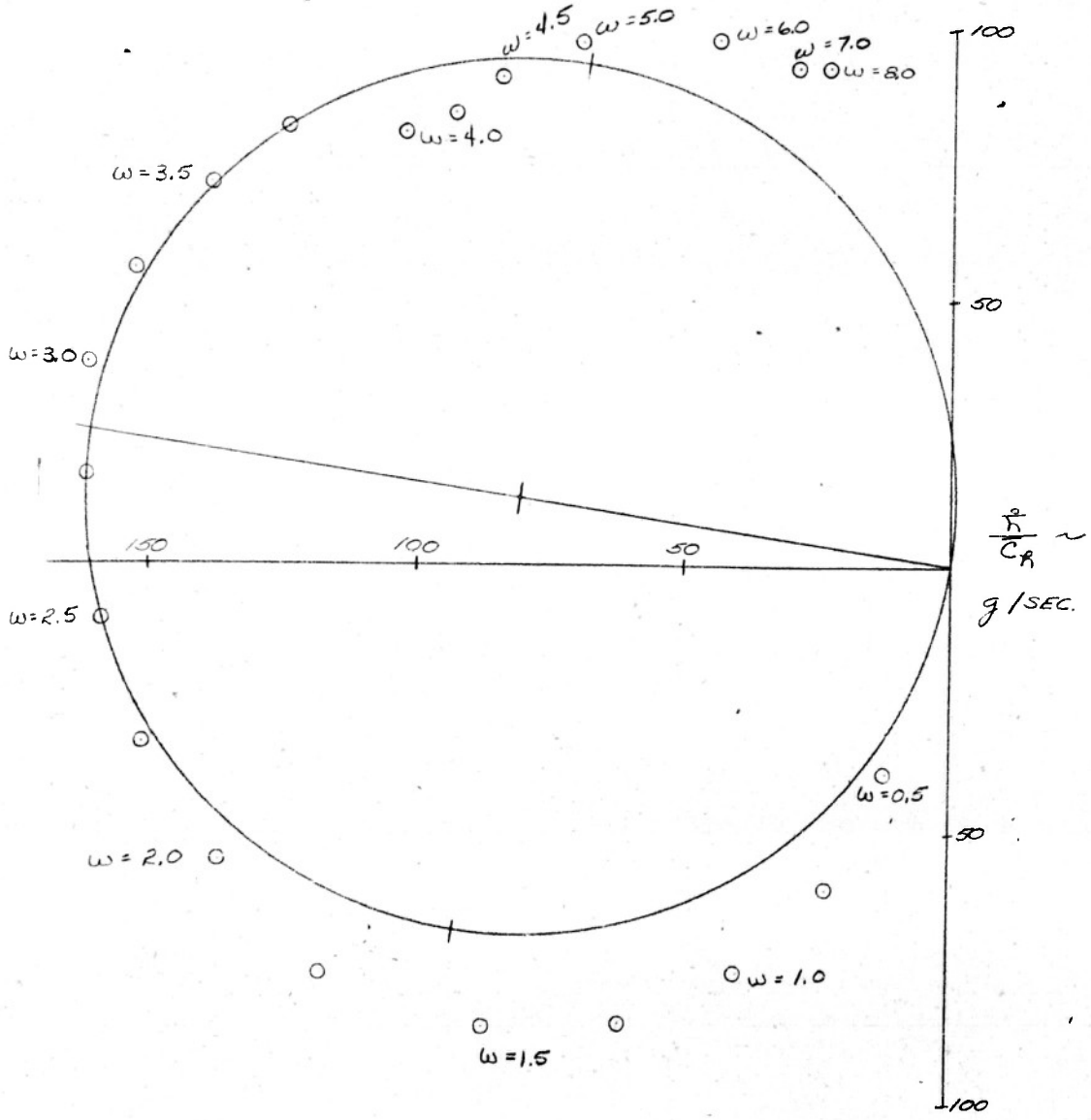

Fig. 15d
Pg. 138

CIRCLE DIAGRAM

VARIATION OF $\frac{\delta}{C_h}\cos(\tan^{-1}\frac{\omega}{2\omega_s})\,\epsilon(\phi_{\delta_e} - \tan^{-1}\frac{\omega}{2\omega^2})$ WITH FREQUENCY

B25J
FLIGHT 80

C.G. = 22% M.A.C.
E.A.S. = 200 M.P.H.

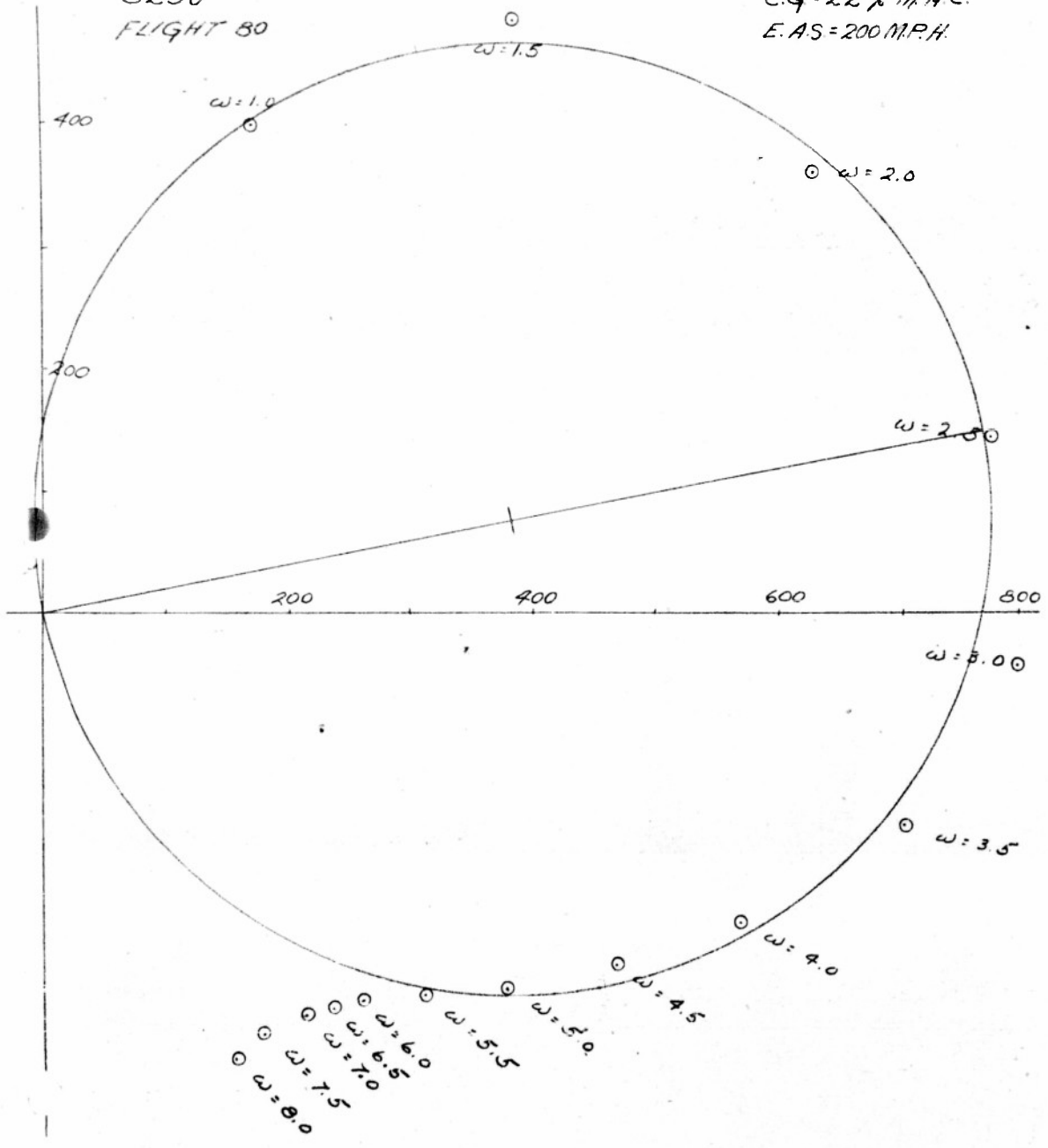

CIRCLE DIAGRAM

VARIATION OF $\frac{|n|}{|\delta|}$ AND $\phi_{\frac{n}{\delta}}^{\circ}$ WITH FREQUENCY

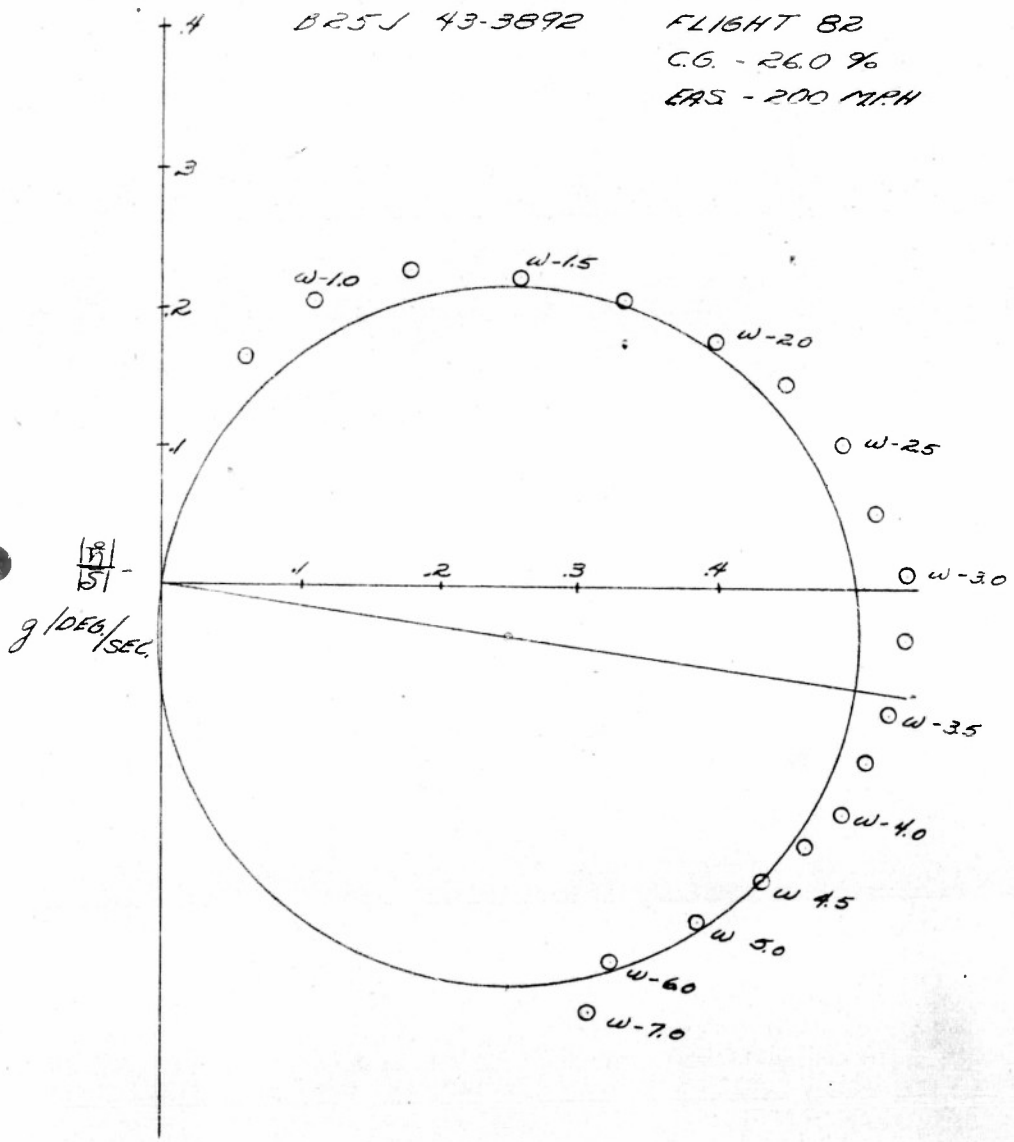

CIRCLE DIAGRAM

VARIATION OF $\frac{a}{\beta}/\beta/\delta|\cos(\tan^{-1}\frac{\omega}{-2\omega}) \angle(\phi^{a}_{\beta\delta} - \tan^{-1}\frac{\omega}{-2\omega})$ WITH FREQUENCY

B25J
FLIGHT 82

C.G. = 26% M.A.C.
E.A.S. = 200 M.P.H.

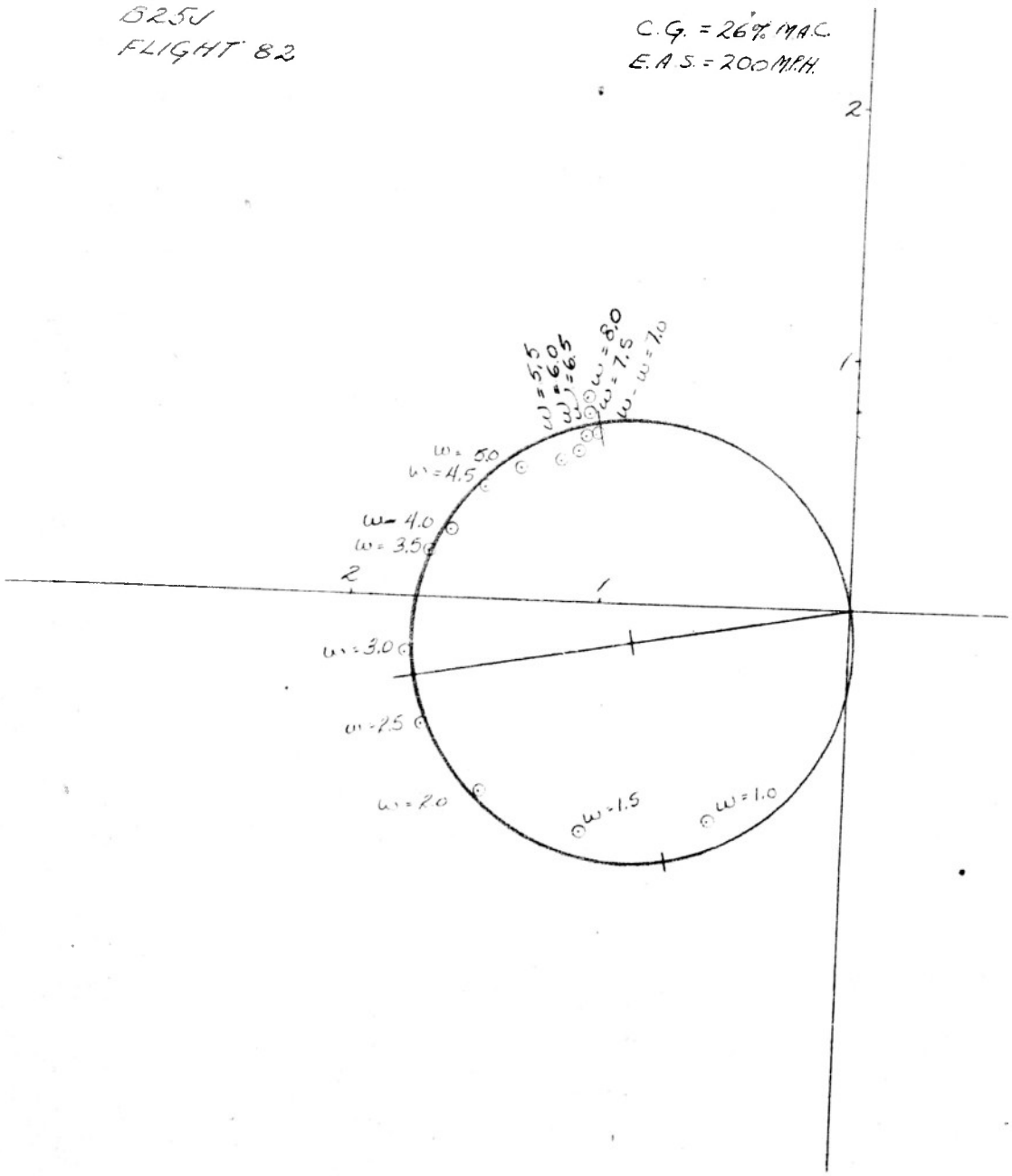

CIRCLE DIAGRAM

VARIATION OF $\frac{\dot{n}}{C_R}$ AND $\phi_{\frac{\dot{n}}{C_R}}$ WITH FREQUENCY

B25J 43-3892
FLIGHT 82

C.G. = 26 %
E.A.S. = 200 M.P.H.

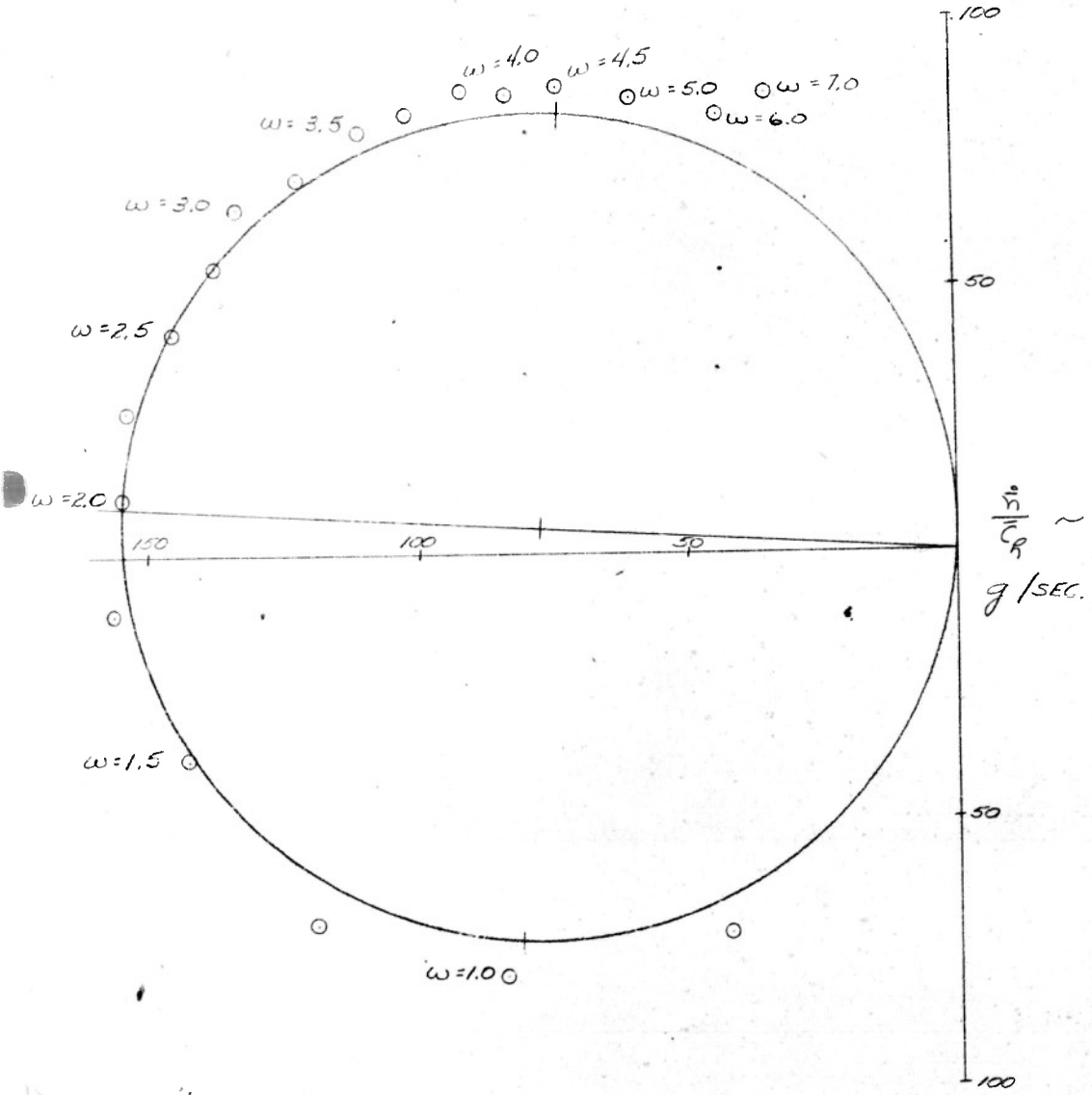

CIRCLE DIAGRAM

VARIATION OF $\frac{\theta}{\theta_{ch}} \cos(\tan^{-1}\frac{\omega}{2\omega_r}) \angle(\phi_\theta - \tan^{-1}\frac{\omega}{2\omega_r})$ WITH FREQUENCY

B25J
FLIGHT 82

C.G. = 26% M.A.C.
E.A.S. = 200 M.P.H.

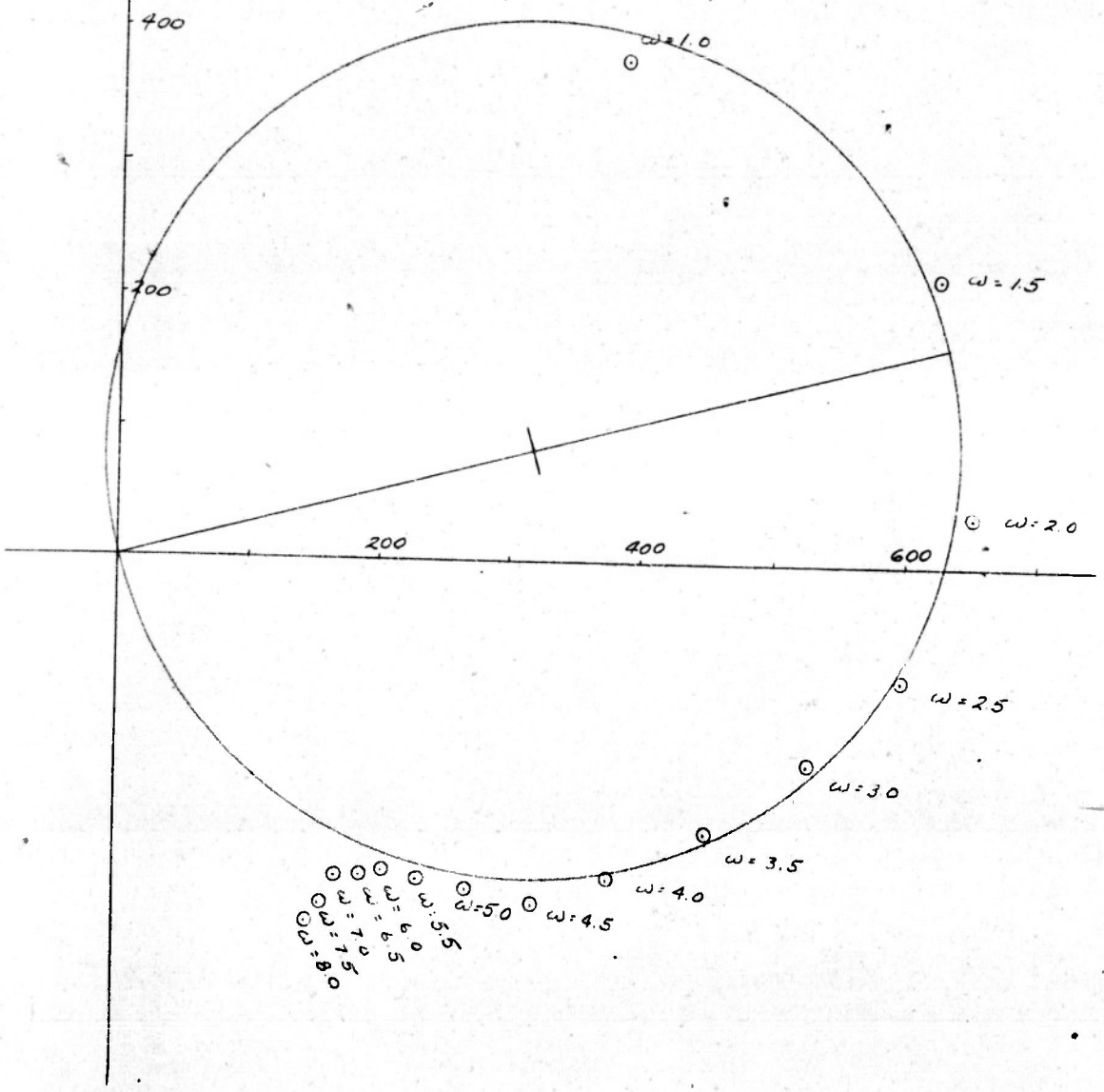

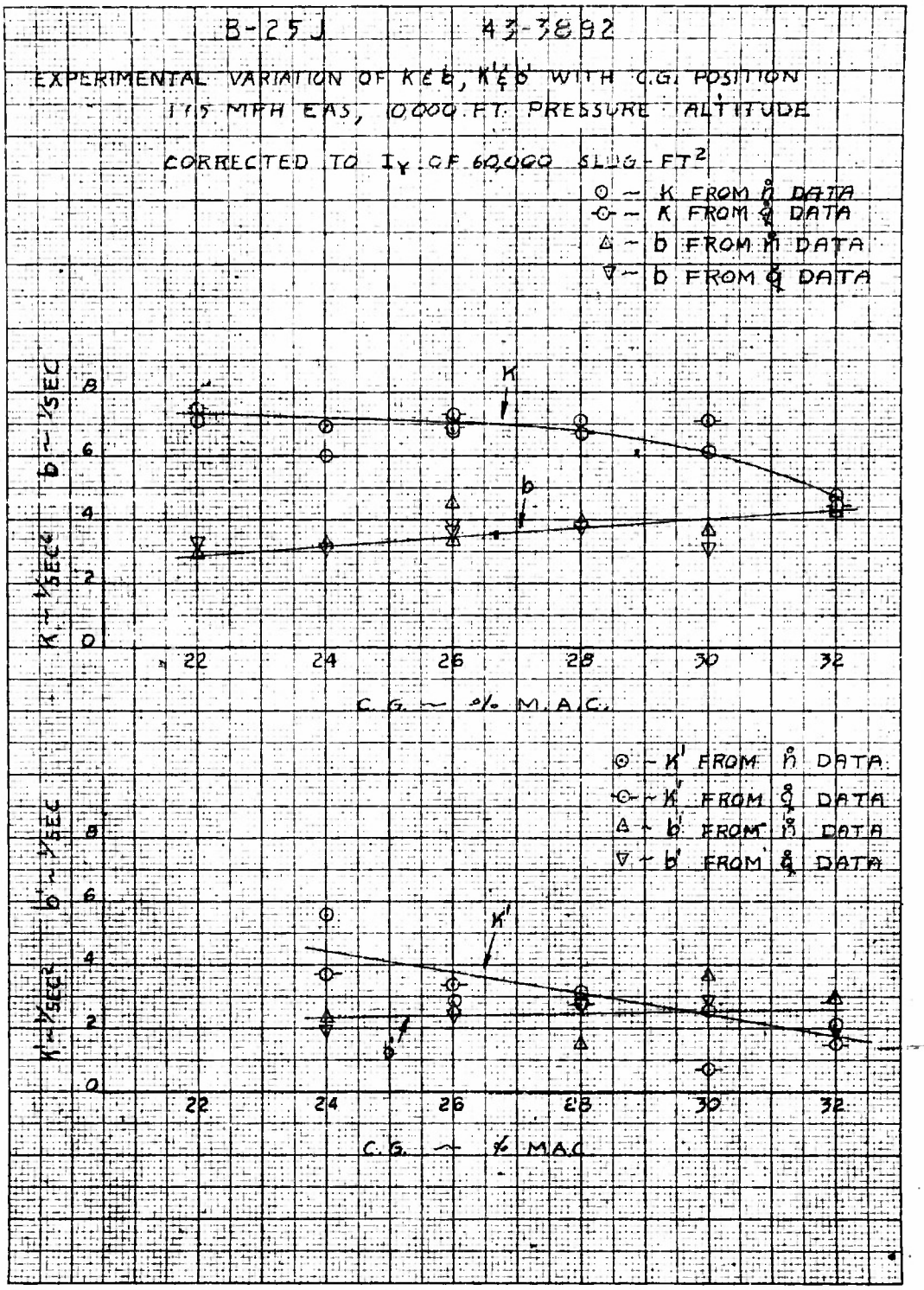
B-25J 43-3892
EXPERIMENTAL VARIATION OF K'E'B', K'E'b' WITH C.G. POSITION
175 MPH EAS, 10000 FT. PRESSURE ALTITUDE
CORRECTED TO I_X OF 60,000 SLUG-FT^2
⊙ – K FROM ṅ DATA
⊙– K FROM q̇ DATA
△ – b FROM ṅ DATA
▽ – b FROM q̇ DATA
K – 1/SEC^2
b – 1/SEC
0
2
4
6
8
22
24
26
28
30
32
C.G. – % M.A.C.
K
b
⊙ – K' FROM ṅ DATA
⊙– K' FROM q̇ DATA
△ – b' FROM ṅ DATA
▽ – b' FROM q̇ DATA
K' – 1/SEC^2
b' – 1/SEC
K'
b'
C.G. – % MAC

B-25 J 43-3892

COMPARISON OF EXPERIMENTAL AND CALCULATED VALUES OF K & b , K' & b'

175 MPH EAS , 10,000 FT. PRESSURE ALTITUDE

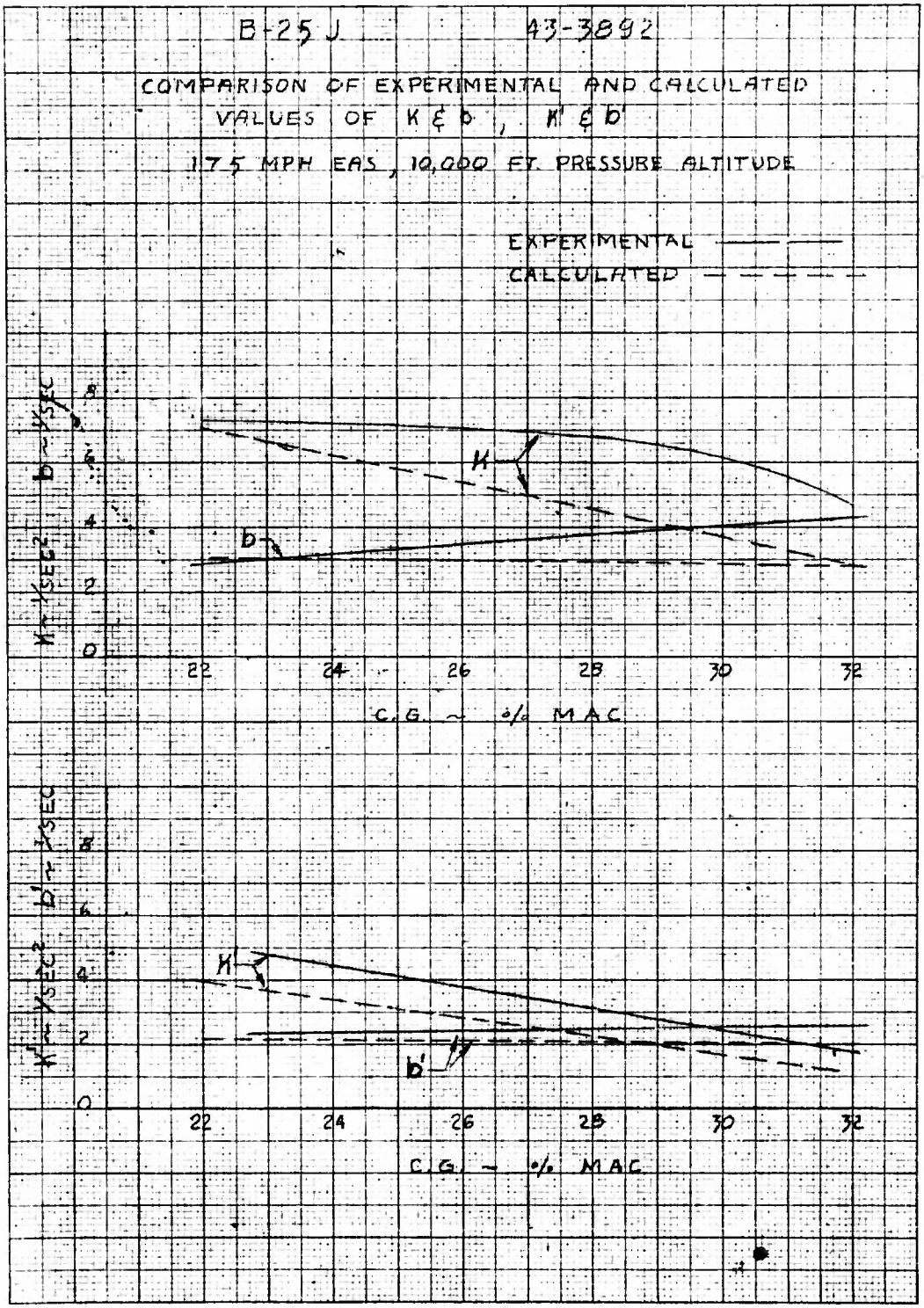

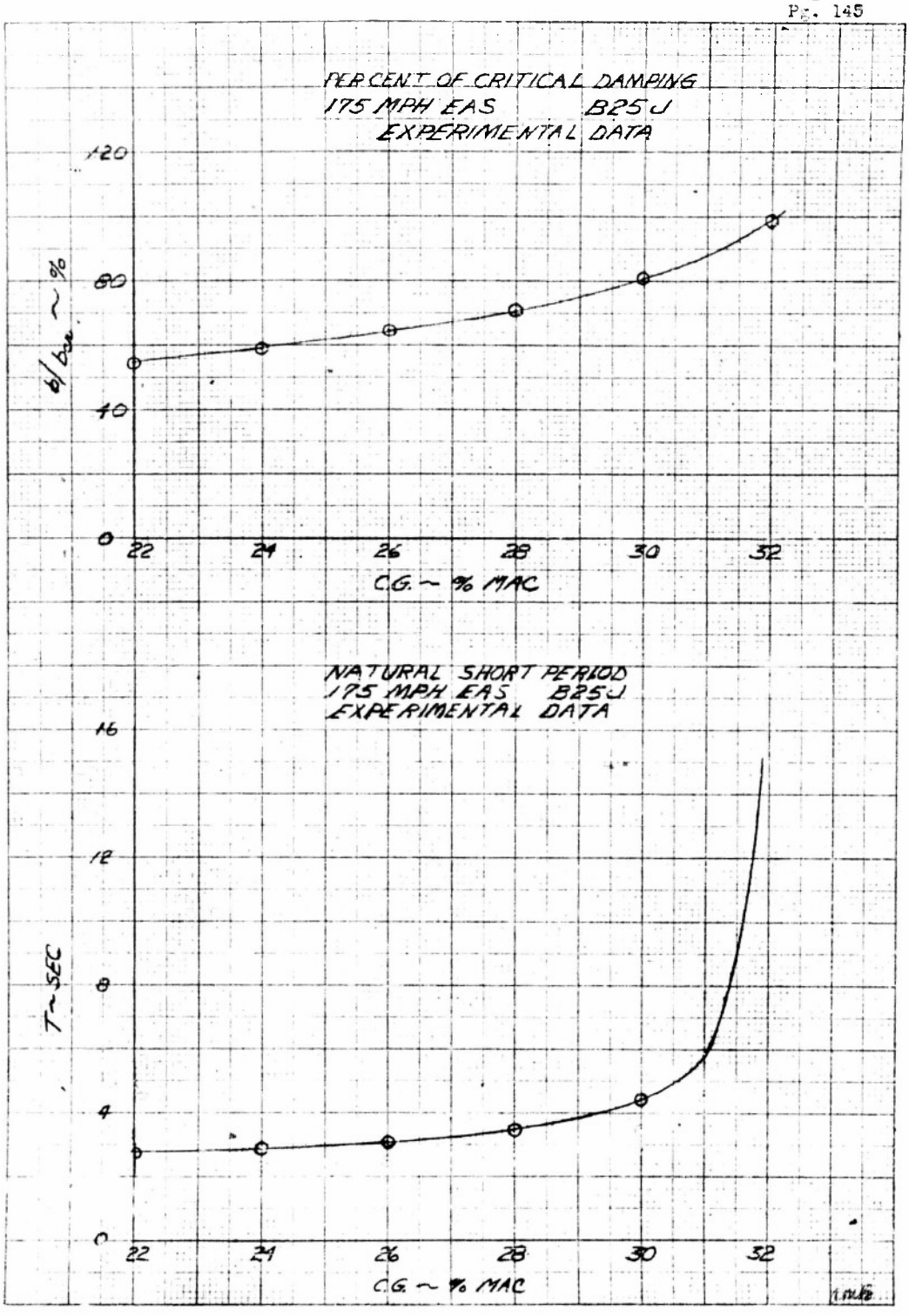
PERCENT OF CRITICAL DAMPING
175 MPH EAS B25J
EXPERIMENTAL DATA
120
80
40
0
b/2a ~ %
22
24
26
28
30
32
C.G. ~ % MAC
NATURAL SHORT PERIOD
175 MPH EAS B25J
EXPERIMENTAL DATA
16
12
8
4
0
T ~ SEC
22
24
26
28
30
32
C.G. ~ % MAC

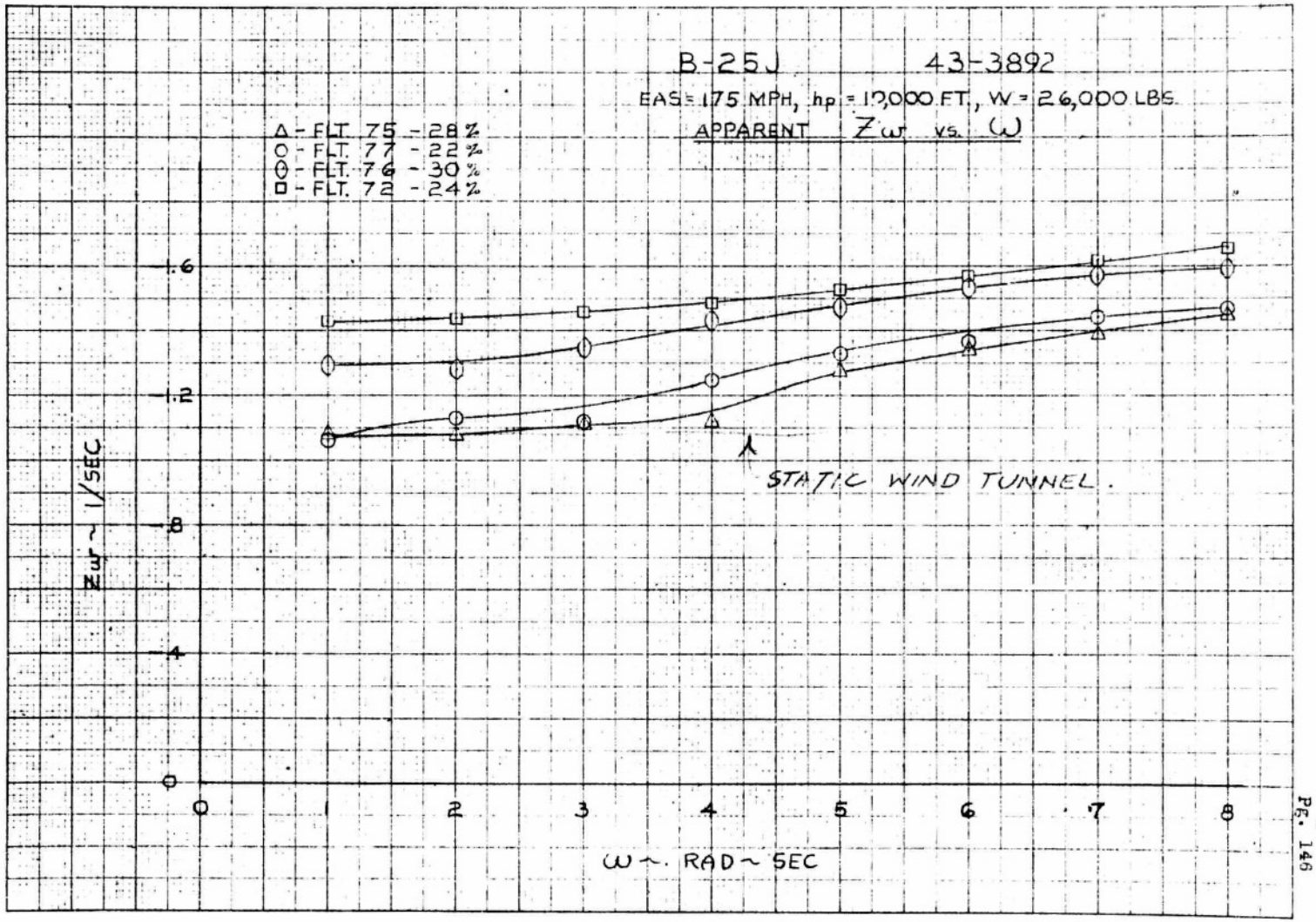
B-25J 43-3892
EAS = 175 MPH, hp = 12,000 FT., W = 26,000 LBS.
APPARENT Z_w vs. (ω)
Δ - FLT. 75 - 28%
○ - FLT. 77 - 22%
Θ - FLT. 76 - 30%
□ - FLT. 72 - 24%
STATIC WIND TUNNEL.
Z_w ~ 1/SEC
ω ~ RAD ~ SEC
0
.4
.8
1.2
1.6
1
2
3
4
5
6
7
8

Fig. 20
Pg. 146

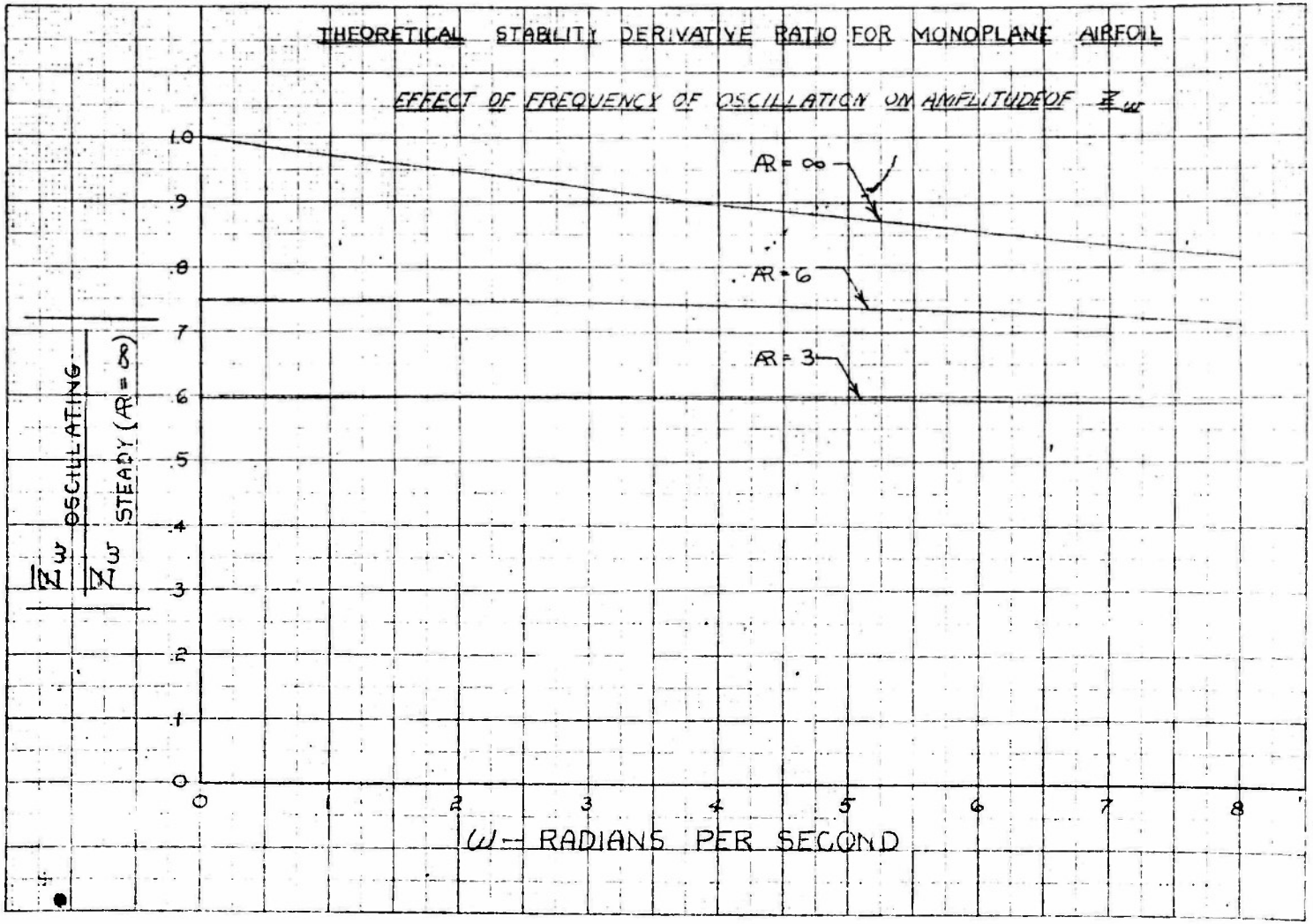

Fig. 21a
p. 147

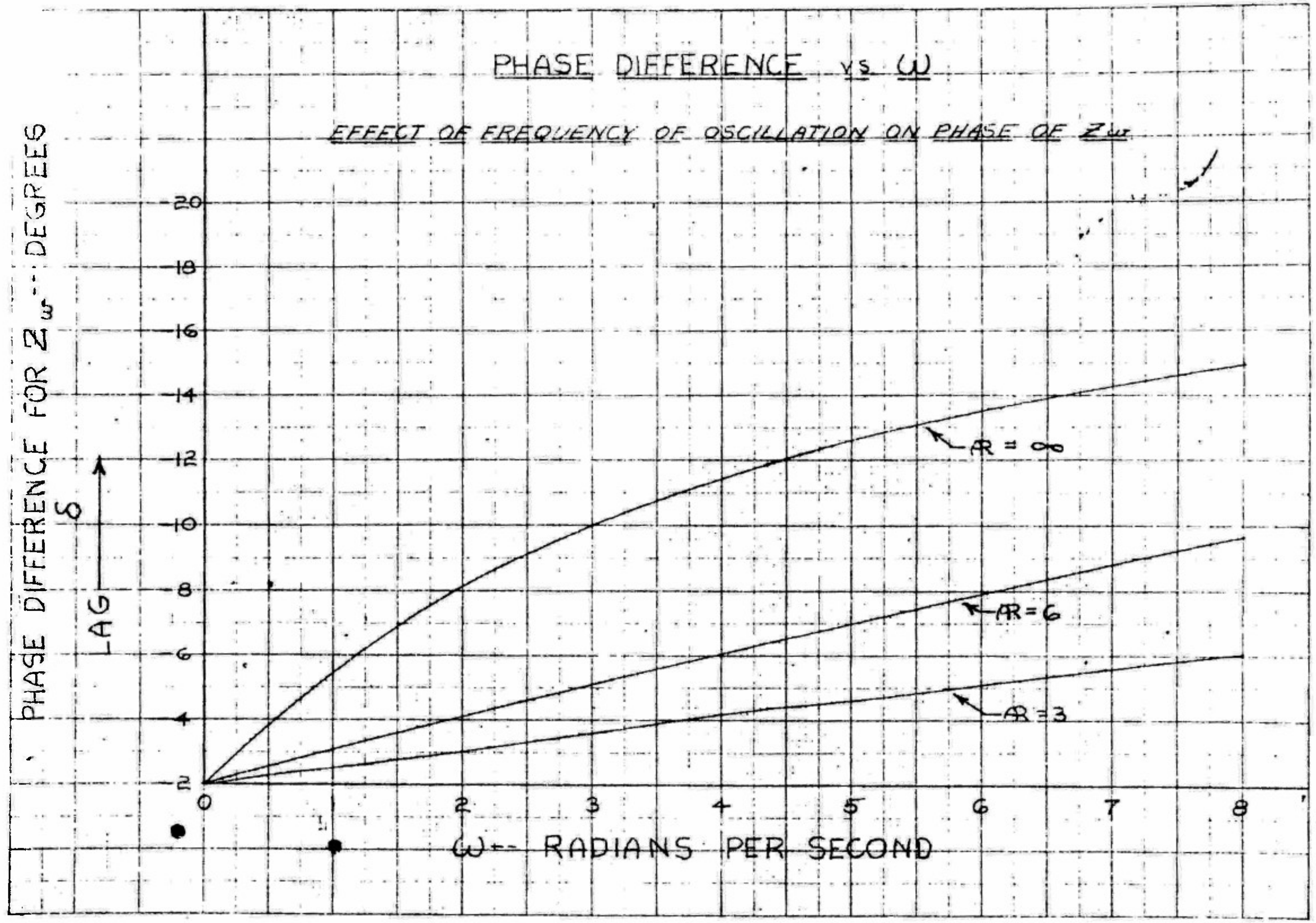
PHASE DIFFERENCE vs ω
EFFECT OF FREQUENCY OF OSCILLATION ON PHASE OF Zω
PHASE DIFFERENCE FOR Zω --- DEGREES
δ
LAG
20
18
16
14
12
10
8
6
4
2
0
1
2
3
4
5
6
7
8
AR = ∞
AR = 6
AR = 3
ω -- RADIANS PER SECOND

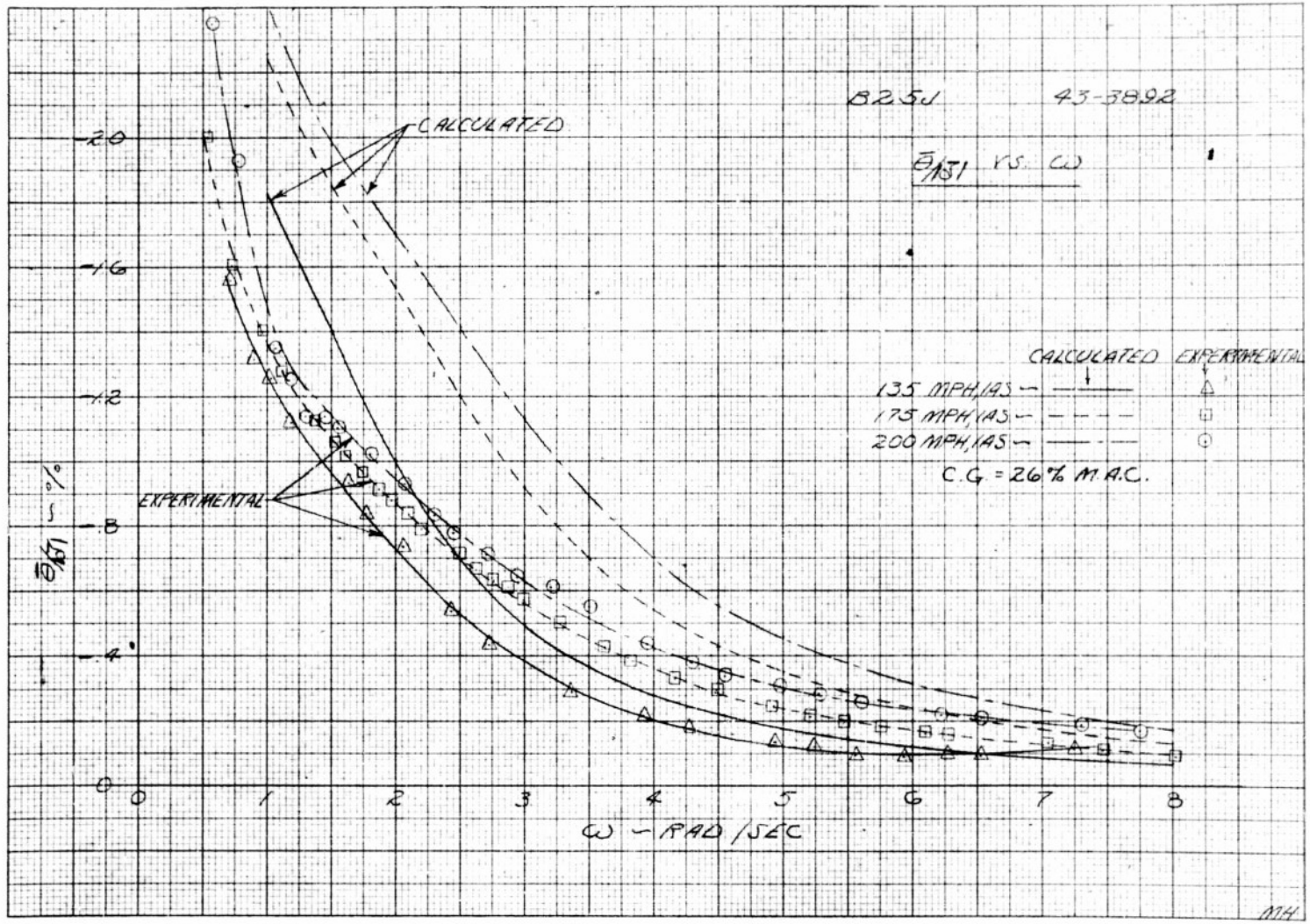

FIG. 22a
PG. 149

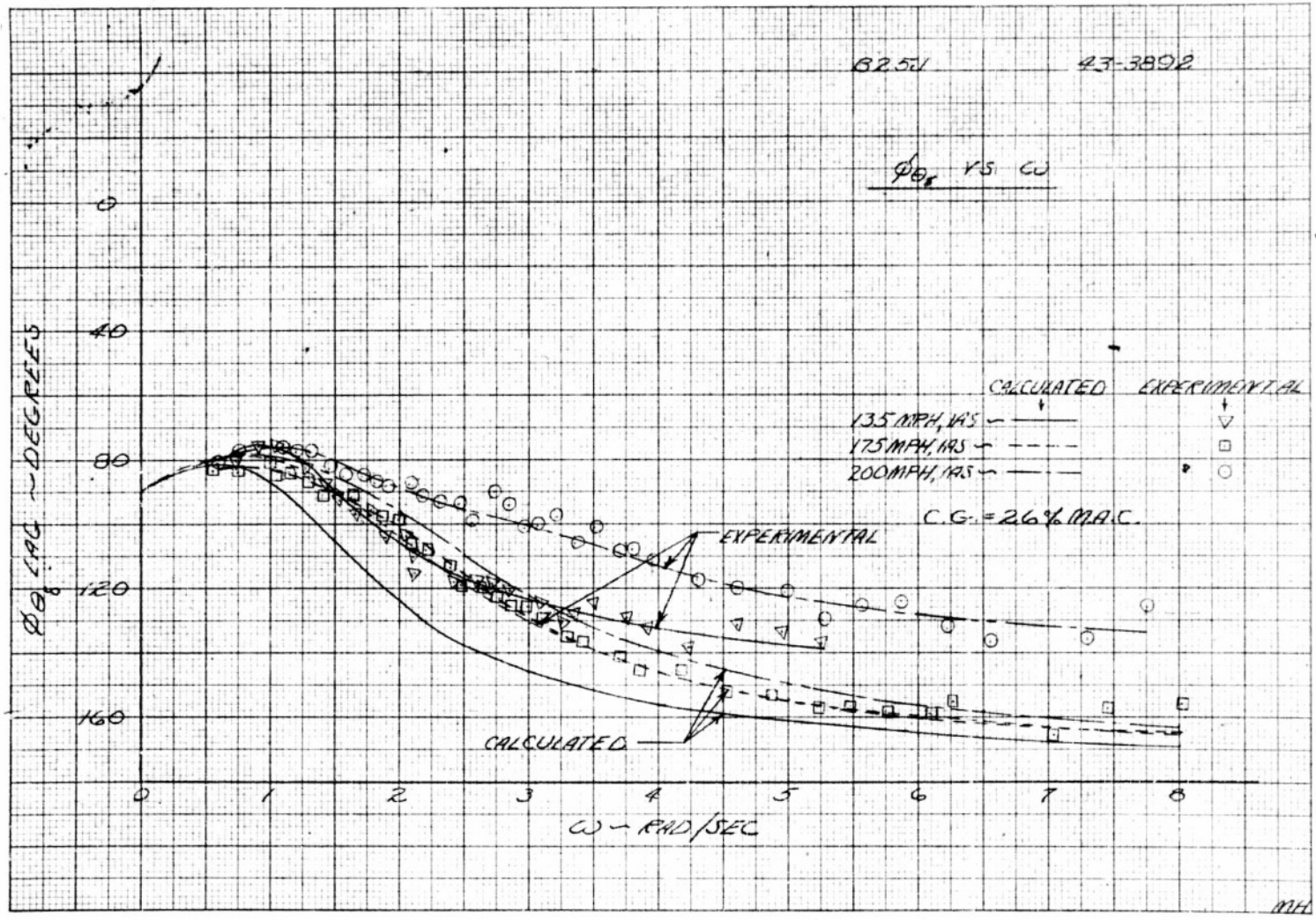

Fig. 22b
Pg. 150

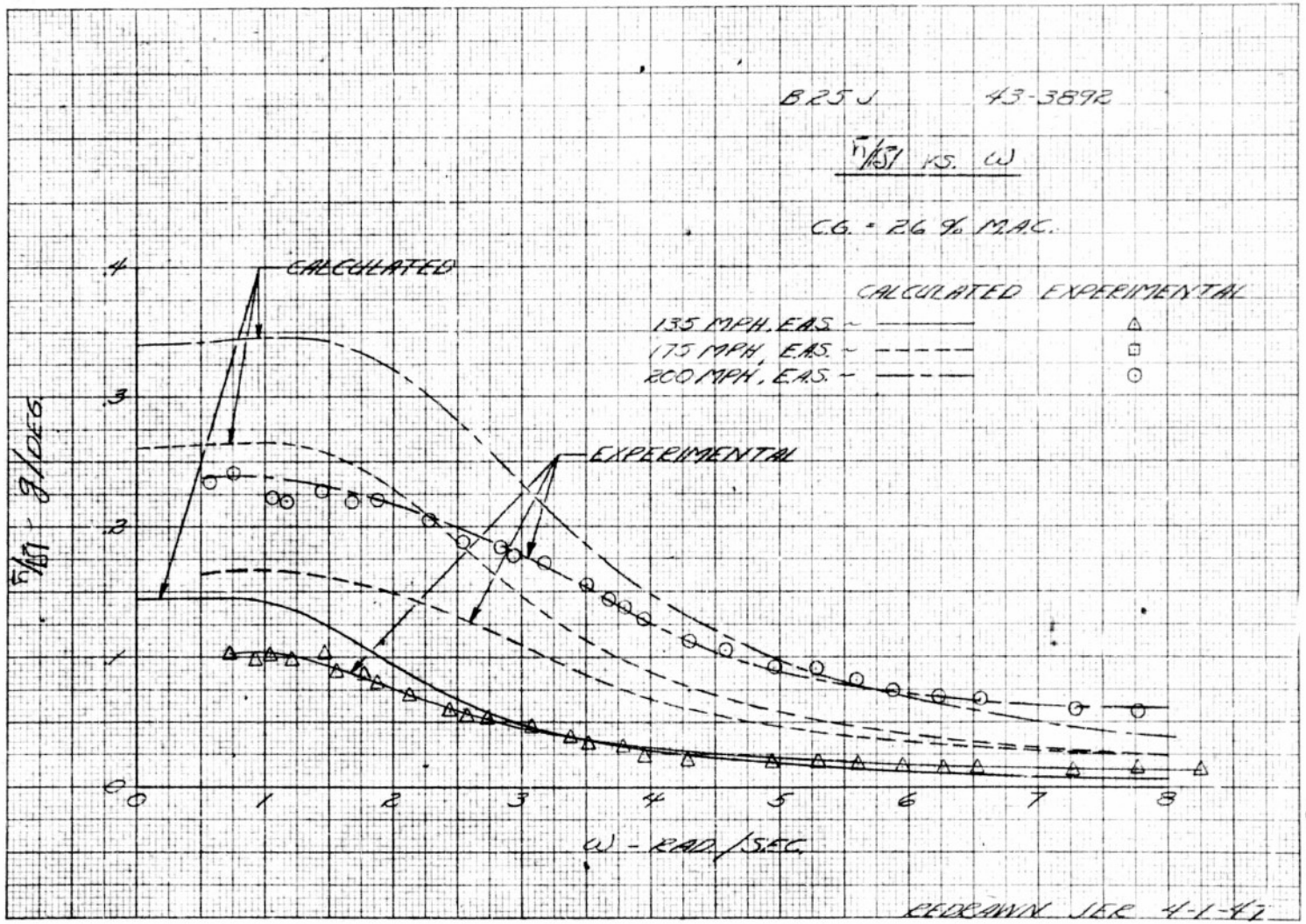

Fig. 23a
Pg. 151

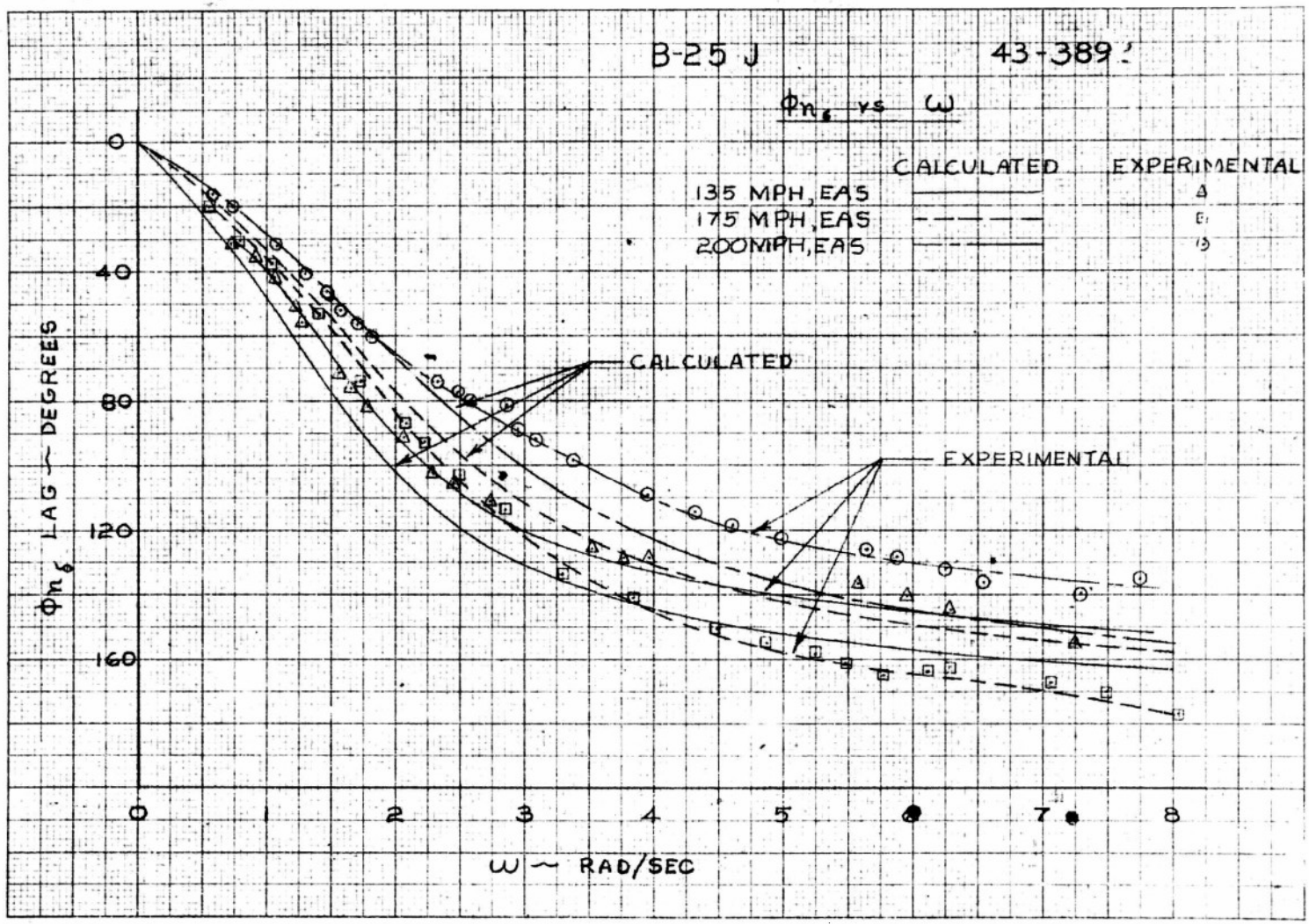

Fig. 23b
Pg. 113

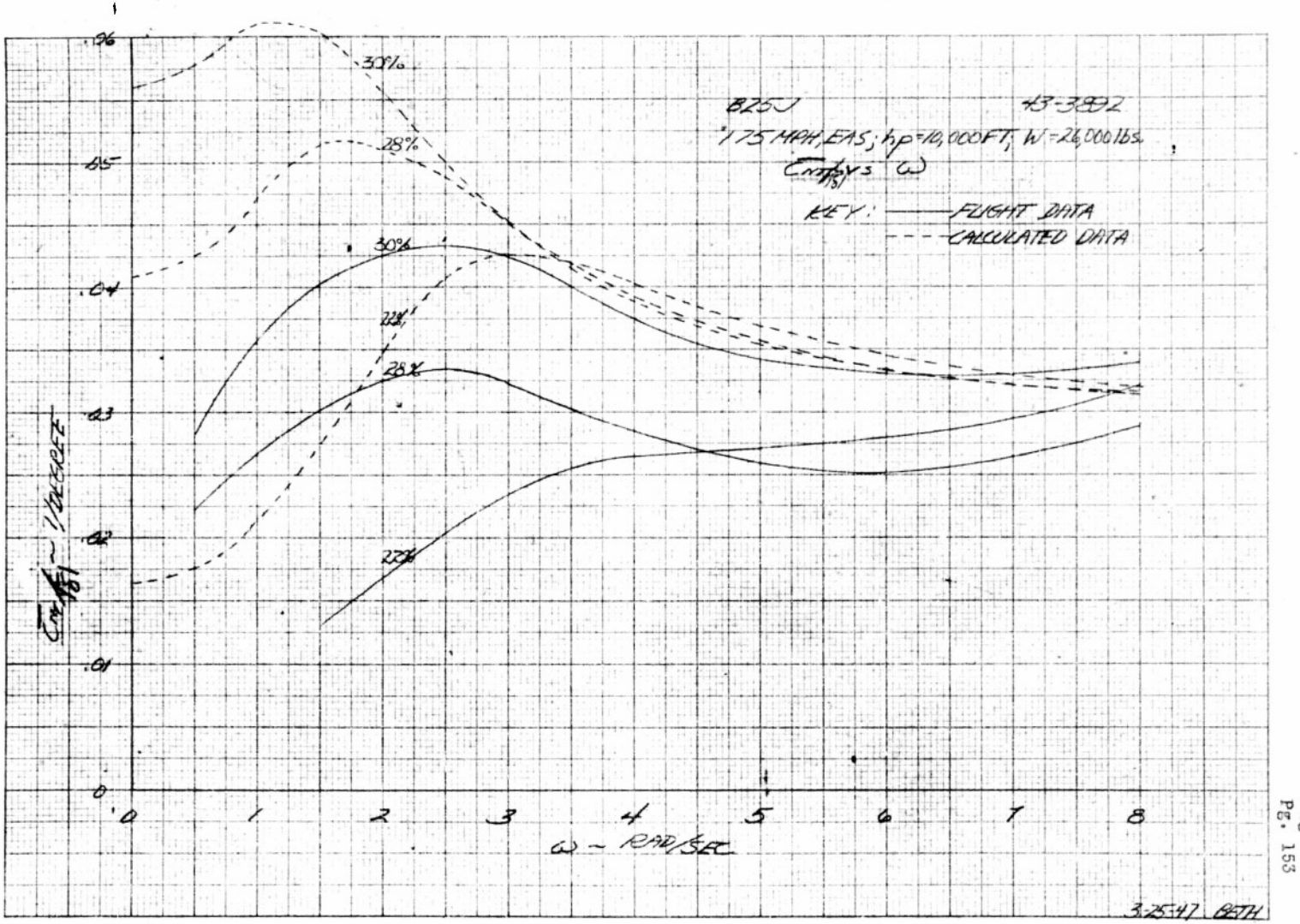

Fig. 24a
Pg. 153

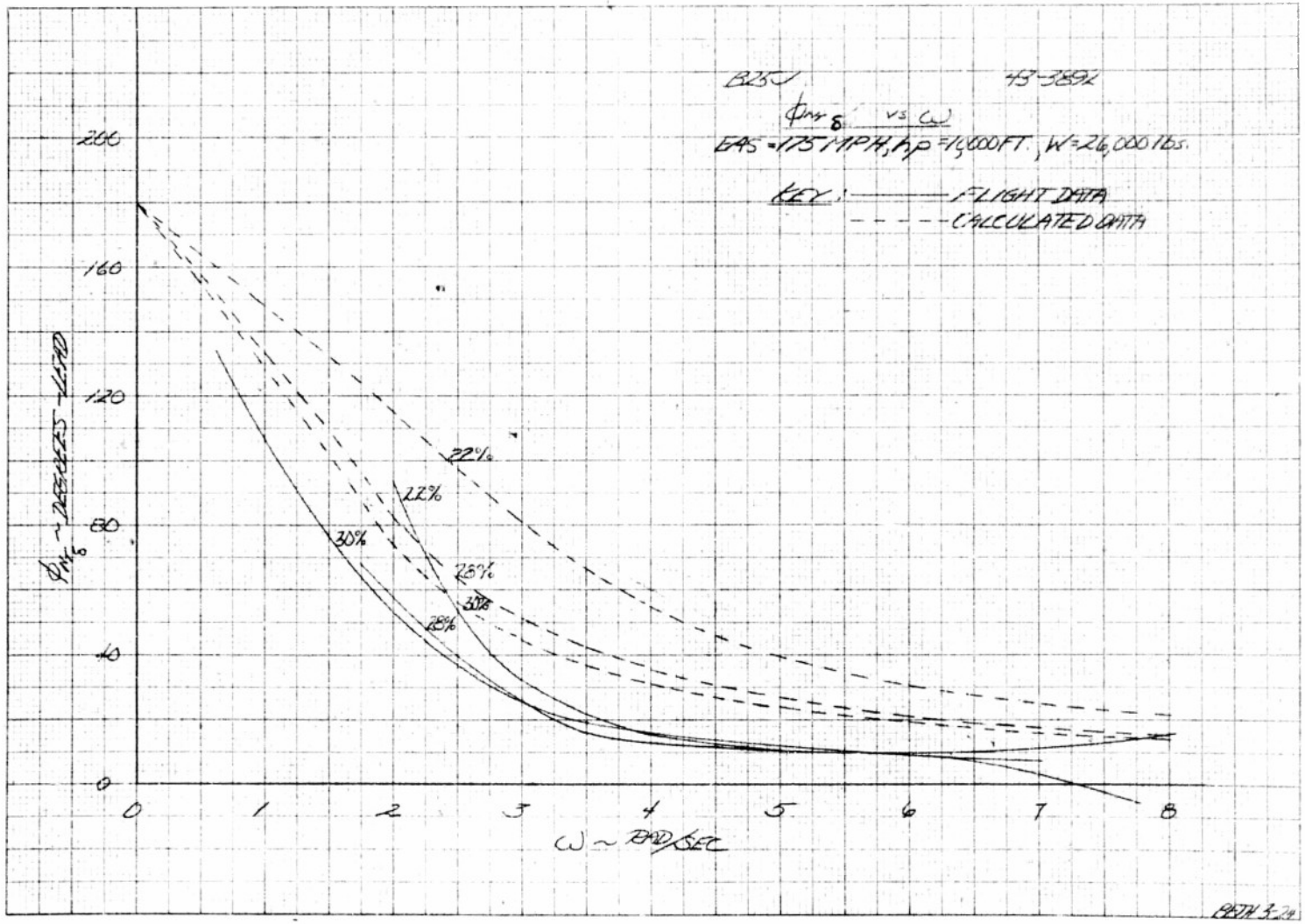

Fig. 24b
Pg. 154

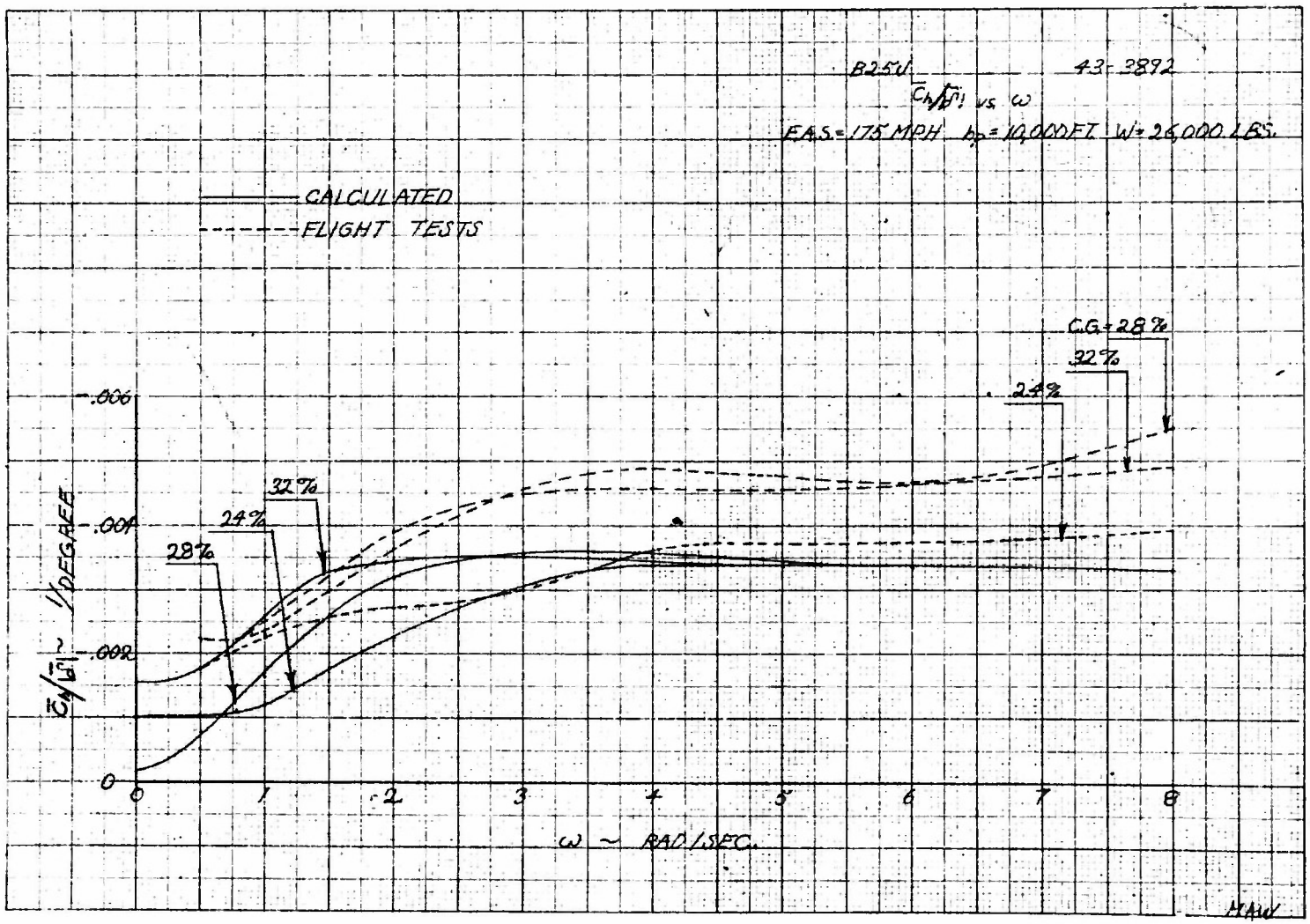

Fig. 25a
Pg. 155

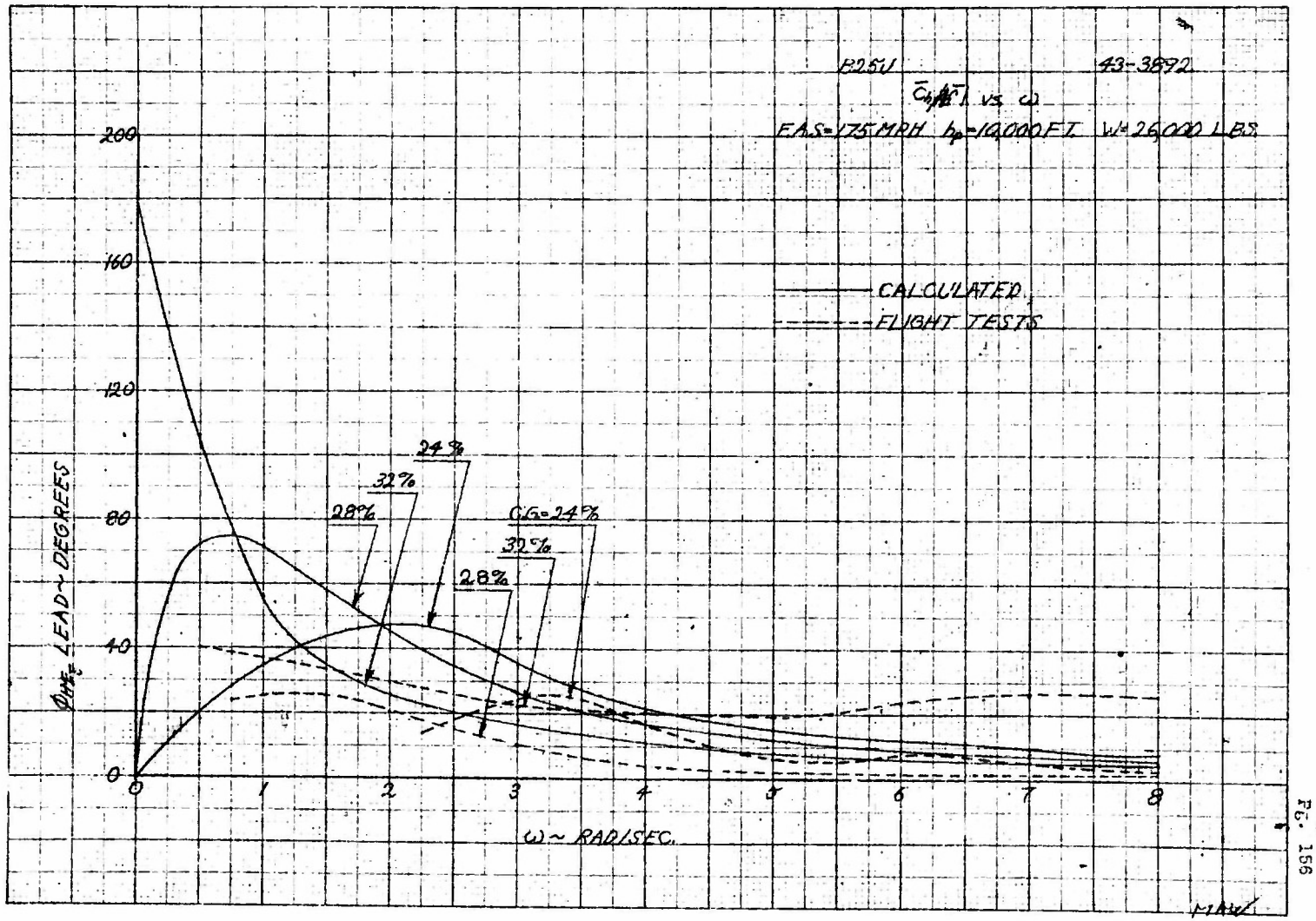

Fig. 25b
Fg. 156

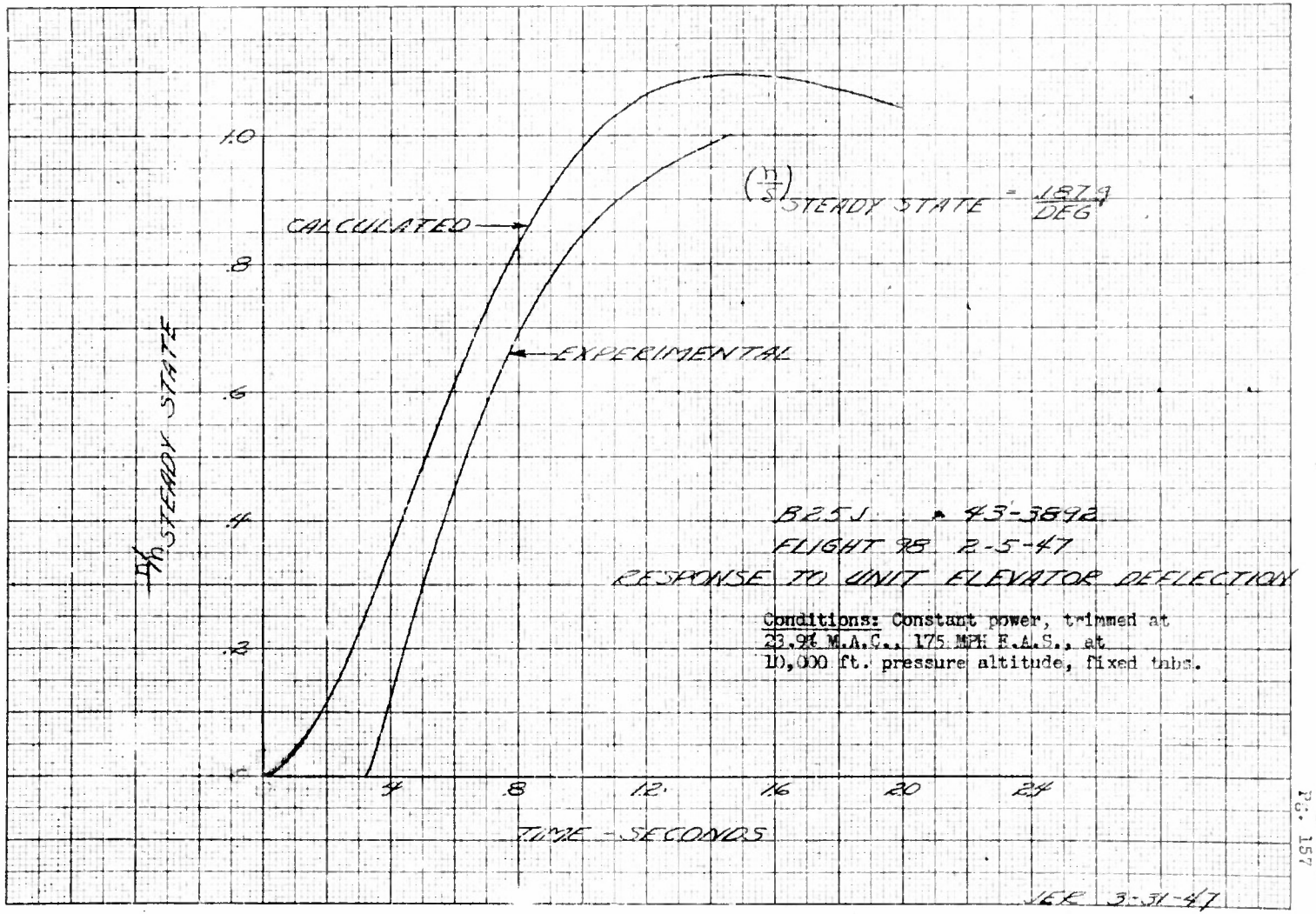

Fig. 20a
Pg. 157

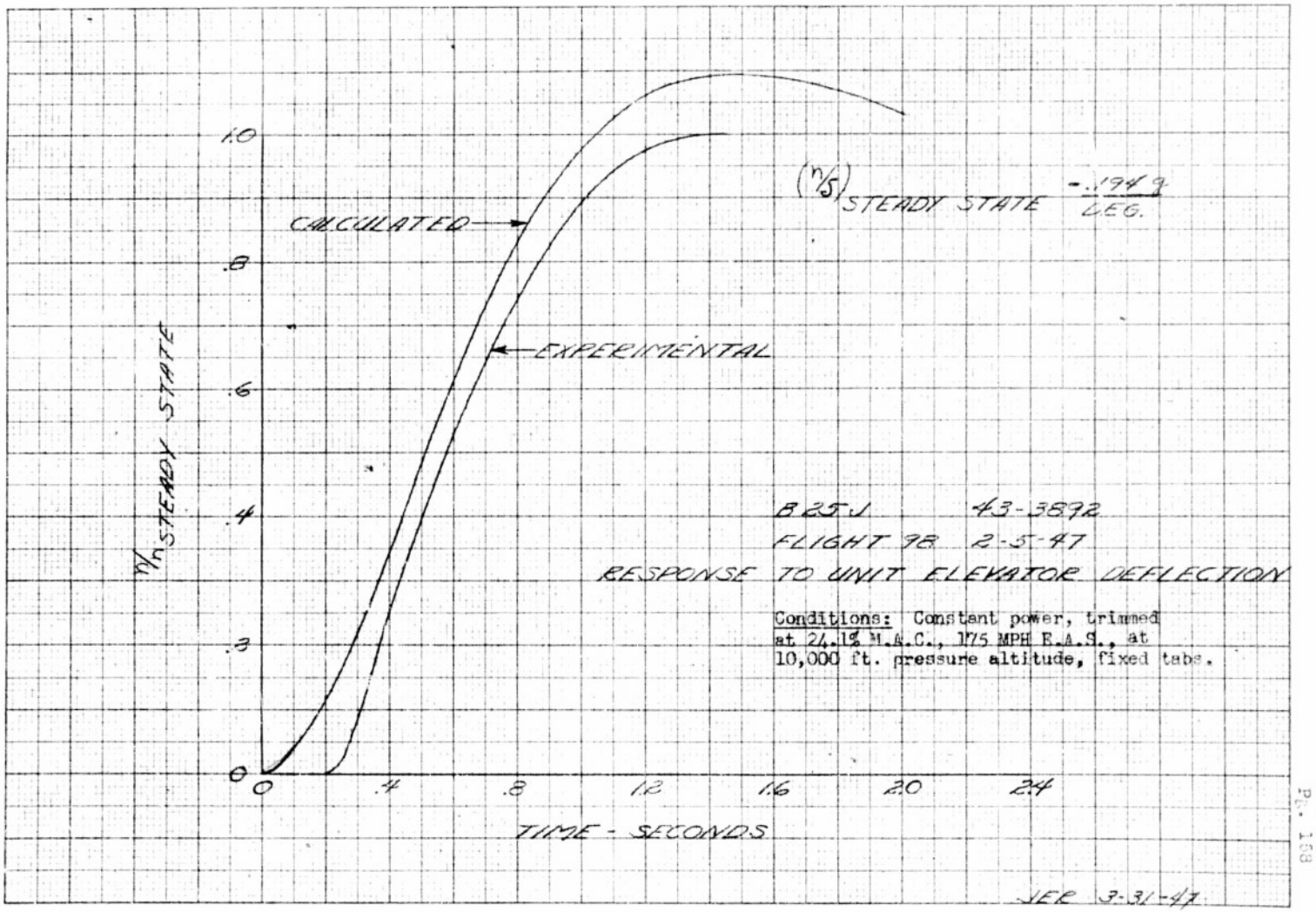

Fig. 203
Pg. 158

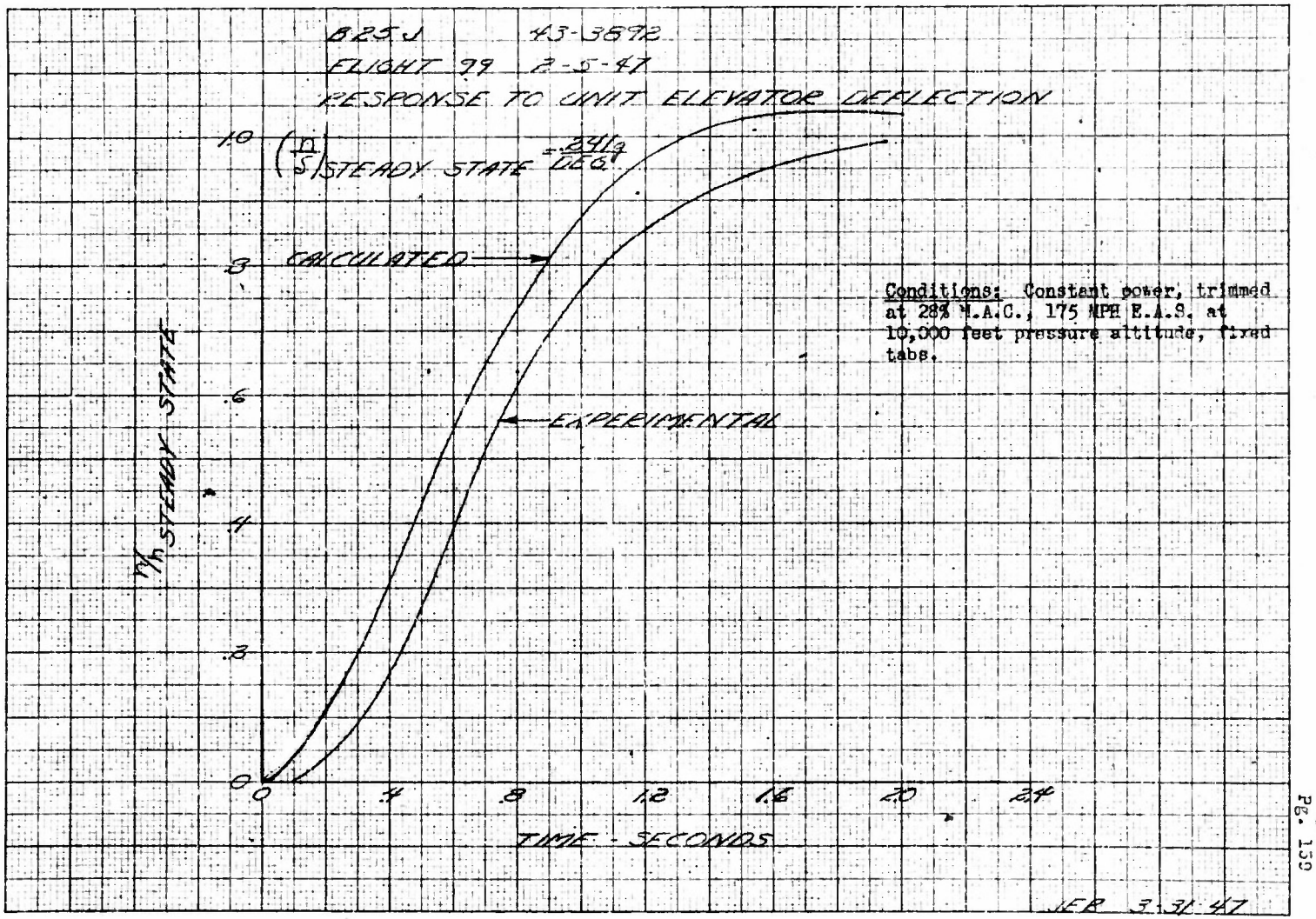

Fig. 25c
Pg. 139

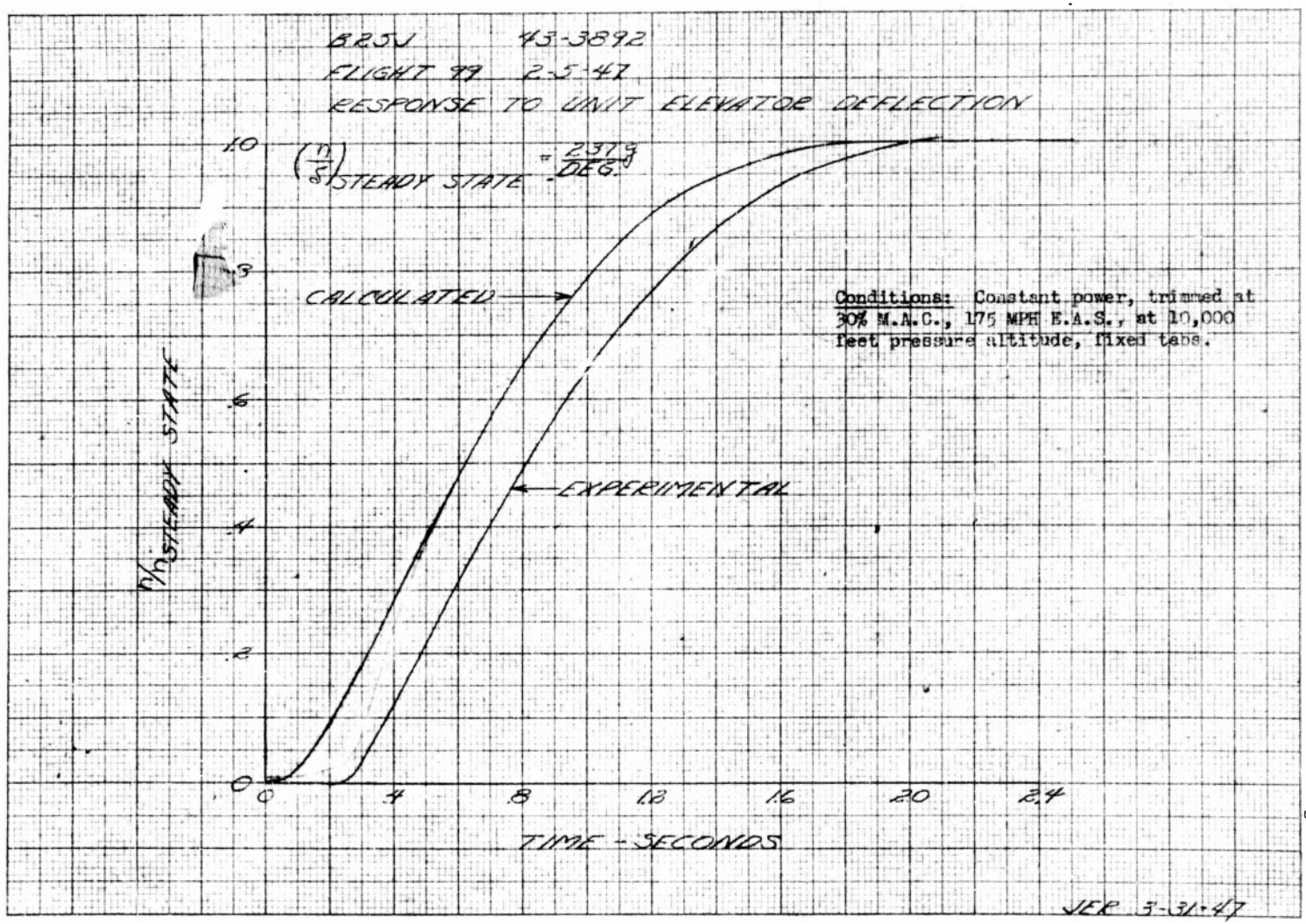

Fig. 26d
Pg. 160

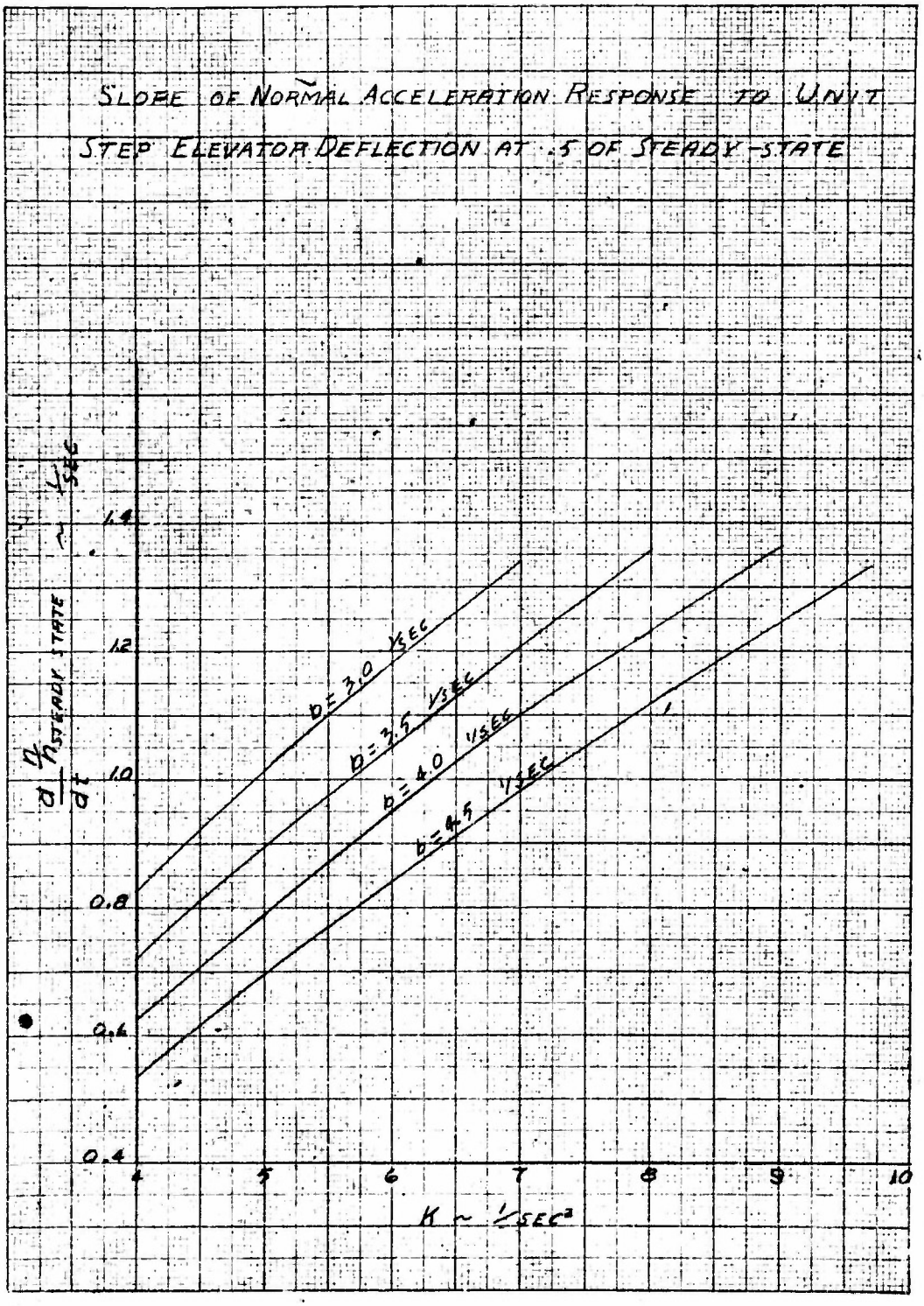

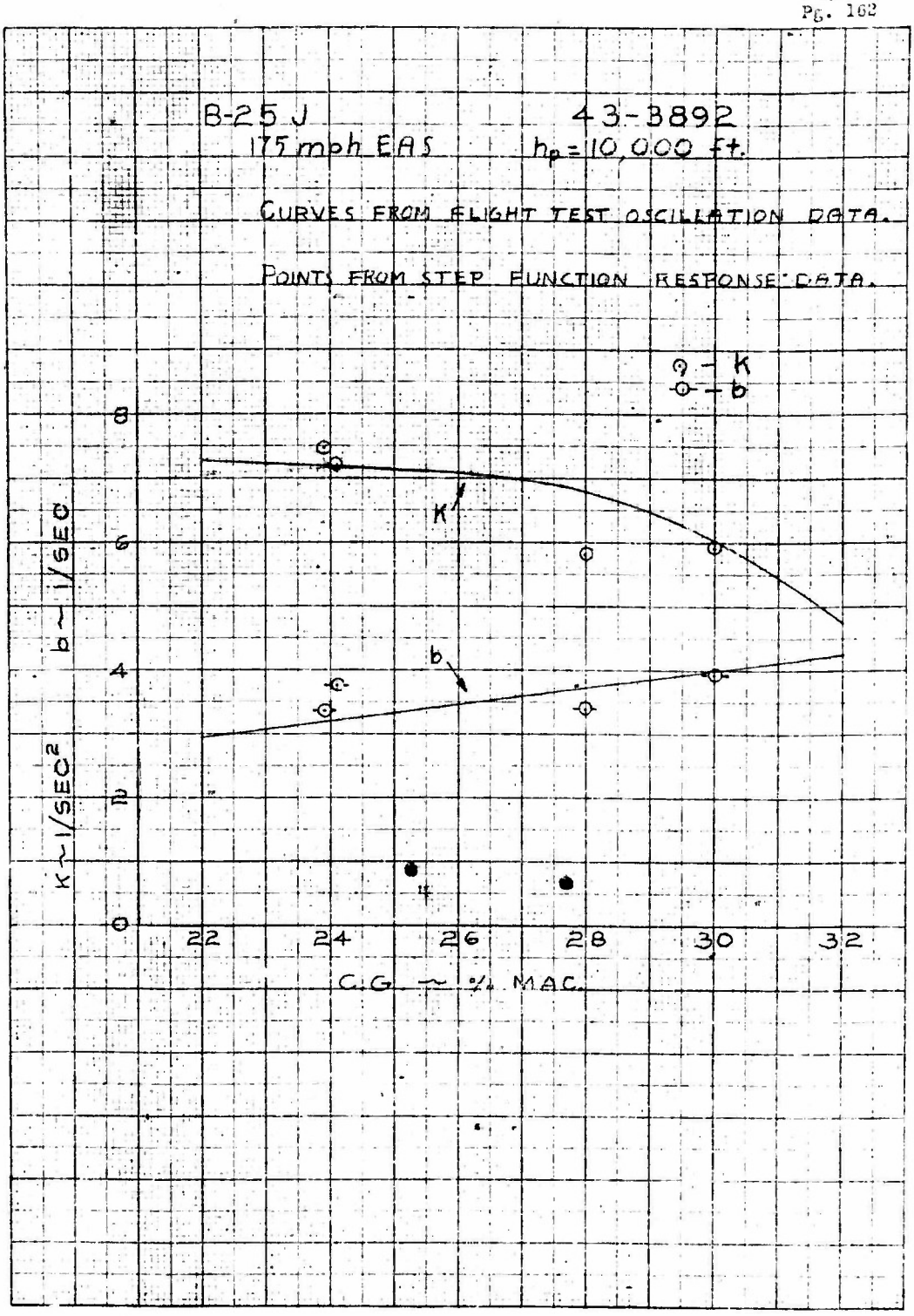
B-25 J
175 mph EAS
43-3892
h_p = 10,000 ft.
CURVES FROM FLIGHT TEST OSCILLATION DATA.
POINTS FROM STEP FUNCTION RESPONSE DATA.
○ - K
○ - b
K
b
b ~ 1/SEC
K ~ 1/SEC²
0
2
4
6
8
22
24
26
28
30
32
C.G. ~ % MAC.

REEL — C

484

A.T.I.

13979